IMPERIAL

Haemostasis and Immunothrombosis in Extracorporeal Circuits

Teresa Mei Ling Lee

BSc, MBBS, MRCP, FFICM

A thesis submitted for the degree of Doctor of Philosophy

at Imperial College London

Funded by:

EuroELSO Young Investigator Award 2021

Imperial - Healthcare Corporation of America Critical Care Fellowship

Royal Brompton and Harefield Hospitals Charity

Supervisors:	**Section of Anaesthetics, Pain Medicine and Intensive Care**
Dr Brijesh Patel	Department of Surgery and Cancer
Dr Kieran O'Dea	Faculty of Medicine
Assistant Supervisor:	Chelsea and Westminster Hospital
Dr Sharon Mumby	Imperial College London

Abstract

ARDS is a debilitating condition within intensive care with high morbidity and mortality. ECMO can be used to support patients with severe ARDS in whom conventional management such as invasive mechanical ventilation and prone positioning has failed. The main complications from ECMO use remain haemostatic with bleeding and thrombosis despite advances in biomaterials and ECMO anticoagulation guidelines. COVID-19 highlighted the importance of immunothrombosis in patients with ARDS. Neutrophil extracellular traps (NETs) and platelet-leucocyte interactions are an increasing area of interest in sepsis and ECMO.

The first aspect of this thesis investigated the presence of immunothrombosis in patients with COVID-19 and non-COVID-19 ARDS who required ECMO. Incidence of ECMO circuit thrombosis was higher in COVID-19 patients which was related to duration of ECMO rather than COVID-19, indicating ECMO itself is immunothrombotic. COVID-19 patients had lower D-dimer levels in the lead up to circuit thrombosis suggesting a different mechanism for thrombosis e.g. reduced fibrinolysis. This highlights the difficulty in predicting circuit thrombosis with current clinical biomarkers. Biomarkers of neutrophil activation and NETosis in patient samples demonstrated increased NETosis after ECMO initiation despite already high levels of neutrophil and platelet activation. The reduced platelet aggregation during ECMO which improved after ECMO discontinuation suggesting ECMO increases NETosis and platelet dysfunction and may be related in ECMO immunothrombosis.

The second aspect of this thesis describes the development of flow cytometry protocols to measure leucocyte-platelet interactions by measuring leucocyte-platelet aggregates (LPA) using the ibidi microfluidics chamber to generate LPA formation under flow conditions. This model demonstrated that LPA form more readily with platelet activation compared to leucocyte activation and can be reduced using a platelet inhibitor. This model can be adapted for use with isolated cells, and endothelial cell providing a platform to investigate the effects of flow on neutrophil and platelet activation, and leucocyte-platelet interactions.

Table of Contents

Abstract 2
Table of Contents 3
Dedication 11
Acknowledgements 12
Statement of Originality 13
Statement of Copyright 13
Publications during candidature 14
Index of Figures 15
Index of Tables 18
Abbreviations 20
Chapter 1: Introduction 24
1.1 Acute Respiratory Distress Syndrome 24
1.1.1 Definition 24
1.1.2 Epidemiology 25
1.1.3 Aetiology of ARDS 25
1.1.4 Pathophysiology of ARDS 26
1.1.5 Management of ARDS 29
1.2 Extracorporeal Membrane Oxygenation and its uses 30
1.2.1 The history of extracorporeal life support 30
1.2.2 Indications for ECMO 31
1.2.3 ECMO circuit 31
1.2.4 The ECMO blood pump 33
1.2.5 The membrane oxygenator 34
1.2.6 The aim of ECMO 36
1.3 Haemostasis 37
1.3.1 The classic model of coagulation 37
1.3.2 The cell-based coagulation model 38
1.3.3 Platelets 40
1.3.4 Platelet activation 41
1.4 Neutrophils 42
1.4.1 Neutrophil activation 42
1.4.2 Neutrophil degranulation 43

1.4.3 Neutrophil death 44
1.4.4 NETosis 45
1.4.5 Neutrophil phenotypes 47
1.4.6 Monocyte Subsets 49
1.5 Immunothrombosis in context 49
1.5.1 What is immunothrombosis? 49
1.5.2 NETosis in ARDS 50
1.5.3 NETs in thrombosis 51
1.5.4 Leucocyte-platelet interactions 51
1.6 ECMO and haemostasis 54
1.6.1 Haemostatic complications are common in ECMO 54
1.6.2 Membrane oxygenator thrombosis: Predicting need for circuit change 55
1.6.3 Why do membrane oxygenators clot? 56
1.6.4 ECMO circuit change 57
1.6.5 Platelet dysfunction in ECMO 58
1.7 Rationale for project 60
1.8 Hypotheses and Aims 60
1.9 Overview of thesis 61
Chapter 2: Methods chapter 63
2.1 Materials 63
2.1.1 Reagents 63
2.1.2 Commercial detection assays 65
2.1.3 Pharmacological agents 69
2.1.4 Instruments, equipment and software 69
2.1.5 Antibodies 72
2.2 Clinical Studies 73
2.2.1 A CLUE Study (COVID-19 Flu ECMO) 73
2.2.2 DeVENT Study 73
2.2.3 HITEC Study 75
2.2.4 HITEC Blood sampling 77
2.2.5 Blood processing 79

2.3 Lab protocols 80
2.3.1 Peripheral blood mononuclear cell (PBMC) and neutrophil isolation 80
2.3.2 Isolated neutrophil stimulation 81
2.3.3 Platelet rich plasma stimulation 81
2.3.4 Whole blood stimulation 82
2.3.5 Ibidi microfluidics pump system 82
2.3.6 Whole blood stimulation in the ibidi microfluidics pump system 84
2.4 Flow cytometry protocols 86
2.4.1 Introduction to spectral flow cytometry 86
2.4.2 Determining particle size using ApogeeMix sizing beads 89
2.4.3 Isolated PMN NETs staining and flow cytometric analysis 90
2.4.4 Whole blood NETs staining and flow cytometric analysis 91
2.4.5 Phenotyping leucocytes and quantifying leucocyte-platelet aggregates by flow cytometry in patient samples 94
2.4.6 Phenotyping leucocytes and quantifying leucocyte-platelet aggregates by flow cytometry for in vitro work 97
2.5 Other protocols for measurement 97
2.5.1 ELISA 97
2.5.2 Cell-free DNA 98
2.5.3 Multiplate Analyzer 98
2.5.4 Thromboelastogram 100
2.6 Statistical Analysis 101
Chapter 3: Clinical observations of immunothrombosis in ECMO patients. 102
Abstract 102
3.1 Introduction 103
3.1.1 Circuit change and importance to outcomes. 103
3.1.2 Predicting need for circuit change in VV ECMO patients is difficult. 103
3.1.3 COVID-19, ARDS and immunothrombosis 104
3.1.4 ECMO use in COVID-19 associated ARDS 105
3.1.5 Oxygenator development and use in practice. 106
3.2 Aims and hypotheses 107

3.3 Methods 107
3.3.1 Study Design and Participants 107
3.3.2 Data collection and definitions 108
3.3.3 Missing Data 109
3.3.4 Statistical Analysis 109
3.4 Results 110
3.4.1 Patient demographics and baseline characteristics 110
3.4.2 Baseline clinical parameters 112
3.4.3 Circuit change and ECMO duration are increased in COVID patients 115
3.4.4 COVID-19 patients more likely to have worse severe respiratory failure and increased ECMO requirements 118
3.4.5 Predictors of circuit change are different in COVID-19 patients 123
3.5 Discussion 129
3.5.1 Clinical differences are observed between COVID-19 and non-COVID-19 patients with severe ARDS requiring ECMO 129
3.5.2 Thrombogenicity of COVID-19 was associated with increased MO dysfunction, and longer ECMO duration. 130
3.5.3 Monitoring membrane oxygenator dysfunction is more difficult in COVID-19. 132
3.5.4 Increased thrombogenicity in COVID-19 due to lack of fibrinolysis 134
3.5.5 ECMO is immunothrombotic 135
3.5.6 Limitations 136
3.6 Concluding remarks 138
Chapter 4: Immune and platelet responses in ECMO patients 140
Abstract 140
4.1 Introduction 141
4.1.1 Neutrophil activation, degranulation and NETosis 141
4.1.2 Neutrophil activation in ARDS 141
4.1.3 NETosis in extracorporeal circuits 142
4.1.4 Platelet activation in ECMO 142
4.2 Aims and hypothesis 144
4.3 Methods 145
4.3.1 Study design and participants 145

4.3.2 Data collection and definitions 145
4.3.3 Sample collection 146
4.3.4 ELISA 146
4.3.5 Flow cytometry for cell-associated NETs 146
4.3.6 Clinical platelet function and viscoelastic assays 146
4.3.7 Statistical Analysis 147
4.4 Results 147
4.4.1 Patient demographics and baseline characteristic of patients with ECMO initiation comparisons 147
4.4.2 Markers of neutrophil activation and NETosis are increased in SARF and undergo a further increase after VV ECMO initiation. 151
4.4.3 Circulating markers of inflammation decrease after ECMO initiation 154
4.4.4 Markers of neutrophil activation and NETosis vary over the ECMO run 156
4.4.5 Markers of neutrophil activation and NETosis decreased after ECMO decannulation. 157
4.4.6 Sub-cohort analysis of neutrophil activation markers between COVID-19 and non-COVID-19 aetiologies of SARF 159
4.4.7 Sub-cohort analysis of neutrophil activation markers pre- and post- membrane oxygenator 160
4.4.8 Measuring cell-associated NETs 160
4.4.9 Platelet activation markers: PF4 and CD62P decreased after ECMO initiation 163
4.4.10 Clinical coagulation assays 166
4.5 Discussion 171
4.5.1 Reductions in inflammatory cytokines after ECMO initiation are likely due to lung rest 171
4.5.2 ECMO initiation leads to increased NETosis and contributes to immunothrombosis in ECMO 173
4.5.3 Comparison of cell-associated and soluble NETs 175
4.5.4 Platelet activation and dysfunction in ECMO patients 177
4.5.5 What is the impact of increased NETosis on platelet activation? 181

4.5.6 The role of platelets in neutrophil activation and NETosis 182
4.6 Concluding remarks 183
Chapter 5: Measuring leucocyte platelet aggregates – challenges of quantification 184
Abstract 184
5.1 Introduction 185
5.1.1 Relationship between neutrophils and platelets in ECMO 185
5.1.2 Leucocyte platelet aggregates 185
5.1.3 Leucocyte phenotypes 188
5.2 Aims and hypothesis 188
5.3 Methods 189
5.3.1 Blood sample processing 189
5.3.2 Whole blood stimulation/in vitro controls 189
5.3.3 Flow cytometry for leucocyte phenotyping and leucocyte-platelet aggregates in patient samples 190
5.4 Results 190
5.4.1 Anticoagulant type affects LPA formation and measurement in vitro. 190
5.4.2 Leucocyte-platelet aggregate formation is calcium dependent and reversible. 193
5.4.3 Measurement of LPA is affected by anticoagulation 195
5.4.4 NPA kinetics and neutrophil phenotypes in ECMO patients 197
5.4.5 Relationship between neutrophil phenotypes, NPA and NETosis 200
5.4.6 MPA kinetics and monocyte subsets in ECMO patients 203
5.4.7 LPA formation was not related to clinically measured cell counts 206
5.5 Discussion 207
5.5.1 Impact of calcium chelation on LPA measurement 208
5.5.2 Impact of other anticoagulants on LPA measurement 209
5.5.3 LPA formation is calcium dependent and is reversible. 210
5.5.4 LPA are present in ECMO patients 212
5.5.5 Neutrophil-platelet aggregates, associated phenotypes, NETosis and thrombocytopenia 213
5.5.6 Monocyte phenotypes in ECMO 215

5.6 Conclusions 216
Chapter 6: Evaluation of leucocyte platelet aggregates in an in vitro model of flow 218
Abstract 218
6.1 Introduction 219
6.2 Aims and hypothesis 219
6.3 Methods 220
6.3.1 Platelet rich plasma stimulation and platelet activity quantification 220
6.3.2 Whole blood stimulation in ibidi microfluidics chamber 220
6.3.3 Flow cytometry for leucocyte phenotyping and leucocyte-platelet aggregates 221
6.4 Results 222
6.4.1 TRAP-6 is a potent platelet agonist, whereas LPS did not induce platelet activation in platelet rich plasma 222
6.4.2 Laminar blood flow appears to generate less LPA than turbulent blood flow. 224
6.4.3 Flow rates did not affect leucocyte-platelet aggregation in vitro 226
6.4.4 Formation of neutrophil-platelet aggregates is increased with platelet stimulation, compared to leucocyte stimulation 228
6.4.5 There is no difference in formation of monocyte-platelet aggregates with leucocyte or platelet stimulation 231
6.4.6 Inhibitors had no effect on baseline LPA formation or leucocyte activation ... 234
6.4.7 Effect of GPIIb/IIIa inhibition and P-selectin pathway inhibition on neutrophil-platelet aggregation 235
6.4.8 There is no effect of GPIIb/IIIa inhibition or P-selectin inhibition on monocyte-platelet aggregation 239
6.5 Discussion 242
6.5.1 Developing an experimental flow model for investigating LPA formation 242
6.5.2 Formation of neutrophil-platelet aggregates under flow conditions is increased with platelet activation. 243
6.5.3 Differential formation of LPA depends on cell type and stimulant 245
6.5.4 Inhibiting GPIIb/IIIa using eptifibatide reduced NPA formation but inhibition of P-selectin pathway by KF38789 did not 246
6.5.5 Significance of leucocyte-platelet aggregates and interactions 250
6.5.6 Limitations 251

6.5.7 Future work using the ibidi model for investigating LPA 253
6.6 Conclusion 254
Chapter 7 Discussion and conclusions 256
7.1 The mechanisms of immunothrombosis in extracorporeal circuits remain unclear 256
7.2 Summary of findings 258
7.2.1 ECMO is immunothrombotic and risk of MO thrombosis increases with ECMO duration 258
7.2.2 The need to distinguish between ECMO initiation or ECMO lung rest 259
7.2.3 The optimal anticoagulant for combined leucocyte and platelet work 261
7.2.4 LPA formation in vitro is dependent on platelet activation and can be reduced by GPIIb/IIIa inhibition 262
7.3 Clinical relevance 263
7.4 Limitations 265
7.4.1 Retrospective data analysis 265
7.4.2 Clinical samples and analysis of biomarkers 266
7.4.3 Developing and optimising protocols 267
7.4.4 In vitro work 269
7.5 Future Work 270
7.5.1 Ongoing HITEC study recruitment 270
7.5.2 Comparison of other ECMO pumps and oxygenators 271
7.5.3 Visualising the thrombotic deposits 272
7.5.4 Developing the in vitro model of ECMO circulation 273
7.5.5 Platelet activation and NETosis 274
REFERENCES 276

Dedication

I would like to dedicate this PhD to my mum Christine for raising me to be a relentless workaholic and my brother Steven for his support and competitiveness. Without them, I would not be the persistent, disciplined person I needed to be to get through many rounds of failed experiments. I also need to dedicate this PhD to my friends Seb and Jim, who have been my colleagues, neighbours, friends and now considered family for their emotional support, motivation, food and wine when needed. The PhD journey is a rollercoaster not least whilst starting it in the middle of a pandemic and through many other life events.

This thesis cannot be complete without dedicating the efforts to the patients and families who have suffered from critical illness, in particular COVID-19. Without the patients and families who have agreed to participate in clinical research, much of this work would not have been possible. I hope this research contributes to knowledge and to the benefit of patients who go through the ICU.

Acknowledgements

Firstly, I want to thank my principal supervisor Dr Brij Patel for encouraging me to take on this project and inspire me to pursue a research doctorate. I had never thought about a research career for myself, but through his mentorship and friendship, it is something I very much see in my future career. Brij has consistently been encouraging and has been there to help circumnavigate the worlds of research and clinical practice. He has now become a good friend and source of sound advice professionally and as a confidant in many other aspects of life.

Many thanks to Dr Kieran O'Dea for taking on another clinical PhD student who was very naïve to the laboratory, but who has been supportive and patient in teaching me the basics of the lab to discussing more worldly topics in the lab or in the pub.

I thank Dr Sharon Mumby, and APMIC lab and colleagues: Virginia, Hera, Eirini and Rhianna for their teaching of lab techniques, guidance and friendship since my first day. I also thank Dr TC Aw for the clinical data extraction which was a mammoth task.

I must thank the Royal Brompton Hospital research team (Mahitha, Anelise, Kamal, Binsu and Kier) for setting up and running the DeVENT and HITEC studies, with excellent recruitment rates and sample collection. Special mention to the ECMO nurses and perfusionists for facilitating research and collecting pre-ECMO bloods whilst on ECMO retrievals even in the middle of the night, without which I would not have such novel results.

I am grateful for the financial support from Healthcare Corporation of America for their sponsorship via the Imperial research fellowship; to the European chapter of the Extracorporeal Life Support Organisation for the research grant that contributed to the funding of work in this thesis; and to Royal Brompton and Harefield Hospitals Charity for their generous donation which funded the running of the HITEC study.

Statement of Originality

No part of this thesis has previously been submitted for a degree in any university and to the best of my knowledge contains no material previously published or written by another person except where due acknowledgment is made in the thesis itself.

All work contained within the thesis was performed by myself or in collaboration with members of the laboratory or Imperial College.

Statement of Copyright

The copyright of this thesis rests with the author and is made available under a Creative Commons Attribution Non-Commercial no Derivatives licence.

Researchers are free to copy, distribute or transmit the thesis on the condition that they attribute it, that they do not use it for commercial purposes and that they do not alter, transform or build upon it. For any reuse of redistribution, researchers must make clear to others the licence terms of this work.

Please seek permission from the copyright holder for uses of this work that are not included in this licence or permitted under UK Copyright Law.

Publications during candidature

Publications and conference abstracts related to this thesis.

[1] Sargeant N, **Lee TM**, Cheriyan R, Aw TC, Garfield B, Ledot S, Patel BV. **Membrane Lung Dysfunction in VV-ECMO: COVID-19 vs non-COVID-19, a comparison**. 32nd Annual ELSO 2021 Conference (Virtual), September 2021. ASAIO 2021. Vol. 67:1-57 doi: 10.1097/MAT.0000000000001565

[2] Patel BV, **Lee TML**, O'Dea K. **CLUSTERINg circulating histones in sepsis.** Am J Respir Crit Care Med. 2023 Jul 15;208(2):125-127. Doi:10.1164/rccm.202305-0935ED. PMID: 37311246

[3] **Lee TML**, Retter A, O'Dea KP, Patel BV**. Extracorporeal membrane oxygenation for severe acute respiratory failure increases serum levels of citrullinated histone H3, a specific marker of neutrophil extracellular traps**. American Thoracic Society, San Diego, May 2024. Am J Respir Crit Care Med 2024;209:A2838. Winner of the ATS Abstract Scholarship for the Critical Care Assembly 2024.

[4] Sivasubramaniam G, Mumby S, **Lee TML**, Patel S, Handslip RT, Ridge C, Desai S, Molyneaux PL, Wilson MR, Patel BV. Alveolar Th2 cytokine upregulation in patients with acute respiratory distress syndrome and non-dependent consolidation. American Thoracic Society, San Diego, May 2024. Am J Respir Crit Care Med 2024;209:A2826

Other publications not related to this thesis during candidature.

[1] Patel BV, Haar S, Handslip R, Auepanwiriyakul C, **Lee TM,** Patel S, Harston JA, Hosking-Jervis F, Kelly D, Sanderson B, Bogatta B, Tatham K, Welters I, Camporota L, Gordon AC, Komorowski M, Antcliffe D, and Prowle JR, Puthucheary Z, Faisal AA; on behalf of the United Kingdom COVID-ICU National Service Evaluation. **Natural history, trajectory, and management of mechanically ventilated COVID-19 patients in the United Kingdom**. Intensive Care Medicine. 2021 May; 45(5):549-565. doi: 10.1007/s00134-021-06389-z.PMID: 33974106

[2] **Lee TML,** Bianchi P, Kourliouros A, Price LC, Ledot S. **Percutaneous oxygenated right ventricular assist device for pulmonary embolism: A case series**. Artif Organs. 2023 Mar;47(3):595-603. doi:10.1111/aor.14420. Epub 2022 Oct 20. PMID: 36265137

Index of Figures

Figure 1.1	Pathology of endothelial dysfunction in ARDS
Figure 1.2	Evidence based interventions for the management of ARDS
Figure 1.3	Schematic diagram of an ECMO circuit
Figure 1.4	Schematic diagram of a roller pump and centrifugal pump used in ECMO.
Figure 1.5	Schematic diagram of gas transfer within the membrane oxygenator
Figure 1.6	Classic model of coagulation
Figure 1.7	Cell-based model of coagulation
Figure 1.8	Platelet activation pathways
Figure 1.9	Neutrophil activation leading to NETosis
Figure 1.10	Neutrophil granulopoiesis and surface marker expression
Figure 1.11	Direct and indirect neutrophil-platelet crosstalk
Figure 1.12	ECMO and patient related factors which increase haemostatic complications
Figure 1.13	Schematic diagram of ECMO circuit change
Figure 1.14	ECMO interacts with coagulation to increase bleeding risk
Figure 2.1	Timelines of patients admitted to RBH via the SARF or cardiogenic shock pathway on ECMO or conventional management
Figure 2.2	Peripheral blood mononuclear cells and neutrophil isolation technique using double density gradient separation
Figure 2.3	Schematic diagram showing set up of the microfluidics pump system
Figure 2.4	Figure showing the experiment set up using four parallel fluidics units
Figure 2.5	The basic principle of flow cytometry
Figure 2.6	Similarity and complexity index for a panel using 8 fluorophores
Figure 2.7	ApogeeMix Sizing beads run Cytek Northern Lights spectral flow cytometer
Figure 2.8	Identification of neutrophils and quantifying cell-associated NETs using flow cytometry
Figure 2.9	Identification of neutrophils and quantifying cell-associated NETs in whole blood using flow cytometry
Figure 2.10	Using SpectroFlo to gate for specific cell types and measure the expression of specific markers
Figure 2.11	Whole blood NETs staining protocol was able to differentiate different levels of cell-associated NETs
Figure 2.12	Neutrophil phenotyping and gating from whole blood samples
Figure 2.13	Monocyte subset and monocyte platelet aggregate gating in patient samples
Figure 2.14	The Roche Multiplate analyser tests platelet response to agonists
Figure 2.15	Thromboelastogram measuring the viscoelastic properties of whole blood
Figure 3.1	Consort diagram of patients included in analysis

Figure 3.2	COVID-19 patients have a higher incidence of circuit change than non-COVID-19 patients
Figure 3.3	COVID-19 and circuit change are both associated with increased ECMO duration
Figure 3.4	Trends in laboratory parameters in the first 7 days of ECMO initiation
Figure 3.5	Trends in ECMO parameters and blood gases in the first 7 days of ECMO
Figure 3.6	Trends in blood parameters in the lead up to circuit change
Figure 3.7	Trends in ECMO device parameters and arterial and post-oxygenator blood gases in the lead up to circuit change
Figure 4.1	Consort diagram showing HITEC study recruitment to date
Figure 4.2	Markers of neutrophil activation and NETosis in healthy volunteers, and ECMO patients
Figure 4.3	Inflammatory markers before and after ECMO initiation
Figure 4.4	Trends in neutrophil activation and NETosis markers over the ECMO run
Figure 4.5	Markers of neutrophil activation and NETosis after ECMO decannulation
Figure 4.6	Markers of neutrophil activation on ECMO initiation separated by COVID-19 status
Figure 4.7	Markers of neutrophil activation before and after the membrane oxygenator
Figure 4.8	Neutrophils undergoing NETosis in patient samples.
Figure 4.9	Correlation matrix between cell-associated NETs and soluble NETosis markers
Figure 4.10	Correlation between platelet count and PF4 and CD62P levels whilst on ECMO.
Figure 4.11	Markers of platelet activation in healthy volunteers and ECMO patients.
Figure 4.12	Trends in platelet count and platelet activation markers over the ECMO run
Figure 4.13	Proportion of platelet aggregation results that were within, under or over the normal range in response to three different agonists
Figure 4.14	Proportion of platelet aggregation results that were within, under or over the normal range in response to three different agonists separated by duration on ECMO.
Figure 4.15	Proportion of Thromboelastogram results that were within, under or over the normal range in ECMO patients
Figure 4.16	Correlation matrix of clinically measured coagulation parameters and the corresponding TEG
Figure 5.1	Platelets bind to leucocytes through specific receptor-ligand interactions to form leucocyte-platelet aggregates
Figure 5.2	Neutrophil-platelet aggregate and monocyte-platelet aggregate formation in vitro
Figure 5.3	Neutrophil-platelet aggregate and Monocyte-platelet aggregate measurement in patient samples in EDTA, heparin and heparin+EDTA samples
Figure 5.4	Effect of different calcium chelators on leucocyte-platelet aggregate measurement and leucocyte phenotyping.

Figure 5.5	Effect of direct thrombin inhibitor on leucocyte-platelet aggregate measurement and leucocyte phenotyping
Figure 5.6	Neutrophil-platelet aggregates, and neutrophil phenotypes in ECMO patients
Figure 5.7	NPA proportions over time in different neutrophil sub populations.
Figure 5.8	Comparison of neutrophil cell surface markers between CD41+ and CD41- neutrophils
Figure 5.8	Correlation matrix of neutrophil-platelet aggregates with cell associated NETs and neutrophil activation markers
Figure 5.10	Monocyte-platelet aggregates and monocyte activation markers in ECMO patients
Figure 5.11	Clinical measured parameters over the ECMO run
Figure 6.1	Platelet count and platelet CD62P expression in response to different agonists
Figure 6.2	Neutrophil and monocyte platelet aggregate formation at static, rotator and flow conditions with no stimulation, LPS and TRAP-6
Figure 6.3	Neutrophil and monocyte platelet aggregate formation with no stimulation (UT), LPS and TRAP-6 at different flow rates.
Figure 6.4	Neutrophil platelet aggregates form under flow conditions and increase with leucocyte and platelet stimulation
Figure 6.5	Platelet activation was increased after TRAP-6 stimulation but not LPS stimulation
Figure 6.6	Monocyte platelet aggregates form immediately and do not change under flow conditions with leucocyte and platelet stimulation.
Figure 6.7	No effect of incubation with P-selectin inhibitor (KF38789) or GPIIb/IIIa inhibitor (Eptifibatide) on neutrophil and monocyte activity and leucocyte-platelet aggregates
Figure 6.8	The effect of Eptifibatide, a GPIIb/IIIa pathway inhibitor on neutrophil platelet aggregation in vitro
Figure 6.9	The effect of KF38789, a P-selectin pathway inhibitor on neutrophil platelet aggregation in vitro
Figure 6.10	There was no effect of Eptifibatide, a GPIIb/IIIa inhibitor or KF38789 a P-selectin pathway inhibitor on neutrophil activation with LPS or TRAP-6 stimulation
Figure 6.11	There was no effect of eptifibatide or KF38789 on monocyte platelet aggregation in vitro
Figure 6.12	There was no difference of Eptifibatide, a GPIIb/IIIa inhibitor or KF38789 a P-selectin pathway inhibitor on monocyte activation with LPS or TRAP-6 stimulation
Figure 7.1	Fluorescent microscopy of neutrophils and platelets stimulated with calcium ionophore

Index of Tables

Table 1.1	The 2012 Berlin Definition of ARDS
Table 1.2	The Murray Score for lung injury
Table 1.3	Causes of ARDS
Table 1.4	Comparison between roller and centrifugal pumps
Table 2.1	Blood separation reagents
Table 2.2	Flow cytometry reagents
Table 2.3	Enzyme-linked immunosorbent assay (ELISA) reagents
Table 2.4	Commercial detection assay reagents
Table 2.5	Agonists, antagonists, and inhibiting agents
Table 2.6	Venepuncture and in vitro blood work consumables
Table 2.7	Instruments for ELISA protocols
Table 2.8	Instrument for flow cytometry protocols
Table 2.9	Instruments for ibidi microfluidics protocols
Table 2.10	Miscellaneous equipment
Table 2.11	Software packages
Table 2.12	In vitro isolated neutrophil NETs – flow cytometry antibodies
Table 2.13	Whole blood NETs – flow cytometry antibodies
Table 2.14	Whole blood cell phenotyping – flow cytometry antibodies
Table 2.15	HITEC blood sample collection
Table 2.16	Summary of patient blood processing for storage
Table 2.17	Range of flow rates and shear stress that can be generated using ibidi microfluidics system
Table 2.18	Fluorochrome peak channels for a 3 laser Northern Lights spectral flow cytometer.
Table 2.19	Flow cytometry panel design for neutrophil and monocyte phenotyping in patient samples.
Table 2.20	Fluorophore conjugated antibodies for quantification of leucocyte-platelet aggregates and phenotyping neutrophils and monocytes for in vitro experiments
Table 3.1	Demographics of the VV ECMO patients included in the study
Table 3.2	Baseline laboratory parameters
Table 3.3	Baseline ECMO device parameters and blood gases
Table 3.4	ECMO circuit change comparisons between COVID-19 and non-COVID-19 patients
Table 3.5	Association between baseline characteristics, ARDS pathology and ECMO duration with need for circuit change
Table 3.6	Differences in clinical parameters from 5 days prior and the day of circuit change in COVID-19 and non-COVID-19 patients

Table 3.7	Differences in ECMO parameters and blood gases from 5 days prior and the day of circuit change in COVID-19 and non-COVID-19 patients
Table 4.1	Demographics of patients from the DeVENT and HITEC studies included in this thesis
Table 4.2	Demographics and admission bloods of healthy volunteers, and ECMO patients included for-pre- and post-ECMO comparisons
Table 4.3	Markers of neutrophil activation and NETosis in healthy volunteers, and ECMO patients
Table 4.4	Inflammatory markers before and after ECMO initiation
Table 4.5	Demographic and bloods of ECMO patients with paired pre- and post-decannulation samples
Table 4.6	Proportion of platelet aggregation results that were within, under or over the normal range in response to three different agonists
Table 5.1	Fluorophore conjugated antibody panels for quantification of leucocyte-platelet aggregates and phenotyping neutrophils and monocytes
Table 5.2	Correlation between NPA and MPA proportions and clinical parameters
Table 6.1	Flow rates and estimated shear stress generated within a 0.4mm microchannel slide using whole blood at 37°C
Table 6.2	Fluorophore conjugated antibodies for quantification of leucocyte-platelet aggregates and phenotyping neutrophils and monocytes for in vitro experiments

Abbreviations

AA	Arachidonic acid
ABG	Arterial blood gas
ACD	Acid citrate dextrose
ADP	Adenosine diphosphate
ALI	Acute lung injury
Ang-2	Angiopoietin-2
APTT	Activated partial thromboplastin time
ARDS	Acute respiratory distress syndrome
ATP	Adenosine triphosphate
AUC	Area under curve
BALF	Bronchoalveolar lavage fluid
BMI	Body mass index
CC	Circuit change
CD11b	Mac-1 / integrin αM
CD62L	L-Selectin
CD62P	P-Selectin
cfDNA	Cell-free DNA
CitH3	Citrullinated Histone H3
CO_2	Carbon dioxide
CPAP	Continuous positive airway pressure
CT	Computerised tomography
COVID-19	Novel Coronavirus Disease 2019
CPB	Cardiopulmonary bypass
DeVENT	Decision support system to evaluate ventilation in the acute respiratory distress syndrome (study)
DVT	Deep vein thrombosis
ECMO	Extracorporeal membrane oxygenation
$ECCO_2R$	Extracorporeal carbon dioxide removal
EDTA	Ethylenediaminetetraacetic acid
ELCS	Extracorporeal life support
ELISA	Enzyme-linked immunosorbent assay
ELSO	Extracorporeal Life Support Organisation
EPR	Electronic Patient Record
EV	Extracellular Vesicles
FBC	Full blood count

FF	Functional fibrinogen
FWB	FACS wash buffer
GPIIb/IIIa	Glycoprotein IIb/IIIa / αIIbβ3 integrin
GPVI	Glycoprotein VI
GSTT	Guy's and St Thomas' Trust
HD	Haemodialysis
HIT	Heparin induced thrombocytopenia
HITEC	Haemostasis and immunothrombosis in extracorporeal circuits (study)
HMGB1	High-mobility group protein B1
HRA	Health Research Authority
HV	Healthy volunteer
ICAM	Intercellular adhesion molecule
ICU	Intensive care unit
IG	Immature granulocytes
IL	Interleukin
INR	International normalised ratio
LOS	Length of stay
LPA	Leucocyte-platelet aggregate
LPS	Lipopolysaccharide
MA	Maximum amplitude
MCP-1	Monocyte chemoattractant protein 1
MFI	Mean fluorescent intensity
MMP-8	Metalloproteinase 8 / Neutrophil collagenase
MMP-9	Metalloproteinase 9 / Gelatinase
MO	Membrane oxygenator
MPA	Monocyte-platelet aggregate
MPO	Myeloperoxidase
NADPH	Nicotinamide adenine dinucleotide phosphate
NE	Neutrophil elastase
NET	Neutrophil extracellular trap
NPA	Neutrophil-platelet aggregate
NuQH3.1	Nucleosome H3.1
PaCO2	Partial pressure carbon dioxide
PaO2	Partial pressure oxygen
PAD4	Peptidylarginine deiminase 4
PAR	Protease activated receptor

PBS	Phosphate buffered saline
PE	Pulmonary embolism
PECAM-1	Platelet-endothelial cell adhesion molecule-1
PEEP	Positive end expiratory pressure
PF	PaO_2/FiO_2
PF4	Platelet factor 4
PMA	Phorbol 12-myristate 13-acetate
PMN	Polymorphonuclear neutrophils
PpostCO2	Post-oxygenator partial pressure carbon dioxide
PpostO2	Post-oxygenator partial pressure oxygen
PSGL1	P-Selectin glycoprotein ligand-1
PT	Prothrombin time
RAGE	Receptor for advanced glycation end products
RBHH	Royal Brompton and Harefield Hospitals
REC	Research ethics committee
ROS	Reactive oxygen species
RPM	Revolutions per minute
SARF	Severe Acute Respiratory Failure
SFC	Spectral flow cytometer
SIRS	Systemic inflammatory response syndrome
SSc	Side scatter
SST	Serum separator tube
TEG	Thromboelastogram
TF	Tissue factor
TLR	Toll-like receptor
TMP	Transmembrane pressure
TNF	Tumour necrosis factor
TRALI	Transfusion related acute lung injury
TRAP-6	Thrombin receptor activating peptide-6
TXA2	Thromboxane A2
UPV	Ultra-lung protective ventilation
UT	Untreated
VA ECMO	Venous-arterial ECMO
VAD	Ventricular assist device
VEGF	Vascular endothelial growth factor
VILI	Ventilator induced lung injury

VV ECMO	Venous-venous ECMO
vWF	Von Willebrand Factor
WCC	White cell count

Chapter 1: Introduction

1.1 Acute Respiratory Distress Syndrome

1.1.1 Definition

Acute respiratory distress syndrome (ARDS) is an acute inflammatory lung injury and was first described in 1967 by Ashbaugh et al who described 12 adult patients with "acute onset tachypnoea, hypoxaemia and loss of compliance after a variety of stimuli" who did not respond to usual methods of respiratory therapy and positive end expiratory pressure (PEEP) and perhaps steroids was the most helpful [1]. In 1994, the American-European Consensus Conference defined acute lung injury (ALI) as a syndrome of inflammation and increased permeability that is associated with clinical, radiological and physiological abnormalities that cannot be explained by, but may co-exist with left atrial or pulmonary hypertension. The separation of ALI and ARDS was dependent on the degree of hypoxia with ALI defined as PaO2/FiO2 (PF) ratio $\leq$ 300 mmHg, and ARDS PF ratio $\leq$ 200 mmHg [2]. In 2012, the definition was revised to include definition of timing, separation of severity using PF ratio, inclusion of PEEP, and clarification of radiological and physiological parameters. This was described as the Berlin Definition of ARDS which recognised 3 grades of severity (Table 1.1).

	Mild	**Moderate**	**Severe**
Timing	Acute onset within 1 week of a known clinical insult or new/worsening respiratory symptoms		
Radiological abnormalities	Bilateral opacities – not fully explained by effusions, lobar/lung collapse, or nodules		
Origin of oedema	Respiratory failure not fully explained by cardiac failure or fluid overload.		
Hypoxaemia PaO2/FiO2	201-300 mmHg with PEEP $\geq$ 5cm H_2O	101-200 mmHg with PEEP $\geq$ 5cm H_2O	<100 mmHg with PEEP $\geq$ 5cm H_2O

Table 1.1 The 2012 Berlin definition of ARDS

Definitions of ALI and ARDS are often supplemented by lung injury scores such as the Murray score, a four-point scoring system which takes into account dynamic lung compliance, degree of radiographic infiltration, PF ratio and level of PEEP (Table 1.2) [3]. It is a more widely used method of quantifying ARDS severity and is often used in clinical studies where a score of >2.5 signifies severe ARDS, and a score $\geq$ 3 is commonly used as a qualifying threshold for support with extracorporeal membrane oxygenation (ECMO) [4, 5].

	0	1	2	3	4
PaO2/FiO2 (mmHg)	≥ 300	225 - 299	175 - 224	100 - 174	< 100
CXR Quadrants	None	1	2	3	4
PEEP (cmH_2O)	≤ 5	6 - 8	9 - 11	12 – 14	≥ 15
Compliance (ml/cmH_2O)	≥ 80	60 - 79	40 - 59	20 - 39	≤ 19
Final Murray score = Average score of all four parameters.					

Table 1.2 The Murray Score for lung injury

1.1.2 Epidemiology

ARDS is a significant cause of morbidity and mortality in the intensive care population. The LUNGSAFE study found that ARDS represented around 10% of total intensive care unit (ICU) admissions and 23% of all mechanically ventilated patients, which when applied to the UK ICU population is 22,000 patients/year [6]. The true incidence of ARDS worldwide may be higher, as recognition and formal diagnosis of ARDS may be lower in some regions. Hospital mortality increases with severity: 34.9% for mild, 40.3% for moderate and 46.1% for severe ARDS [6]. Mortality is one measure of the impact of ARDS, and many survivors have prolonged physical dysfunction with ongoing breathlessness, and poor mobility after recovery from ARDS. There is also the psychological impact of long ICU and hospital admissions on the patient and their families.

1.1.3 Aetiology of ARDS

ARDS can be caused by a number of insults, which result in a syndrome of non-cardiogenic pulmonary oedema, hypoxaemia, and inflammation often requiring mechanical ventilation. Aetiologies can be separated into pulmonary (direct) or extra-pulmonary (indirect) insults. Direct insults usually involve the alveolar space, and common causes include infection (bacterial pneumonia, viral pneumonitis), aspiration pneumonitis, lung trauma (including drowning, smoke inhalation), or pulmonary embolism (PE). Extra-pulmonary insults usually arise from systemic injury e.g. extra-pulmonary sepsis, polytrauma, pancreatitis, cardiopulmonary bypass (CPB) and transfusion related acute lung injury (TRALI) (Table 1.3). The heterogeneity of ARDS aetiology contributes to difficulties in diagnostics and the development of therapies.

	Pulmonary (direct)	Extra-pulmonary (indirect)
Common	Pneumonia (bacterial, fungal, parasitic) Viral pneumonitis (Influenza, COVID-19) Aspiration pneumonitis	Systemic non-pulmonary sepsis Polytrauma (with shock and transfusion) Acute pancreatitis
Less common	Pulmonary embolism Pulmonary contusion/thoracic trauma Drowning Inhalation injury Reperfusion lung injury (after transplantation) Fat embolism	Cardiopulmonary bypass Transfusion related acute lung injury Drug overdose

Table 1.3 Causes of ARDS

1.1.4 Pathophysiology of ARDS

In ARDS, the lung injury is due to a combination of alveolar epithelial and capillary endothelial damage which leads to release of cytokines and chemokines including but not limited to angiopoietin-2 (Ang-2), Interleukin-6 (IL-6), Interleukin-8 (IL8), tumour necrosis factor alpha (TNFα), vascular endothelial growth factor (VEGF). These pro-inflammatory mediators disrupt the endothelial barrier, and allows movement of fluid, proteins and cells into the interstitial and alveolar space. In addition, the released cytokines and chemokines attract and recruit more neutrophils and macrophages into the alveolar space (Figure 1.1) [7].

TNFα is one of the most widely studied proinflammatory cytokines and is produced by many cells types (endothelial, immune cells, smooth muscle cells etc) after stimulation and has been implicated ARDS pathophysiology by increasing ROS production, and activation of proinflammatory receptors such as receptor for advanced glycation end products (RAGE) and intercellular adhesion molecule 1 (ICAM-1) [8], leading to increased vascular permeability, increasing inflammation and cell death [9]. Increased levels of sRAGE is associated with increased risk and severity of ARDS [10] and its inhibition could reduce the degree of ALI [11, 12]. Ang-2 and VEGF have key roles in angiogenesis and are both involved in many physiological processes. In ARDS, they both increase vascular permeability and assist in the recruitment of monocytes and neutrophils to the alveolar space [13, 14]. Circulating monocytes and macrophages migrate into the alveolar space in response to monocyte chemoattractant protein-1 (MCP-1). Resident alveolar macrophages release cytokines to recruit neutrophils or monocytes which promote inflammation and the later recruited macrophages mainly function to phagocytose neutrophils and other apoptotic cells and play an important role in

regulation of the inflammatory process [15]. IL-6 is also a major pro-inflammatory mediator implicated in sepsis and ARDS and more recently in COVID-19, contributing to the vascular leak, lung injury and organ dysfunction [16, 17].

Endothelial damage and activation of neutrophils is associated with expression of neutrophil and endothelial adhesion molecules such as E-selectin, P-selectin and ICAM-1. These bind neutrophils to the endothelium and facilitate their movement via the platelet-endothelial cell adhesion molecule-1 (PECAM-1) to infection/inflamed sites along a chemokine gradient [18]. Once in the alveolar space, the activated neutrophils release their own cytotoxic products including reactive oxygen species (ROS), granular enzymes, and neutrophil extracellular traps (NETs) to defend against the invading pathogens and also interact with the epithelium increasing cytokine release [19].

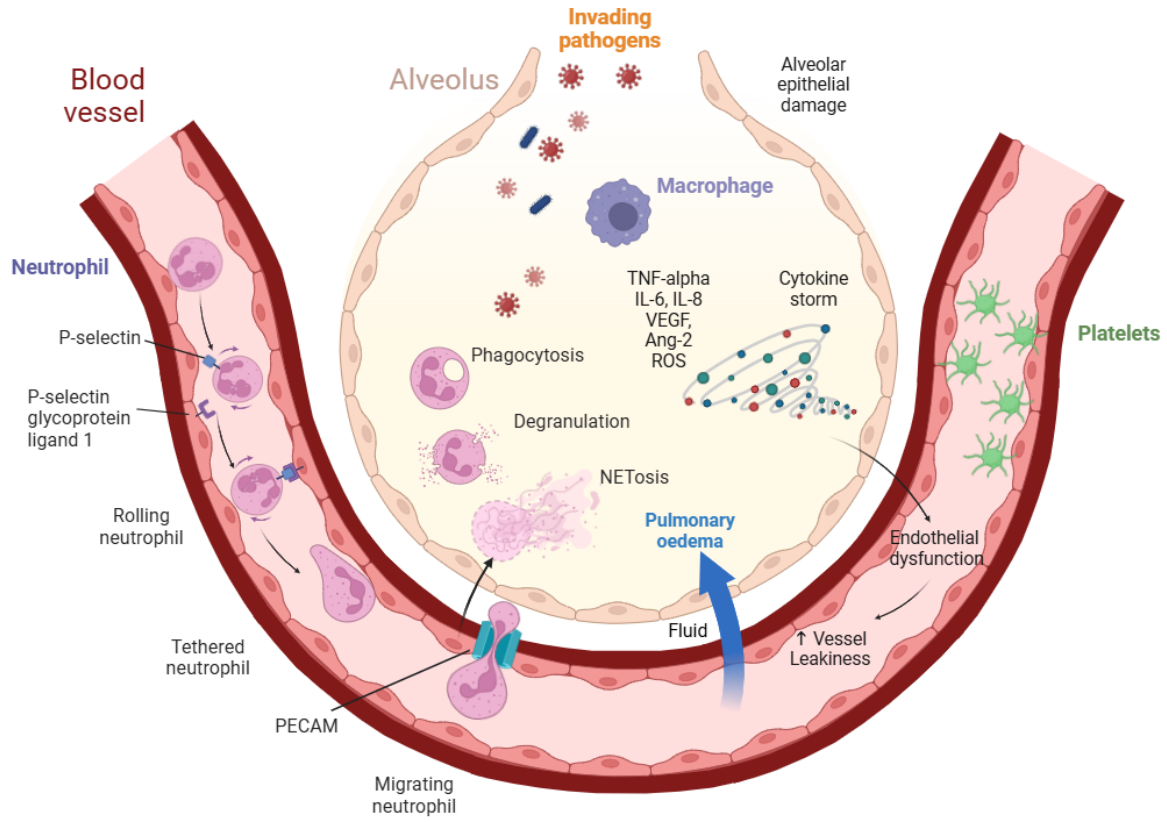


Figure 1.1 Pathology of endothelial dysfunction in ARDS.

Damage to the alveolar capillary endothelium and epithelium from invading pathogens leads to release of inflammatory cytokines (TNFα, IL-6, IL-8, VEGF, Ang-2) and reactive oxygen species. This cytokine storm leads to disruption of the endothelial barrier allowing movement of fluid, macromolecules and cells into the interstitial and alveolar spaces. Neutrophils and macrophages are recruited into the alveolar space and are activated to eliminated invading pathogens. Upon activation, neutrophils may undergo NETosis, degranulation releasing enzymes such as neutrophil elastase and myeloperoxidase, and also phagocytosis.

Angiotensin-2, Ang-2; interleukin, IL; neutrophil extracellular trap, NET; platelet-endothelial cell adhesion molecule, PECAM; tumour necrosis factor alpha, TNFα; reactive oxygen species, ROS; vascular endothelial growth factor, VEGF. Image created on Biorender.

In overwhelming pathological conditions such as in ARDS, this defence mechanism can become deleterious. The excess endothelial activation and cytokine release can result in a “cytokine storm” leading to increased leakiness of the pulmonary vasculature, resulting in pulmonary oedema. There is excess recruitment and activation of neutrophils and macrophages which themselves may become harmful to the alveolar environment as they release their own proteins and enzymes through degranulation and NETosis, which can further activate and induce further alveolar damage. The cytokine storm was particularly evident in Novel Coronavirus Disease-2019 (COVID-19) ARDS patients [20].

1.1.5 Management of ARDS

Early recognition of ARDS is key to identifying patients who are at risk of deterioration or who may benefit from specific therapies/interventions. The mainstay of ARDS ventilation management remains conservative fluid management and lung protective ventilation as per the ARDSnet ventilatory protocol. This includes low tidal volume (6ml/kg) ventilation, PEEP titration to PF ratio where the level of PEEP is often increased proportional to the level of hypoxaemia, whilst aiming for a plateau pressure < 30cmH_2O. Patients with severe ARDS (PF ratio < 100mmHg) and refractory hypoxaemia will be considered for trial of prone positioning or neuromuscular blockade. In some cases, inhaled pulmonary vasodilators such as nitrous oxide may be considered. If refractory to conventional therapies, patients may be considered for extracorporeal membrane oxygenation (ECMO) (Figure 1.2).

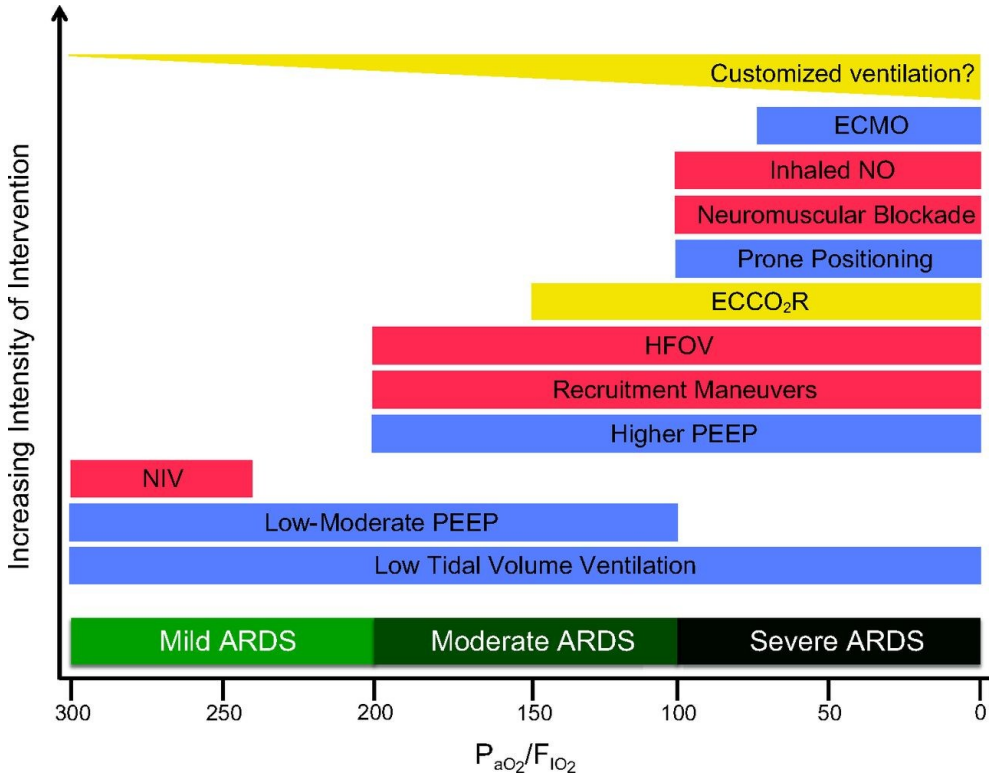


Figure 1.2 Evidence based interventions for the management of ARDS

This figure represents the potential interventions that could be used in the management of patients with ARDS. The blue boxes are interventions that are supported by current evidence including ECMO for severe ARDS. Boxes in red are interventions that are not recommended according to current evidence. Boxes in yellow are interventions that still require confirmation though clinical trials including $ECCO_2R$. Taken from Ratano and Fan (2020) [21]

Acute respiratory distress syndrome, ARDS; extracorporeal carbon dioxide removal, $ECCO_2R$ Extracorporeal membrane oxygenation, ECMO; high-frequency oscillatory ventilation, HFOV; non-invasive ventilation, NIV; nitric oxide, NO; positive end expiratory pressure, PEEP.

The use of ECMO is to prevent further ventilator induced lung injury (VILI) caused by excess pressures (barotrauma), high tidal volumes (volutrauma), and increased respiratory rates (atelectotrauma) from aggressive mechanical ventilation. ECMO therefore, should not be used routinely in patients with ARDS as long as adequate gas exchange with lung protective ventilation is maintained [4, 22]. The evidence for use is in selected patients with severe ARDS (Murray score > 3, or pH < 7.2 due to uncompensated hypercapnia), alongside conventional therapies, to allow for lung rest or lung protective ventilation. Regarding extracorporeal CO2 removal ($ECCO_2R$), there is currently not enough evidence for its use in ARDS, but it could allow for low tidal volume ventilation in select groups of patients e.g. those with a predominantly hypercapnic respiratory failure [4]. ECMO may also be used as a bridge to transplant in some patients who are on the lung transplant list in selected circumstances, or as a bridge to recovery following lung transplant.

1.2 Extracorporeal Membrane Oxygenation and its uses

1.2.1 The history of extracorporeal life support

ECMO is a form of extracorporeal life support (ECLS) that has been developed from CPB and is widely used for cardiac and respiratory support with increasing numbers year on year [23]. ECMO is used to support patients severe cardiac or respiratory failure who are refractory to conventional management strategies and the underlying disease is considered to be reversible. ECMO allows more time for the underlying condition to be treated or may be a bridge to other therapies such as transplant. ECLS includes venous-venous (VV) and venous-arterial (VA) ECMO, ventricular assist devices (VAD) and CPB.

The first bubble and later membrane oxygenator (MO) was developed in the 1980s but it was not until the 1930-1950s where further advancements of the MO were made. In 1953 the first successful intra-cardiac operation was carried out with the patient on CPB. The first ECMO survivor for ARDS was in 1972 [24], with several more cases following, and it looked like ECMO may be the answer to support patients with ARDS, however at the time the pumps were large and required a large volume of blood products. In the 1880s ECMO was largely used for neonatal respiratory failure with survival rates improving to 70-90% with experience [25]. The Extracorporeal Life Support Organisation (ELSO) was founded in 1989 and through the 1990s to 2000s there were rapid advances in the development of centrifugal pumps, and MOs, leading to the modern ECMO circuits in use today.

ECMO use increased worldwide in the adult population following the 2009 H1N1 influenza epidemic and COVID-19 pandemic [23]. In the 2000s adult ECMO studies such as the CESAR [5] and EOLIA trials [26] showed better efficacy and safety with ECMO use. Following the COVID-19 pandemic, there is now increased interest in optimising the management of patients on ECMO and to minimise complications the most common of which are haemostatic.

1.2.2 Indications for ECMO

The indications for respiratory ECMO are potentially reversible severe acute respiratory failure (SARF) of known aetiology (as described in 1.1.3) for which there is no improvement despite maximising conventional therapies such as mechanical ventilation, sedation, paralysis and fluid management, and where risk of mortality remains high or, the patient is at risk of harm such as increased risk of barotrauma, volutrauma and oxygen toxicity which can prevent lung recovery [4, 22]. Patients may have hypoxaemic or hypercapnic respiratory failure as described in Section 1.1.3.

Indications for cardiac ECMO include refractory cardiogenic shock, post-cardiac arrest, and post-cardiotomy shock where recovery is expected, and also as a bridge to other long-term therapies such as VAD, or organ transplant [27].

In the UK, the referral criteria for VV ECMO include severe hypoxic respiratory failure with PF ratio <50mmHg, lung injury score of 3 or higher, and uncompensated hypercapnia with a pH 7.2 or lower despite respiratory rate > 35 breaths per minute, or due to life threatening airway disease (e.g asthma, airway trauma). Other criteria for considering ECMO include patients who have not responded to prone positioning for at least 6 hours or where prone positioning is contraindicated, and unsuccessful optimal respiratory management with lung protective ventilation after discussion with a tertiary ECMO centre. ECMO centres may also consider the patients potential to recover (e.g. a Respiratory ECMO Survival Prediction score [RESP] ≤ 3) and how long the patients have been ventilated before agreeing to ECMO. Exclusion criteria include refractory or established multi-organ failure, evidence of severe neurological injury and cardiac arrest for > 15minutes [28].

1.2.3 ECMO circuit

This thesis will mainly discuss principles in relation to ECMO, but these can be applied to other forms of ECLS. The two main forms of ECMO are VA, to support cardiac failure or VV,

to support respiratory failure. The basic ECMO circuit consists of a large bore central vascular access cannula usually in the inferior or superior vena cava that drains venous blood from the body, a centrifugal pump which pumps the blood through a MO to oxygenate the blood and remove carbon dioxide, and another large central access cannula through which the blood is returned to the venous system in VV ECMO or the arterial system in VA ECMO (see Figure 1.3).

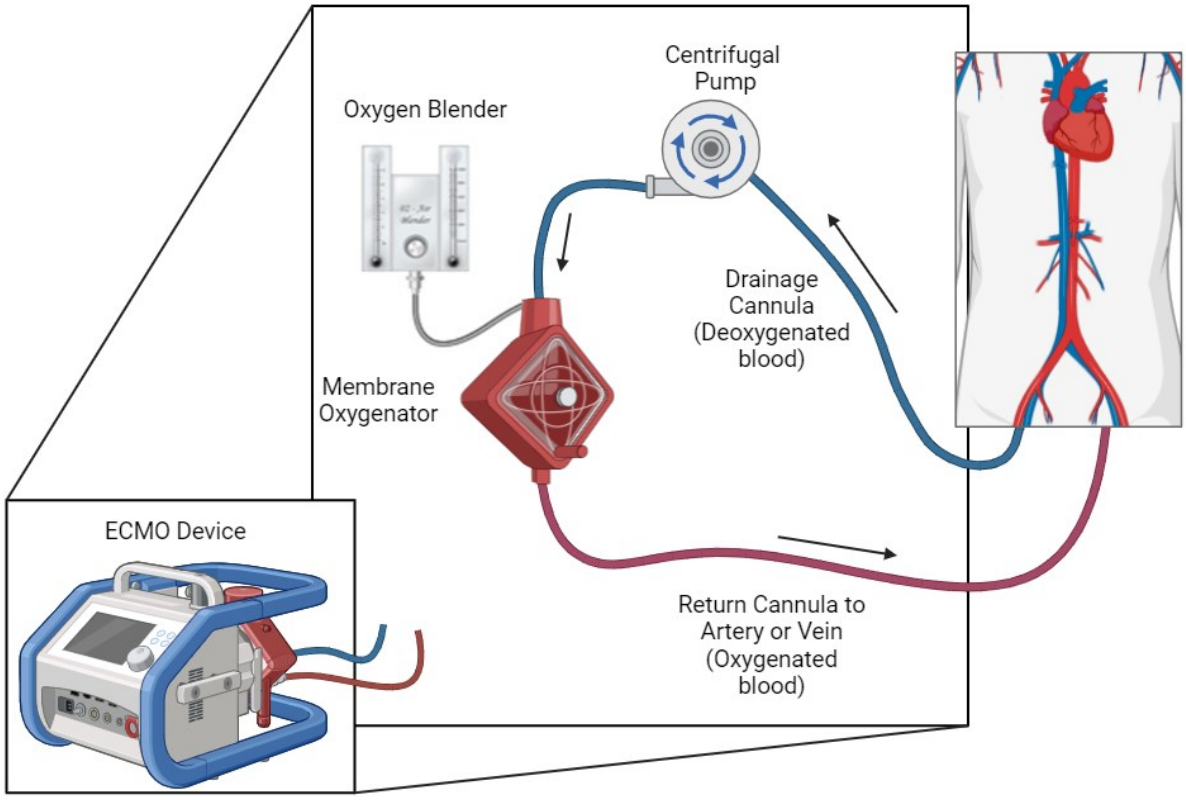


Figure 1.3 Schematic diagram of an ECMO circuit.

Many ECMO devices come as a complete unit for portability e.g. Cardiohelp device with integrated oxygenator. It can be broken down into the console, ECMO pump, membrane oxygenator attached to oxygen blender. Blood is drained from a drainage cannula usually in the femoral vein, pumped via a centrifugal pump through a membrane oxygenator with oxygen blender attached, and returned to the patient via a return cannula. This can be in the other femoral vein or internal jugular vein for VV ECMO or into the femoral artery for VA ECMO. Direction of blood flow indicated by arrows. Image created on Biorender.

More complex configurations of the ECMO circuit can be achieved by adding extra drainage and/or return cannulas and connectors in special circumstances. ELSO have recommended standardised nomenclature for these complex configurations [29].

The key components of the ECMO circuit are the pump and the MO. There have been many developments over the years in optimising the ECMO circuit, such as using centrifugal

pumps as opposed to roller pumps, and developing new materials for the ECMO cannulae, tubing and MO.

1.2.4 The ECMO blood pump

The function of the pump is to help drain blood from the body and propel it through the MO and back to the body. The ideal ECMO blood pump should be able to provide a wide range of flows without exerting excessive shear stress on the blood causing haemolysis, platelet and leucocyte activation. The two main types of ECMO pumps are roller and centrifugal pumps (Figure 1.4).

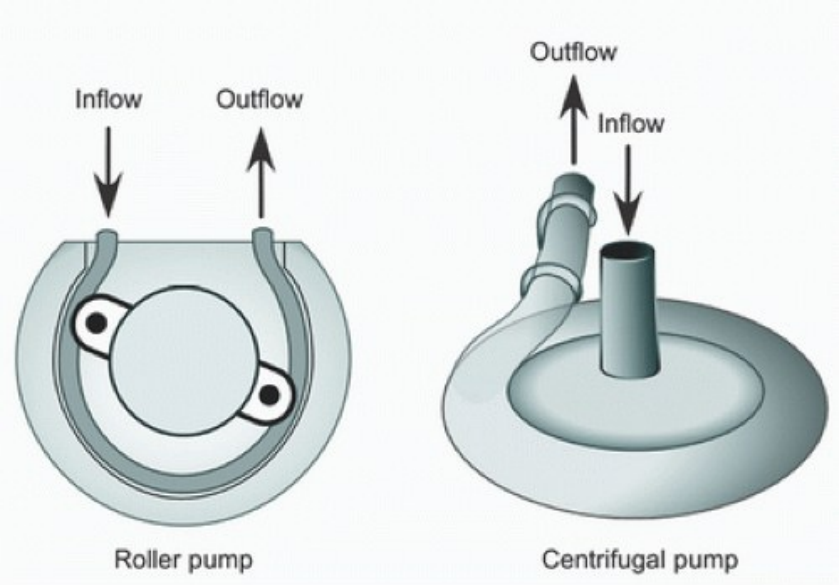


Figure 1.4 Schematic diagram of a roller pump and centrifugal pump used in ECMO.

The arrows show the flow of blood. Image taken from https://thoracickey.com/extracorporeal-membrane-oxygenation-in-infants-and-children/ [30]

Roller pumps use two rollers to sequentially compress a segment of tubing generating forward flow of blood in a peristaltic motion. They require a bladder or reservoir between the cannula and the pump and utilises gravity for drainage into the reservoir. Roller pumps are still used for most CPB machines and were used in older ECMO pumps. Centrifugal pumps are non-occlusive pumps that contain a spinning rotor (pump head) contained within a cone shaped polycarbonate structure. The pump head, driven by a magnetic field to levitate it rotates at high speed (revolutions per minute; RPM) creating a vortex which draws blood in and uses the centrifugal force to eject the blood passively. Blood pump rate is increased by increasing the RPM and therefore the centrifugal force exerted [31].

Each pump has different advantages and disadvantages:

	Roller Pump	Centrifugal Pump
Advantages	No backflow due to gravity Smaller priming volume (good for paediatrics) Good for short term use Reliable constant flow rate	Less blood trauma and haemolysis Don't require gravity – can be placed at any height Can generate higher blood flows Longer term use Portable Less risk of air embolism No damage to tubing
Disadvantages	Blood trauma and haemolysis Tubing and blood trauma limits long term use. High risk of air embolism	Can generate high negative pressures (haemolysis) Retrograde flow possible if pump speed too slow or pump stops Heat generation in pump head (haemolysis, clotting) Larger priming volume More difficult to prime Magnetic decoupling

Table 1.4 Comparison between roller and centrifugal pumps

Roller pumps were used in the majority of all ECMO cases until the 2010s. Since the mid-2000s centrifugal pumps became the predominant pump used, which coincided with the increase in adult cases [32]. Roller pumps are not used in adults in modern ECMO but do remain in use mostly in neonatal and paediatric populations largely due to the smaller priming volume and shorter ECMO runs. Many comparative studies have found fewer complications with the use of roller pumps in the paediatric population including less haemolysis, fewer mechanical complications, renal and cardiac complications and less inotrope use [33, 34]. However, this is not true for the adult population. As the centrifugal pump does not require a reservoir, nor gravity, it is better suited to portable ECMO. There is less trauma and haemolysis and can generate higher blood flows with much lower risk of air embolism. However one study found the shear forces generated by the continuous flow in a centrifugal pump associated with von Willebrand factor (vWF) deficiency and increased bleeding complications [35].

1.2.5 The membrane oxygenator

The MO in ECMO mimics the human lung. It is made up of hollow microfibres (0.3 to 0.8μm pores) that are permeable to gas but not liquid. The blood passes in counter current around the outside of the fibres with gas flowing within the fibres. This facilitates the transfer of

oxygen into the blood and carbon dioxide out (Figure 1.5). Oxygen is poorly diffusible in plasma and the transfer of oxygen is dependent on the differential gas pressures across the membranes therefore, whereas carbon dioxide is highly diffusible in plasma, so it is easily removed from the blood due to the concentration gradient.

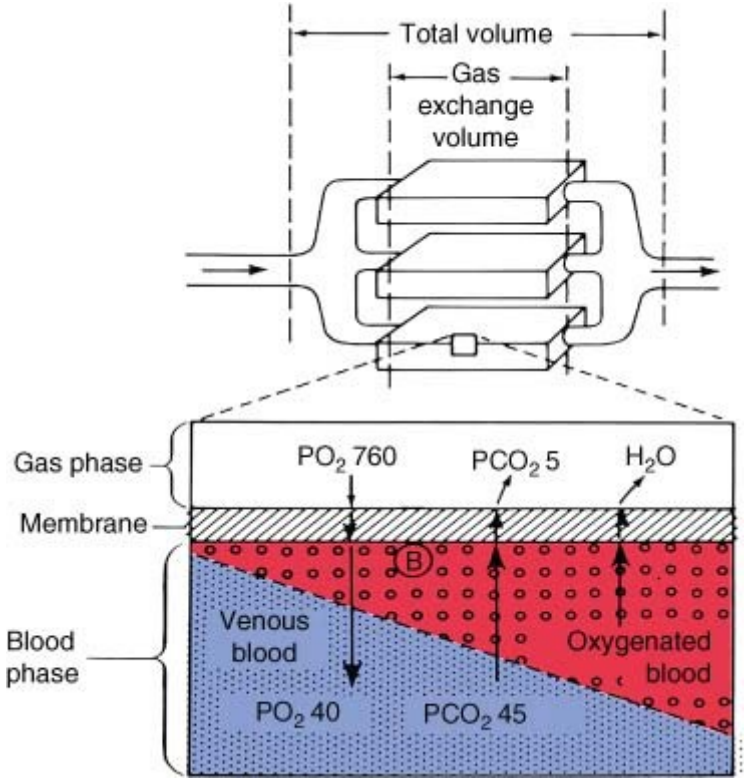


Figure 1.5 Schematic diagram of gas transfer within the membrane oxygenator

Venous blood flows in a laminar fashion past the gas exchange membrane. Oxygen passes through the membrane in response to the partial pressure gradient. Desaturated red cells at the membrane surface become oxygenated quickly but the adjacent red cells are exposed to a lower gradient. The amount of oxygen transferred per membrane surface area is controlled by this "boundary layer" of oxygenated red cells. CO_2 is cleared in response to the partial pressure gradient but is not limited by a boundary layer. Taken from Bartlett et al. (2000) [36].

Early oxygenators were made from silicone rubber until the 2000s when polypropylene (PP) and polymethylpentene (PMP) were introduced. In CPB, the standard oxygenators are made of PP because they have small priming volumes, high gas transfer rates and low resistance. However, over time the micropores can become permeable to fluid leading to plasma leak into the gas phase and adhering to the membrane surface. This reduces gas exchange and leads to development of coagulopathy limiting their long-term use [31]. Since 2009, almost all modern ECMO uses PMP oxygenators [32]. PMP oxygenators, like PP, have low resistance, low priming volume but are also associated with reduced haemolysis, reduced red cell and

platelet transfusion and improved gas exchange. [37]. Plasma leak occurs very rarely with PMP and therefore can be used for longer ECMO runs compared to the shorter duration of CPB.

The MO represents the largest source of non endothelialised surface area in an ECMO circuit ranging between 1.5 - 2.5m^2 in adult circuits with a volume of 100-250mls depending on manufacturer and size. The large surface area is required to optimise gas exchange, but it is also the part of the circuit most likely to interact with coagulation and form thrombi.

1.2.6 The aim of ECMO

ECMO is used in patients who are not able to deliver oxygen to tissues to maintain normal metabolic activities. This can be due to respiratory failure where there is failure to oxygenate the blood, or cardiac failure where there is failure of blood flow to the tissues.

Oxygen delivery (DO_2) is dependent on the cardiac output (CO), which is around 5L/minute in an adult, and the arterial oxygen content (CaO_2).

$$DO_2 = CO \times CaO_2$$

The CaO_2 of arterial blood includes the haemoglobin bound oxygen and dissolved oxygen. Hb-bound O_2 is determined by the oxygen carrying capacity of blood (haemoglobin x Hufner's constant [1.34]) and the oxygen saturation (SaO_2). Dissolved oxygen is proportional to the partial pressure of oxygen (PaO_2) and its solubility coefficient (0.003).

$$CaO_2 = \text{Hb-bound } O_2 + \text{dissolved } O_2$$

$$CaO_2 = ([Hb \times 1.34] \times SaO_2) + 0.003 \times PaO2$$

Oxygen delivery in a critically unwell intensive care patient can be affected by several factors including cardiac output, haemoglobin levels, and blood oxygenation. The tissue oxygen consumption (VO_2) is affected by fever, paralysis, drugs, and cooling in critical care. The aim of ECMO is to provide at least 2/3 of the patient's own cardiac output in order to provide adequate tissue oxygen delivery. This can be difficult to achieve in VV ECMO where the respiratory failure is often due to infection (viral or bacterial), or systemic inflammatory states where patients have high native cardiac output (up to 10-12 L/min) and high VO_2. Most ECMO circuits can supply up to 7L/min of blood flow, however increasing blood flow through the ECMO increases risks of complications such as haemolysis and coagulopathy due to shear and blood exposure to the MO leading to increased risk of thrombosis.

1.3 Haemostasis

Haemostasis is the normal physiological process by which the clotting cascade is activated to seal vascular damage to reduce blood loss after injury. Disruptions to haemostasis lead to uncontrolled bleeding or thrombosis which are pathological and common complications in patients receiving ECMO.

1.3.1 The classic model of coagulation

The classic coagulation cascade describes a process of sequential activation of plasma coagulation proteins, through two distinct paths, the intrinsic and extrinsic pathways, that converge in the final common pathway and ultimately result in a fibrin clot (Figure 1.6).

The extrinsic pathway, also known as the tissue factor pathway, is triggered when a protein which is usually extrinsic to blood e.g. tissue factor (TF) or Factor III (FIII), is exposed to blood from vascular endothelial injury. Tissue factor is normally embedded within the vascular endothelium, and when exposed or activated, binds to coagulation factor VII (FVII), forming a complex with activated FVII (FVIIa). The TF:FVIIa complex is a potent activator of FX in the common pathway. The intrinsic pathway, also known as the contact pathway, begins when blood comes into contact with anionic surfaces within the vessel, such as collagen, kallikrein and high molecular weight kininogen that are exposed after vascular endothelial damage. Other anion foreign surfaces such as an ECMO circuit, and cell-free DNA (cfDNA) from neutrophils also initiate the contact pathway. This leads to activation of FXII, and subsequent activation of FXI, and FIX, and finally FX. In addition, Factor VIII is found in the blood and is activated by thrombin (FIIa).

The common pathway may result from the activation of either the intrinsic or extrinsic pathway and begins when FXa, FVa and calcium bind together to form the prothrombinase complex. This activates prothrombin (FII) into thrombin (FIIa) which cleaves fibrinogen (FI) into fibrin (FIa). Fibrin then polymerises to form a fibrin clot where platelets can bind.

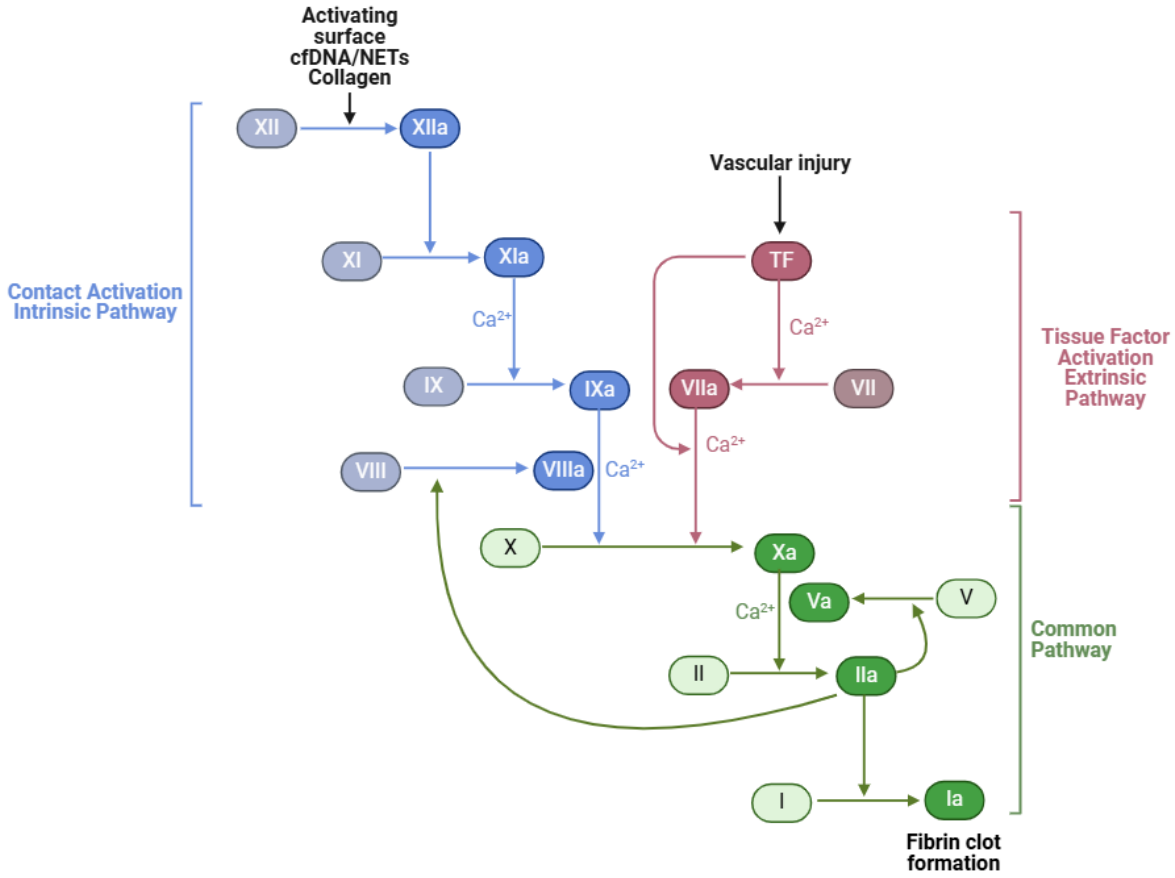


Figure 1.6 Classic model of coagulation

The activation of the intrinsic pathway via factor XII, and extrinsic pathway via tissue factor, leads to sequential activation of plasma coagulation proteins, that converge in the final common pathway and ultimately result in a fibrin clot. Image created on Biorender.

Calcium, Ca; Cell-free DNA, cfDNA; Neutrophil extracellular traps, NETs; Tissue factor, TF.

The coagulation protein cascade model correlates well with the clinically used laboratory assays. The activated partial thromboplastin test (APTT) measures the activity of the intrinsic (Factors XII, IX, IX and VIII) and common (Factors X, V, II, and I) pathways. The prothrombin time (PT) or INR measures the activity of extrinsic (Factor VII) and common pathways [38]. Heparin and many anticoagulants work by inhibiting the common pathway and many tests of anticoagulant function, measure anti-Xa levels.

1.3.2 The cell-based coagulation model

The classic coagulation model suggests that the extrinsic and intrinsic pathways are independent of each other with little interaction and does not consider the interactions with cells. Understanding of the coagulation system has improved significantly in recent years and the traditional coagulation cascade model has been superseded by the cell-based

coagulation model, proposed about 20 years ago [39]. In this model, TF-bearing cells (endothelial cells, and leucocytes) and platelets are the two key cellular components with thrombin and fibrinogen the main coagulation proteins involved in haemostasis [38]. The cell-based model of coagulation has three phases (Figure 1.7).

The first stage is initiation; this is where TF-bearing cells such as vascular endothelial cells and fibroblasts are activated by inflammation or injury. The damaged cells have increased expression of TF on their cell surface and interact with FVII in blood to form the TF:FVIIa complex which activates FX and initiates coagulation. The thrombin generated in the initiation phase is essential for progression to amplification phase where platelets and cofactors FV, FVIII and FXI, vWF become activated to prepare for more significant thrombin generation in the propagation phase. In the propagation phase FIXa accelerated by FVIIIa binds to activated platelets causing further FX activation. The forming of the prothrombinase complex (FXa, FVa and calcium) on membrane surfaces (as seen in common pathway) leads to a burst of thrombin generation and the cleavage of fibrinogen to form fibrin monomers which polymerise to consolidate the initial platelet plug into a stable fibrin clot (Figure 1.7) [38].

This model has a strong emphasis on TF-bearing cells and platelets and how they interact with different coagulation factors. There are many cells that express TF including endothelial cells, fibroblasts, platelets, epithelial cells, monocytes and macrophages. These cells are activated by vascular injury, infection or inflammation, and therefore the cell-based coagulation model can help explain the increased coagulopathy and thrombosis in septic or hyperinflammatory conditions such as ARDs.

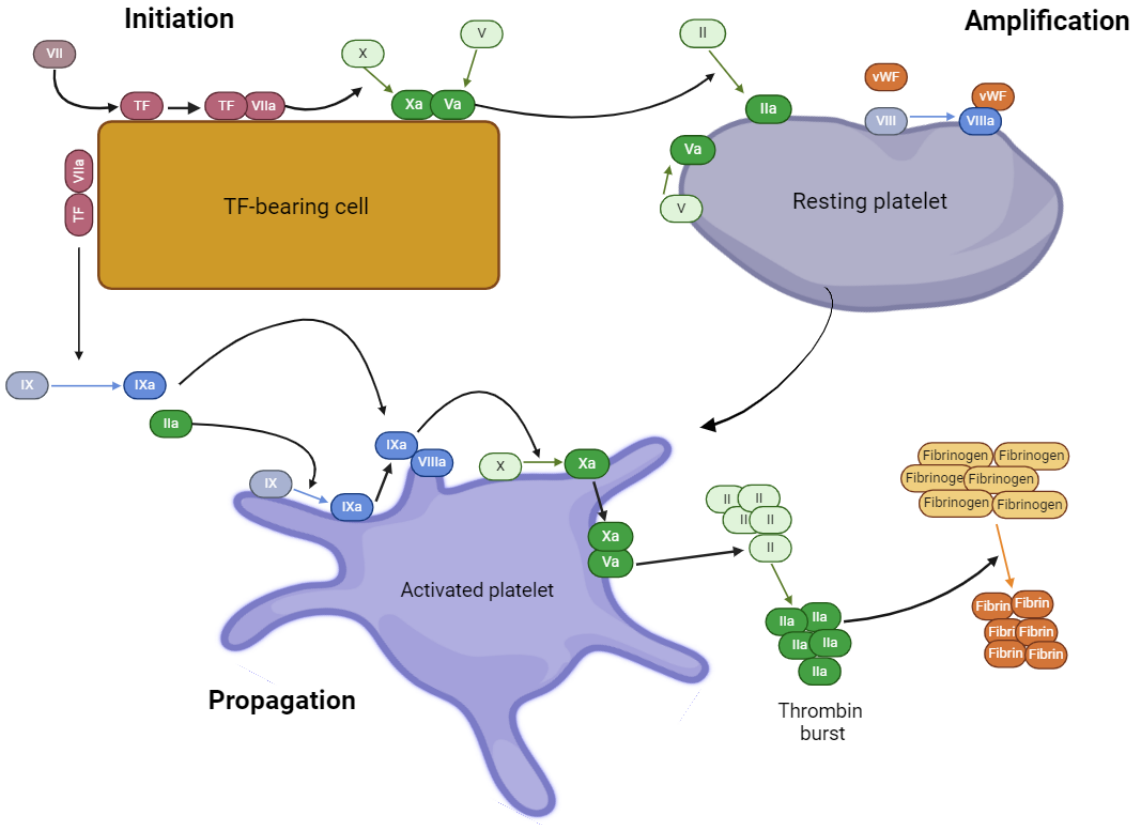


Figure 1.7 Cell-based model for coagulation.

In the initiation phase, tissue factor on the cell surface of tissue factor bearing cells interacts with Factor VII leading to activation of Factor X which initiates coagulation and thrombin (FIIa) generation. Thrombin leads to platelet activation in the amplification phase where cofactors Factor V, VIII, XI and von Willebrand factor (vWF) are activated to prepare for thrombin burst in the propagation phase. Image created on Biorender.

1.3.3 Platelets

Platelets, also known as thrombocytes, are key cells in haemostasis and thrombosis. They are derived from megakaryocytes in the bone marrow and enter the blood stream without nuclei. There is continuous production and clearance of 10^{11} platelets daily to maintain 150 - 400 x 10^{9}/L in circulation [40]. Inactive platelets are a discoid shape but upon activation, the cytoplasm restructures to form an elongated shape with extensions to increase their surface area, known as pseudopods (Figure 1.7). Platelets have many different surface receptors and adhesion molecules and contain numerous granules or intracellular vesicles which are released upon activation. There are three types of platelet intercellular vesicles: alpha granules, dense granules and lysosomes. Alpha granules are the most abundant granules within platelets (50-80 per platelet) and contain a wide range of proteins that comprise the bulk of the platelet secretome including haemostatic factors (fibrinogen, vWF, platelet factor 4 [PF4], coagulation factors), angiogenic factors (angiogenin VEGF), proteases, and

cytokines. Proteins from alpha granules contribute to platelet adhesion and activation, and subsequent thrombus formation and stabilisation. Dense granules are the second major secretory compartment of platelets (3-8 per platelet) and contain small molecules such as adenosine diphosphate (ADP), adenosine triphosphate (ATP), calcium, phosphates, purines and bioactive amines. Lysosomes contain enzymes for protein, lipid and carbohydrate degradation and have a role in digestion of phagocytic and cytosolic components similar to nucleated cells [41, 42].

1.3.4 Platelet activation

Platelets flow in blood vessels in a resting state and can be activated via multiple pathways. The normal endothelium is a non-adhesive surface to platelets but when vessel injury occurs, there is exposure of collagen from the subendothelium. Collagen is one of the most thrombogenic components of the subendothelial matrix and initiates platelet adhesion. Platelets bind to collagen via the α2β1 receptor which allows for further binding to collagen via the glycoprotein VI (GPVI) receptor initiating transmembrane and intracellular signalling (Figure 1.8). Exposed collagen also attaches to vWF, a large globular multimeric glycoprotein which unfolds to a string-like structure. Platelets adhere to tethered vWF via the GPIb-IX-V receptor complex or directly through collagen and the GPVI receptor [43]. Adhesion of platelets to the exposed endothelium is influenced by shear rates. At high shear α2β1 and GPVI are not sufficient to bind platelets to collagen, and binding of the GPIb-IX-V receptor to vWF becomes essential in platelet adhesion. Platelet adhesion at the site of tissue damage initiates events that result in aggregation. Platelet aggregation also stimulates release of thromboxane A2 (TXA2) via the arachidonic acid (AA) cascade, and thrombin is formed via the coagulation pathway from prothrombin on the surface of the activated platelet (Figure 1.7). ADP, TXA2 and thrombin bind to specific membrane receptors (P2Y12 and P2Y1 receptors, TXA2 receptor and protease-activated receptors [PAR]) and stimulate platelet aggregation on and around the platelets adherent to the subendothelium [40].

Binding of any of these agonists to their respective receptors initiates pathways that increase cytoplasmic calcium, resulting in granule release, and the conversion of glycoprotein IIb/IIIa (GPIIb/IIIa; also known as integrin αIIbβ3) from a low affinity state to a high affinity active state for cross-linking vWF or fibrinogen leading to further platelet aggregation [44]. Furthermore, activated platelets undergo dramatic shape change from a round sphere to an irregular sphere with multiple filipodia spreading on the subendothelium which increases their area of contact. Activated platelets contribute to the inflammatory cascade by release of

their storage granules containing adhesion ligands and proteins such as P-selectin (CD62P) and signalling molecules, such as CD40L, platelet factor 4 (PF4; also known as CXCL4) and other inflammatory molecules like histamine and ADP [40, 44]. This provides a high local concentration of molecules essential for platelet plug formation.

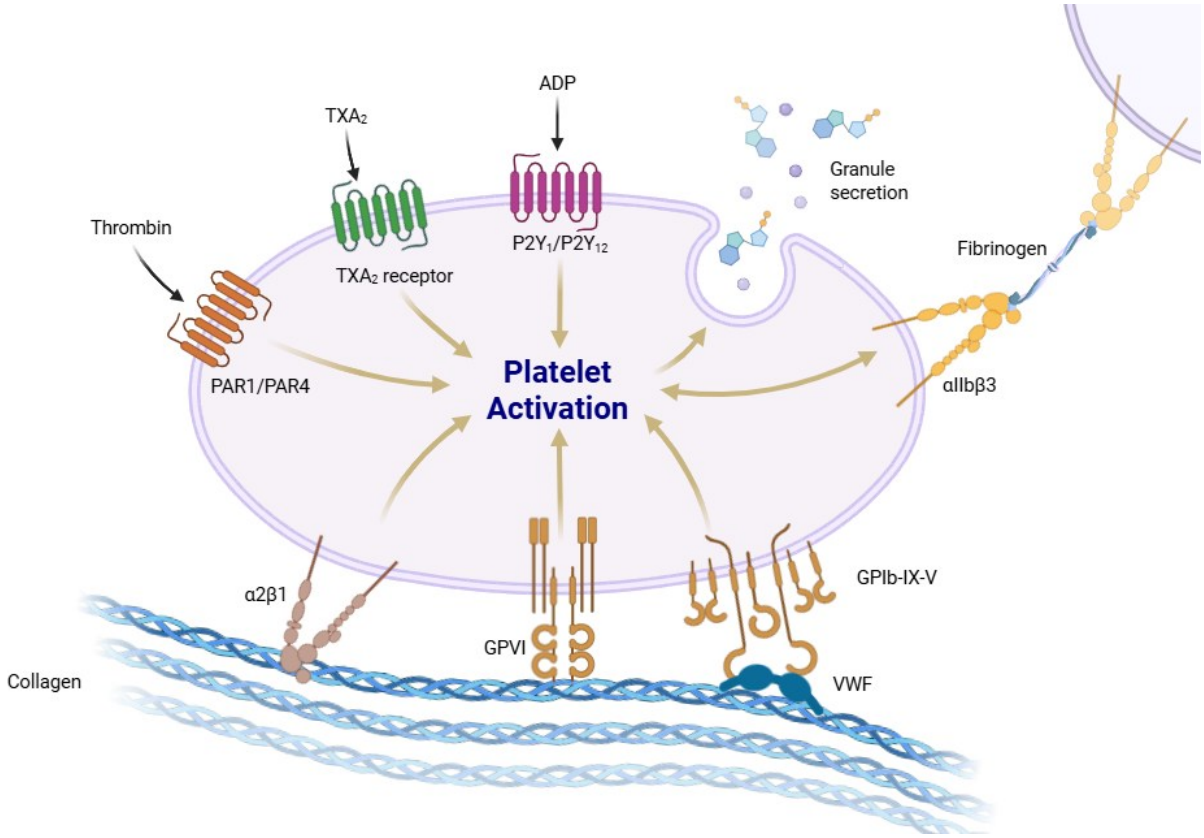


Figure 1.8 Platelet activation pathways

Exposed collagen in damaged endothelium binds to platelet α2β1 and GPVI receptors initiating transmembrane and intracellular signalling. Collagen also attaches to vWF which binds to the platelet GPib-IX-V receptor. Thrombin, TXA2 and ADP also bind to their respective receptors PAR1/PAR4, TXA2R and P2Y1/P2Y12 leading to further platelet activation and aggregation. Activated platelets release storage granules and their contents and GPIIb/IIIa (αIIbβ3) binds to fibrinogen and vWF.

Adenosine diphosphate, ADP; Protease activated receptors, PAR; Glycoprotein, GP; Thromboxane A2, TXA2; von Willebrand factor, vWF.

1.4 Neutrophils

1.4.1 Neutrophil activation

Neutrophils are among the first cells to arrive at sites of infection and have a key role in inflammation and the host response to infection [45]. Neutrophils account for 50-70% of all circulating leucocytes and are generated at a rate of 10^{11} to 10^{12} per day during infection. Neutrophils are terminally differentiated and have a short lifespan of 12-20 hours in circulation in most reports [46].

Under homeostatic conditions, neutrophils patrol the blood and tissues to detect pathogens and in response become activated by ligands (antibodies, pathogens, cytokines, activated platelets etc.) binding to neutrophil receptors such as toll-like receptor (TLR) 4, P-selectin glycoprotein ligand 1 (PSGL-1), high-mobility group protein B1 (HMGB1) and Fc-γ receptors [47]. This leads to an influx of calcium into the cells activating nicotinamide adenine dinucleotide phosphate (NADPH) oxidase and generation of ROS also known as oxidative burst [48] and the downstream activation of neutrophil functions. There are three mechanisms by neutrophils kill invading pathogens. Firstly, activated neutrophils can engulf pathogens into a vacuole in a process called phagocytosis. Internalised pathogens are destroyed by the oxidative burst and fusion of the phagosome with granules releasing bactericidal enzymes myeloperoxidase (MPO) and neutrophil elastase (NE). Secondly, neutrophil degranulation happens, where the bactericidal proteins and enzymes stored within the granules are mobilised to the phagosome or plasma membrane, where they fuse with the plasma membrane to release their cargo into the extracellular space. Lastly, the generation of ROS from NADPH oxidase and MPO initiates a process called NETosis, which releases neutrophil extracellular traps (NETs) to ensnare pathogens and kill them or assist with phagocytosis by other neutrophils or macrophages [46, 48].

ROS are harmful to lung tissues and play an important role in inflammatory lung injury as they induce pulmonary endothelial and epithelial barrier dysfunction, further release of inflammatory cytokines, increased leucocyte infiltration into lung tissues, and worsening pulmonary tissue damage enhancing the progression of ARDS [49]. The release of these inflammatory cytokines activate inflammatory pathways as well as directly attacking pathogens and initiating phagocytosis of microorganisms [46]. Neutrophils also contribute to various physiological functions such as angiogenesis, coagulation and tissue repair [50].

1.4.2 Neutrophil degranulation

The neutrophil cytotoxic proteins are stored in granules which are categorized based on their enzyme content and function. Primary or azurophilic granules contain the bactericidal enzymes such as MPO, which is the most abundant neutrophil protein, defensins and serine proteases (such as NE, cathepsin G and proteinase 3). Secondary or specific granules contain antimicrobial peptides such as lactoferrin, lysozymes and some matrix metalloproteinases e.g. MMP-8 (or collagenase) and tertiary granules containing MMP-9 (or gelatinase) [46, 51].

Generation of ROS is essential to neutrophil degranulation and release of bactericidal enzymes from the azurophilic granules. MPO is one of the most abundant proteins in neutrophils. When neutrophils are activated, MPO is released from the neutrophil cytoplasm, and into the extracellular plasma, or alveolar space. MPO catalyses the oxidation of chlorides and halides in the presence of hydrogen peroxide to form ROS [49, 52] in addition to the ROS produced by NADPH oxidase. The excess ROS production contributes to intracellular chromatin decondensation and ultimately NETosis. NE is a neutrophil specific serine protease found in azurophilic granules. When released, NE hydrolyses several proteins, promotes inflammation, and is bactericidal [52, 53]. NE can degrade the extracellular matrix proteins, disrupt alveolar cell-cell adhesion, and damage pulmonary vascular glycocalyx during the pulmonary inflammatory process. Both MPO and NE are required for NET formation. And they have been shown to regulate the formation of NETs by disrupting the charge of intracellular chromatin, and also degrade specific histones (Papayannopoulos et al., 2010).

1.4.3 Neutrophil death

Since neutrophils contain cytotoxic proteins and enzymes, their development and clearance mechanisms must be tightly regulated to prevent unintended inflammation or injury to the host. The number of neutrophils generated daily is high and with their short life span, neutrophil turnover is high to maintain homeostasis. Due to the nature of their cytotoxic contents, non-lytic cell death is the predominant cell death pathway in steady states to protect the host from injury. Programmed neutrophil cell death (apoptosis) is a non-inflammatory or non-lytic form of cell death activated in quiescent neutrophils by cytokines in a similar way as in other cells. Apoptosis can also be activated in neutrophils after phagocytosis and ROS production. Neutrophil apoptosis is characterised by changes in cell structure and shape, reduction of cell volume, and chromatin condensation. The neutrophils are then no longer functional and lose their chemotaxis, and degranulation mechanisms [54]. Neutrophil turnover can be increased or delayed in inflammatory states [46]. In hyperinflammatory states such as in infection, severe sepsis or critical illness, lytic forms of cell death lead to the release of the cytotoxic proinflammatory proteins, enzymes and chemokines into the extracellular space causing local inflammation and tissue injury. These lytic cell death pathways include necroptosis, pyroptosis and NETosis [54, 55].

1.4.4 NETosis

Since NETs were first discovered in 2004, they have been an increasing area of interest because of their role in a variety of conditions. They were first discovered for their role in infection [45], but have also been implicated in cancer, thrombosis, stroke, and cardiovascular disease [56, 57].

Neutrophil activation and generation of ROS by NADPH oxidase also triggers activation of the calcium dependent enzyme peptidylarginine deiminase 4 (PAD4) which is primarily expressed in neutrophils [48]. PADs convert arginine residues into the amino acid citrulline. When histones are citrullinated, there is a loss of positive charge leading to chromatin decondensation, the initial step in NETosis. The unravelling of the chromatin material exposes intracellular DNA, nucleosomes and free histones and allows mixing with cytoplasmic and nuclear proteins and enzymes such as NE and MPO (see Figure 1.9). The protein decorated chromatin is then released as the neutrophil swells up and its cell membrane disintegrates, ultimately leading to neutrophil cell death [48]. Release of NETs leads to entrapment of pathogens within a localised environment of bactericidal proteins and enzymes leading to degradation of the pathogens as well as assisting in macrophage phagocytosis [58].

Histone H3 citrullination by PAD4 is essential for NET production, therefore citrullinated histone H3 (CitH3) is seen as a NET-specific biomarker [59] with many studies using this as an early biomarker for NETosis [60-63]. The unravelling of chromatin material exposes intracellular DNA and nucleosomes (Figure 1.9) hence nucleosomes can be used as a surrogate marker for NETosis [64].

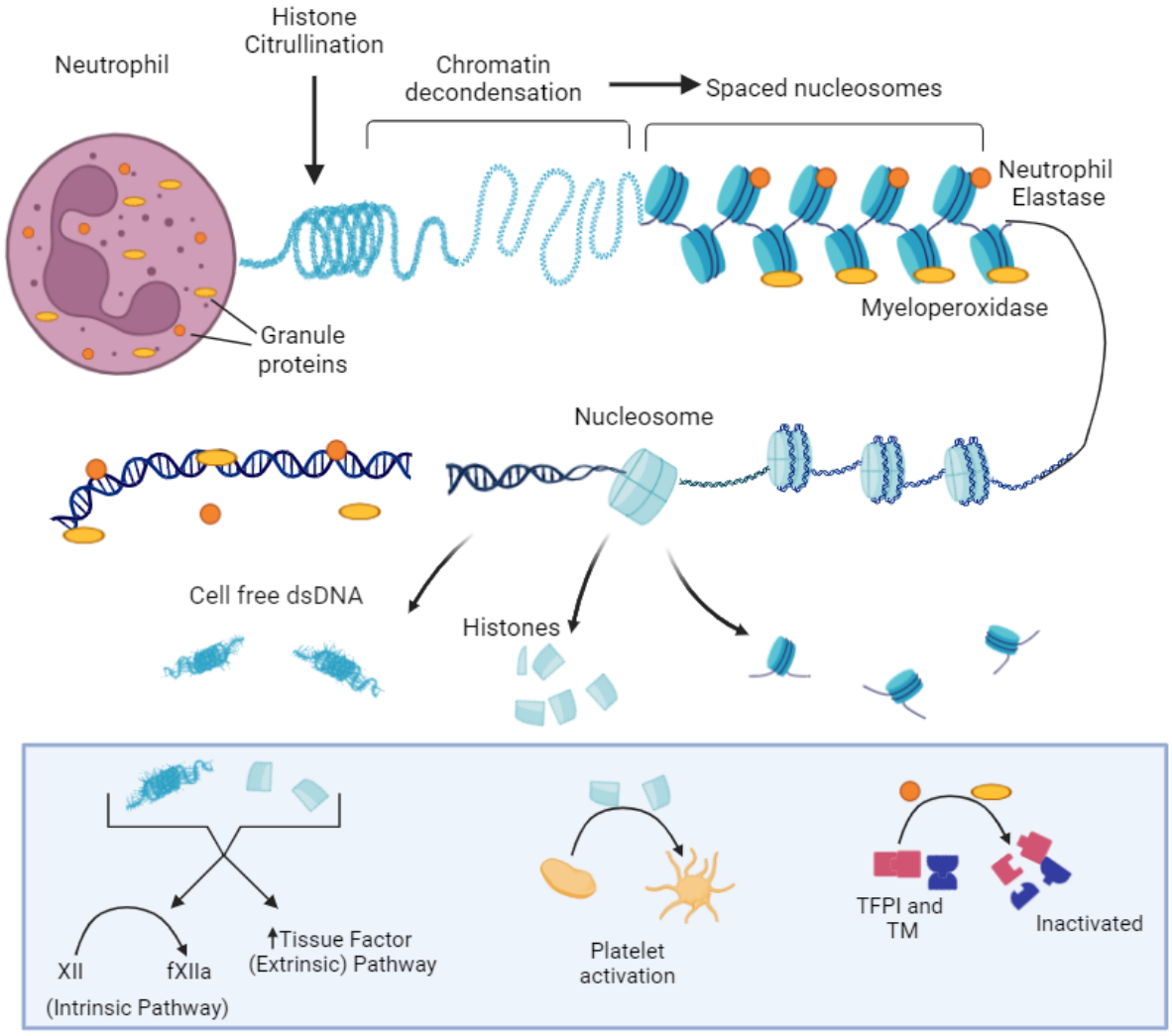


Figure 1.9. Neutrophil activation leading to NETosis

Histone citrullination leads to loss of positive charge on chromatin causing chromatin decondensation. This leads to release of nucleosomes, free histones, cell free DNA mixing with cytoplasmic and nuclear proteins and enzymes such as neutrophil elastase and myeloperoxidase. Disintegration of the cell membrane and release of these contents is called NETosis. Each NET component can interact with different aspects of the coagulation cascade. Image created in Biorender.

Tissue factor pathway inhibitor, TFPI; Thrombomodulin, TM; Factor 12, fXII. Adapted from AJRCCM 2023;208(2):125-127 [65].

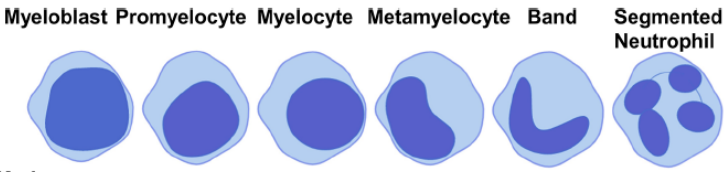
There have been two pathways of NETosis described: suicidal or lytic NETosis and vital NETosis. Lytic NETosis is the classic model of NETosis and is recognised as a form of cell death. It is dependent on NADPH oxidase [48], causing chromatin decondensation and mixing with cytoplasmic proteins. The NETs are released into the extracellular space after disintegration of the plasma membrane causing cell lysis which can take several hours from stimulus to cell lysis. The neutrophil loses its functions such as chemotaxis and phagocytosis [48, 66].

In contrast, vital NETosis occurs without cell death and is a NADPH oxidase independent process. Here the intracellular chromatin is expelled from the cell without cell lysis e.g. by release of vesicles, and granule proteins are released by degranulation. These components then assemble extracellularly to form NETs leaving the remaining neutrophil cytoplast that retains some functions such as phagocytosis. This process occurs within a shorter time 5-60 minutes. [66-68]. However, there remains a lack of consensus on whether there are indeed two forms of NETosis [66, 67].

Neutrophil activation and NETosis is required in response to infection, but if left uncontrolled in severe inflammatory or septic states, overactivation can lead to a dysregulated inflammatory response, and also increased thrombosis, which may become harmful.

1.4.5 Neutrophil phenotypes

Neutrophils have been referred to by many names since their discovery, including phagocytes, polymorphonuclear neutrophils (PMN), low density neutrophils and granulocytes. They have phenotypically distinct subtypes during granulopoiesis and are highly versatile and sophisticated cells that respond and adapt to a variety of stimuli. Under pathological conditions neutrophils may differentiated into discrete subsets with distinct phenotypic and functional profiles [69, 70]. During granulopoiesis, hematopoietic stem cells differentiate into myeloblasts, which become promyelocytes, myelocytes, metamyelocytes, band cells and, finally, segmented neutrophils (Figure 1.10). At the different stages of neutrophil development different cell surface markers are expressed to varying degrees. As the neutrophils develop, they gain neutrophil specific granule components such as MPO, and NE and other granule proteins and enzymes. Therefore, as the neutrophil matures there is increased granularity and increased cell size proportional to the cell's density which allows for separation by density gradient centrifugation [70].



Surface Marker						
CD66b	-	+++	+++	++	++	++
CD15	+	+++	+++	+++	+++	++
CD33	+++	+++	++	+	+	+
CD62L	++	++	++	++	++	++
CXCR2	+	+	+	+	+ +	++
CXCR4	++	++	++	++	+	+
CD18	++	+	+++	++	++	++
CD24	-	-	++	++	++	++
CD11b	-	-	+/++	++	++	++
CD11c	-	-	++	++	++	++
CD177	-	-	+	+	+	+
CD16	-	-	-	+	++	+++
CD87	-	-	-	-	++	++
CD10	-	-	-	-	-	++
CD35	-	-	-	-	++	++
HLA-DR	+	-	-	-	-	-
CD34	+	-	-	-	-	-
CD49d	++	++	++	+	-	-

+ Low intensity ++ Medium Intensity +++ High Intensity

Figure 1.10 Neutrophil granulopoiesis and surface marker expression

Taken from Front. Immunol. 12:602963 [70]

The markers of interest to this thesis are CD66b and CD11b (also known as Mac-1 or integrin αM) which help to identify neutrophils and have increased expression when activated. CD66b is expressed on neutrophils once they reach the promyelocyte stage, and CD11b from the myelocyte stage. L-selectin (CD62L) is a cell adhesion molecule which is part of the selectin family of ligands. It helps neutrophils attach to activated endothelium, helping neutrophils roll and migrate to site of inflammation and is shed when neutrophils are activated [71].

Neutrophil heterogeneity has been linked to sepsis progression and severity. The presence of immature granulocytes (IG; $CD10^{low}$ $CD16^{low}$) is associated with increased severity of sepsis and Daix et al found patients with IG <30% was associated with a better survival than IG > 30% [72]. CD64, is a high-affinity immunoglobulin Fc-γ receptor 1 expressed on

leucocytes. CD64 expression on resting neutrophils is low and is rapidly upregulated after activation. Neutrophil CD64 expression is increased in inflammatory bowel disease [73], inflammatory autoimmune diseases, [74] and in sepsis with high sensitivity and specificity in distinguishing patients with bacterial infections and active disease from healthy controls or inactive disease. Interest in neutrophil CD64 expression has increased in recent years with many studies exploring its diagnostic value in early adult sepsis and in critically ill patients [72, 75].

1.4.6 Monocyte Subsets

Monocytes are the largest mononuclear leucocyte and account for approximately 5% of circulated nucleated cells in normal adult blood. They have a circulating half-life of 1-3 days. Monocytes differentiate into macrophages and dendritic cells and play an important role in innate and adaptive immunity, inflammation and homeostasis. Monocytes patrol the body for invading pathogens and migrate from the circulation to infected or inflamed tissues within hours. They function as phagocytes and antigen presenting cells to remove pathogens and dead or damaged cells [76]. Monocytes are divided into three phenotypically and functionally distinct populations based on differences in CD14 and CD16 expression. Classic monocytes are $CD14^{++}$ $CD16^{-}$, intermediate $CD14^{++}$ $CD16^{++}$, and non-classic $CD14^{+}$ $CD16^{++}$, with classic monocytes accounting for 80-90% of circulating monocytes, intermediate 2-5% and non-classic 2-10% [77]. The different subtypes of monocytes have different gene expression resulting in differing responses to bacterial infection and inflammation. [78]. Monocytes also express HLA-DR, a Major Histocompatibility Complex class II receptor, which is often seen as a monocyte activation marker [79, 80]. It has been reported that increased numbers of intermediate and non-classic monocytes as well as HLA-DR shedding are related to increased sepsis and inflammation in patient samples [72, 80, 81].

1.5 Immunothrombosis in context

1.5.1 What is immunothrombosis?

Immunothrombosis is the interaction between the innate immune pathways (neutrophils, monocytes and lymphocytes) and coagulation and thrombus formation (platelets, coagulation cascade). The term immunothrombosis often refers to the aberrant thrombus formation or hypercoagulability seen in infective or inflamed states, such as sepsis and ARDS.

The majority of VV ECMO patients often have ARDS and therefore increased systemic inflammation. Platelet activation and thrombocytopenia is also widely reported in sepsis and in ECMO [82]. NETs are an emerging area of interest and could be a potential link between thrombosis, immunity and inflammation in sepsis and in the context of ECMO. It is also thought that the increased platelet activation during ECMO can lead to increased activation of neutrophils and therefore NETosis [82-84]. There is increasing focus on platelet-leucocyte interactions in disease.

1.5.2 NETosis in ARDS

Neutrophils are recruited to the alveolar space in ALI and contribute to the pathogenesis of ARDS (section 1.1.4, figure 1.1). There is increasing evidence that NETosis is one of the most important mechanisms to ALI. Many studies have found NETosis markers in plasma of patients with ALI caused by pneumonia, acid-aspiration, and TRALI [64, 85-89]. NETs were increased in patients with COVID-19 related ARDS [90-92] and many hypothesised that NETs were involved in the immunothrombosis of COVID-19 [93-95].

Some studies compared concentrations in the alveolar space to plasma and found NETosis markers in higher concentrations in bronchoalveolar lavage fluid (BALF) than plasma of patients with pneumonia and ARDS [85, 89]. Furthermore, BALF from patients with ARDS can induce NETosis in neutrophils from healthy donors and contribute to further epithelial cell damage [96]. There are many mechanisms by which NETosis is triggered, and this may depend on the type of lung injury. For example, it has been found platelets induce NETosis in TRALI and VILI via TLR4 [86, 97].

Indeed, the presence of NETs correlates with disease severity and mortality [64, 87, 88]. NET components, NE and MPO, are also increased in patients with ALI, SIRS and sepsis and associated with increased mortality [98-100]. Inhibiting or reducing NETosis could be a useful therapeutic strategy to reduce morbidity and mortality in this cohort of patients. To date there have only been studies targeting NET production in animal models. Lefrancais found PAD4 deficient mice and dissolving NETs with DNase treatment, led to reduced lung injury and improved survival [87] and in another mouse model, Alvelestat (an NE inhibitor) was able to reduce the degree of acid aspiration ALI [88]. These are possible therapeutic targets for NETs in ARDS but there is not yet work in human subjects.

1.5.3 NETs in thrombosis

As well as their primary role in host defences against pathogens, there is building evidence that NETs play a role in coagulation and immunothrombosis [101-103]. NETs are present in thrombi of patients with ischaemic stroke [56], acute coronary syndromes [104], and venous thromboembolism [57]. They are increased in patients on extracorporeal circuits such as CPB [105-107], and haemodialysis [108-110] and are associated with increased risk of thrombosis.

NETs have been shown to interact with coagulation in various ways (Figure 1.9) [111]. Firstly, the expelled cfDNA forms a scaffold for platelet and red cell adhesion and activation, leading to thrombus formation [112]. In addition, the released cfDNA and histones can activate platelets and increase thrombin generation [113] which may be mediated by TLR-2 and TLR4 [114, 115], and also increase contact activation via factor XII. Secondly purified histones, NE and MPO can bind to thrombomodulin preventing activation of protein C, increasing further thrombin generation as well as increasing TF expression [116], and also inactivate tissue factor pathway inhibitor [117]. The relationship between NETosis and thrombosis is bidirectional with overactivation of coagulation cascade and platelets or uncontrolled neutrophil activation and NETosis leading to propagation of immunothrombosis.

1.5.4 Leucocyte-platelet interactions

Leucocytes and platelets are the first cells to be recruited to sites of tissue injury and inflammation and in recent years, the link between coagulation and inflammation is better understood. Activation of coagulation is part of the host defence to prevent systemic spread of pathogens, and platelets interact with monocytes and neutrophils leading to further activation and recruitment.

In normal circulation, platelets and leucocytes do not readily interact. Known platelet-leucocyte interactions require the platelets or leucocytes to be activated or primed to promote cell-cell interactions [118]. Interactions between platelets and leucocytes can be mediated by direct contact between platelet and leucocyte surface proteins and receptors, or indirectly via secreted ligands or molecules in the plasma and these interactions lead to reciprocal activation in each cell type. Activated platelets present adhesion ligands and signalling molecules such as P-selectin, CD40L, GPIIb/IIIa, and ICAM-2 on the platelet surface which interact with PSGL-1, CD40 and Mac-1 on the leucocyte cell surface. Interaction of ligands to their receptors, particularly of P-selectin to PSGL-1, and GPIIb/IIIa

via intermediary proteins to Mac-1, leads to formation of leucocyte-platelet aggregates (LPA) [119-121]. Activated platelets also degranulate and release granule contents such as fibrinogen, vWF, PF4, HMGB1, VEGF directly into the plasma or within extracellular vesicles which activate leucocytes such as neutrophils via the aforementioned receptors as well as RAGE, TLR2 and TLR4 (Figure 1.11) [122]. Activated leucocytes present TF on their cell surface leading to further activation of platelets as described in the cell-based model of coagulation, and NETs interact with coagulation as described in section 1.4.4 [118, 123] .

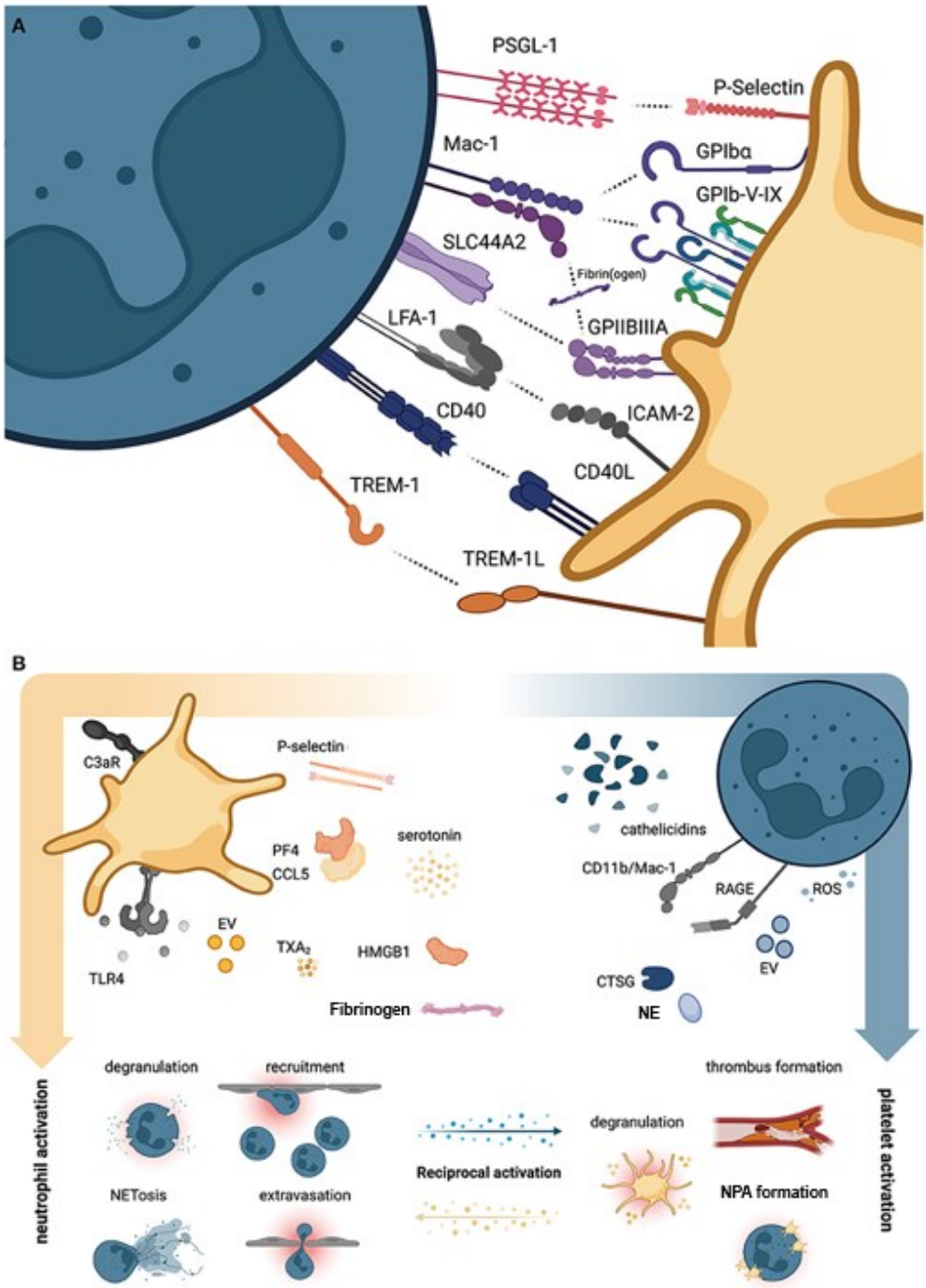


Figure 1.11 Direct and indirect neutrophil-platelet crosstalk

A) Neutrophil (left, blue) and platelet (right, yellow) receptor pairs that directly interact and promote reciprocal activation B) soluble agonists secreted by platelets promoting neutrophil activation (left) and agonists secreted by platelets promoting platelet activation (right).

Cathepsin G, CTSG; extracellular vesicles, EV; high-mobility group protein B1, HMGB1; intercellular adhesion molecule 2, ICAM-2; lymphocyte function-associated antigen 1, LFA-1; neutrophil elastase, NE; neutrophil-platelet aggregate, NPA; platelet factor 4, PF4; P-selectin glycoprotein ligand-1, PSGL-1; receptor for advanced glycation end-products, RAGE; reactive oxygen species, ROS; toll-like receptor, TLR; thromboxane A2, TXA2; triggering receptor expressed on myeloid cells 1, TREM-1. Taken from Front.Cardiovasc. Med. 8:824112 [122]

1.6 ECMO and haemostasis

1.6.1 Haemostatic complications are common in ECMO

Exposure of blood to negatively charged synthetic surfaces of an ECMO circuit leads to activation of the coagulation cascade, platelets, leucocytes and complement which are then returned to the patient [124]. This can lead to a systemic inflammatory response and a prothrombotic state leading lead to thrombosis in the patient or device failure. The rates of ECMO thrombosis are unknown however clots are reported in the MO in up to 11% of patients and cerebral infarction in up to 7% of adult patients [125]. The consequences of ECMO related thrombosis are severe and therefore, patients are often anticoagulated whilst on ECMO, usually with unfractionated heparin infusions. Heparin reduces thrombin generation and also demonstrates less platelet and leucocyte activation [126, 127]. In addition, the use of hydrophobic PMP and PP materials in the MO and the development of heparin bound circuits to reduce the prothrombotic nature of ECMO surfaces has led to reduced complications [126, 128]. Despite advances in biomaterials and anticoagulation regimes, haemostatic complications, both bleeding and thrombosis, remain the leading causes of morbidity and mortality in patients managed with ECMO [125, 129].

The most common areas for thrombus formation in the ECMO circuit is the MO, where there is a high surface area exposed to blood [130, 131], and tubing connector junctions where there is increased turbulence [132]. The most feared complication is MO thrombosis, which if severe necessitates a circuit change, a high-risk intervention in patients who are completely dependent on ECMO. According to the ELSO registry up to 2016, MO failure accounted for 9.1% of VV ECMO, and 6.6% of VA ECMO complications [125]. The need for circuit change is associated with increased time on ECMO, and increased morbidity and mortality [133, 134].

The interaction between haemostasis and ECMO is complex and depends on patient factors and ECMO related factors which can be summarised in Figure 1.12.

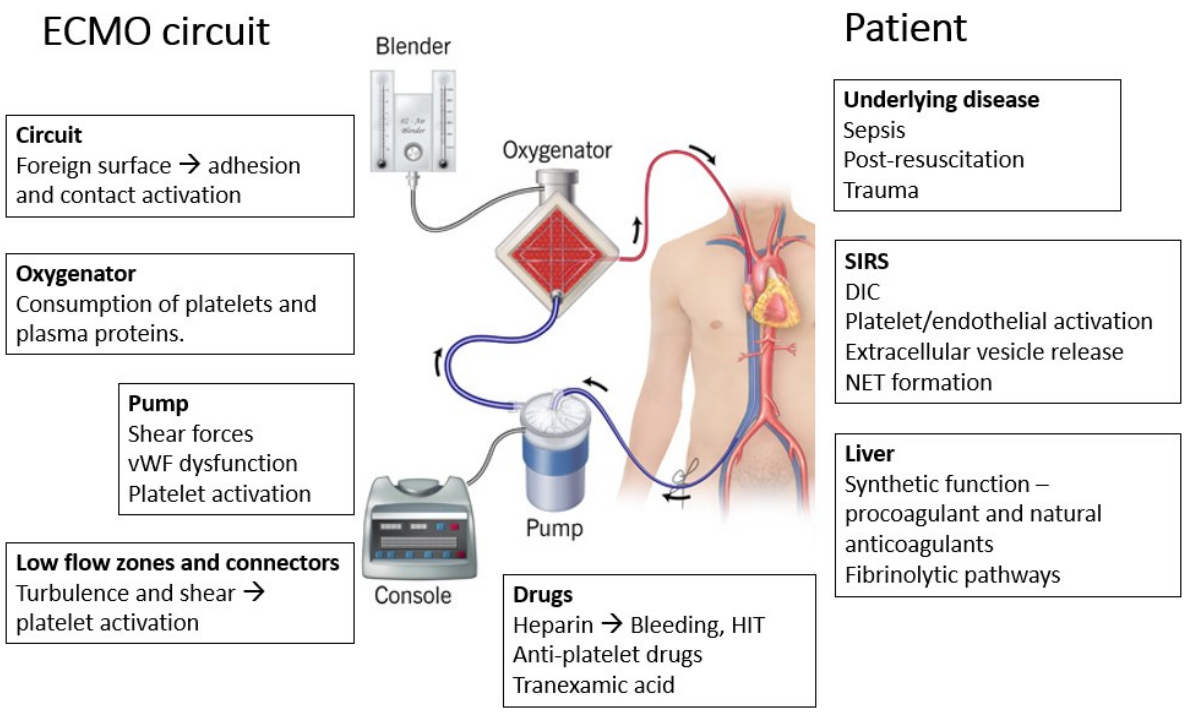


Figure 1.12 ECMO and patient related factors which increase haemostatic complications
Adapted from Transfusion Medicine Reviews (2015) 29;90–101 [129].

1.6.2 Membrane oxygenator thrombosis: Predicting need for circuit change

Predicting when patients have significant MO thrombosis that requires a circuit change can be difficult. It is a decision based on the observation of macroscopic clots and fibrin strands within the circuit or MO, and a combination of changes in blood markers such as increasing D-dimer, falling fibrinogen, and falling platelet count, all indices of consumptive coagulopathy [131, 135]. There are changes in ECMO mechanics such as rising transmembrane pressure (TMP; pressure difference before and after the MO) and increasing transmembrane resistance (TMR; blood flow to motor pump RPM ratio) [136] as well as the decrease in MO gas exchange efficiency which is measured as the post-oxygenator PaO2 (PpostO2) [137]. However, it is not always straightforward, and no single parameter can predict the need for circuit change, nor is there a set threshold for which a circuit change is indicated. Moreover, these clinical variables are often affected by the underlying critical illness and disease and must be evaluated in the context of the patient's clinical condition.

Monitoring for the presence of fibrin or macroscopic clots within the ECMO circuit and MO is usually part of the daily ECMO checks, however, this may not be a useful parameter. In many oxygenators (Cardiohelp Quadrox, Nautilus), it is the oxygenated (outlet) side of the

MO that is visible. CT evidence shows thrombi are present in most ECMO circuits after decannulation, but the clots form mostly on the deoxygenated/venous side of the MO [130, 138], which is not visible in most devices. In these studies, all circuits were from patients who had successfully weaned and therefore decannulated from ECMO. There were no patients who required a circuit change and therefore conclusions regarding the clot burden and impact on MO function cannot be answered.

1.6.3 Why do membrane oxygenators clot?

Firstly, the geometric structure of the MO and the location of the inlet and outlet as well as the design of the flow path can impact the haemodynamics within the MO. It has been suggested that the square structures have increased low flow areas in the corners and therefore increased thrombus formation compared to circular models [139]. However, the thrombus deposition within MO is also affected by the position of the blood inlet and outlets. Using computational flow dynamic models many groups have compared the most commercially used square oxygenators (Cardiohelp Quadrox, and Cardiohelp HLS Oxygenator, [Getinge, Sweden]) with circular models such as the Nautilus ECMO oxygenator (Medtronic, USA), both of which are commonly used in the UK and in our centre. However no clear conclusions have been made from these models [139]. Other studies have shown using CT imaging that clot formation is more likely on the venous side of the MO particularly around the blood inlet [130].

Secondly there is the impact that the ECMO circuit has on haemostasis as outlined in section 1.6.1. Histological analysis of thrombi from ECMO circuits demonstrates that the major thrombus components are fibrin, vWF, red blood cells and platelets [132, 140, 141]. Staessens et al, found in VA ECMO circuits there were two typical thrombus types: red blood cell rich/fibrin poor and red blood cell poor/fibrin rich thrombi but the thrombus composition was not associated with thrombus location in the device. They did however find higher amounts of CitH3 found in pump and oxygenator thrombi compared to tubing samples and patients who had fibrin rich thrombi had higher blood leucocyte counts and lactate dehydrogenase levels [141]. These results suggest a role of immunothrombosis and specifically NETs in MO thrombosis.

1.6.4 ECMO circuit change

A circuit change is a complete or partial exchange of the MO, pump head and part of the circuit tubing. The circuit change procedure requires expertly trained personnel including intensivist/cardiothoracic surgeons who are trained in ECMO, ECMO trained nursing staff, and perfusionists, who follow standard operating procedures. The ECMO circuit is clamped to restrict blood flow, the circuit is cut between the clamps, ensuring adequate tubing length to connect to a new circuit, the new circuit is connected under an underwater seal via 3/8" tubing connectors, the clamps removed and the new ECMO pump is started to generate blood flow through the new circuit (Figure 1.13). A circuit change adds in extra connectors to the circuit introducing two areas of increased turbulence as well as exposing blood to a new non-endothelialised circuit.

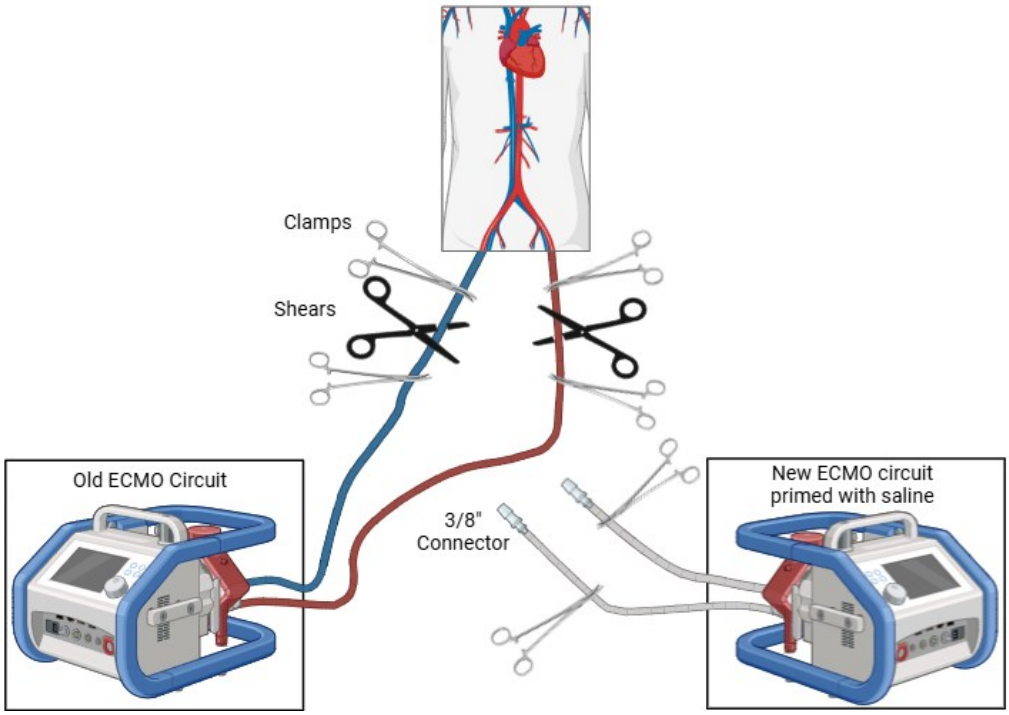


Figure 1.13 Schematic diagram of ECMO circuit change

The drainage and return tubing are clamped twice. The tubing is cut between the clamps, and the old ECMO circuit (left; pump, membrane oxygenator, and part of the tubing) is exchanged for the new ECMO circuit (right) which has been primed with saline. The new circuit is connected to the drainage and return tubing using additional connections. The clamps are removed to allow blood to flow through the new circuit. Image created in Biorender.

The circuit change procedure is usually competed within 10-30 seconds from time of clamping to running back onto the new ECMO circuit. During the time the circuit is clamped, the patient is not receiving any ECMO support. Patients are usually put onto 100% oxygen via the ventilator prior to starting a circuit change but for patients with severe respiratory

failure who are completely dependent on ECMO this may not be enough, and patients can become hypoxaemic and develop the consequences of hypoxia very quickly, e.g. bradycardia, hypotension or cardiac arrest, making this a high-risk procedure in patients who are dependent on ECMO.

1.6.5 Platelet dysfunction in ECMO

There are several mechanisms by which platelet function is affected by ECMO. Platelets can become both activated and functionally impaired during ECMO. The exposure of blood to the negatively charged artificial surfaces of the ECMO circuit leads to adsorption of plasma proteins, such as fibrin, vWF, as well as red blood cells, leucocytes and platelets, to the ECMO tubing and MO [142, 143]. Both the classic and cell-based models of coagulation suggest that on initiation of ECMO there is increased exposure of TF and contact activation both leading to thrombin generation and clot formation which creates the platelet plug. Using scanning electron microscopy, platelets have been found within fibrin networks in MO surfaces [130, 144]. The adsorption of platelets to the ECMO surfaces could contribute to the thrombocytopenia observed in ECMO patients.

Thrombocytopenia commonly develops during ECMO although this is not related to its duration [145-147]. During ECMO there is increased shear to blood due to the ECMO pump, which can lead to platelet receptor shedding of key platelet adhesion proteins GPIbα and GPIV with loss of high molecular weight vWF multimers [148, 149]. This leads to reduced platelet response (measured by aggregometry test) to platelet agonists collagen, ADP, AA, and thrombin receptor activating peptide-6 (TRAP-6) whilst on ECMO [145, 148, 150]. Flow cytometry of platelets in ECMO patients shows reduced expression of platelet activation markers such as P-selectin in addition to the GPIbα receptors, GPIV and GPIIb/IIIa [148, 151]. This loss of platelet aggregation may lead to the increased risk of bleeding seen in patients receiving ECMO.

In addition to reduced intrinsic platelet function there is also development of acquired von Willebrand syndrome during ECMO. vWF is a large multimeric glycoprotein that has 2 essential functions in haemostasis: it mediates platelet tethering to the subendothelial matrix at sites of vascular injury (e.g. to collagen) and forms a complex with coagulation factor VIII. Normally vWF does not interact with platelets unless it undergoes conformational change. When collagen is exposed, vWF binds to collagen and exposes the contact site for platelet

receptor GPIbα allowing circulating platelets to rapidly bind to the collagen bound vWF leading to platelet aggregation and thrombus formation [152].

In ECMO the shear stress leads to unfolding of the high molecular weight vWF. This creates mores sites for ADAMTS13 to bind and cleave high molecular weight vWF into low molecular weight vWF. This reduces the adhesive activity of vWF to collagen and platelets, and therefore increased risk of bleeding [148, 152] (Figure 1.14).

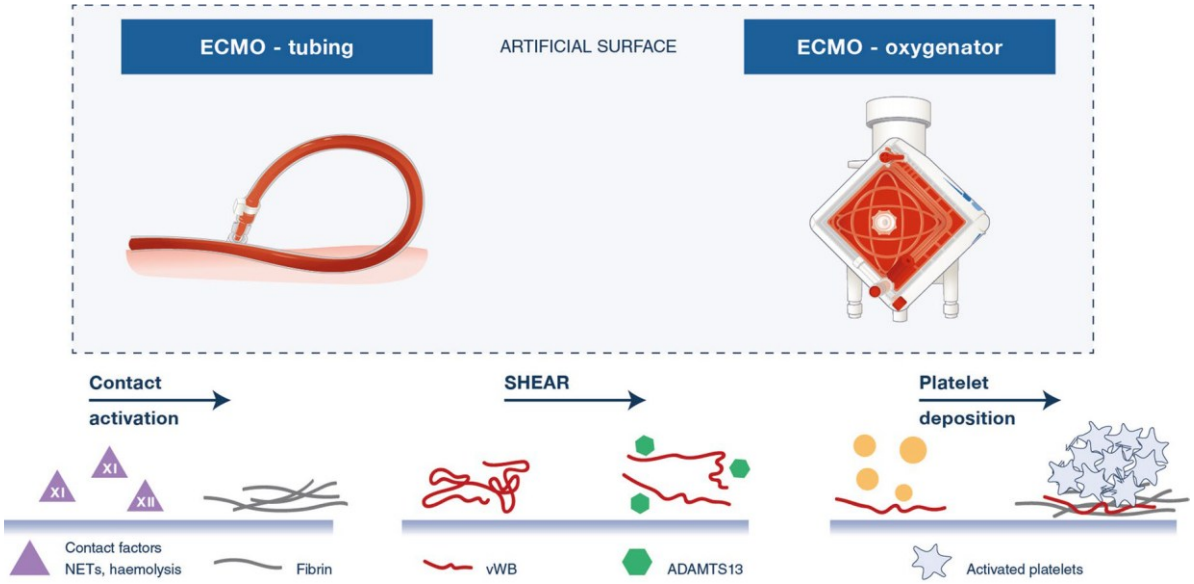


Figure 1.14 ECMO interacts with coagulation to increase bleeding risk

Taken from Intensive Care Med (2020); 46(4):771-774) [143]

1.7 Rationale for project

ECMO is the highest form of respiratory and cardiac support that can be offered clinically, and its use is increasing year on year. The most common complications are haemostatic with bleeding and thrombosis particularly of the MO. It is therefore important to further develop scientific understanding of the processes and cell-cell interactions that occur during ECMO to find new treatments to reduce complications and therefore morbidity and mortality.

1.8 Hypotheses and Aims

It is unknown why MO thrombosis occurs more in some patients than others but immunothrombosis specifically neutrophil-platelet interactions is likely to be a driving mechanism. The main aim of this PhD is to investigate the role of neutrophil and platelet activation in ECMO patients and the impact on circuit thrombosis. This overarching aim can be split into the following sub-aims:

1) Analyse clinical data to determine levels of immunothrombosis in ECMO patients by comparing incidence and monitoring of MO thrombosis using COVID-19 as an immunothrombotic cohort.

2) Develop and validate methods and protocol for measuring NETs, leucocyte phenotypes and LPA from *in vivo* patient samples.

3) Determine the kinetics of leucocyte and platelet activation (including NETosis and LPA formation) in ECMO patients:

    a. Across the ECMO run (during initiation, continuation, and cessation of EMCO)
    b. Between ECMO patients with and without circuit thrombosis requiring a circuit change.

4) Using in vitro models to investigate the effects of flow and shear on leucocyte-platelet interactions and NET formation.

I hypothesise that NETosis is a key mechanism for the development of immunothrombosis in patients on ECMO, particularly those who require circuit change, and that it is shear stress across the MO that leads to activation of inflammation, and LPA formation, and subsequent NET formation.

1.9 Overview of thesis

The introduction will hopefully have delivered a background into the history of ECMO and the challenges of using ECMO in an already inflamed cohort of patents, how current research into immunothrombosis may help us to understand the problems caused by biological-machine interactions, and how these cell-cell interactions may need further investigation.

The data presented in this thesis is separated into the clinical observational data, biological data from exploratory analyses using samples from clinical studies, development of a protocol for measuring LPA, leucocyte phenotypes and NETs, and in vitro work designed to mimic the extracorporeal circuit in order to investigate these cell-cell interactions.

Chapter 2 describes the methods and materials used to explore these ideas. The clinical data has been extracted from the hospital's clinical systems and all the exploratory analyses have been mapped to clinical data where possible. The HITEC study was designed to support this thesis, with ethical approval gained in January 2022 and recruitment starting in May 2022. This is the first project within our lab to primarily investigate leucocyte-platelet interactions and many of the methods and protocols were developed and optimised during this project.

Chapter 3 aims to look at the impact of ECMO thrombosis in clinical practice in the Royal Brompton Hospital and evaluates the clinical parameters currently in use to predict ECMO thrombosis. Within this analysis, I looked at the impact of immunothrombosis in ECMO by comparing COVID-19, an immunothrombotic condition, to non-COVID-19 patients.

To achieve aim 2, I first needed to determine if markers of inflammation, neutrophil and platelet activation, and NETosis could be measured in ECMO patient samples. Chapter 4 details the results of exploratory analyses using existing patient samples from the DeVENT and HITEC studies. The levels of neutrophil activation, NETosis, and platelet activation could be measured using ELISA of patient plasma samples. This chapter shows that ECMO is indeed immunothrombotic with increased levels of NETosis. Chapter 5 describes the challenges in developing flow cytometry protocols for measuring LPA and identifying leucocyte phenotypes in whole blood for use in patient samples. A protocol for measuring NETs in whole blood was also developed. By linking the ELISA data from chapter 4, and data from the newly developed protocols described in chapter 5, I was able to describe some of the changes in neutrophil and platelet activation across the ECMO to achieve aim 3.

Chapter 6 describes the development of an experimental model using the ibidi microfluidics chamber for investigating leucocyte-platelet interactions in whole blood under continuous

flow. Using the flow cytometry LPA quantification protocol as described in chapter 5, LPA formation and changes in leucocyte activation were measured over time perfused within the ibidi system. Using this model, I found that LPA formation depends on platelet activation, and there were different neutrophils and monocytes have different relationships with platelets. I was able to reduce LPA formation using a platelet inhibitor which could be a potential therapeutic target to mediate immunothrombosis.

As a clinician in intensive care, I feel it is important to investigate clinically relevant problems by measuring indices that can be used in patients and in experimental lab models, and hence the scope of work presented in this thesis. I developed a protocol for measuring LPA, and leucocyte phenotypes in patient whole blood using spectral flow cytometry and these protocols were adapted for use for in vitro work. The ibidi parallel microfluidics chamber work described in chapter 6 is aimed to mimic the continuous blood flow in an extracorporeal circuit. Although this work may still need some optimising it has produced promising pilot data for future work within the laboratory. I hope this is the beginning of my journey within basic translational research within critical care.

Chapter 2: Methods chapter

2.1 Materials

The following tables describe the materials (reagents and equipment) utilised withing this thesis, as well as their application and where they were obtained.

2.1.1 Reagents

Table 2.1 Blood separation reagents

Reagent	Constituents	Application	Source
Dulbecco's phosphate buffered saline (PBS) – modified, without calcium (1X)	-	Diluent	Sigma Aldrich
Distilled water, sterile filtered, bioreagent, suitable for cell culture	-	Diluent	Sigma Aldrich
Ethylenediaminetetraacetic acid (EDTA) (0.5M)	-	Cation chelator (Calcium and magnesium)	Sigma Aldrich
Histopaque ® 1077	Polysucrose and sodium diatrizoate, adjusted to a density of 1.077 g/ml	Density gradient cell separation	Sigma Aldrich
Histopaque ® 1119	Polysucrose and sodium diatrizoate, adjusted to a density of 1.119 g/mL	Density gradient cell separation	Sigma Aldrich
Red Cell Lysis Buffer (10X)	Ammonium chloride Potassium carbonate EDTA	Red cell lysis	Biolegend
RPMI 1640 Media (1X)	-	Resuspending isolated cells	Sigma Aldrich

Penicillin-Streptomycin-glutamine (PSG)	10000U/ml Penicillin 10000µg/ml streptomycin 29.2mg/ml L-glutamine	For cell resuspension media	Gibco
Human Albumin Solution (HAS) 25%		Cell culture media	BioIVT, GEM-800-120-S

Table 2.2 Flow cytometry reagents

Reagent	Constituents	Application	Source
FACS wash buffer	1X PBS 2% foetal calf serum (FCS) (w/v) 0.1% sodium azide 5 mM EDTA	Flow cytometry for in vitro isolated neutrophil work. (Not for whole blood or platelet work)	Sigma Aldrich Invitrogen, Thermo Scientific
BD FACS Lysing Solution (10X) Cat: 349202	-	Red cell lysis and fixation of whole blood samples	BD Biosciences
Annexin V Binding Buffer Cat: 422201	-	Buffer with calcium for staining samples with Annexin V	Biolegend
PBS without calcium	1X PBS	Washing of samples, diluent	Sigma Aldrich
PBS with calcium, magnesium	1X PBS with calcium/magnesium	Diluent for samples with Annexin V	Sigma Aldrich
Paraformaldehyde (PFA) solution, 4% in PBS		Fixative	Thermo Scientific
SpectroFlo Quality control (QC) beads	-	Daily flow cytometer QC check	Cytek Biosciences
Apogee Mix sizing beads	Polystyrene and silica beads of known size and fluorescence	Calibrating size on acquisition settings	Apogee Flow

Sheath Fluid (30X)	-	Flow cytometer maintenance	Cytek Biosciences

Table 2.3 Enzyme-linked immunosorbent assay (ELISA) reagents

Reagent	Constituents	Application	Source
PBS	1X PBS	ELISA	Sigma Aldrich
ELISA assay buffer	1X PBS 0.05% Tween-20 (v/v)	ELISA	Sigma Aldrich Invitrogen
Bovine serum albumin		ELISA	Sigma Aldrich
Streptavidin-HRP Cat: N100		ELISA	Thermo Scientific
ELISA substrate reagent	3,3', 5'5'-Tetramethyl-benzidine (TMB)	ELISA	Invitrogen
ELISA stop solution	Sulphuric acid (2N H_2SO_4)	ELISA	Invitrogen

2.1.2 Commercial detection assays

Table 2.4 Commercial detection assay reagents

Kit	Constituents	Source
Quant-iT Pico Green dsDNA kit Cat: P7589	Quant-iT PicoGreen dsDNA reagent (Component A) TE buffer (20X) (Component B) Lambda DNA standard (Component C)	Invitrogen Molecular Probes
Myeloperoxidase ELISA Cat: BMS2038INST	Microwell plate (12 strips of 8 wells each) coated with monoclonal antibody to human MPO, Biotin-Conjugate (anti-human MPO monoclonal antibody), Streptavidin-HRP and sample diluent, lyophilized Human MPO standard curve (coloured) Wash buffer concentrate (20X) (phosphate-buffered saline with 1% Tween™ 20) Sample diluent Tetramethyl-benzidine (TMB) substrate solution Stop solution (1M Phosphoric Acid 1M)	Invitrogen

Human Neutrophil Elastase ELISA Cat: BMS269	Microwell Plate (12 strips of 8 wells each) coated with polyclonal antibody to human PMN Elastase HRP-Conjugate anti-α 1-Polyclonal antibody Human PMN Elastase Standard lyophilized Control high, lyophilized Control low, lyophilized Sample Diluent Wash buffer concentrate (10x) TMB substrate solution Stop solution (2M hydrochloric acid)	Invitrogen
Citrullinated Histone H3 (Clone 11D3) ELISA Cat: 501620	Anti-histone H3 HRP conjugate Anti-Citrullinated Histone H3 ELISA strip plate Citrullinated Histone ELISA standard Immunoassay buffer B (10X) Wash buffer concentrate (400X) Polysorbate 20 TMB substrate solution HRP stop solution	Cayman Chemical
NuQ H3.1 Assay kit Cat: 53511	Wash buffer Assay buffer Control diluent Detection diluent Streptavidin-HRP conjugate Substrate solution NuQ H3.1 Plate NuQ H3.1 detection antibody NuQ H3.1 positive control	Volition Rx Limited Active Motif
Cell Death Detection ELISA Cat: 11 544 675 001	Anti-histone monoclonal antibody (cloneH11-4) Anti-DNA Peroxidase (POD) conjugate Coating buffer (10X) Washing buffer (10X) Incubation buffer Substrate buffer ABTS substrate tablets	Roche Diagnostics
Human Angiopoietin-2 Duoset ELISA	Mouse anti-human Ang-2 capture antibody Mouse anti-human Ang-2 detection antibody	R&D Systems

Cat: DY623	Recombinant human Ang-2 standard Streptavidin-HRP	(BioTechne)
Human IL-1β Duoset ELISA Cat: DY201	Mouse anti-human 1L-1β capture antibody Goat anti-human 1L-1β detection antibody Recombinant human IL-1β standard Streptavidin-HRP	R&D Systems (BioTechne)
Human IL-6 Duoset ELISA Cat: DY206	Mouse anti-human IL-6 capture antibody Goat anti-human IL-6 detection antibody Recombinant human IL-6 standard Streptavidin-HRP	R&D Systems (BioTechne)
Human IL-8 Duoset ELISA Cat: DY208	Mouse anti-human IL-8 capture antibody Goat anti-human IL-8 detection antibody Recombinant human IL-8 standard Streptavidin-HRP	R&D Systems (BioTechne)
Human IL-10 Duoset ELISA Cat: DY217B	Mouse anti-human IL-10 capture antibody Goat anti-human IL-10 detection antibody Recombinant human IL-10 standard Streptavidin-HRP	R&D Systems (BioTechne)
Human MCP-1 Duoset ELISA Cat: DY279	Mouse anti-human MCP-1 capture antibody Goat anti-human MCP-1 detection antibody Recombinant human MCP-1 standard Streptavidin-HRP	R&D Systems (BioTechne)
Human MMP-9 Duoset ELISA Cat: DY911	Mouse anti-human MMP-9 capture antibody Goat anti-human MMP-9 detection antibody Recombinant human MMP-9 standard Streptavidin-HRP	R&D Systems (BioTechne)
Human Myeloperoxidase Duoset ELISA Cat: DY3174	Rat anti-human MPO capture antibody Goat anti-human MPO detection antibody Recombinant human MPO Standard Streptavidin-HRP	R&D Systems (BioTechne)
Human Platelet Factor 4 (CXCL4) Duoset ELISA Cat: DY795	Mouse anti-human PF4 capture antibody Goat anti-human PF4 detection antibody Recombinant human PF4 Standard Streptavidin-HRP	R&D Systems (BioTechne)

Human P-selectin (CD62P) Duoset ELISA Cat: DY136	Mouse anti-human CD62P capture antibody Sheep anti-human CD62P detection antibody Recombinant human CD62P Standard Streptavidin-HRP	R&D Systems (BioTechne)
Human Tissue Factor/Coagulation Factor III Duoset ELISA Cat: DY2339	Mouse anti-human TF capture antibody Goat anti-human TF detection antibody Recombinant human TF standard Streptavidin-HRP	R&D Systems (BioTechne)
Human TNFα Duoset ELISA Cat: DY210	Mouse anti-human TNFα capture antibody Goat anti-human TNFα detection antibody Recombinant human TNFα standard Streptavidin-HRP	R&D Systems (BioTechne)
Human VEGF Duoset ELISA Cat: DY293B	Mouse anti-human VEGF capture antibody Goat anti-human VEGF detection antibody Recombinant human VEGF standard Streptavidin-HRP	R&D Systems (BioTechne)
Human von Willebrand Factor A2 Duoset ELISA Cat: DY2764-05	Mouse anti-human vWF-A2 capture antibody Sheep anti-human vWF-A2 detection antibody Recombinant human vWF-A2 standard Streptavidin-HRP	R&D Systems (BioTechne)
Duoset ancillary reagent kit Cat: DY008B	Clear polystyrene microplates (five 12x8-well strip microplates) ELISA plate sealers (24 plate sealers) TMB ELISA substrate (1X, five 12.5 mL vials) Stop solution (1X, three 11 mL vials) ELISA plate-coating buffer (1X, one 60 mL vial) Reagent diluent concentrate 2 (10X, two 21 mL vials) Wash buffer (25X, six 21 mL vials)	R&D Systems (BioTechne)

2.1.3 Pharmacological agents

Table 2.5 Agonists, antagonists, and inhibiting agents

Reagent	Application	Source
Calcium ionophore (A23187) Cat: C7522	Leucocyte and platelet agonist	Sigma Aldrich
Eptifibatide (Cat: 4725/1)	Glycoprotein IIb/IIIa inhibitor	Tocris (BioTechne)
Lipopolysaccharide (LPS) from Escherichia coli O111:B4 Cat: tlrl-3pelps	Leucocyte agonist	Invivo Gen
Phorbol 12-myristate 13-acetate (PMA)	Neutrophil agonist (NETosis)	Tocris (BioTechne)
P-selectin pathway inhibitor KF38789 Cat: 2748	Platelet antagonist	Tocris (BioTechne)
Thrombin (Coagulation Factor II) Cat: 2196-SE-200	Coagulation agonist	Tocris (BioTechne)
Thrombin receptor activating peptide-6 (TRAP-6) Cat: 34967	Platelet agonist	Tocris (BioTechne)

2.1.4 Instruments, equipment and software

Table 2.6 Venepuncture and in vitro blood work consumables

Equipment	Application	Source
Safety-Lok blood collection Set + Holder 21G Cat: 367282	Venepuncture	Becton Dickinson
Trisodium citrate (0.129 M, 3.8%; 4.5ml) vacutainer tubes Cat: 363080	Venepuncture	Becton Dickinson
Lithium heparin (10ml) vacutainer tubes Cat: 368884	Venepuncture	Becton Dickinson
Lithium heparin (4ml) vacutainer tubes Cat: 368480	Venepuncture	Becton Dickinson
K3 EDTA (10ml) vacutainer tubes Cat: 367525	Venepuncture	Becton Dickinson

K3 EDTA (3ml) vacutainer tubes Cat: 368856	Venepuncture	Becton Dickinson
Serum (SST) (8.5ml) vacutainer tubes Cat: 367953	Venepuncture	Becton Dickinson
Serum (SST) (4ml) vacutainer tubes Cat: 368967	Venepuncture	Becton Dickinson
S-Monovette hirudin (1.6ml) tube Cat: 04.1959.001	Venepuncture	Sarstedt
Vacuette ACD-A (9ml) tube Cat: 455055	Venepuncture	Greiner Bio-One
Paxgene blood RNA tubes Cat: 762165	Venepuncture	Qiagen

Table 2.7 Instruments for ELISA protocols

Equipment	Application	Source
Plate washer	ELISA	Dynex Technologies
Stat-Matic manual plate washer	ELISA	Merck
96 well plate – clear	ELISA	Thermo Fisher
96 well plate – black	Immunofluorescence	Thermo Fisher
ELx800 absorbance microplate reader	ELISA Colorimetric plate reader	BioTek

Table 2.8 Flow cytometry protocols

Equipment	Application	Source
Northern Lights 3-Laser spectral flow cytometer	Flow Cytometry	Cytek

Table 2.9 ibidi microfluidics protocols

Equipment	Source
Ibidi pump system quad (4 fluidics units)	Thistle Scientific
Perfusion set, 1.6mm ID, 15cm length	Thistle Scientific
0.4mm u-slide, ibiTreat	Thistle Scientific
Injection port	Thistle Scientific
Terumo 10mls syringes	Scientific laboratory supplies
Terumo 1ml syringe	Scientific laboratory supplies
18G blunt fill needle	Scientific laboratory supplies

Table 2.10 Miscellaneous equipment

Equipment	Application	Source
FLx800 fluorescence microplate reader	Fluorescence plate readings	BioTek
Multifuge 3-SR swing out centrifuge	Centrifugation	Heraeus
Centrifuge 5417R	Centrifugation	Eppendorf
Centrifuge 5427R	Microcentrifuge	Eppendorf
Centrifuge 5702R	Microcentrifuge	Eppendorf

Table 2.11 Software packages

Software	Application	Source
FlowJo v10.8.7	Flow cytometry	Tree Star Inc
Prism 9.5.1	Statistical analysis	GraphPad
SpectroFlo	Flow cytometry software for use with Northern Lights	Cytek

2.1.5 Antibodies

Table 2.12 In vitro isolated neutrophil NETs – Flow cytometry antibodies

Antigen	Clone	Fluorophore	Final concentration	Source
CD66b	G10F5	PE-Cy7	1:400	Biolegend
Myeloperoxidase	455-8E6	PE	1:80	BD Biosciences
Neutrophil Elastase	950344	APC	1:80	Novus Biologicals
Histone H3	D1H2	AF647	1:100	Cell Signalling
Sytox Green	-	FITC	10ul/ml	Invitrogen

Table 2.13 Whole blood NETs – Flow cytometry antibodies

Antigen	Clone	Fluorophore	Final concentration	Source
CD66b	G10F5	PE-Cy7	1:100	Biolegend
Myeloperoxidase	455-8E6	PE	1:40	BD Biosciences
Histone H3	D1H2	AF647	1:40	Cell Signalling
Sytox Green	-	FITC	10ul/ml	Invitrogen

Table 2.14 Whole blood cell phenotyping – Flow cytometry antibodies

Antigen	Clone	Fluorophore	Final concentration	Source
Annexin V	-	FITC	1:50	Biolegend
Bovine Lactadherin	-	FITC	1:40	Prolytix
CD10	HI10a	BV605	1:100	Biolegend
CD11b	ICRF44	BV605	1:100	Biolegend
	ICRF44	PE-Cy5	1:100	Biolegend
CD14	HCD14	APC-Fire 750	1:100	Biolegend
CD16	3G8	FITC	1:100	Biolegend
CD41	HIP8	PE-Cy7	1:100	Biolegend
	HIP8	APC	1:100	Biolegend

CD45	2D1	BV421	1:100	Biolegend
	2D1	PE-Cy7	1:100	Biolegend
CD61	VI-PL2	PE-Cy7	1:100	Biolegend
	VI-PL2	AF647	1:100	Biolegend
CD62L	DREG05	AF647	1:100	Biolegend
CD62P	AK4	BV605	1:100	Biolegend
	AK4	PE	1:100	Biolegend
CD64	10.1	APC-Fire750	1:100	Biolegend
CD66b	6/40c	BV421	1:100	Biolegend
	G10F5	PE-Cy7	1:100	Biolegend
CD142	NY2	PE	1:100	Biolegend
HLA-DR	LN3	AF647	1:100	Biolegend

2.2 Clinical Studies

2.2.1 A CLUE Study (COVID-19 Flu ECMO)

The retrospective observational analysis of the Royal Brompton and Harefield Hospitals (RBHH) ECMO database was approved by the Research Ethics Committee (REC) Healthcare research authority (HRA) Reference 20/EM/0204 [153]. This is a retrospective cohort study comparing the differences in baseline characteristics and outcomes in patients with influenza and COVID-19 ARDS treated with VV ECMO and conventional therapy in a SARF unit. All patients lacked capacity, and the need for individual informed consent was waived for retrospective analysis of data collected prospectively for routine care, with no breach of privacy or anonymity.

2.2.2 DeVENT Study

The Decision Support System to Evaluate VENTilation in ARDS (DeVENT) trial was a multi-centre, international, prospective randomised control superiority trial that investigated whether an open-loop computer-based decision system (Beacon Caresystem) can reduce mechanical ventilation time in ARDS patients. The study also aimed to examine the biological and physiological factors that determine the worsening of ARDS and the processes involved in recovery from ARDS by collecting longitudinal blood, urine and bronchoalveolar fluid samples [154]. The DeVENT study was conducted across three adult intensive care units (one each in the UK, France and Austria).

In the UK, the study received ethical approval by the London South-East REC HRA Reference 19/LO/1606, Integrated Research Application System (IRAS) 266521, clinicaltrials.gov NCT04115709 on 15 January 2020. Ethical approval for subsequent prospective studies using blood, bronchoalveolar fluid and urine samples collected from this study has been granted by REC. The study protocol was approved by the French Ethics Committee (Comité de Protection des Personnes Sud Mediterranee III; approved on July 30, 2020, under number 2019.12.06 ter_19.11.15.76132) and Medicine Agency (Agence Nationale de Sécurité du Médicament; approved on July 3, 2020, under number 2019-A02610-57-A). The study protocol was approved by the ethics committee of Medical University of Vienna, Austria (EC No. 2056/2019) on 28 April 2020. Monitoring and oversight were provided by the Imperial Clinical Trials Unit, and independent trials steering and data monitoring and ethics committees. The study was conducted in accordance with Good Clinical Practice guidelines, local regulations, and the ethical principles described in the Declaration of Helsinki.

For the purposes of this thesis only the patients recruited in the UK will be described. Adult patients were included if they fulfilled ARDS criteria (as per Berlin definition: a known clinical insult with new worsening respiratory symptoms; chest radiograph with bilateral infiltrates consistent with evidence of pulmonary oedema but not fully explained by cardiac failure; hypoxemia as defined by PF ratio of ≤300mmHg (or ≤40kPa) (pre-ECMO PaO_2/FiO_2 should patient be placed on extracorporeal support) [155]. Exclusion criteria included age <18 years old; absence of an arterial catheter, decline in consent, greater than 7 days of mechanical ventilation, treatment withdrawal imminent within 24 hours, a do not attempt resuscitation order being in place, severe chronic respiratory disease requiring domiciliary ventilation and/or home oxygen therapy (except for sleep disordered breathing); requirement of VA ECMO; head trauma or other conditions with requirement of tight regulation of arterial CO2 level. Informed consent was obtained from the patient, personal consultee, or independent nominated professional, with retrospective consent obtained from the patient or personal consultee if possible.

Blood samples were collected within 6 hours before ECMO initiation, and after enrolment to the study. For the DeVENT study, samples were labelled in relation to the day of recruitment e.g. day of recruitment is baseline (BL), D1, D2, D3 etc. DeVENT sample collection included

the following time points: pre-ECMO, study enrolment (baseline), Day1 (D1), Day 3 (D3), D5, D7, D10, D14, and weekly thereafter.

All samples were taken from an already indwelling arterial line or central venous catheter. The DeVENT study recruited 55 patients between March 2020 to April 2021 in the UK site. Of these, 44 (80%) had COVID-19, and 43 (78%) were on VV ECMO..

2.2.3 HITEC Study

The Haemostasis and Immunothrombosis in Extracorporeal Circuits study (The HITEC Study) is a prospective observational cohort study designed to support this research PhD. The aim of this study is to examine the biological and ECMO mechanical changes during patients' ECMO runs with emphasis on changes before and after initiation of ECMO, in patients who develop thrombotic complications leading to circuit change, and before and after decannulation of ECMO. The study protocol and supporting documents (consent forms, recruitment logs, case report forms) were developed and written during the first year of this PhD. HRA REC approval was granted in January 2022 (HRA reference 21/WA/0395, IRAS 294477) [156] and the study opened for recruitment in May 2022 at the Royal Brompton Hospital. The study is conducted in accordance with Good Clinical Practice guidelines, local regulations, and the ethical principles described in the Declaration of Helsinki.

Eligible patients include critically ill adult patients (age >18years) who are transferred from referral sites to the Royal Brompton Hospital through the ECMO service, with severe respiratory and cardiac failure who may require extracorporeal life support (ECLS), including but not limited to ECMO (VV and VA), VAD, and CPB. Exclusion criteria include age <18 years old, decline in consent, and treatment withdrawal imminent within 24 hours. As this was an observational exploratory study there was not enough information to base a power calculation.

The sampling timeline differs to the DeVENT timeline. Samples are labelled in relation to the day of ECMO, e.g. blood samples are collected pre-ECMO, after consent, and once a week (every 5-7 days) from initiation of ECMO e.g. Day 0 (D0), Day 1 (D1), D7, D14 etc. All samples were taken from an already indwelling arterial line or central venous catheter. See Figure 2.1 for the patient journey whilst on ECMO.

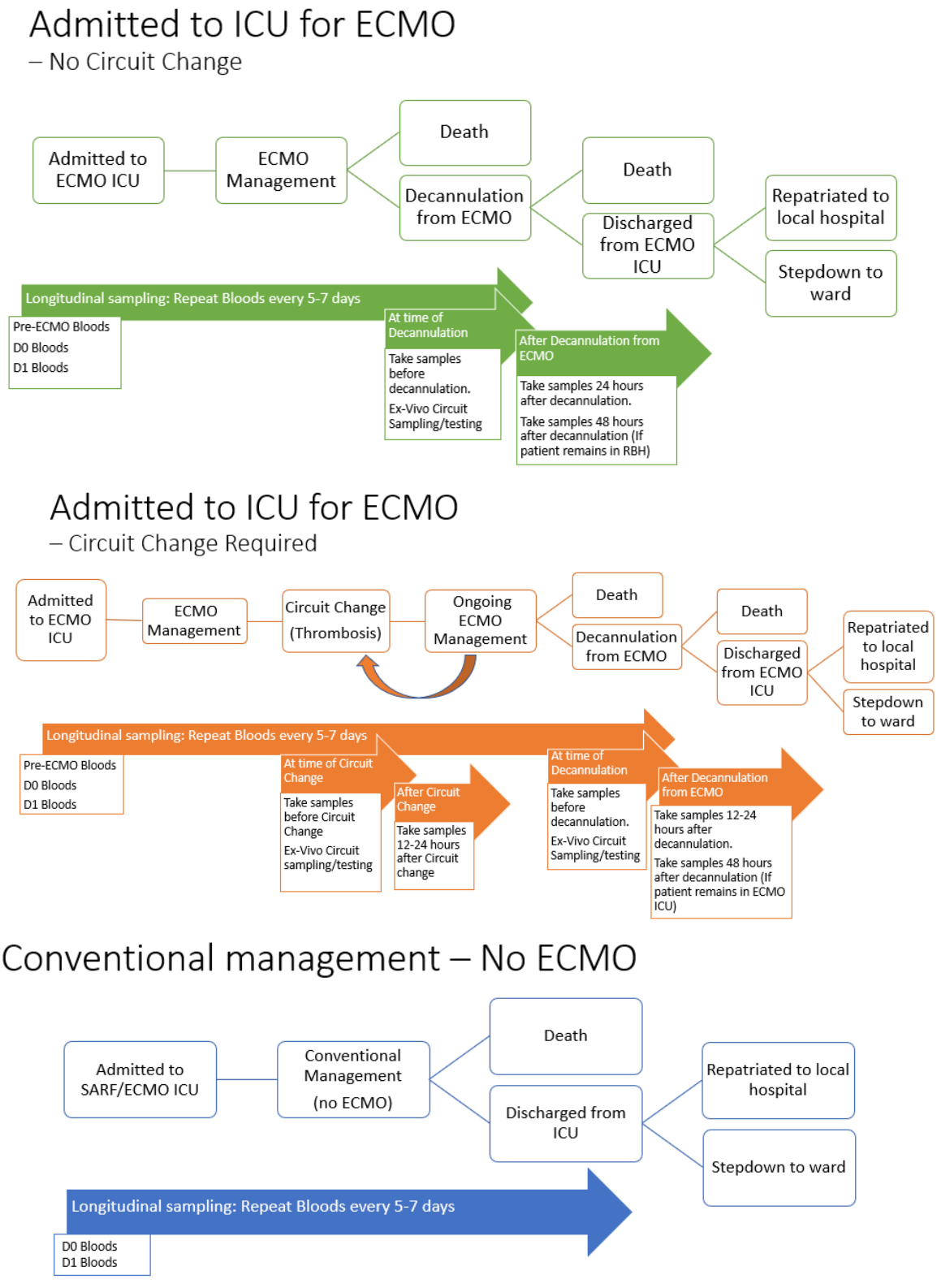


Figure 2.1 Timelines of patients admitted to RBH via the SARF or cardiogenic shock pathway on ECMO or conventional management.

If recruited to HITEC study the patients have bloods taken pre-ECMO initiation, after recruitment to the HITEC study and once a week thereafter until decannulation. Additional blood samples are taken if a circuit change is required. Samples are labelled in relation to the day of ECMO.

2.2.4 HITEC Blood sampling

Informed consent or assent was obtained for all patients and informed consent for all healthy volunteers (HV) enrolled in the DeVENT and HITEC studies. Blood samples from patients were taken from already inserted vascular access devices (arterial line or central vascular catheter) and did not require additional venepuncture. Blood from HV was collected by standard venesection technique using a 21G vacutainer system (Becton Dickinson).

Pre-ECMO bloods were collected by the ECMO retrieval team in the hours before ECMO initiation at the referral centre. They were stored in a fridge (4°C) and not processed until the patient was recruited into the study. For some samples this could be up to 48hours later. Once recruited, blood samples were collected from patients at baseline after ECMO initiation (Day 0 and Day 1), and every 5 days thereafter until decannulation from ECMO. Additional samples were taken at key events such as ECMO circuit change and ECMO decannulation. If a patient required a circuit change, bloods were collected on the day of circuit change prior to circuit change (CC), occurring, and also the next day (CC+1) where possible. If the patient had more than once circuit change the subsequent samples was labelled CC2 and CC2+1 as appropriate. At decannulation from ECMO, samples were taken on the day of decannulation (DC) and the day after (DC+1) (See table 2.16 for sample collection schedule).

		Blood tubes required						0.5ml taken from total samples Citrate or Li-Heparin bottles		
	Volume per tube (mls)	EDTA	ACD	Citrate	SST	Li-Hep	PAX Gene	TEG (Citrate blood)	Multiplate	Total blood (mls)
		8	8.5	4.5	4.5	9	2.5	0.5	1	
Pre-ECMO Bloods (If possible)	Once	X	X	X	X	X				32.5
Longitudinal Sampling (All Patients)	D0 (Bloods on arrival to RBH)	X	X	X	X	X	X			35
	D1	X	X	X	X	X				34.5
	Every 5-7 days (4-6 weeks)	X	X	X	X	X	X			34.5
Circuit Change Sampling (Clinical decision)	On the day	X	X	X	X	X				34.5
	12-24 hours after	X	X	X	X	X				34.5
Decannulation Sampling (All Patients)	On the day	X	X	X	X	X				34.5
	12-24 hours after	X	X	X	X	X				34.5
Ex-Vivo circuit (After circuit change or decannulation)	250mls blood	X	X	X	X	X				250
	Take for storage	12mls	17mls	9mls	9mls	18mls				

Table 2.15 HITEC blood sample collection.

The blood tubes and volumes required per sampling point.

Study day (in relation to ECMO), D; Extracorporeal membrane oxygenation, ECMO; cardiopulmonary bypass, CPB; ethylenediaminetetraacetic acid, EDTA; Anticoagulant Tri-sodium Citrate with Citric Acid and Dextrose, ACD; serum separation tube, SST; Lithium-Heparin, Li-Hep; and Thromboelastogram, TEG.

If samples were taken in hours, then a Thromboelastogram (TEG, Haemonetics) and platelet function tests using the Multiplate analyser (Roche Diagnostics) were also performed at the same time. Platelet function tests were only performed if the platelet count was >100 x 10^9/ml. Some samples were missed due to events happening out of hours.

At some timepoints, samples were collected pre-oxygenator and post-oxygenator rather than from an indwelling line, to investigate if there were any differences pre- and post-membrane. This sampling method could only be done as clinical experience of the research team allowed due to the risks of air entrainment into the ECMO circuit.

Samples were only taken if there were research staff available for processing of bloods. As such if a circuit change or decannulation occurred out of hours, samples would not have been taken and therefore there are some timepoints with missing samples.

2.2.5 Blood processing

Bloods from both DeVENT and HITEC studies were processed in the same way. After collecting blood from patients, all specimen tubes were inverted 5-10 times to ensure thorough mixing with the tube additive. All samples, except SST were placed on ice and processed within 4 hours of collection.

Small aliquots of whole blood were used for platelet function assay and TEG at the time of sampling. In addition, whole blood aliquots from patient samples are analysed using flow cytometry within 4 hours.

The remaining blood in ethylenediaminetetraacetic acid (EDTA), anticoagulant tri-sodium citrate with citric acid and dextrose (ACD), citrate and lithium-heparin tubes were centrifuged to collect platelet rich plasma (PRP) and platelet poor plasma (PPP) fractions (see table 2.17). SST tubes were allowed to clot for 30 minutes before centrifugation at 20°C. The plasma and serum were aliquoted as 1ml samples and stored in 1.5ml Eppendorfs at -80°C until analysis performed.

	No spin	2000 *x g* 10 mins	1st spin. 400 x *g* 10mins	2nd spin. 1500 *x g* 15mins
EDTA	Whole blood flow cytometry for NET quantification	Plasma for cytokines		
Li-Heparin	Whole blood flow cytometry for leucocyte phenotyping and LPA quantification	In vitro assays		
SST		Serum		
ACD			PRP	PPP for EV quantification
Citrate	Thromboelastogram		PRP	PPP
Hirudin	Multiplate			

Table 2.16 Summary of the patient blood processing for storage

Centrifugation speeds and time to obtain plasma samples from each vacutainer blood tube. All centrifugation (apart from SST) carried out at 4°C.

Anticoagulant tri-sodium citrate with citric acid and dextrose, ACD; Ethylenediaminetetraacetic acid, EDTA; extracellular vesicles, EV; leucocyte-platelet aggregate, LPA; serum separator tube SST; relative centrifugal force (RCF), x g; platelet poor plasma, PPP; platelet rich plasma, PRP.

The majority of samples were processed by the Royal Brompton Hospital Research Sample Processing Lab. Out of hours samples, where taken, were processed by me at Imperial College London APMIC labs, Chelsea and Westminster Hospital. All samples were stored in the Imperial College London APMIC labs, at Chelsea and Westminster Hospital, London. All samples followed the same processing and labelling protocol.

2.3 Lab protocols

2.3.1 Peripheral blood mononuclear cell (PBMC) and neutrophil isolation

Blood was taken from HV using EDTA vacutainers. Histopaque-1077 (Sigma Aldrich) and Histopaque-1119 (Sigma Aldrich) double density gradient separation was performed at room temperature. Histopaque-1077 (3mls) was carefully layered onto Histopaque-1119 (3mls) in a 15ml polypropylene tube (Falcon™, VVR). Whole blood (4-6mls) was then layered onto the Histopaque-1077 as the upper layer and centrifuged at 700 x *g* in a swing-out rotator for 30 minutes at room temperature with no brake. Following centrifugation, blood was separated into distinct layers (as shown in Figure 2.2): plasma, peripheral blood mononuclear cells (PBMC), Histopaque, neutrophils, and red blood cells.

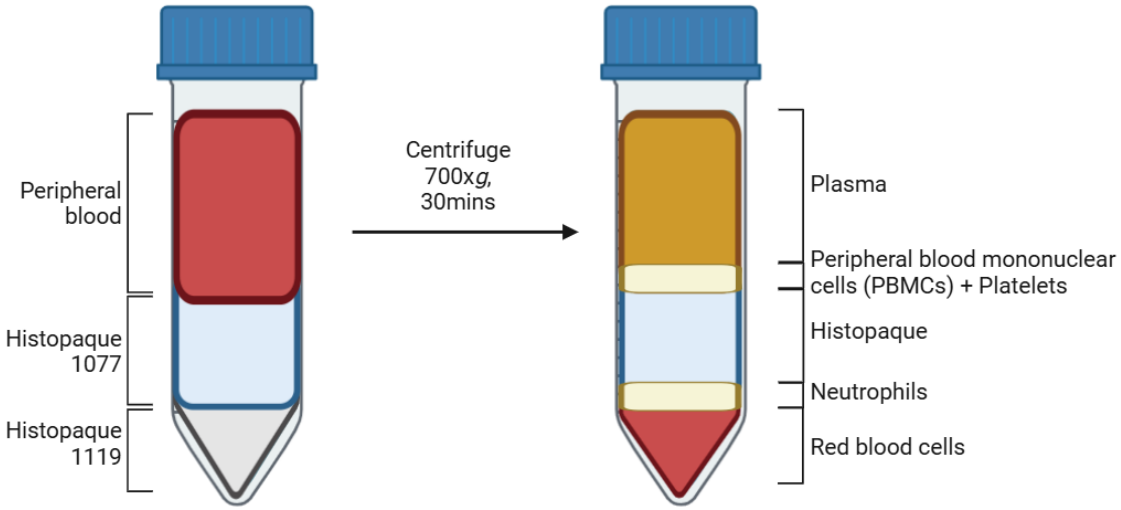


Figure 2.2 Peripheral blood mononuclear cells and neutrophil isolation technique using double density gradient separation.

Layered Histopaque-1119 (3mls), Histopaque-1077 (3mls) and blood (4-6mls) is centrifuged at 700 x g for 30 minutes and room temperature. Distinct layers are seen after centrifugation. The PBMC and neutrophil layer are aspirated using Pasteur pipettes. Created with Biorender.com.

The plasma layer was aspirated and stored in 1ml aliquots in 1.5ml Eppendorfs as control samples. The PBMC layer was gently collected using a sterile Pasteur pipette and transferred to a new 15ml Falcon tube. The PBMC layer was discarded if monocytes were

not required. Using a fresh Pasteur pipette, the neutrophil layer was collected into a new 15ml Falcon tube. Cold, sterile phosphate-buffered saline (PBS, without Ca^{2+}/Mg^{2+}) (Sigma), was added to the Falcon to a final volume of 15mls, and centrifuged at 400 x *g* for 7 minutes at 4°C. The supernatant was discarded to leave the cell pellet. Any remaining erythrocytes were lysed by suspension with 5ml red blood cell lysis buffer (Biolegend) for 10 minutes as per manufacturer's instructions. The cells were washed (centrifugation at 400 x *g*, 7 minutes, 4°C) with PBS twice. After washing, the cells were resuspended in 1ml of RPMI-1640 media (Sigma-Aldrich) with 0.5% human albumin solution (BioIVT, GEM-800-120-S) or 10% autologous serum, Hanks Balanced Salt Solution (HBSS) or PBS as appropriate for experiment conditions. The cells were counted using flow cytometry by diluting 5µl of cells into a FACS tube containing 500µl of FACS wash buffer. Different populations were identified by the forward and side scatter and cell counts determined using volumetric-based counting method.

2.3.2 Isolated neutrophil stimulation

Freshly isolated neutrophils (PMN) were cultured in RPMI-1640 medium with antibiotics penicillin-streptomycin-glutamine (Life Technologies) and 0.5% HAS. Cells were added to 12-well polystyrene tissue culture plate at 3.75 x 10^6 cells/well (750µl of 5 x 10^6 cells/ml suspension). Phorbol 12-myristate 13-acetate (PMA) (Sigma-Aldrich) at 50nM or 100nM was used to stimulate NET production. The plates were placed in a 37°C incubator with 5% CO_2 in air, for 1 hour, 2 hours, or 3 hours. Cells left on ice unstimulated served as untreated controls. After stimulation, using a 1ml micropipette, the wells were rinsed with the media within the well to gently detach the neutrophils and NETs. All material and media (cell-NET mix) were collected into 1.5ml Eppendorfs and kept on ice until further processing.

2.3.3 Platelet rich plasma stimulation

Whole blood was taken from HV into vacutainers containing heparin or ACD anticoagulant. The vacutainers were centrifuged at 400 x *g*, for 10 minutes at 20°C, to obtain PRP. PRP was stimulated in 1.5ml Eppendorfs with agonists (thrombin receptor activating peptide-6 [TRAP-6], thrombin, calcium ionophore [A23187], lipopolysaccharide [LPS]) for 1 hour in a rotator, at 37°C. Aliquots of PRP at room temperature, on ice or in the rotator untreated served as controls. After stimulation, PRP was stained to quantify platelet activation.

2.3.4 Whole blood stimulation

Whole blood stimulation assays were used for pilot data and to validate protocols. Heparinised and EDTA anticoagulated whole blood was used depending on the protocol. Whole blood was stimulated at 37°C in Eppendorfs left static, in a rotator for continuous mixing, or in flow conditions using the ibidi microfluidics pump system (see below). Whole blood was stimulated with LPS 100ng/ml, PMA 100nM, TRAP-6 10uM or left unstimulated for 1-4 hours depending on the protocol.

Following stimulation, aliquots of whole blood were analysed directly by flow cytometry (Section 2.4), and remaining blood was centrifuged at 2000 x *g,* for 10 minutes at 4°C to obtain cell- and platelet-free plasma. The plasma was stored at -20°C for further downstream processing.

2.3.5 Ibidi microfluidics pump system

The ibidi microfluidics pump system was used for experiments under flow conditions. The ibidi pump system can produce unidirectional laminar flow within a microchannel slide, allowing different flow rates and shear rates to be applied within the slide. This was used to simulate physiological conditions of blood flow over 'foreign' or synthetic surfaces, such as that in the ECMO circuit or in the ECMO oxygenator in vivo.

The microfluidics pump system consists of an air pump connected with the pump control software, and four fluidics units. Each fluidic unit includes two reservoirs (syringes) sealed with air filters, a perfusion set (tubing) of various inner diameters, and a microchannel slide of various channel heights. The fluidic unit's active component are the two switching valves which create the unidirectional flow. There are two connectors at the back of the fluidic unit: one electrical connection for the valve control and one for the pressurised air. Both connect the fluidic unit to the pump. The set up of the ibidi microfluidic parallel pump system is shown in Figure 2.3. The pump system can be set up with 4 fluidics units in parallel allowing different conditions to be run at the same time. The air pressure generated flow, rather than standard peristaltic flow avoids physical compression and potential activation of cells.

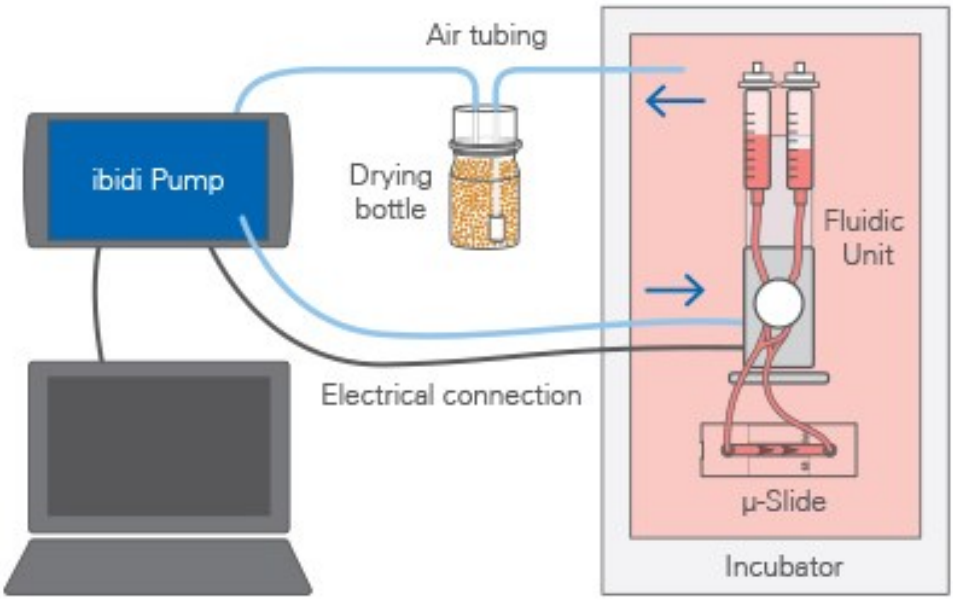


Figure 2.3. Schematic diagram showing set up of the ibidi microfluidics pump system.

The ibidi air pump is connected to a computer with the ibidi Pump control Software. Air tubing connects the pump to the fluidics unit via air filters at the top of the reservoirs. Each fluidics unit consists of two reservoirs (syringes) containing the perfused medium, connected to the perfusion set, and a microchannel slide. The blue arrows indicate the direction of air flow.

The air pump generates a constant pressure (mbar) that pumps the medium from one reservoir to another across the microchannel slide. The applied pressure results in a specific flow rate (ml/minute), that is dependent of pressure input, the tubing size, channel height, and the viscosity of the medium (e.g. blood or media). The specific flow rate produces a shear stress (dyn/cm^2) on adhered cells within the microchannel slide (Table 2.17). A wide range of flow rates and shear stress can be generated to simulate physiological flow patterns.

Microchannel Slide height (mm)		Pressure (mbar)	Flow rate (ml/min)	Shear stress (dyn/cm^2)
0.8	Min	5	0.92	0.96
	Max	95	11.71	12.21
0.6	Min	5	0.91	1.64
	Max	95	11.66	21.02
0.4	Min	5	0.88	3.48
	Max	95	11.06	43.68
0.2	Min	5	0.43	6.62
	Max	95	6.37	98.02

Table 2.17 Range of flow rates and shear stress that can be generated using the ibidi microfluidics system

These are the minimum and maximum flow and shear rates that can be generated when using whole blood at 37°C (with an assumed viscosity 0.03 dyn·s/cm^2) and 1.6mm ID, 15cm perfusion sets. The flow rates change with different microchannel slide heights.

Before each reservoir empties, a computer controlled 2-way valve system switches the direction of flow, therefore continuous unidirectional flow within the microchannel slide is achieved. The software allows users to customise the flow parameters to design a regimen for different volumes of fluid by adjusting the switch time.

2.3.6 Whole blood stimulation in the ibidi microfluidics pump system

This system was used to investigate leucocyte-platelet interactions in heparinised whole blood under flow conditions approximating to flow within the membrane oxygenator. The microfluidics pump was placed in a cell culture incubator with 5% CO_2 at 37°C. The pump moves the blood in a closed tubing system which maintains sterility. To allow repeated sampling from the system without interrupting flow, injection ports were included into the circuit after the microchannel slide, from which samples were aspirated with a 18G blunt non-filter needle and 1ml syringe. See figure 2.4 to see a typical experiment set up with 15cm 1.6mm perfusion sets, and 0.4mm microchannel slides. The assumed viscosity of blood at 37°C is between 2-5 Centipoise (cP) or 0.02-0.04 dyn·s/cm^2 (as measured by the ibidi pump system). For the purposes of these experiments a standard blood viscosity of 0.03 dyn·s/cm^2 was assumed.

Blood was taken from HV into heparin vacutainers and decanted into 5ml Eppendorfs. Agonists were added as required for the experiment: LPS 100ng/ml or TRAP-6 10nM. All Eppendorfs were vortexed gently to allow adequate mixing. For inhibition experiments eptifibatide (1µg/ml) and KF38789 (20µM) were added to whole blood and incubated for 10 minutes prior to adding the agonist.

Using a Pasteur pipette, the blood was added to syringe A of the perfusion unit and allowed to fill the perfusion set, and equilibrate the volumes in both syringe A and B. The whole ibidi system was placed in the incubator at 37°C. Once all perfusion sets had equilibrated, the experiment was started with the required pressure to generate a flow rate of 2.5ml/minute through a 0.4mm microchannel slide which equates to a shear stress of 10dyn/cm^2 on cells adhered within the microchannel slide. Samples were taken from the injection port at set time points. Unused blood was reinjected into the system via the injection port.

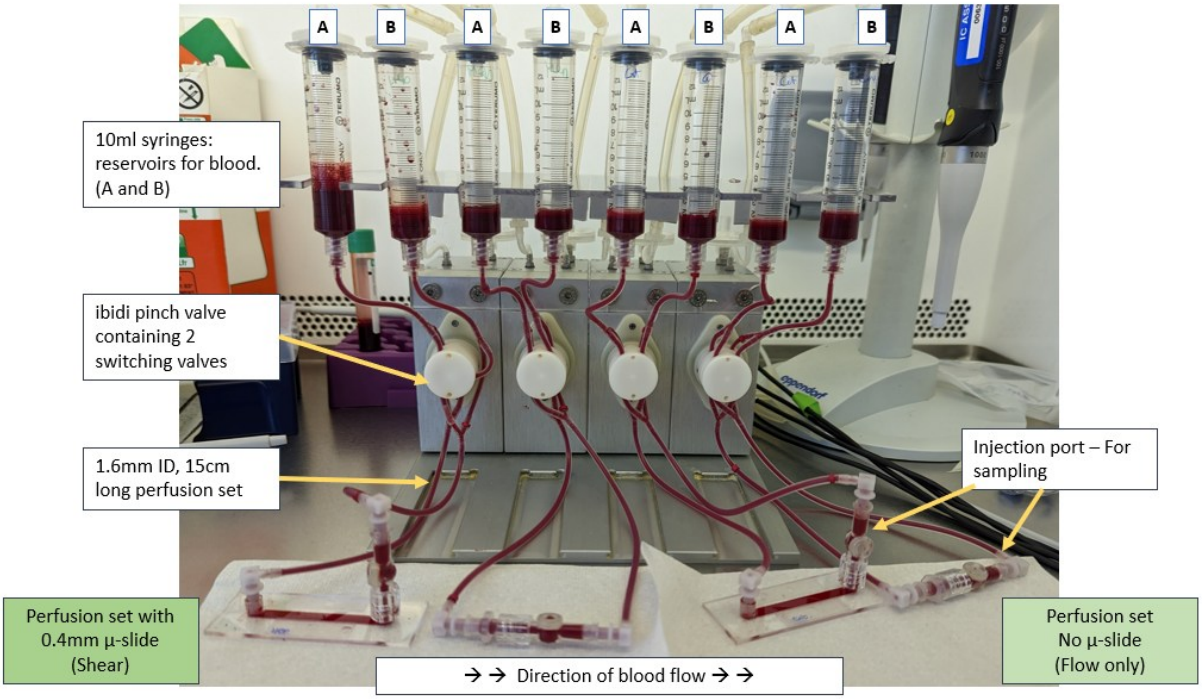


Figure 2.4 Figure showing the experiment set up using four parallel fluidics units.

Using this set up four different conditions can be run simultaneously. In the experiments described, blood is the medium with an assumed viscosity of 0.03 dyn·s/cm^2 at 37°C. Using the 1.6mm ID 15cm perfusion sets, 0.4mm microchannel slides, and a blood flow rate of 2.5ml/minute.

2.4 Flow cytometry protocols

2.4.1 Introduction to spectral flow cytometry

Flow cytometry is a well-established and widely used cell analysis technique which allows the identification of different subpopulations of cells. A cell suspension is hydrodynamically focussed using sheath fluid and a small nozzle into a single cell stream which passes through a laser beam (Figure 2.5). The cells are identified based on cell size (detected as forward scatter; FSc), granularity (detected as side scatter; SSc), and expression of various combinations of cell surface markers, receptors or intracellular molecules.

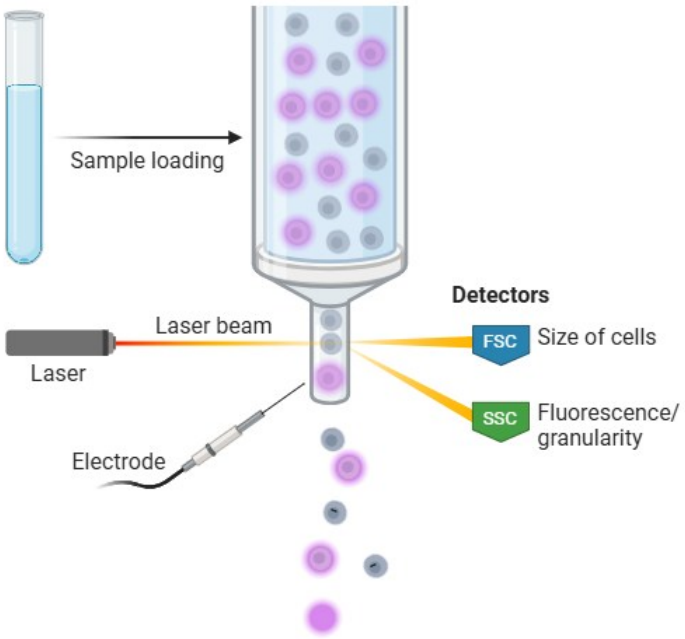


Figure 2.5 The basic principle of flow cytometry

The detection of some fluorescent protein or fluorochrome combinations by conventional flow cytometry presents a challenge due to high amounts of spectral overlap which limits the number of fluorophores that can be used and therefore limits differentiation of different sub populations of cells. Spectral flow cytometry (SFC) provides more information for each fluorophore which allows for increased resolution and sensitivity. Unlike conventional flow cytometers that direct specific bandwidths of fluorescence light into discreet detectors or photomultiplier tubes, SFC uses solid-state multi-channel, narrow-beam detector array for each laser. Each array can be configured with up to 16 detectors that are used to capture a part of the emission spectrum from each particle passing through the laser beam. Using mathematical algorithms and reference controls, spectral deconvolution or “unmixing” can distinguish different fluorophores which have similar emission maxima but differing off-peak emissions. This provides greater flexibility and capability in panel design even if populations are co-expressed.

The flow cytometer used for work in this thesis is Northern Lights spectral flow cytometer (Cytek), which utilises 3 lasers. The violet, blue and red lasers have 16, 14 and 8 detection channels respectively. The Northern Lights SFC can analyse samples with up to 24 fluorophores, with careful panel design (Table 2.18).

Violet Excited Fluors	Peak Channel	Blue Excited Fluors	Peak Channel	Red Excited Fluors	Peak Channel
BV421	V1	BB515, sVio515, Vio515	B1	APC	R1
Alexa Fluor 405, Super Bright 436, Zombie Violet, Live/Dead Blue	V2	Alexa Fluor 488, FITC, VioBright FITC, Zombie Green	B2	Alexa Fluor 647, Vio 667, sVio 667, Live/Dead Far Red, eFluor 660	R2
eFluor 450, VioBlue, Pacific Blue, Live/Dead Violet	V3	Alexa Fluor 532, Live/Dead Green	B3	APC-Cy5.5	R3
BV480	V4	PE	B4	Alexa Fluor 700, APC-R700	R4
eFluor 506	V5	PE/Dazzle 594, PE-CF594, PE-eFluor 610, PE-Texas Red	B6	APC-Alexa 750, APC/Fire 750, APC-Cy7, APC-Vio 770, APC-eFluor 780, APC-H7, Live/Dead NIR	R7
BV510, VioGreen, Zombie Aqua, Live/Dead Aqua	V7	PE-Cy5, PerCP	B8		
BV570, Pacific Orange, Live/Dead Yellow	V8	PE-Cy5.5, PerCP-Cy5.5, BB700	B9		
BV605, Super Bright 600, Qdot 605, Live/Dead Red, Zombie Yellow	V10	PerCP Vio700, PerCP-eFluor 710	B10		
BV650, Super Bright 645, Qdot 655	V11	PE Vio770, PE-Cy7	B13		
BV711, Super Bright 702, Qdot 705	V13				
BV750	V14				
BV785, BV786, Qdot 800	V15				

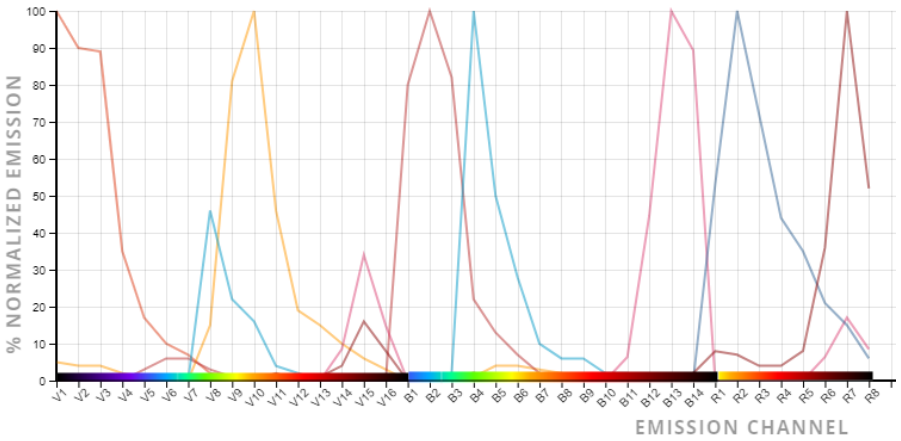
Table 2.18 Fluorochrome peak channels for a 3 laser Northern Lights spectral flow cytometer. *The violet, blue and red lasers have 16, 14 and 8 detection channels respectively.*

Similarity index and complexity index

Fluorophores are compared to each other using the similarity index. A value close to 0 indicates spectral signatures that are not similar, and a value close to 1 indicates spectral signatures that are similar. In order to use two fluorophores together, and be able to distinguish one from another, the similarity index should be $\leq$0.98.

The complexity Index is a measure of how distinguishable a collection of spectral signatures are from each other when unmixed together. It calculates this by looking at the ratio of the similarity index of the worst overlapping combination of signatures to the best overlapping combination of signatures. The lower the better. If designed well, the complexity of 10-fluorophore panels will be 2-3, and a 40-fluorophore panel will be 40-50.

For the leucocyte phenotyping panels, 8 fluorophores were selected which created a panel with complexity index 1.99 and no similar fluorophores (Figure 2.6). Flow cytometry data was acquired using SpectroFlo Software and data was analysed using FlowJo 10.8 Software (Three Star, Ashland, OR, USA).



BV421	1							
BV605	0.06	1						
FITC	0.01	0.01	1					
PE	0	0.25	0.08	1				
PE-Cy5	0	0.21	0.01	0.12	1			
PE-Cy7	0	0.04	0	0.03	0.15	1		
Alexa Fluor 647	0	0.03	0	0.01	0.32	0.03	1	
APC-Cy7	0	0.02	0	0	0.09	0.29	0.22	1

Complexity™ Index: 1.99

Figure 2.6 Similarity and complexity index for a panel using 8 fluorophores.

There were no similar emission profiles, and the complexity index is low.

2.4.2 Determining particle size using ApogeeMix sizing beads

Particle size using flow cytometry is usually determined by light scatter (FSc and SSC), however same sized particles of different refractive index (e.g. biological vs synthetic particles) can give different signal strengths. The ApogeeMix sizing beads are a mixture of 6 populations of non-fluorescent silica beads, which have a similar refractive index to biological vesicles, and 2 populations of fluorescent polystyrene beads which can be used to prepare flow cytometers for the analysis of small biological particles such as extracellular vesicles. Figure 2.7 shows the flow plots for ApogeeMix sizing beads acquired on extracellular vesicle settings.

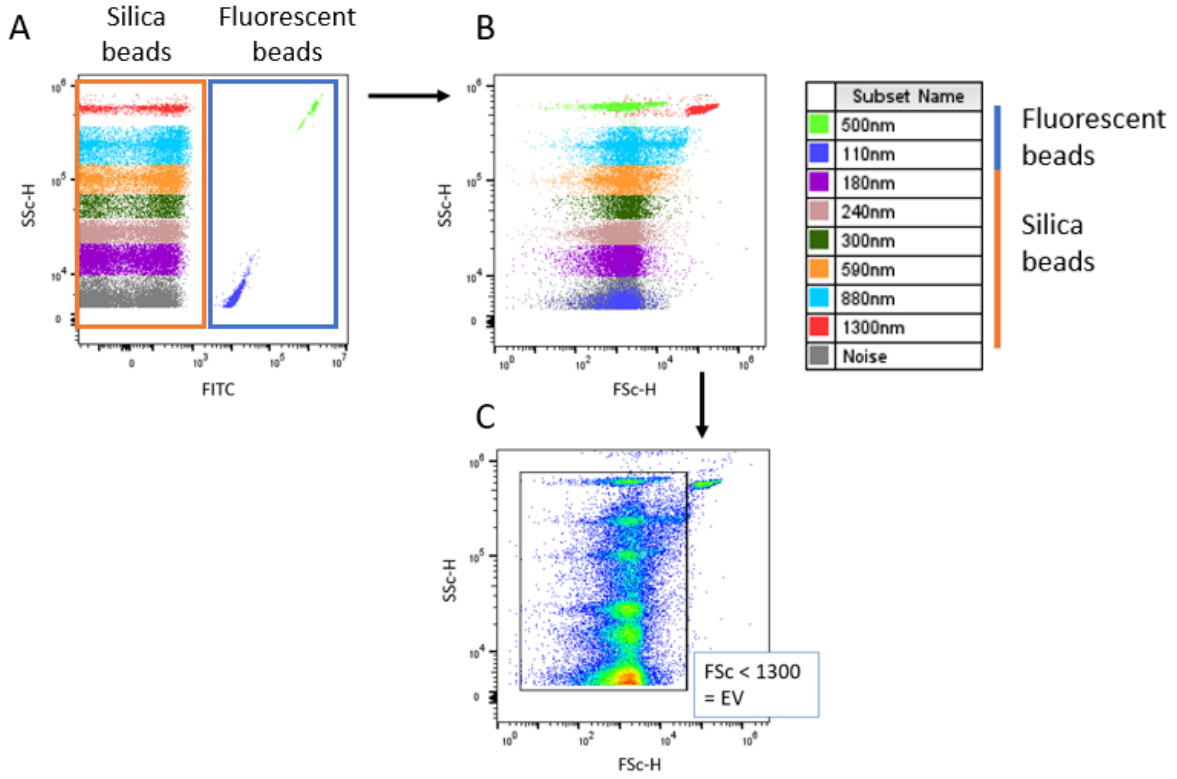


Figure 2.7. ApogeeMix Sizing beads run Cytek Northern lights spectral flow cytometer.

Samples acquired on modified settings for extracellular vesicles. A) The 2 populations of fluorescent beads (110nm and 500nm) were differentiated from each other and the silica beads using the FITC channel. B) The silica bead populations were able to be differentiated from each other based on light scatter. C) Particles that were smaller than FSc 1300nm were gated as extracellular vesicles.

2.4.3 Isolated PMN NETs staining and flow cytometric analysis

Neutrophils and media from stimulation in tissue culture plates (as described in 2.3.2) were collected and kept on ice until further processing. The fluorochrome-conjugated antibody cocktails for NET quantification were prepared in FACS wash buffer (FWB) at the final concentrations stated in table 2.12. Cell suspensions (10µl) were incubated with fluorochrome-conjugated antibody cocktail (10µl) for 30minutes in the dark at 4ºC. After incubation, 480µl of FWB and 5µl Sytox green was added and vortexed to ensure adequate mixing. The samples were left for 15 minutes in the dark at room temperature, before acquisition on the flow cytometer (Figure 2.8). Neutrophils were identified by their CD66b expression, and those that were double positive for MPO and cfDNA or HistoneH3 and cfDNA were considered cell-associated NETs.

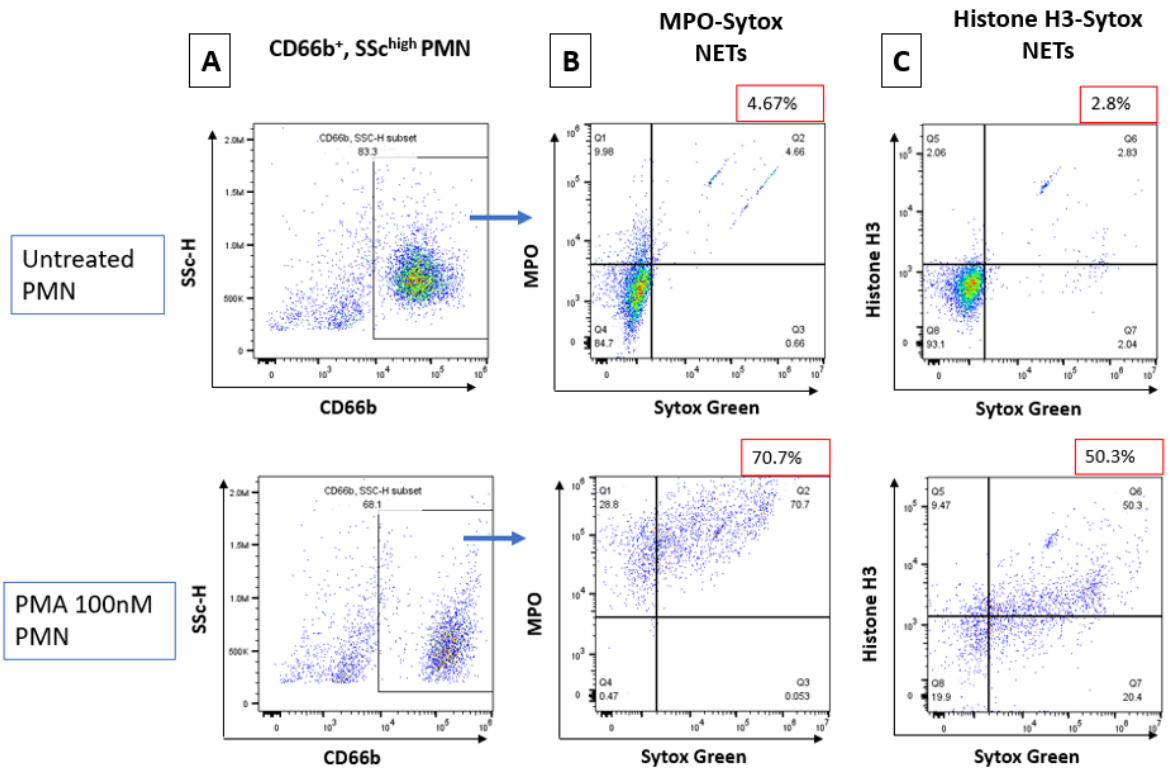


Figure 2.8 Identification of neutrophils and quantifying cell-associated NETs using flow cytometry.

(A)Neutrophils were identified by CD66b expression and high side scatter. Neutrophils were gated for Sytox green staining and (B) myeloperoxidase (MPO) or (C) histone H3. Neutrophils that were double positive for (B) MPO and Sytox Green or (C) Histone H3 and Sytox Green were considered cell-associated NETs. The proportion of NETs was quantified as a percentage. PMA is a very potent stimulator for NETosis. The proportion of NETs increased after PMA stimulation.

2.4.4 Whole blood NETs staining and flow cytometric analysis

To determine the proportion of neutrophils undergoing NETosis in patient samples, cell-associated NETs were quantified using flow cytometry. This allows for immediate and efficient quantification of NETs from multiple patient whole blood samples on the same day and less handling and processing of samples with other methods of quantification such as fluorescent microscopy, which often require 2-day staining protocols; or ELISA, requiring samples to be centrifuged to obtain plasma or serum and stored for downstream batch analysis.

EDTA whole blood (20µl) was incubated with antibody cocktails (20µl) (Table 2.13) for 30minutes in the dark at 4ºC. After incubation, 460µl of FWB and 5µl Sytox green added and vortexed to ensure adequate mixing. The samples were left for 15 minutes in the dark at room temperature before acquisition on the flow cytometer to collect 10000 PMN events (Figure 2.9).

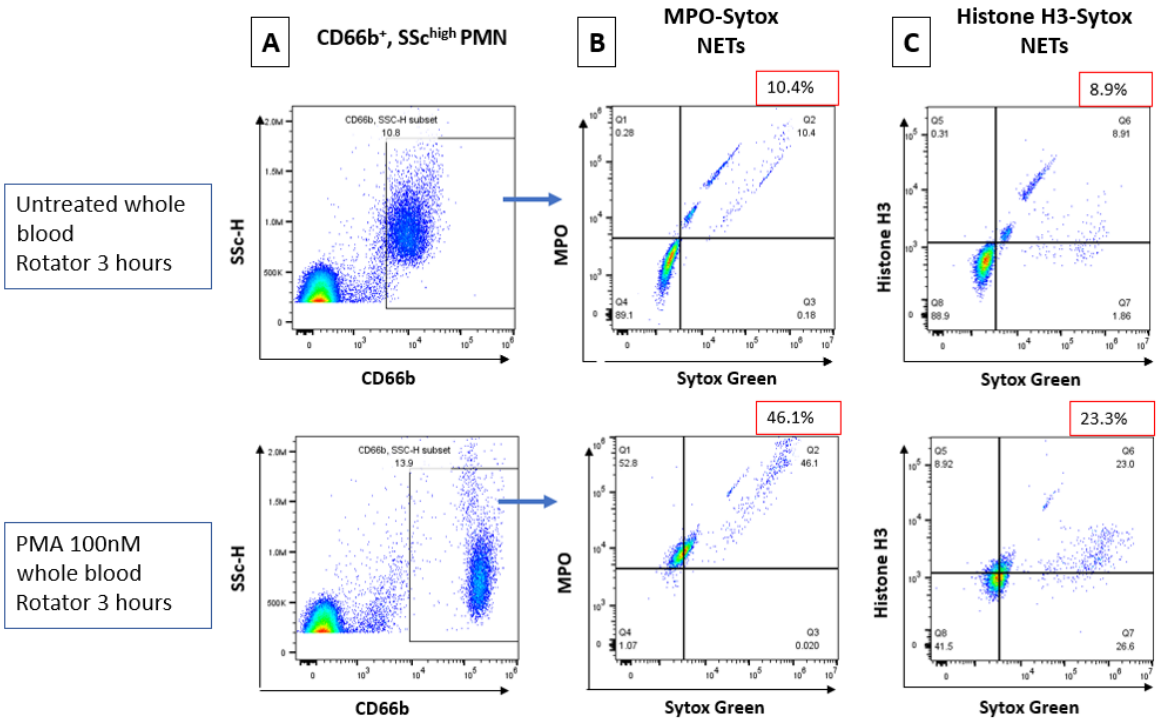


Figure 2.9 Identification of neutrophils and quantifying cell-associated NETs in whole blood using flow cytometry.

(A) Neutrophils were identified by CD66b expression and high side scatter. Neutrophils were gated for Sytox green expression and (B) myeloperoxidase (MPO) or (C) histone H3. Neutrophils that were double positive for (B) MPO and Sytox Green or (C) Histone H3 and Sytox Green were considered cell-associated NETs. The proportion of NETs was quantified as a percentage.

When running non-lysed whole blood on a flow cytometer, the smaller erythrocytes, platelets, and other debris from dead cells produces a lot of noise, which may interfere with the acquisition of the target cells. To exclude debris from being counted in a sample, a gating threshold can be set based on size, or expression of a specific marker. In the whole blood samples, a minimum threshold for the neutrophil specific marker CD66b was set to gate for neutrophils and exclude erythrocytes, monocytes and lymphocytes. As well as quantifying the proportion of cell-associated NETs, the expression of certain proteins can be quantified by measuring the mean fluorescent intensity (MFI) of those markers (Figure 2.10).

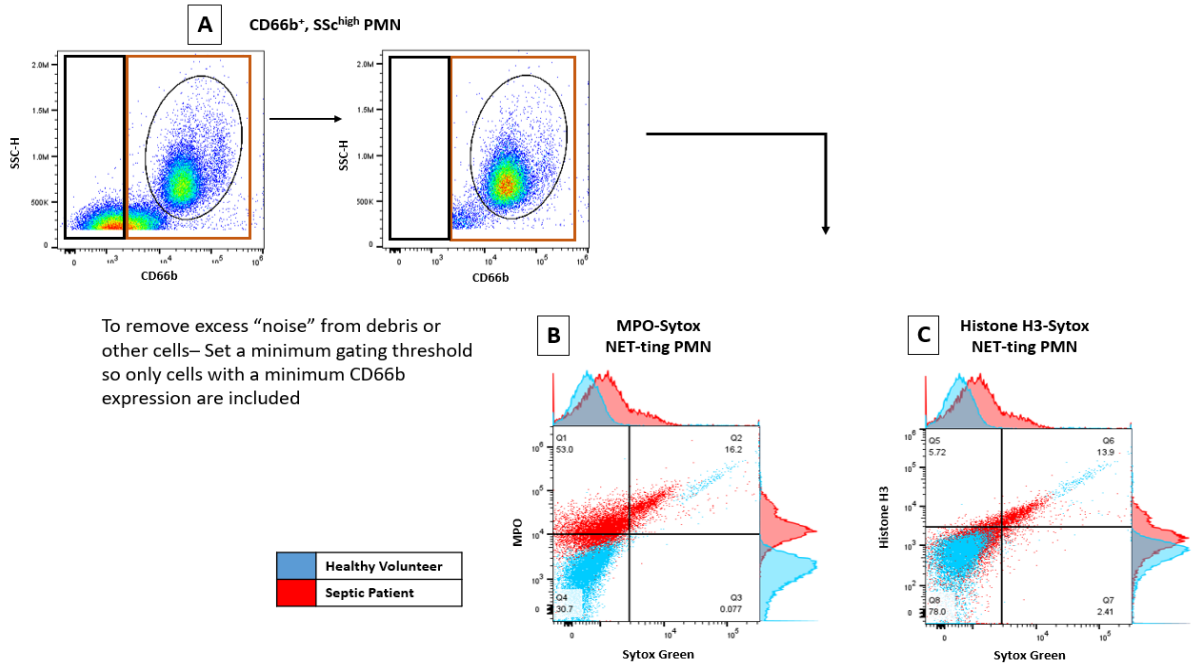


Figure 2.10 Using SpectroFlo to gate for specific cell types and measure the expression of specific markers.

(A)Neutrophils were identified by CD66b expression and high side scatter. To exclude debris/noise, only events that had CD66b expression over a set threshold were included. Neutrophils were gated for Sytox green expression and (B) myeloperoxidase (MPO) or (C) histone H3. The mean fluorescent intensity of cell surface markers can be measured as shown by the histograms. The sample from a septic patient (red) has increased MPO, Histone H3 and Sytox green expression compared to healthy volunteer sample (blue).

Detection of NETs in WB was validated by spiking WB with NETs generated from PMA stimulated neutrophils (Figure 2.11).

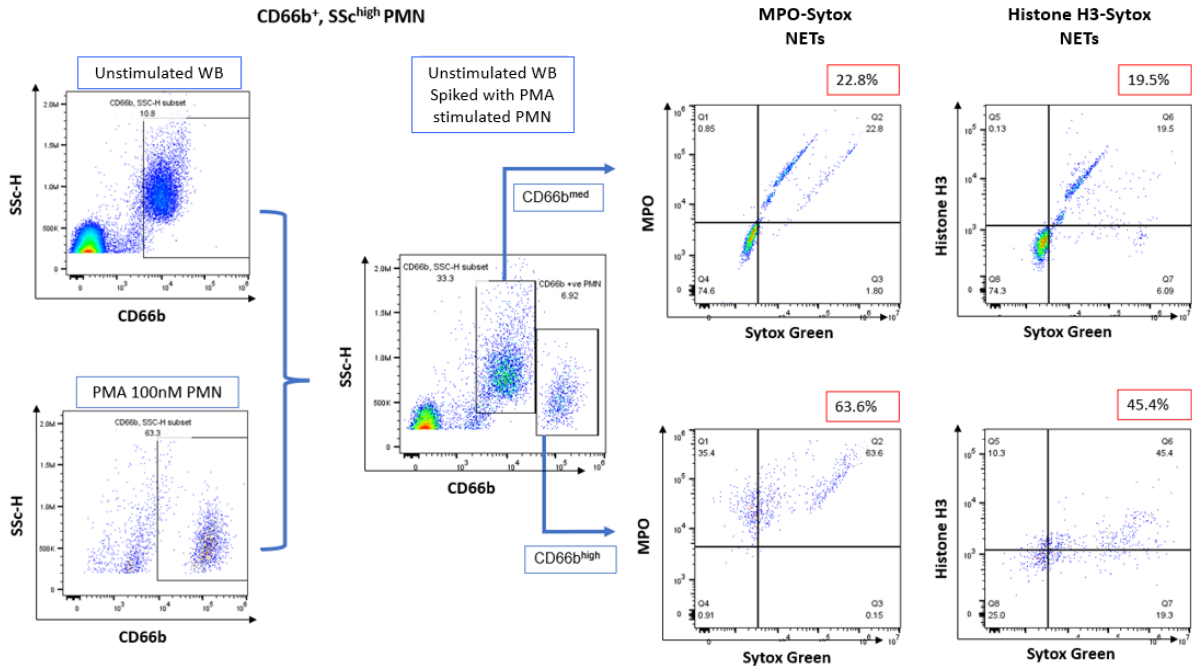


Figure 2.11 Whole blood NETs staining protocol was able to differentiate different levels of cell-associated NETs.

In a sample of unstimulated whole blood spiked with PMA stimulated neutrophils, two populations of CD66b +ve events (neutrophils) were detected. These two populations expressed different levels of MPO, histone H3 and Sytox green which corresponded with the respective stimulation. This demonstrates this protocol was able to detect differing levels of cell-associated NETs in whole blood.

2.4.5 Phenotyping leucocytes and quantifying leucocyte-platelet aggregates by flow cytometry in patient samples

Careful panel design allowed the use of 8-fluorophore panels for patient leucocyte phenotyping and leucocyte-platelet aggregates (Table 2.19).

Fluorophore	Neutrophils	Monocytes
BV421	CD66b	CD45
BV605	CD10	CD11b
FITC	CD16	CD16
PE	CD142	CD142
PE-Cy7	CD41	CD41
AF647	CD62L	HLA-DR
APC-Fire 750	CD64	-
APC-Cy7	-	CD14

Table 2.19 Flow cytometry panel design for neutrophil and monocyte phenotyping in patient samples.

All antibodies were diluted to final concentration of 1:100.

Whole blood (10-20µl depending on protocol) from patients and HV was incubated with antibody cocktails for 15 minutes, in the dark at room temperature. After incubation 500-750µl of BD FACS lyse was added to the FACS tubes for 10 minutes to lyse the erythrocytes and fix samples. Samples were diluted with 2ml PBS and centrifuged at 300 x *g* for 7 minutes at 4ºC. The supernatant was discarded and stained cells were resuspended in 500µl of PBS and run on the flow cytometer to collect 10,000 PMN (Figure 2.12) or 5,000 classic monocyte events (Figure 2.13) depending on the panel.

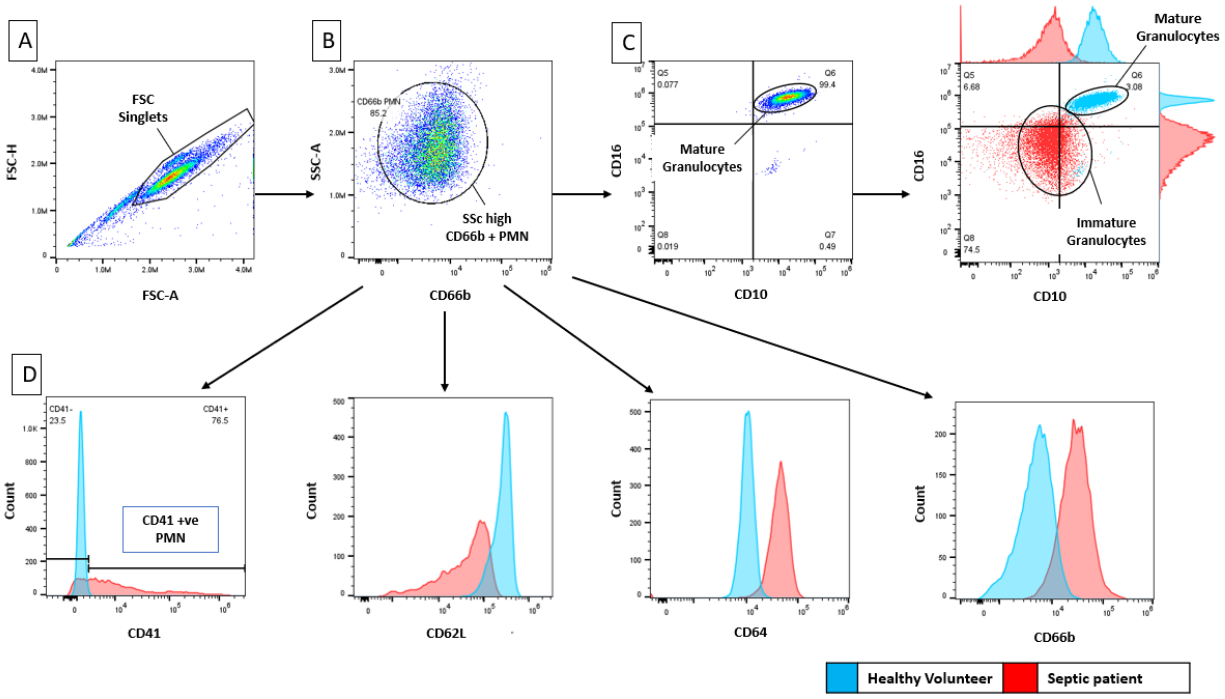


Figure 2.12 Neutrophil phenotyping and gating from whole blood samples

A) Only FSc singlets were counted, B) neutrophils are identified as CD66b+, SSc^{high} events, C) Mature granulocytes are identified as CD16^{high} and CD10^{high} neutrophils, D) Neutrophils that are positive for the platelet marker CD41 are counted as neutrophil-platelet aggregates. Cell surface expression of each marker: CD16, CD10, CD41, CD62L, CD64 and CD66b were measured as mean fluorescent intensity. The histograms and dot plot overlays show the difference in expression of each marker between a healthy volunteer (blue) and a septic patient (red).

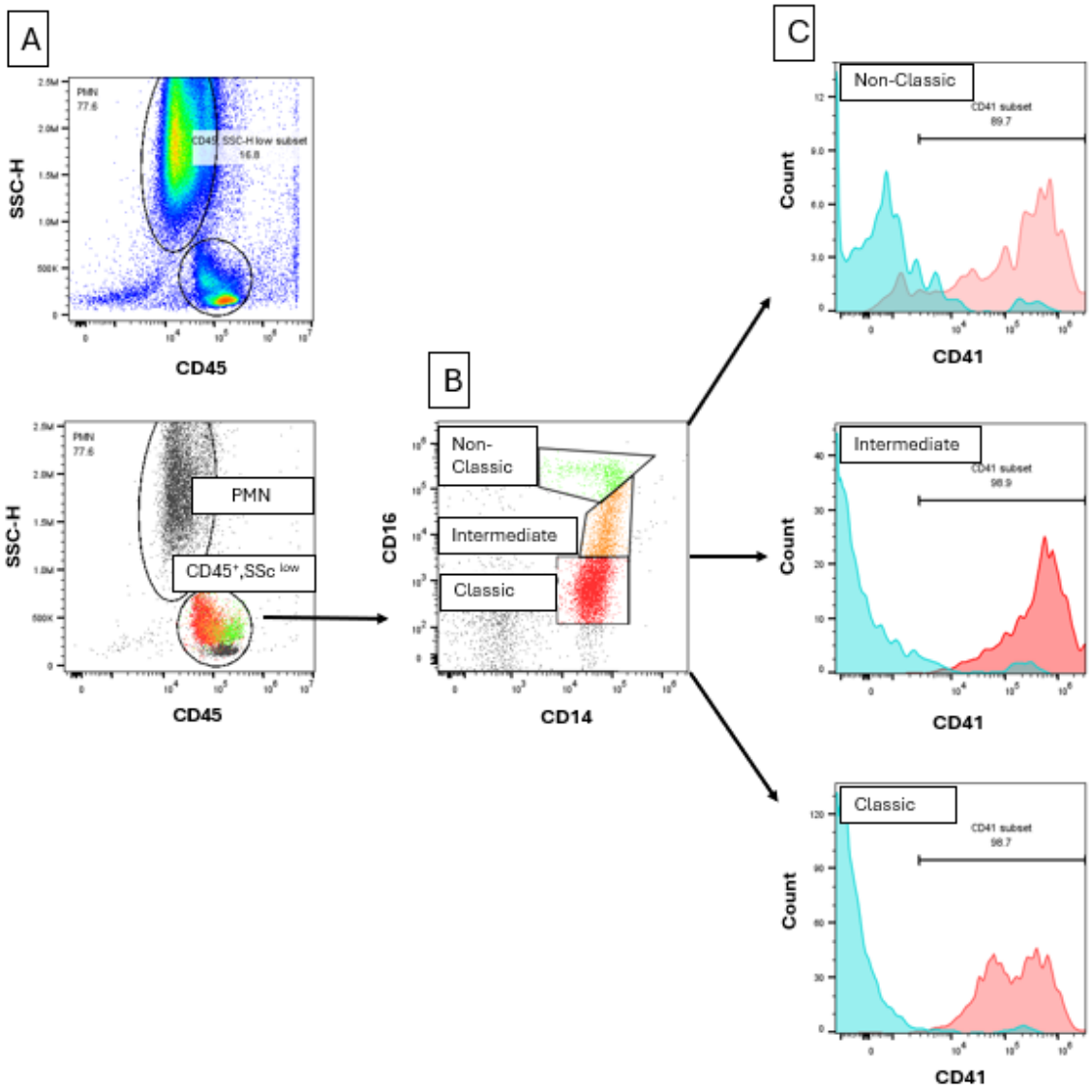


Figure 2.13 Monocyte subset and monocyte platelet aggregate gating in patient samples.

A) Monocytes are identified as CD45^{+} and SSc^{low} B) monocyte subtypes are gated based on their CD14 and CD16 expression: Classic monocytes are CD14^{++}, CD16 $^{-}$, intermediate monocytes CD14^{++}, CD16 $^{+}$ and non-classic monocytes are CD14^{+}, CD16^{++} C) Monocytes that are positive for the platelet marker CD41 are counted as monocyte-platelet aggregates. The histograms show the difference in expression of each marker between EDTA sample (blue) and heparin sample (red).

2.4.6 Phenotyping leucocytes and quantifying leucocyte-platelet aggregates by flow cytometry for in vitro work

A single neutrophil and monocyte panel was used for quantifying neutrophils and monocytes from the in vitro experiments using the ibidi system. The fluorophore panel is shown in table 2.21.

Fluorophore	Marker
BV421	CD45
BV605	CD62P
FITC	BLAC
PE	CD41
PE-Cy5	CD11b
PE-Cy7	CD66b
AF647	CD62L
APC-Cy7	CD14

Table 2.20 Fluorophore conjugated antibodies for quantification of leucocyte-platelet aggregates and phenotyping neutrophils and monocytes for in vitro experiments.

All antibodies were diluted to a final concentration of 1:100.

Whole blood (20µl) was incubated with antibody cocktails for 15 minutes, in the dark at room temperature. After incubation 750µl of BD FACS lyse was added to the FACS tubes for 10 minutes to lyse the erythrocytes and fix samples. Samples were diluted with 2ml PBS and centrifuged at 300 x *g* for 7 minutes at 4ºC. The supernatant was discarded and stained cells were resuspended in 500µl of PBS and run on the flow cytometer to collect 5,000 classic monocyte events.

2.5 Other protocols for measurement

2.5.1 ELISA

Soluble markers were measured using validated DuoSet sandwich ELISA kits according to manufacturer's instructions: Ang-2, IL-1β, IL-6, IL-8, IL-10, MMP-9, MPO, PF4, P-selectin, TNFα, TF, and VEGF. Prior to the assay, 96-well microplates were coated with 50µl of capture antibody diluted to the specific working concentration in PBS. Plates were washed with ELISA wash buffer (1X PBS + 0.05% Tween-20) three times and blocked with 200µl of reagent diluent (1% BSA in PBS) for 1 hour. A seven-point standard curve was made by diluting a reconstituted standard in reagent diluent, using 2-fold serial dilutions. Plates were washed again before addition of 50µl standards and samples and incubating for 2 hours at room temperature on an orbital shaker 450rpm. After another wash step, 50µl of detection

antibody was added to each well and left to incubate on the orbital shaker for a further 2 hours. Plates were washed again and 50µl of streptavidin-conjugated horseradish peroxidase (HRP) was added to each well and incubated in the dark for 20 minutes. After a final wash step, 50µl of 3,3',5,5' Tetramethylbenzidine (TMB) substrate solution was added and incubated in the dark for 30 minutes or until there was visible colour change of the lowest. The reaction was stopped by addition of 50µl stop solution 2M sulphuric acid. The plates were read at 450nm using a microplate reader (BioTek ELx800).

Neutrophil cytoplasmic enzymes and NET components can be released on activation or detach from the neutrophil during NETosis therefore soluble neutrophil activation, and NETosis markers were also measured using ELISA in addition to the flow-based assay described in section 2.4.4. The following commercial detection kits for neutrophil activation and NETosis were used: Human Myeloperoxidase (Invitrogen, BMS2038INST), Human Neutrophil Elastase (Invitrogen, BMS269), Citrullinated Histone 3 (Clone 11D3) (Cayman, 501620); NuQ H3.1 (Volition). These assays were performed as per manufacturer's instructions.

2.5.2 Cell-free DNA

Cell-free DNA (cfDNA) was measured using the Quant-iT PicoGreen fluorometric assay (Invitrogen P7589) as per manufacturer's instructions. In brief, 100µl of EDTA plasma samples and standards were loaded onto black 96-well plates in duplicate. PicoGreen or buffer solution were added to relevant wells and the plate covered with foil and left to incubate for 5 minutes on a plate shaker (200RPM). The plate was read using a fluorescent plate reader (480nm excitation and 520nm emission) (BioTek FLx800). The sample autofluorescence (measured in the column with buffer solution) was subtracted from the sample cfDNA autofluorescence (measured in the column with PicoGreen solution) to calculate the cfDNA concentration against the standard curve.

2.5.3 Multiplate Analyzer

The Multiplate analyser (Roche, Switzerland) is used to determine platelet function in response to platelet agonists. The testing method is called multiple electrode aggregometry and has up to 5 channels. The analysis is based on the principle that activation of platelets leads to platelet aggregation and adherence onto two metal sensor wires in the Multiplate test cuvette. This increases the electrical impedance between the two wires and therefore

the electrical resistance which can be measured. The electrical software calculates the area under the curve (AUC) and reaction velocity. The AUC indicates the agonist induced platelet aggregation capacity.

The common tests used for platelet function testing are the ADP, ASPI and TRAP which tests different pathways of platelet activation (Figure 2.17). The ADP test uses ADP 6.5µM, to stimulate ADP receptors on the platelet surface leading to platelet activation. This tests the pathway for P2Y12 antagonists such as Clopidogrel, Prasugrel or Ticagrelor. The Aspirin (ASPI) test uses arachidonic acid (AA) 0.5mM as the agonist, a substrate for cyclooxygenase (COX) which produces TXA2, a potent platelet agonist. This tests response to COX inhibitors such as aspirin and some non-steroidal anti-inflammatory drugs. Thrombin receptor activating peptide 6 (TRAP-6) mimics thrombin by activating protease activated receptor-1 (PAR-1) on the platelet surface leading to platelet activation. [145, 157]. TRAP-6 32µM is used for the Multiplate test.

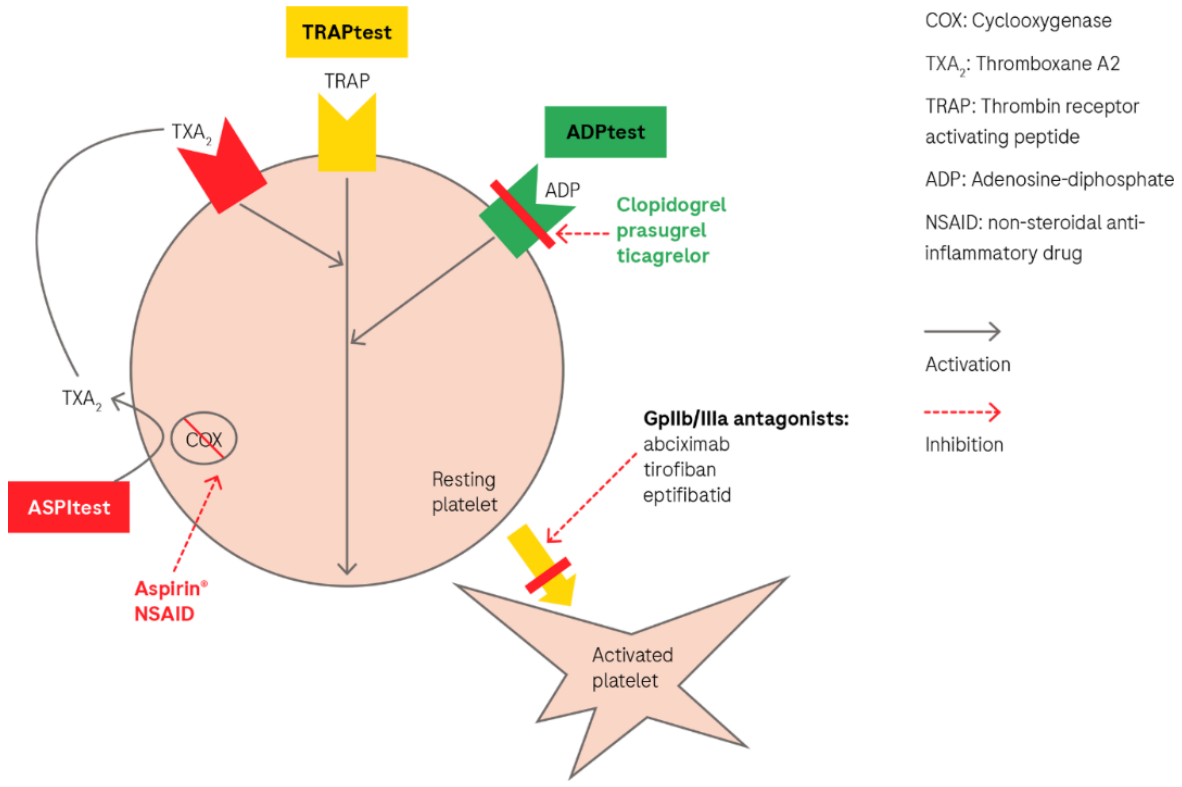


Figure 2.14 The Roche Multiplate analyser tests platelet response to agonists.

Image from Roche Diagnostics [158]

2.5.4 Thromboelastogram

The thromboelastogram is performed in a cup where the blood sample is placed, and a detection pin suspended in its centre. The cup oscillates around the detection pin which records movement. Initially in blood with low viscosity, little pin movement is detected. As the blood coagulates, forming fibrin mesh with platelet aggregation on the mesh, it adheres to the cup and the pin, and the movement of the cup will therefore induce movement of the pin. The greater the viscoelasticity of the clot the higher the amplitude of pin motion. Later as fibrinolysis starts, and the fibrin-platelet clot dissolves, contact with the detection pin is lost and less motion is detected. Newer machines such as the TEG6 (Haemonetics) no longer uses the “pin-in-cup” technique, but resonance where the blood is exposed to a fixed vibration frequency range and the detector measures the vertical motion of blood meniscus under LED and transforms the movement in a tracing of clot dynamics.

The recorded amplitude of movement over time is recorded as a Thromboelastogram (Figure 2.16). The R-time (or reaction time) is the time to initial fibrin formation and is dependent on clotting factors and represents the initiation phase of clot formation. The K-time (or kinetics) is the time taken to achieve a certain level of clot strength (an amplitude of 20mm), which represents the amplification phase of clot formation. The alpha angle (the slope of the line between the end of R and end of K) measures the speed at which fibrin build up and cross linking takes place i.e. the rate of clot formation, and represents thrombin burst or propagation phase. Both K time and alpha angle are dependent on fibrinogen. The maximum amplitude (MA; mm) represents the final strength of the fibrin clot. This is dependent on platelets (80%) and fibrin (20%). The A30 is the amplitude measured at 30 minutes after MA. It is expressed as a % decrease of MA and represent fibrinolysis.

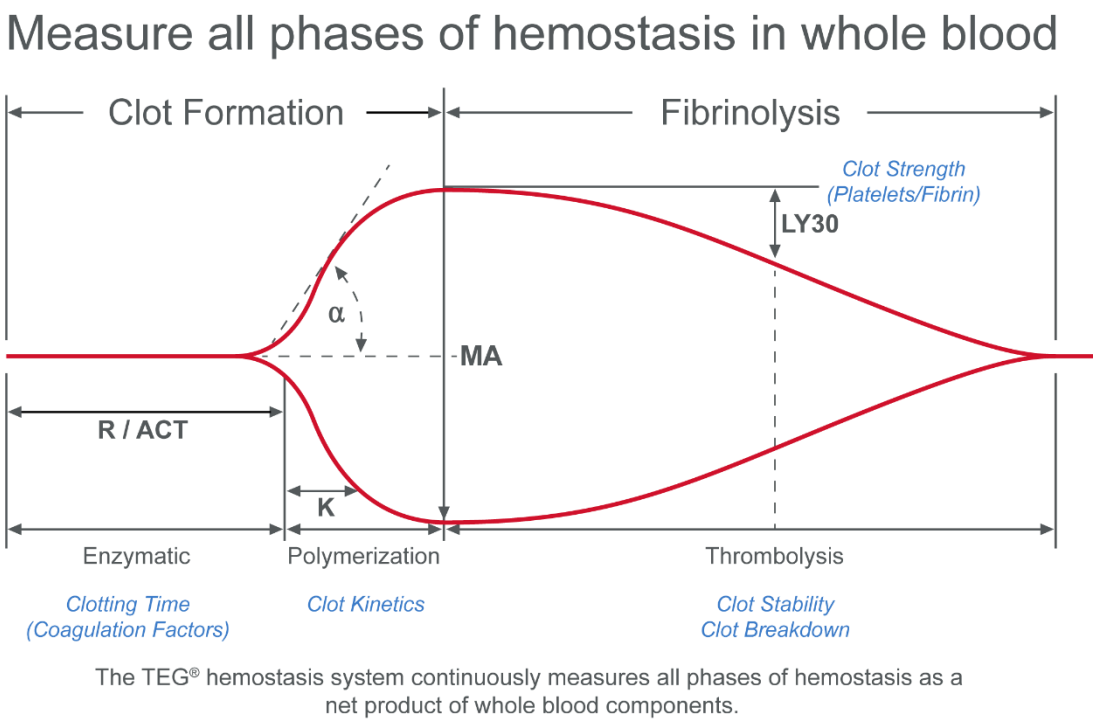


Figure 2.15 Thromboelastogram measuring the viscoelastic properties of whole blood.

The measured amplitude is recorded as a function over time and represents different phases of clot formation. Each phase is dependent on clotting factors, fibrin mesh formation or platelet aggregation and final clot integrity. The R-time or clotting time is dependent on clotting factors. Prolongation of the R-time indicates need for plasma. The K-time and α-angle represent fibrin mesh formation. A longer K-time or shallow α-angle indicates need for cryoprecipitate. The MA of the clot indicates the clot strength and is dependent on platelets and fibrin and therefore indicates the need for platelets +/- cryoprecipitate. Reaction time, R time; Activated clotting time, ACT; Kinetics, K -time; alpha angle, α; Maximum Amplitude, MA; lysis at 30 minutes after MA, LY30. Image taken from Haemonetics (www.teg.haemonetics.com).

2.6 Statistical Analysis

Descriptive statistics were used to summarise the data. Results are presented as mean and standard deviations, or medians and interquartile range, as appropriate. Categorical values were summarised as counts and percentages. Normality testing was carried out with Kolmogorov-Smirnov tests. Differences between groups were compared with the Mann-Witney, t-test, Kolmogorov-Smirnov or Kruskal-Wallis tests as appropriate.

Trends in variables over time and between groups were analysed using two-way ANOVA with repeated measures, or mixed-effects model with Geisser-Greenhouse correction as appropriate.

All statistical tests were 2-sided and $P<0.05$ was considered statistically significant. Analyses were performed using Prism GraphPad Version 9.5.1.(225) Software.

Chapter 3: Clinical observations of immunothrombosis in ECMO patients.

Abstract

The most common component at risk for thrombosis in an ECMO circuit is the membrane oxygenator (MO), often necessitating a circuit change, a high-risk procedure in patients completely dependent on ECMO. Use of VV ECMO increased significantly during the Coronavirus Disease 2019 (COVID-19) pandemic. COVID-19 has been associated with an immunothrombotic phenotype with increased pulmonary angiopathy, hypercoagulability and thrombosis, including deep vein thrombosis, PE and limb ischaemia. The mechanisms of immunothrombosis in COVID-19 include a combination of endothelial dysfunction, cytokine production and activation of leucocytes and platelets.

Within this chapter we evaluated whether the immunothrombotic phenotype of COVID-19 influenced MO thrombosis in VV ECMO patients. This was a single centre retrospective cohort study comparing incidence and clinical indices prior to first circuit change for MO dysfunction, between consecutive COVID-19 and non-COVID-19 patients.

COVID-19 patients had significantly increased incidence of circuit thrombosis requiring circuit change compared to non-COVID-19 patients (62.4% vs 34.0%; P<0.0001). The incidence of circuit change was associated with longer ECMO duration, but there was no difference in mortality between COVID-19 patients who required a circuit change and COVID-19 patients who did not. The time to first circuit change was longer in COVID-19 patients compared to non-COVID-19 patients (13 vs 9 days; P=0.0018). In multivariate analyses, the main risk factor for MO thrombosis was ECMO run time (OR 1.103 [1.073 – 1.140]; P<0.0001).

COVID-19 patients had significantly greater increases in MO resistance in the lead up to circuit change compared to non-COVID-19 patients. Increase in D-dimer prior to a circuit change is widely regarded as a useful marker for monitoring ECMO circuit thrombosis and need for circuit change. However, in COVID-19 patients the rise in D-dimer in the lead up to circuit change was less exaggerated than in non-COVID-19 patients (Δ D-dimer: +1404 vs +8276 ng/ml; P=0.0067). This is likely to represent the lack of fibrinolysis seen in COVID-19.

The altered pathophysiology in COVID-19 patients was able to highlight the impact of immunothrombosis in ECMO which requires further investigation.

3.1 Introduction

3.1.1 Circuit change and importance to outcomes.

The MO is the most common place for thrombosis to occur in patients on ECMO and is associated with increased morbidity and mortality (Murphy et al., 2015; Thiagarajan et al., 2017). MO thrombosis necessitates the need for a circuit change, a high-risk procedure in patients who are completely dependent on ECMO. Occasionally patients require a circuit change due to other mechanical problems such as mechanical pump failure, rupture of tubing or circuit components or leak. Nevertheless, MO thrombosis requiring circuit change is associated with a longer ECMO duration [133, 134].

A circuit change is a partial or complete exchange of the MO, pump head and part of the circuit tubing (Chapter 1.6.4). The ECMO circuit is clamped to restrict blood flow, the circuit is cut between the clamps, and the new circuit is connected under an underwater seal, the clamps removed and the new ECMO pump is started to generate blood flow through the new circuit. The circuit change procedure is usually competed within 10-30 seconds from time of clamping to running back onto the new ECMO circuit. During the time the circuit is clamped, the patient is not receiving any ECMO support and for patients who are completely dependent on ECMO this short period without ECMO support can be very high risk as patients can become hypoxaemic and develop the consequences of hypoxia very quickly, e.g. bradycardia, hypotension or cardiac arrest.

Circuit change remains a common problem associated with ECMO despite advances in circuit component materials and anticoagulation regimes [125, 129]. The initial effect of establishing ECMO creates an overall procoagulant effect. The artificial surfaces of the ECMO circuit leads to contact activation of the coagulation cascade, thrombin generation and fibrin deposition [124]. This procoagulant state necessitates the need for anticoagulation whilst on ECMO. However, patients still develop circuit related thrombosis despite adequate anticoagulation.

3.1.2 Predicting need for circuit change in VV ECMO patients is difficult.

Because of the risks associated with a circuit change, it is important to perform this procedure in patients who truly require it. However, predicting the need for circuit change is difficult in patients who may already have coagulopathy from their underlying disease,

activation of various inflammatory and coagulation pathways from the initiation of ECMO and the need for anticoagulation whilst on ECMO [124, 159].

MO dysfunction is not uncommon and the decision to change a circuit is multifaceted but there are no clear guidelines on this aspect of ECMO management. There are a range of parameters that are measured clinically which help to guide the decision for circuit change, which can be categorised as ECMO mechanical parameters and haemostatic markers. Changes in ECMO mechanical parameters include increasing transmembrane pressure (TMP; mmHg), reducing blood flow (L/min), with the same/increasing mechanical power required (revolutions per minute; RPM) to generate the same blood flow (RPM/blood flow) or increase in transmembrane resistance (TMR; TMP/blood flow) [137, 144]. There is also reduction in gas exchange capacity of the MO as measured by post-oxygenator blood gases demonstrating a reduction in post-oxygenator PaO2 (PpostO2). Changes in laboratory markers include decreasing platelet count and fibrinogen count due to consumption, increase in D-dimers due to increased clot volume, and increasing plasma free haemoglobin (PFH) due to haemolysis [135, 137]. There is no single marker which predicts the need for circuit change; some propose D-dimer as the most sensitive marker for circuit dysfunction, whilst others may promote reduction in PpostO2, or increases in TMP or MO resistance as the most useful [160, 161]. These markers are used in combination along with visual inspection of the circuit and should be monitored daily to determine circuit health [137].

There is no optimal time for circuit change and these decisions are usually dependent on the institution, and a multi-disciplinary discussion between the ECMO physicians and perfusionists.

3.1.3 COVID-19, ARDS and immunothrombosis

The coronavirus disease 2019 (COVID-19) outbreak started in Wuhan, China in December 2019 and was declared a global pandemic by the World Health Organisation (WHO) in March 2020 [162]. It is caused by severe acute respiratory syndrome coronavirus 2 (SAR-CoV-2) and spreads more rapidly than its predecessors SARS-CoV-1, and Middle East respiratory syndrome coronavirus (MERS-CoV) [163]. At the time of writing there have been over 750 million cases and 7 million deaths worldwide [162]. Hypoxic respiratory failure was the dominant complication resulting from COVID-19 resulting in ARDS and ICU admission [164].

Whilst patients who had COVID-19 pneumonia and required invasive mechanical ventilation fulfilled the Berlin definition criteria of ARDS, they were also found have distinct features that were not seen in severe ARDS. Gattinoni and colleagues describe two phenotypes of COVID-19 pneumonia; Type L with low elastance, V/Q mismatch due to perfusion defects, and little pulmonary oedema, compared to the Type H which more closely resembles a severe ARDS patients with high elastance, increased lung weight due to oedema and high right-to-left shunt [165]. COVID-19 also highlighted the important interplay between inflammation and coagulation in critically ill patients with thrombosis a dominant feature with increased incidence of PE, deep vein thrombosis (DVT) and arterial thromboses in COVID-19 patients as compared to non-COVID-19 patients [93, 95, 166-168]. Using dual energy CT scans, it was possible to show significant impairment of pulmonary perfusion, most likely as a consequence of combined pulmonary angiopathy, hypercoagulability, and immunothrombosis [95].

COVID-19 patients demonstrate other biochemical signs of increased hypercoagulability with increased platelet count, increased fibrinogen and D-dimer concentrations compared to non-COVID-19 patients [166, 167]. D-dimer was used as a marker of severity of COVID-19 disease particularly in patients who also had low lung compliance [169]. Furthermore, D-dimer concentrations are consistently higher in patients with severe COVID-19 than in general ICU patients and patients with severe pneumonia not related to COVID-19 [170].

3.1.4 ECMO use in COVID-19 associated ARDS

As with ARDS, the most severe COVID-19 patients required invasive mechanical ventilation and those who were refractory to conventional therapies may be initiated on ECMO [95, 171]. There was a substantial surge in ECMO use during the pandemic with over 16,000 patients requiring ECMO for COVID-19 worldwide [172, 173]. ECMO is usually used as rescue therapy for refractory ARDS patients who can no longer be managed safely with conventional ventilation. Consensus guidelines for the use of ECMO in COVID-19 patients and for ECMO during a pandemic were developed by ELSO [174]. Most COVID-19 patients who required ECMO were supported on VV ECMO for ARDS. Early referral to ECMO centres was recommended and whilst there were no data to suggest deviation from conventional ECMO management, contraindications for ECMO use may have been more stringent as ECMO capacity diminished [28, 174]. Use of ECMO for patients with COVID-19 related ARDS has been reported to have similar survival outcomes compared to patients who required ECMO for non-COVID-19 related ARDS [175-177].

COVID-19 associated coagulopathy includes both thrombotic and bleeding events. The risk of thrombosis dominates over the risk of bleeding therefore anticoagulation was recommended for critically ill patients with COVID-19 with no significant increase in bleeding complications [178]. Specific haemostatic complications related to ECMO include circuit thrombosis, increased rates of PE and intracranial haemorrhage in COVID-19 patients on ECMO [129]. Early single centre studies suggested increased MO thrombosis in COVID-19 patients compared to non-COVID-19 patients [179, 180]. Many ECMO centres adopted increased anticoagulation targets early in the pandemic due to the increased thrombotic risk. However, the ELSO guidelines (2021) recommended that bleeding was still a concern for all ECMO patients and that there was insufficient data to suggest deviation from conventional anticoagulation targets for COVID-19 patients receiving ECMO [174]. Furthermore, the biochemical markers of hypercoagulability that are elevated in COVID-19 are the same markers used to monitor ECMO circuit health e.g. d-dimer.

3.1.5 Oxygenator development and use in practice.

Many factors may contribute to the ECMO induced haemostatic complications. It is commonly believed that the exposure of blood to ECMO circuit components (pump, oxygenator, cannulas and tubing) activate inflammation and the coagulation cascade [124]. The ECMO tubing is negatively charged and can activate the coagulation cascade, leucocytes and platelets. The MO has the largest surface area of the ECMO circuit and therefore contact activation and is the most common place for thrombotic deposits to occur [130, 132, 144]. ECMO coagulopathy is described in detail in section 1.6.

Over the years there have been technical developments to ECMO materials, which have transformed the equipment we use today. As mentioned in section 1.2.3 the ECMO tubing is “bio-lined”/coated with heparin, the oxygenators are made with PMP, a hydrophobic material, and there are developments into cannula design. The development of oxygenators to improve their performance has led to variations in oxygenator shape, blood inlet and outlet position, as well as modifications in membrane materials. Computational models suggest the oxygenator shape, inlet and outlet number and position influence the rheology and laminarity of blood flow across the oxygenator and therefore the thrombotic risks [139]. The standard mobile ECMO device used in many ECMO centres and our own, is the Cardiohelp pump (Getinge, Sweden) with the HLS Advance 7L oxygenator (Maquet, Germany) which has a transverse flow path with a square profile, with four inlets and one outlet. Newer oxygenators

in use include the Nautilus™ (Medtronic, USA) which has a transverse flow path with a circular profile, one inlet and one outlet at the bottom edge of each side. Medtronic report that their design minimises surface contact area whilst achieving a low blood side pressure drop; and the circular profile eliminates corners were low flow and stasis are known to occur. These modifications aim to reduce clotting at the MO and allow for longer term performance [181]. The Royal Brompton Hospital uses both the Cardiohelp motor (Getinge, Sweden) with integrated HLS Advance oxygenator and the Centrimag (Abbott, USA) pump with Nautilus oxygenator.

3.2 Aims and hypotheses

This chapter aims to investigate whether ECMO related thrombosis, in particular circuit change frequency was impacted by disease aetiology or ECMO equipment.

The primary outcome was to investigate whether the increased thrombosis risk in COVID-19 patients would increase MO thrombosis and the need for circuit change.

The secondary outcome was to investigate whether the markers for circuit change were different in COVID-19 patients compared to non-COVID 19 patients,

3.3 Methods

3.3.1 Study Design and Participants

Data was extracted from clinical systems in accordance with the A CLUE study (Section 2.2.1). This single centre, retrospective, observational, cohort study describes consecutive adult (age ≥18 years) patients who were admitted through a specialist severe acute respiratory failure (SARF) and ECMO service. Patients were transferred from referral sites to The Royal Brompton and Harefield Hospitals (RBHH) between 20th February 2019 and 4th February 2023.

Patients retrieved for ECMO by the RBH team were initiated onto mobile ECMO using bifemoral cannulation and a Cardiohelp motor with integrated HLS Advance oxygenator. Due to the nature of the ECMO network in the UK, some patients admitted to RBH are retrieved by other teams who may use a femoral-jugular cannulation approach or CentriMag pump with other oxygenators e.g. A.L.ONE (Euroset, Italy) or Nautilus™. ECMO was initiated with a blood flow of 3-4L/min and sweep gas flow of 1-3l/min. Thereafter, ECMO blood flow was adjusted to PaO2, and sweep gas flow according to PaCO2 and pH. Patients are usually

started on a heparin infusion after arrival to the ECMO centre with target anti-Xa levels of 0.2-0.3Units/L. Daily bloods include ECMO circuit health parameters such as platelet count, D-dimer, fibrinogen, PFH, and post-oxygenator blood gases where possible.

Eligible patients were 1) age ≥16 years 2) had ARDS from any aetiology requiring VV ECMO and 2) supported on a Cardiohelp pump with integrated HLS Advance oxygenator. Patients were excluded if 1) the first circuit was a CentriMag pump 2) on any ECMO configuration other than VV ECMO 3) the reason for the first circuit change was for reconfiguration to/from VV ECMO or equipment fault (not thrombosis), or 4) there was insufficient data e.g. transferred to/from another centre.

The study was approved by the Research Ethics Committee (A CLUE study; REC reference 20/EM/0204). All patients lacked capacity, and the need for individual informed consent was waived for retrospective analysis of data collected prospectively for routine care, with no breach of privacy or anonymity.

3.3.2 Data collection and definitions

Demographic, clinical, laboratory, ECMO mechanical and ventilatory data were extracted from electronic medical records (Intellispace Critical Care and Anaesthetics Information Systems; Phillips, Netherlands). Clinical data were reviewed and collated by investigating clinicians.

Start of ECMO is defined as cannulation; end of ECMO is defined as decannulation or death (if the patient died whilst on ECMO); circuit change is defined as a change of all components of the circuit (including the MO) excluding the access and return cannulae for presumed MO failure. Reconfiguration is defined as changing the configuration of ECMO circuit to/from VV ECMO to VVV ECMO, VA ECMO or VVA ECMO with or without changing the MO.

Extracted data included variables that were recorded hourly (ECMO mechanical data), and several times a day (laboratory bloods and arterial blood gas [ABG] data). All data was organised into 24-hour periods for analysis and averaged over the 24-hour period. 24-hour periods relating to ECMO duration were calculated from ECMO cannulation. 24-hour periods

relating to circuit change were calculated from the time of circuit change. Baseline (BL) is defined as the average value over the first 24 hours of ECMO support; day of circuit change (D0) is the 24-hour period prior to circuit change, the days preceding circuit change (D-1, -2, -3 etc) describe each sequential 24-hour period prior to circuit change. Trends analyses are performed on average values relating to the day of ECMO initiation or day of circuit change. Only occurrences of circuit change for MO thrombosis were included. In patients who had multiple circuit changes this related to the day of the first circuit change.

The lower threshold of detection for PFH is 0.3 g/L; values <0.3 g/L were assigned to be 0.15 g/L (half the lowest value of detection).

3.3.3 Missing Data

The threshold of data missingness was set to 25% missingness for the required analyses. Variables exceeding this threshold were excluded from trends analysis. Patients were excluded from trends analysis if the circuit change occurred within 120 hours (5 days). Missing data were imputed by linear interpolation where appropriate (D-dimer, fibrinogen).

3.3.4 Statistical Analysis

Normality testing was carried out with Kolmogorov-Smirnov tests. Descriptive statistics were used to summarise the data. Results are presented as mean and standard deviations, or medians and interquartile range, as appropriate. Categorical values were summarised as counts and percentages. Differences between groups were compared with the Mann-Whitney, t-test, Kolmogorov-Smirnov, Kruskal-Wallis or Chi-squared tests as appropriate.

Trends in variables over time and between groups were analysed using two-way ANOVA or mixed effects analysis with Geisser-Greenhouse correction, and Dunnett's multiple comparisons test.

All statistical tests were two-sided and $P<0.05$ was considered statistically significant. Analyses were performed using Prism GraphPad Version 9.5.1 (733) Software.

3.4 Results

3.4.1 Patient demographics and baseline characteristics

A total of 364 patients were admitted to RBH for VV ECMO for SARF between 20th February 2019 and 4th February 2023. After exclusions, 279 patients who were initiated on VV ECMO on a Cardiohelp with integrated HLS Advance oxygenator for ARDS were included for further analysis (See Figure 3.1 for exclusions).

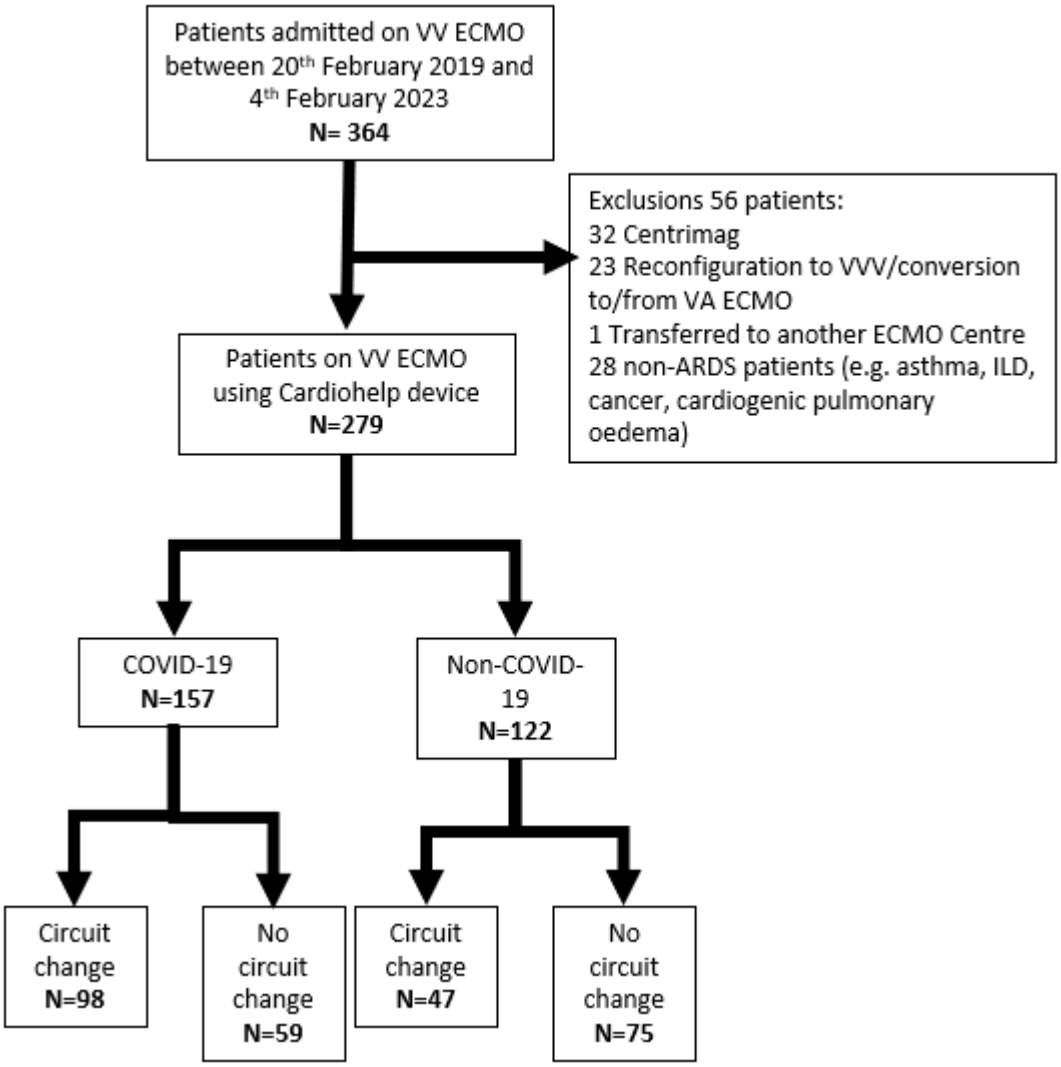


Figure 3.1 Consort diagram of patients included in analysis.

364 patients were eligible for inclusion. 28 patients had non-ARDS aetiologies for their respiratory failure, 32 patients had a Centrimag as their initial circuit, 23 patients were on other ECMO modalities or configurations, and 1 patient had insufficient data as they were transferred to another centre. A total of 279 patients were included in final analysis with 157 COVID-19 patients and 122 non-COVID-19 patients.

There were 157 COVID-19 patients and 122 non-COVID-19 patients. The COVID-19 patients were mostly, from non-Caucasian ethnic groups (49.7 vs 37.7%; P<0.0001) and had

higher BMI (31.1 vs 26.8 kg/m^2; P=0.0006) but slightly lower SOFA scores than non-COVID-19 patients (6 vs 9; P<0.0001) (See Table 3.1).

			All N=279	COVID-19 N=157	Non-COVID-19 N=122	P-value
Age (median, IQR)			45 (35-52)	46 (37.5-51)	43 (30.8-54.0)	0.1366
Male (n, %)			177 (63.4)	106 (67.5)	71 (58.2)	0.1089
SOFA Score (not incl. resp)			7 (6-10)	6 (5-8)	9 (7-12)	**<0.0001**
Non-COVID pathology	**Known bacterial pneumonia** *(Pneumococcal, Staph, Strep, TB)*		-	-	28 (23.0)	
	Aspiration pneumonia		-	-	23 (18.9)	
	Viral pneumonitis *(Influenza, Adenovirus and MPV)*		-	-	23 (18.9)	
	Pneumonia (unknown pathogen)		-	-	19 (15.6)	
	Extra-pulmonary ARDS *(TRALI, , pancreatitis, polytrauma)*		-	-	17 (13.9)	
	Lung injury *(Post-op, pulmonary haemorrhage, inhalational, trauma)*		-	-	9 (7.4)	
	Other resp pathology *(PE,)*		-	-	3 (2.5)	
Ethnicity (n, %)		**Asian**	72 (25.8)	51 (32.5)	21 (17.2)	**<0.0001**
		Black	39 (14.0)	25 (15.9)	14 (11.5)	
		Caucasian	127 (45.5)	51 (32.5)	76 (62.3)	
		Mixed	6 (2.)	2 (1.3)	4 (3.3)	
		Other	20 (7.2)	16 (10.2)	4 (3.3)	
		Unknown	15 (5.4)	12 (7.6)	3 (2.5)	
BMI (kg/m^2) (n, %)		**Weight (kg)**	84 (70-100)	90 (75-107)	75 (65-95)	**<0.0001**
		BMI (kg/m^2)	28.1 (23.8-34.0)	31.1 (25.8-36.4)	26.8 (22.4-31.7)	**0.0006**
ECMO cannulation (n, %)		**Bifemoral**	265 (95.0)	153 (97.5)	112 (91.8)	0.0682
		Femoral-jugular	12 (4.3)	4 (2.5)	8 (6.5)	
		Dual lumen cannula	2 (0.7)	0	2 (1.6)	
Survival (n, %)		**ECMO**	219 (78.5)	117 (74.5)	102 (83.6)	0.0783
		Hospital	193 (69.2)	111 (70.7)	82 (67.2)	0.6014
ECMO duration (days) (Median, IQR)			17.8 (10-34)	25.8 (12.6-21.7)	12.5 (6.6-16.6)	**<0.0001**

Table 3.1 Demographics of the VV ECMO patients included in the study

Normality was determined using Kolmogorov-Smirnov test. Differences between groups were compared with Mann Whitney, and unpaired t-tests as appropriate. Differences between groups with categorical data were compared with Chi-squared tests and duration to first circuit change with Log-rank (Mantel-Cox test).

Body Mass Index; BMI; Extracorporeal Membrane Oxygenation, ECMO; Sequential Organ Failure Assessment, SOFA; transfusion related acute lung injury, TRALI.

The majority of patients (95%) were initiated on ECMO via bifemoral cannulation as this was convention in the retrieving institution. Those canulated in a femoral-jugular approach were retrieved from a different centre or had patient related complications for which a bifemoral approach was not appropriate e.g. femoral vein thrombus. There was no difference in survival to ECMO decannulation or hospital discharge between COVID-19 and non-COVID-19 patients. In patients who survived to decannulation, COVID-19 patients had significantly longer ECMO duration compared non-COVID-19 patients (21.7 v 12.5 days; p<0.0001).

3.4.2 Baseline clinical parameters

Routine admission bloods for all ECMO patients were compared between COVID-19 and non-COVID-19 ECMO patients (Table 3.2). The admission bloods served as the baseline bloods for further comparisons.

COVID-19 patients had a higher platelet count (221 [152-298] vs 158 [84-238] x 10^9/L; P<0.0001), but lower CRP (147 [55-221] vs 189 [124-307] mg/L; P=0.0021), lower , serum creatinine (62 [46.5-97.0] vs 90 [59-147] mg/dL; P=0.0016), bilirubin (32 [22-44.5] vs 52 [34-92] µmol/L; P<0.0001) and AST (43 [31-64] vs 81 [45-167] U/L; P=0.0003) than non-COVID-19 patients. The lower creatinine, bilirubin and higher platelet count likely contribute to lower SOFA scores in COVID-19 patients. COVID-19 patients had higher heparin anti-Xa level (0.32 [0.21-0.46] vs 0.15 [0.05-0.26] units/ml; P<0.0001) due to the higher anticoagulation targets that were recommended for COVID-19 patients at the beginning of the pandemic.

There were no significant differences in the baseline ECMO circuit health lab parameters such as D-dimer, fibrinogen or PFH. Both groups had similar inflammatory markers such as neutrophil, monocyte counts, and procalcitonin.

	Blood parameters	COVID-19		Non-COVID-19		P-value
		N=157		N=122		
Haematology	**Haemoglobin (g/L)**	157	96 (88-106)	122	94 (85–103)	0.8921
	Platelet Count (10^9/L)	157	221 (152-298)	122	158 (84–238)	**<0.0001**
	Mean platelet volume (fL)	118	8.6 (7.9-9.1)	65	8.8 (7.8–9.3)	0.9996
	White Blood Cell Count (10^9/L)	157	10.6 (8.2-13.3)	122	13.0 (8.9-18.6)	0.1209
	Neutrophil Count (10^9/L)	157	9.3 (7.1-11.6)	122	10.9 (7.1-16.7)	0.2797
	Monocyte Count (10^9/L)	157	0.6 (0.3--.8)	122	0.5 (0.3-0.9)	0.9996
Coagulation	**PT (seconds)**	157	12.8 (11.8-14.1)	121	14.2 (12.6 – 17.0)	**<0.0001**
	INR	157	1.0 (1.0-1.2)	121	1.2 (1.0-1.4)	**<0.0001**
	APTT (seconds)	157	40.8 (33.4-50.6)	121	41.7 (32.6 – 58.7)	0.9933
	Fibrinogen (g/L)	156	4.6 (3.3-6.9)	121	4.4 (3.1-6.4)	0.9302
	Heparin anti-Xa level (units/ml)	157	0.32 (0.21-0.46)	118	0.15 (0.05-0.26)	**<0.0001**
	Antithrombin	54	64 (44.8-78.5)	16	51.5 (40.8-79)	0.9912
	D-dimer (ng/ml)	155	2753 (1109-4586)	121	2452 (1169–2452)	0.9996
Biochemistry	**Urea (mmol/L)**	157	8.6 (6.3-12.0)	122	8.6 (5.2-13.2)	0.9985
	Creatinine (mg/dL)	157	62 (46.5-97.0)	122	90 (59-147)	**0.0016**
	Bilirubin (µmol/L)	157	32 (22-44.5)	122	52 (34-92)	**<0.0001**
	Alkaline Phosphate (U/L)	157	89 (67-119)	122	90 (60-154)	0.9981
	Alanine Aminotransferase (U/L)	157	43 (28-69)	122	42 (26-86)	0.9991
	Aspartate transaminase (U/L)	78	43 (31.8-64.3)	122	81 (45-167)	**0.0003**
	Albumin (g/dL)	156	24 (22-27)	122	25 (22-27)	0.9512
	Corrected Calcium (mg/dL)	157	2.30 (2.20-2.38)	122	2.34 (2.26-2.42)	0.1451
	C-Reactive Protein (mg/L)	157	147 (55-221)	122	189 (124-307)	**0.0021**
	Lactate dehydrogenase (U/L)	140	994 (760-1219)	80	921 (656-1412)	0.9996
	Plasma Free Haemoglobin (g/L)	129	0.15 (0.15-0.3)	104	0.15 (0.15-0.3)	0.8515
	Procalcitonin (ng/ml)	85	0.9 (0.3-4.4)	17	5.5 (1.3-24.1)	0.0906
	Troponin I (ng/ml)	118	32.7 (13.1-87.2)	34	66 (20-536)	0.6247
Immunology	**C3**	108	1.2 (1.0-1.4)	91	0.9 (0.6-1.3)	0.0563
	C4	98	0.2 (0.1-0.3)	85	0.2 (0.1-0.3)	0.9996
	IGA	106	1.9 (1.4-2.5)	92	1.8 (1.3-2.6)	0.9981
	IGG	106	7.5 (6.1-9.73)	92	7.0 (4.8-10.3)	0.9573
	IGM	106	0.8 (0.6-1.2)	91	0.5 (0.4-0.8)	**<0.0001**

Table 3.2 Baseline laboratory parameters.

Normality was determined using Kolmogorov-Smirnov test. Some parameters have missing values as data was not recorded or available. Mann-Whitney and unpaired t-tests were carried out as appropriate. All tests were two-sided and P<0.05 was considered statistically significant.

Activated partial thromboplastin time APTT; International normalised ratio, INR; Prothrombin time, PT.

Within the first 24 hours of ECMO initiation there were no significant differences in ECMO requirements (RPM, blood flow, sweep gas flow) between COVID-19 and non-COVID-19

and no difference in MO resistance as measured by TPM, TMR or RPM:blood flow ratio (Table 3.3). There was also no difference in MO efficiency as demonstrated in the post-oxygenator blood gases, specifically the PpostO2.

There were significant differences in the patient's baseline arterial blood gas parameters. Despite similar ECMO blood flow and sweep gas requirements, COVID-19 patients were more hypoxaemic with a lower arterial PaO2 (11.4 [9.8-13.7] vs 12.7 [10.5-15.3] kPa; P=0.0177) and had worse ventilation with higher arterial PaCO2 (7.4 [6.9-7.7] vs 6.7 [6.2-7.4] kPa; P<0.0001). The arterial pH was also statistically different however values of both groups remain within normal range.

		N	**COVID-19 N=157**	N	**Non-COVID-19 N=122**	**P-Value**
ECMO Device Parameters	**Blood Flow (L/minute)**	157	4.33 (± 0.31)	122	4.24 (±0.65)	0.1993
	Revolutions per minute (RPM/min)	157	2974 (±317)	122	2971 (±3604)	0.9446
	Sweep Gas Flow (L/minute)	157	4.0 (3.0 – 5.0)	122	4.0 (3.0 – 5.0)	0.5459
	Transmembrane pressure (TMP; mmHg)	157	23 (20 – 28)	122	22 (18 – 26)	0.2881
	RPM:Blood Flow (RPM/L/minute)	157	685 (658 – 723)	122	687 (663 – 732)	0.7341
	Transmembrane resistance (TMR) (mmHg/L/minute)	157	5.39 (4.96 – 6.16)	122	5.27 (4.61 – 5.79)	0.1667
Blood gases	**Post-oxygenator pH**	118	7.47 (7.42 – 7.52)	93	7.44 (7.39 – 7.49)	**0.0177**
	Post-Oxygenator PaO2 (PpostO2; kPa)	118	64.7 (57.5 – 68.0)	93	63.8 (56.9 – 67.3)	0.3197
	Post-Oxygenator PaCO2 (PpostCO2; kPa)	118	5.5 (4.9 – 5.8)	93	5.2 (4.6 – 5.9)	0.1830
	Arterial pH	157	7.38 (7.34 – 7.41)	122	7.36 (7.31 – 7.4)	**0.0177**
	Arterial PaO2 (kPa)	157	11.4 (9.8 – 13.7)	122	12.7 (10.5 – 15.3)	**0.0177**
	Arterial PaCO2 (kPa)	157	7.4 (6.9 – 7.7)	122	6.7 (6.2 – 7.4)	**<0.0001**

Table 3.3 Baseline ECMO device parameters and blood gases in COVID-19 (N=157) and non-COVID-19 (N=122) patients.

Normality was determined using Kolmogorov-Smirnov test. ECMO blood flow and ECMO RPM are parametric. Some parameters have missing values as data was not recorded or available. Mann-Whitney and unpaired t-tests were carried out as appropriate. All tests were two-sided and P<0.05 was considered statistically significant.

Kilopascal, kPa; Partial pressure of oxygen, PaO2; Partial pressure of carbon dioxide, PaCO2; Revolutions per minute, RPM; Transmembrane pressure, TMP, Transmembrane resistance, TMR.

3.4.3 Circuit change and ECMO duration are increased in COVID patients

A total of 145 (52.0%) patients required circuit change for MO thrombosis. When separated into COVID-19 and non-COVID-19 groups, incidence of circuit change was significantly higher in COVID-19 patients compared to non-COVID-19 (62.4% vs 38.5%, P<0.0001) and at all time points (Mantel-Cox test [X^2=11.46, P=0.0007]) (Figure 3.2). There was no difference in circuit change frequency in non-COVID-19 patients from before and during the COVID-19 pandemic (16th March 2020 onwards) (Table 3.4).

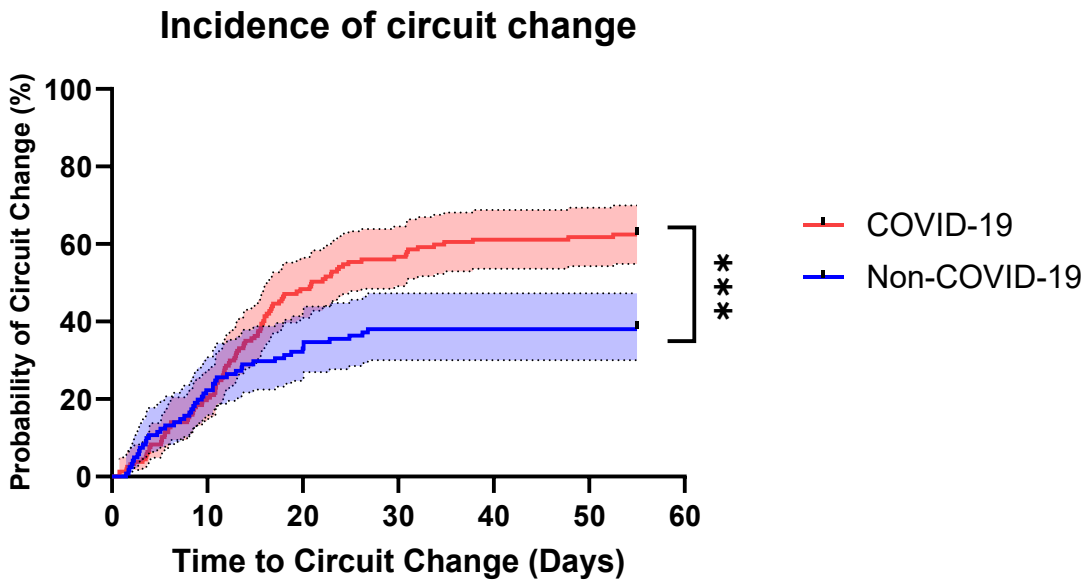


Figure 3.2 COVID-19 patients have a higher incidence of circuit change than non-COVID-19 patients.

Kaplan-Meir curve comparing circuit change incidence between all COVID-19 (N=157) and non-COVID-19 (N=122) ECMO patients. 62.4% of COVID-19 patients required circuit change compared to 38.5% of non-COVID-19 patients. Curves are significantly different when compared using Log-rank (Mantel-Cox) test (X^2=11.46, P=0.0007). Lines represent hazard ratio ± 95% CI ratio.

Of all patients who required circuit change, most patients (63.1%) required only one circuit change for MO failure, and there was no difference in circuit change frequency between COVID-19 and non-COVID-19 patients (Table 3.4). The median ECMO run time to first circuit change was longer in COVID-19 patients compared to non-COVID-19 patients (13.0 [8.1-19.4] vs 9.0 [3.6-13.6] days; p=0.0047). In patients who survived their ECMO run, ECMO run time was significantly longer in COVID-19 patients compared to non-COVID-19 patients (21.7 [11.5-38.0] vs 12.3 [7.4-18.5] days; P<0.0001). When separated by circuit change frequency, total ECMO duration was longer in COVID-19 patients who required one circuit change (27.1 [17.8-43.8] vs 12.7 [11.2-19.5]; P = 0.0005). The need for multiple circuit changes was not associated with any difference in ECMO duration between COVID-19

cohorts (Table 3.4). Both COVID-19 and requirement for circuit change are associated with increased ECMO duration (Mantel-Cox test; X2=101.722.1, P<0.0001, P<0.0001) (Figure 3.3).

		All N=307	COVID-19 N=157	Non-COVID-19 N=122	P-value
Circuit Change (n, %)	**All**	149 (48.5)	98 (62.4)	47 (38.5)	**0.0001**
	Pre-COVID-19 pandemic	-	-	27/69 (39.1)	0.8753
	Post-COVID-19	-	-	20/53 (37.7)	
Time to first CC (days) (median, IQR)		11.5 (6.0-17.3)	13.0 (8.1-18.4)	9.0 (3.6-13.6)	**0.0047**
CC Frequency (n, %)	**One CC**	94 (63.1)	64 (65.3)	30 (63.8)	0.8617
	Multiple CC	51 (34.2)	34 (34.7)	17 (36.2)	
ECMO duration (days) (Median, IQR)	**All patients**	17.8 (10-34.)	25.8 (12.6-42.2)	12.5 (6.9-21.7)	**<0.0001**
	All ECMO survivors	**N=219**	**N=117**	**N=102**	
		15.8 (9.7-28.0)	21.7 (11.5-38.0)	12.3 (7.4-18.5)	**<0.0001**
	- No CC	9.0 (5.9-13.9)	10.5 (6.9-17.2)	9.7 (5.7-13.6)	0.0895
	- One CC	20.9 (12.7-36.7)	27.1 (17.8-43.8)	12.7 (11.2-19.5)	**0.0005**
	- Multiple CC	37.4 (24.6-45.4)	37.1 (24.8-53.4)	37.5 (22.9-40.6)	**0.3378**

Table 3.4 ECMO circuit change comparisons between COVID-19 (n=157) and non-COVID-19 (n=122) patients.*Chi-squared test for categorical data and t-tests and Mann-Whitney test as appropriate were performed to compare between groups. All tests were two-sided and P<0.05 was considered statistically significant. Pre-COVID-19 pandemic defined as before 16th March 2020, and post-COVID-19 pandemic defined as after 16th March 2020.*

Circuit change, CC; extracorporeal membrane oxygenation, ECMO.

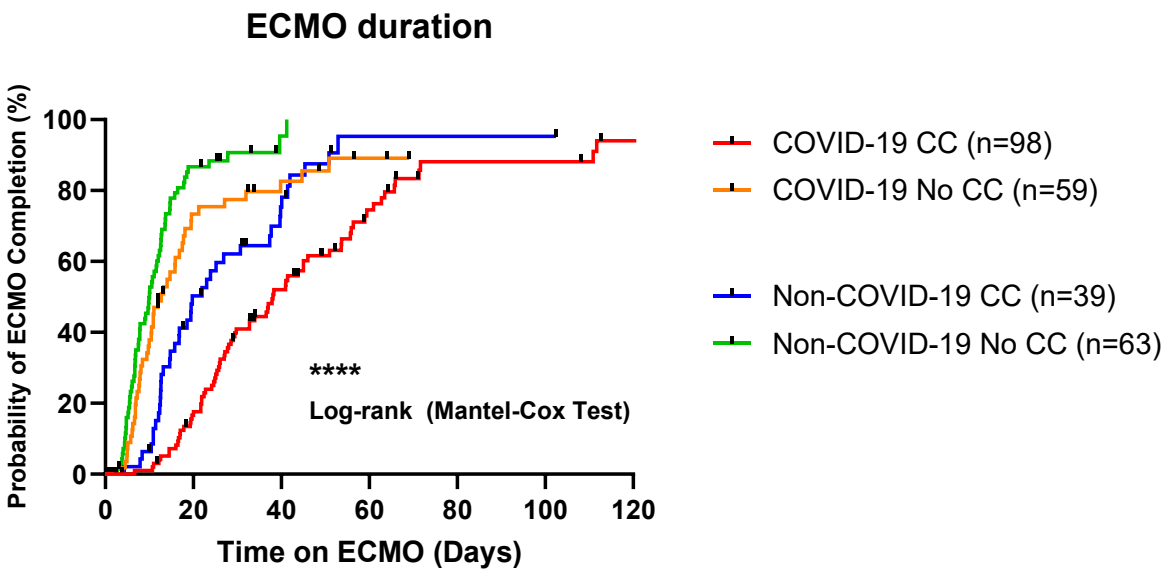


Figure 3.3 COVID-19 and circuit change are both associated with increased ECMO duration.

Kaplan-Meier curves demonstrating differences in ECMO duration between COVID-19 and non-COVID-19 patients who did and did not require a circuit change. Patients were censored for ECMO decannulation and death. Log-rank (Mantel-Cox) test (X^2=101.7, P<0.0001). The median ECMO duration was 9.73 days for non-COVID-19 no circuit change [green], 19.4 days for non-COVID-19 circuit change [blue], 13.23 days for COVID-19 no circuit change [orange] and 38.1 days for COVID-19 circuit change [red].

Circuit change, CC; Novel coronavirus 2019, COVID-19; Extracorporeal membrane oxygenation, ECMO.

Multivariate logistic regression

The association between SARF aetiology, demographics (age, BMI, ethnicity), admission SOFA, and ECMO duration to requirement for circuit change were analysed using multivariate logistic regression (Table 3.5). SARF aetiology (including COVID-19) was not an independent risk factor for circuit change , but longer ECMO duration was (OR 1.094 [1.068-1.127]; P<0.0001). Since COVID-19 patients had significantly longer ECMO duration (Table 3.4) compared to non-ECMO patients regardless of circuit change frequency, these are confounding factors. The increased circuit change frequency seen in COVID-19 patients is likely a consequence of the increased ECMO duration rather than as a risk factor in itself.

Variable	Estimate	Standard error	Odds ratio	95% CI	P value
SARF Aetiology					
COVID	0.2670	0.7469	1.306	0.3017 to 5.905	0.7207
Aspiration pneumonia	0.3096	0.8800	1.363	0.2411 to 7.898	0.7250
Extra-pulmonary ARDS	0.3663	0.9680	1.442	0.2091 to 9.786	0.7051
Bacterial Pneumonia	0.4984	0.78661	1.646	0.3568 to 8.125	0.5263
Viral Pneumonitis	-0.1149	0.9061	0.8914	0.1500 to 5.437	0.8991
Age	-0.0064	0.01339	0.9936	0.9677 to 1.020	0.6293
BMI					
18.5-24.9	-2.020	1.401	0.1327	0.0048 to 1.681	0.1493
25-29.9	-1.858	1.423	0.1561	0.0054 to 2.062	0.1917
>30	-0.1.089	1.400	0.3365	0.01212 to 4.260	0.4366
Ethnicity					
Caucasian	-0.5507	0.4635	0.5765	0.2284 to 1.417	0.2348
Black	-0.9673	0.4986	0.3801	0.1379 to 0.9860	0.0524
Asian	-0.3954	0.40455212	0.6734	0.3006 to 1.477	0.3283
Other	0.5507	0.4635	1.735	0.37055 to 4.379	0.2348
ECMO Duration (Days)	0.09013	0.01367	1.094	1.067 to 1.126	**<0.0001**
Admission SOFA	-0.08473	0.0559	0.9191	0.8219 to 1.024	0.1314

Table 3.5. Association between baseline characteristics, ARDS pathology and ECMO duration with need for circuit change.

A Multivariate logistic regression analysis was carried out to examine the relationship between need for circuit change and predictor variables from admission demographics (age, gender, BMI, ethnicity), ARDS pathology, SOFA score, and ECMO duration. P<0.05 was considered statistically significant.

3.4.4 COVID-19 patients more likely to have worse severe respiratory failure and increased ECMO requirements

To explore why there is a difference in circuit change frequency and duration of ECMO between COVID-19 and non-COVID-19 patients, trends in blood and ECMO parameters for the first week after ECMO initiation were compared between the two groups. Patients who

had an ECMO run time of less than 3 days were excluded. After exclusions comparisons were made between 155 COVID-19 patients and 115 non-COVID-19 patients.

In the first 7 days after ECMO initiation, trends such as decreasing haemoglobin and platelet count, increasing d-dimer, and decreasing CRP were observed in both groups as expected with all ECMO patients (Figure 3.4). There were some significant haematological differences such as increased haemoglobin, platelet count, and lower leucocytes (both neutrophil and monocytes) in COVID-19 patients compared to non-COVID-19 patients which remain unchanged from admission. Both groups had similar D-dimers at ECMO initiation, but the D-dimer levels were more elevated by day 7 in non-COVID-19 patients compared to COVID-19 patients (D7: 8403 ± 8504 vs 5364 ± 5577; P=0.0009). COVID-19 patients were anticoagulated to a higher target as shown by the higher heparin anti-Xa levels. COVID-19 patients continued to have lower bilirubin, creatinine, and CRP than non-COVID-19 patients throughout the early stages of ECMO which contribute to lower SOFA scores and demonstrates COVID-19 patients were more likely to have single organ failure.

To eliminate the effect of potential MO thrombosis on these initial trends, patients who had a circuit change within 10 days of ECMO initiation were also excluded in a separate analysis. After exclusion of these patients, the difference in the D-dimer levels at day 7 between COVID-19 and non-COVID-19 patients remained (6976 [± 7066] vs 4832 [± 4680] ng/ml; P=0.01205). Other differences between groups remained similar (graphs not shown).

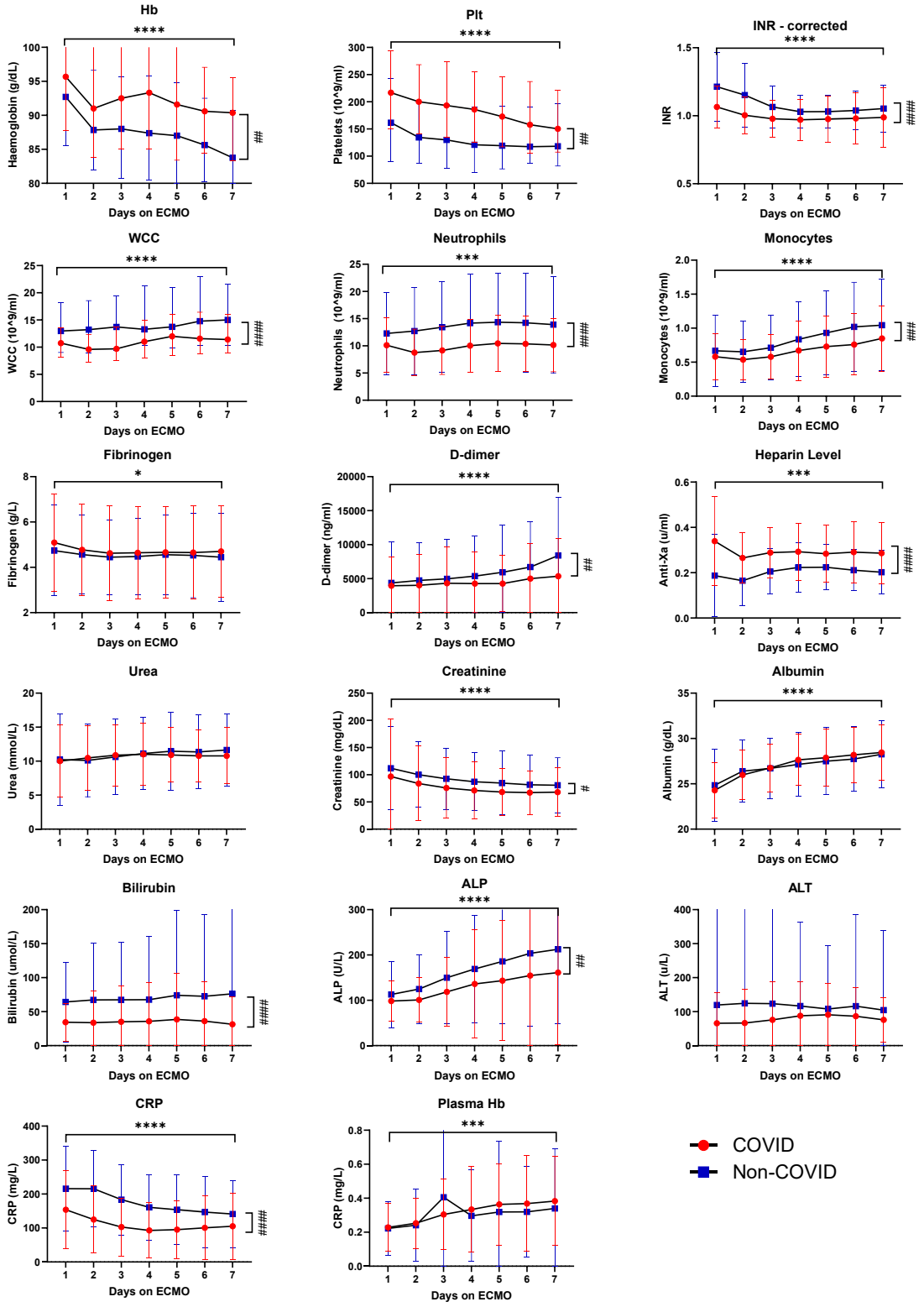


Figure 3.4 Trends in laboratory parameters in the first 7 days of ECMO initiation.

*Comparisons were made between 155 COVID-19 patients and 115 non-COVID-19 patients. Mixed-effects group analyses with Geisser-Greenhouse correction and Dunnett's multiple comparison test were performed. Displayed as median, IQR. * trends over time, # comparison between COVID-19 cohorts. All tests were two-sided and P<0.05 was considered statistically significant * p<0.05, ** p<0.01, *** p<0.001, **** p<0.0001. Activated partial thromboplastin time, APTT; Alanine Transaminase, ALT; Alkaline Phosphatase, ALP; C-Reactive Protein, CRP; Haemoglobin, Hb; International normalised ratio, INR; Prothrombin time, PT; White Cell Count, WCC.*

Regarding ECMO mechanical parameters, COVID-19 patients maintained higher ECMO blood flow and sweep gas flow in the first 7 days of ECMO whereas for non-COVID-19 patients, both blood flow and sweep gas reduced by day 7. There was some variation in TMP and slight increase in TMR over the first 7 days of ECMO in all patients, but no difference between COVID-19 and non-COVID-19 patients (Figure 3.5). COVID-19 patients continued to be more hypoxic and hypercarbic than non-COVID-19 patients after ECMO initiation demonstrating the degree of ongoing respiratory failure and explains the need for increased ECMO blood flow and sweep gas flow.

When patients who had a circuit change within 10 days were excluded from this analysis, there was no difference in ECMO device requirements (RPM, blood flow and sweep gas flow) in the initial stages after ECMO initiation, and no difference in MO function as measured by TMP and post-oxygenator blood gases.

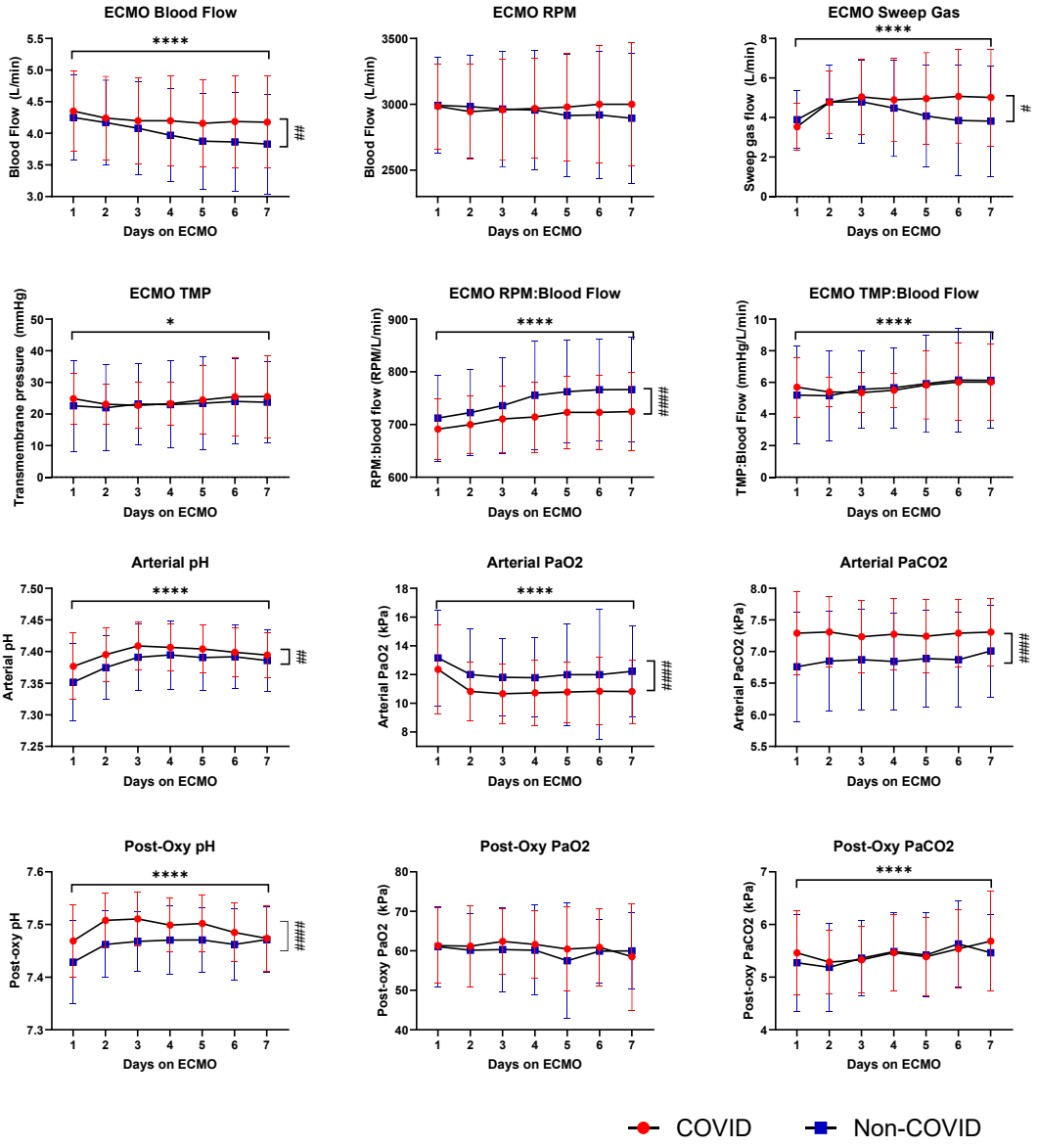


Figure 3.5 Trends in ECMO parameters and blood gases in the first 7 days of ECMO initiation.

*Comparisons were made between 155 COVID-19 and 115 non-COVID-19 patients for ECMO mechanical parameters, 142 COVID-19 patients and 107 non-COVID-19 patients for arterial blood gases, and 131 COVID-19 and 94 non-COVID-19 patients for post-oxygenator blood gases. Mixed-effects group analyses with Geisser-Greenhouse correction and Dunnett's multiple comparison test were performed. Displayed as median, IQR. * trends over time, # comparison between COVID-19 cohorts. All tests were two-sided and P<0.05 was considered statistically significant * p<0.05, ** p<0.01, *** p<0.001, **** p<0.0001.*

Extracorporeal membrane oxygenation, ECMO; post-oxygenator PaO2, PpostO2; post-oxygenator PaCO2, PpostCO2; revolutions per minute, RPM; transmembrane pressure, TMP; transmembrane resistance, TMR.

3.4.5 Predictors of circuit change are different in COVID-19 patients

Trends in parameters from 5 days prior to circuit change (D-5, D-4 etc) to the day of circuit change (D0) were compared between COVID-19 and non-COVID-19 cohorts. After excluding patients who had circuit change within 5 days of ECMO initiation, and those who had more than 25% data missingness, comparisons were made between 85 COVID-19 patients and 32 non-COVID-19 patients who required a circuit change (Tables 3.6 and 3.7). The most clinically relevant and significant results are shown in figures 3.6 and 3.7.

There were significant changes in some laboratory parameters in the 5-day lead up to circuit change (D-5 to D0) with decreasing haemoglobin, platelet count and fibrinogen and increasing PFH as expected, but no difference in these trends between COVID-19 and non-COVID-19 patients. However, the increase in D-dimer was less exaggerated in COVID-19 patients compared to non-COVID-19 patients (Δ D-dimer: 1404 (348.0 – 7493.0) vs 8951 (536 – 27841) ng/ml; P<0.0001 interaction) (Figure 3.6). COVID-19 patients had higher APTT and anti-Xa levels due to the higher anti-coagulation targets set for COVID-19 patients. In the 2 days following circuit change, platelet count and fibrinogen levels started to recover and D-dimer and PFH decreased in both cohorts of patients.

Regarding ECMO mechanical parameters, in the lead up to circuit change, higher ECMO blood flow was maintained in COVID-19 patients compared to non-COVID-19 patients. This is usually to maintain adequate oxygenation and may reflect the degree of hypoxia seen in COVID-19 patients as demonstrated by the lower arterial PaO2 seen in COVID-19 patients (Figure 3.7). There was no significant difference in TMP or TMR in the 5-day lead up to circuit change. However, the power required to generate the same blood flow (RPM:blood flow) was lower in COVID-19 patients (P=0.0366) which is maintained from ECMO initiation.

Changes in ECMO device parameters following circuit change were not analysed as many patients were changed to a Centrimag pump with various MO models, as well as the Cardiohelp 5L or 7L for their second circuit. In the lead up to circuit change there was decreasing MO efficiency as expected as measured by the decrease in PpostO2 and increase in PpostCO2 but no differences between COVID-19 groups. There were no differences over time in arterial PaCO2 and PaO2 but COVID-19 patients were consistently more hypoxic and hypercarbic compared to non-COVID-19 patients reflecting the degree of respiratory failure in these patients (Figure 3.7).

	D-5 to D0 (Median, IQR)				
Trends in Blood Parameters	**COVID-19 (N=85/98)**		**Non-COVID-19 (N=32/51)**		**Trend P Value: Time (T), COVID (C), Interaction (T x C)**
Δ Haemoglobin (g/L)	85	-3.50 (-9.46 – 6.75)	32	-3.13 (-12.06 – 0.94)	**T: 0.0018** **C: 0.0192** T x C: 0.4400
Δ Platelet Count (10^9/L)	85	-20.4 (-74.6 – 14.5)	32	-4.5 (-76.77 – 21.63)	**T: 0.0005** C: 0.1266 T x C: 0.9109
Δ White Blood Cell Count (10^9/L)	85	-0.65 (-3.53 – 2.28)	32	-0.90 (-5.59 – 5.13)	T: 0.8286 **C: 0.0053** T x C: 0.9450
Δ Neutrophil Count (10^9/L)	85	-0.58 (-4.07 – 1.95)	32	-0.60 (-5.85 – 4.13)	T: 0.8218 **C: 0.0020** T x C: 0.9630
Δ Monocyte Count (10^9/L)	85	0.07 (-0.13 – 0.27)	32	0.075 (-0.29 – 0.38)	T: 0.5138 **C: 0.0111** T x C: 0.9932
Δ INR	85	0.05 (-0.03 – 0.10)	32	0.04 (-0.03 – 0.10)	**T: 0.0016** C: 0.0991 T x C: 0.8797
Δ APTT (seconds)	85	1.15 (-7.77 – 8.93)	32	-0.33 (-6.41 – 6.36)	T: 0.7869 **C: 0.0239** T x C: 7066
Δ Heparin anti-Xa (units/ml)	66	-0.030 (-0.184 – 0.051)	20	-0.067 (-0.102 – -0.001)	**T: 0.00007** **C: 0.0064** T x C: 0.8511
Δ Fibrinogen (g/L)	85	-1.21 (-2.50 – -0.02)	35	1.86 (-2.92 – -0.28)	**T: <0.0001** C: 0. 1335 T x C: 0.9166
Δ D-dimer (ng/ml)	83	**1404 (348.0 – 7493.0)**	**35**	**8951 (536 – 27841)**	**T: <0.0001** **C: 0.0077** **T x C: <0.0001**
Δ Urea (mmol/L)	85	1.50 (-1.16 – 3.89)	35	0.5 (-1.58 – 4.96)	**T: 0.0090** C: 0.3591 T x C: 0.9962
Δ Creatinine (mg/dL)	85	-1.0 (-7.5 – 5.5)	35	-1.1 (-11.4 – 8.9)	T: 0.0566 C: 0.3370 T x C: 0.8967
Δ Bilirubin (µmol/L)	85	1.0 (-4.8 – 10.8)	35	-1.0 (-11.5 – 15.5)	T: 0.3198 **C: 0.0003** T x C: 0.3150
Δ Alkaline Phosphate (U/L)	85	1.8 (-19.4 – 51.0)	35	16.8 (-20.9 –65.9)	**T: 0.0230** C: 0.9223 T x C: 0.1208
Δ Alanine Aminotransferase (U/L)	85	-5.4 (-26.3 – 7.5)	35	-1.7 (-10.0 – 19.9)	T: 0.1702 C: 0.2678 **T x C: 0.0405**
Δ Albumin (g/dL)	85	1.3 (-0.5 – 3.0)	35	2.0 (-1.3 – 4.0)	**T: <0.0001** C: 0.5199 T x C:0.8958
Δ Corrected Calcium (mg/dL)	85	0.04 (-0.04 – 0.11)	35	0.04 (-0.08 – 0.11)	**T: 0.0040** C: 0.2639 T x C: 0.3691
Δ CRP (mg/L)	85	-11.8 (-88.9 – 67.9)	35	-31.9 (-111.4 – 38.0)	T: 0.1813 C: 0.6875 T x C: 0.6011
Δ Plasma Free Haemoglobin (g/L)	56	0.00 (-0.325 – 0.323)	23	0.00 (0.00 – 0.18)	**T: 0.0107** C: 0.4366 T x C: 0.7307

Table 3.6 Differences in clinical parameters from 5 days prior and the day of circuit change in COVID-19 and non-COVID-19 patients.

In patients who had circuit change, the differences between parameters from five days prior to circuit change (D-5) and the 24 hours prior to circuit change (D0) were compared between COVID-19 and non-COVID-19 patients. Kolmogorov-Smirnov normality testing, RM Two-way ANOVA or mixed-effect group analyses with Geisser-Greenhouse correction, and Dunnett's multiple comparison for hypothesis testing were performed. All data were non-parametric and presented as median (interquartile range). P values presented for change over time (T), between COVID-19 and non-COVID-19 (C), and interaction between time and COVID-19 status (T x C). Statistical significance defined as $p<0.05$.

Activated partial thromboplastin time APTT; C-reactive protein, CRP; Extracorporeal membrane oxygenation, ECMO; International normalized ratio, INR; prothrombin time, PT.

Trends in Device parameters (Median, IQR)	COVID-19 N=85		Non-COVID-19 N=32		Trend P Value: Time (T), COVID (C), Interaction (T x C)
Δ Blood Flow (L/minute)	85	0.060 (-0.237 – 0.474)	32	-0.209 (-0.555 – 0.276)	T: 0.5890 C: 0.0924 **T x C: 0.0415**
Δ Motor pump speed (RPM)	85	105.2 (-157.5 – 392.2)	32	-103.6 (-420.5 – 216.2)	T: 0.8104 C:0.7954 **T x C: 0.0093**
Δ Transmembrane pressure (mmHg)	85	3.7 (-0.1 – 8.7)	32	1.2 (-2.2 – 7.2)	**T: 0.0040** C: 0.1956 **T x C: 0.0003**
Δ Gas Flow (L/minute)	85	1.0 (-0.9 – 2.6)	32	-0.7 (-2.0 – 0.6)	T: 0.5196 C: 0.3631 **T x C: <0.0001**
Δ Motor RPM to blood flow ratio	85	6.79 (-32.21 – 48.77)	32	-4.96 (-50.84 – 57.16)	T: 0.47226 **C: 0.03660** T x C: 0.7732
Δ TMP to blood flow ratio (mmHg/L/minute)	85	0.93 (0.03 – 1.73)	32	0.62 (-0.18 – 1.89)	**T: <0.0001** C: 0.5262 T x C: 0.2165
Trends in blood gas parameters (Median, IQR)					
Δ Arterial pH	85	-0.009 (-0.039 – 0.021)	32	0.012 (-0.029 – 0.037)	T: 0.4221 C: 0.9455 T x C: 0.8481
Δ Arterial PaO_2 (kPa)	85	-0.823 (-1.669 – 1.089)	32	0.454 (-1.230 – 3.122)	T: 0.2099 **C: 0.0361** T x C: 0.2099
Δ Arterial $PaCO_2$ (kPa)	85	0.116 (-0.194 – 0.396)	32	-0.005 (-0.549 – 0.230)	T: 0.7211 **C: <0.0001** T x C: 0.4029
Δ Post-oxygenator pH	52	-0.011 (-0.065 – 0.023)	15	-0.020 (-0.087 – 0.040)	**T: 0.0239** C: 0.8200 T x C: 0.8022
Δ Post-oxygenator PaO_2 (kPa)	52	-6.34 (-18.23 – -0.58)	15	-9.92 (-22.99 – -1.025)	**T: <0.0001** C: 0.8267 T x C: 0.3992
Δ Post-oxygenator $PaCO_2$ (kPa)	52	0.183 (-0.523 – 0.801)	15	0.215 (-0.495 – 0.769)	T: 0.0592 C: 0.0918 T x C: 0.8327

Table 3.7 Differences in ECMO mechanical parameters and blood gases from 5 days prior and the day of circuit change in COVID-19 and non-COVID-19 patients.

In patients who had circuit change, the differences between ECMO mechanical parameters and blood gases from five days prior to circuit change (D-5) and the 24 hours prior to circuit change (D0) were compared between 85 COVID-19 and 32 non-COVID-19 patients. Kolmogorov-Smirnov normality testing, RM Two-way ANOVA or mixed-effect group analyses with Geisser-Greenhouse correction, and Dunnett's multiple comparison for hypothesis testing were performed. All data were non-parametric and presented as median (interquartile range). P values presented for change over time (T), between COVID-19 and non-COVID-19 (C), and interaction between time and COVID-19 status (T x C). Statistical significance defined as p<0.05.

Extracorporeal membrane oxygenation, ECMO; partial pressure of carbon dioxide, PaCO2; partial pressure of oxygen, PaO2; revolutions per minute, RPM.

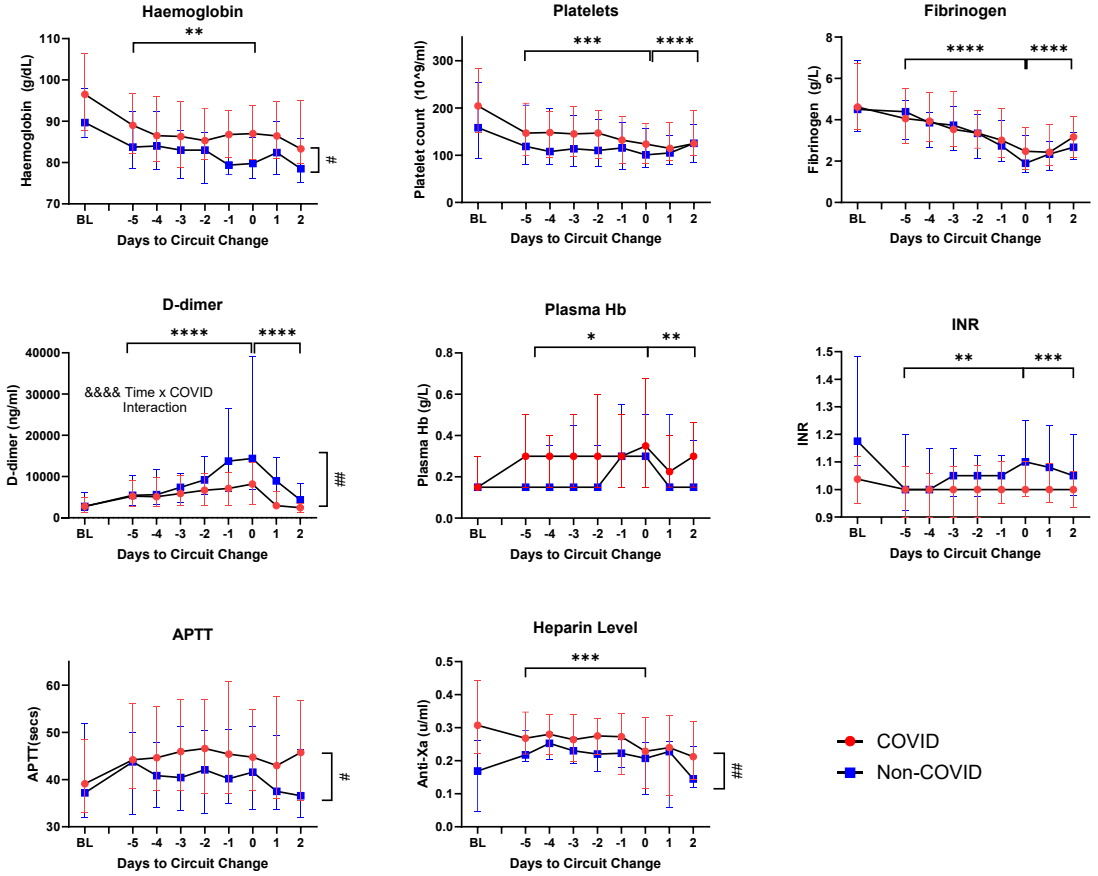


Figure 3.6 Trends in blood parameters in the lead up to circuit change.

*Comparisons of blood parameters from baseline i.e initiation of ECMO (BL), five days prior to circuit change (D-5) to circuit change day (D0) and 2 days after circuit change (D2) in COVID-19 (n=85) and non-COVID-19 (n=32) patients. Trends comparisons made between D-5 and D0, and D0 to D2. Kolmogorov-Smirnov normality testing, RM Two-way ANOVA or mixed-effect group analyses with Geisser-Greenhouse correction, and Dunnett's multiple comparison for hypothesis testing were performed. All data were non-parametric and presented as median (interquartile range). * trends over time, # comparison between COVID-19 cohorts, & interaction between COVID-19 cohorts and time. * p<0.05, ** p<0.01, *** p<0.001, **** p<0.0001.*

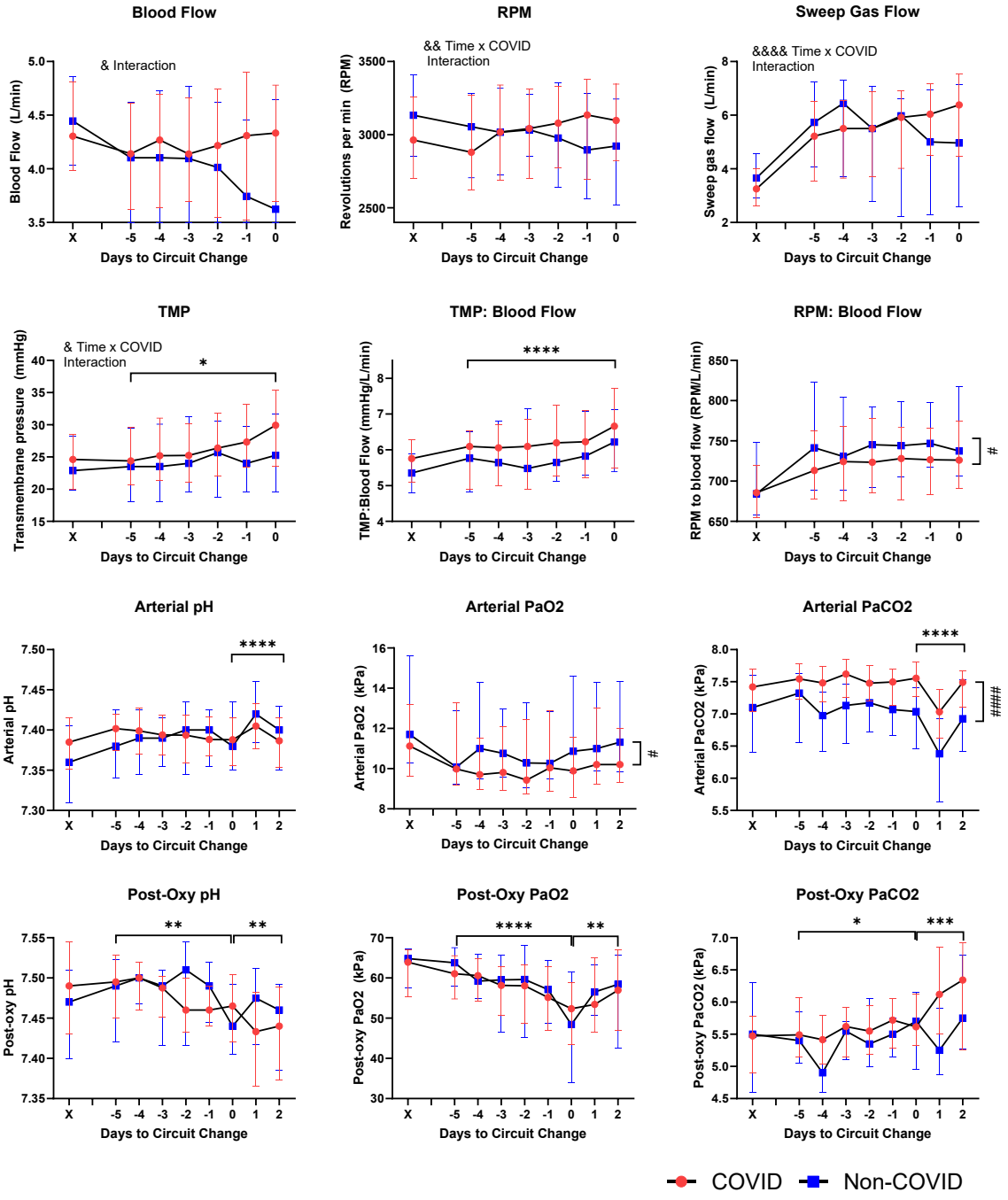


Figure 3.7 Trends in ECMO device parameters and arterial and post-oxygenator blood gases in the lead up to circuit change.

*Comparisons of ECMO device parameters, and blood gases between COVID-19 (n=85) and non-COVID-19 (n=32) from initiation of ECMO (Day X), five days prior to circuit change (D-5) to circuit change day (D0) and 2 days after circuit change (D1,2) for blood gases. Revolutions per minute, RPM; transmembrane pressure, TMP. Kolmogorov-Smirnov normality testing, RM Two-way ANOVA or mixed-effect group analyses with Geisser-Greenhouse correction, and Dunnett's multiple comparison for hypothesis testing were performed. All data were non-parametric and presented as median (interquartile range). Trends comparisons made between D-5 and D0, and D0 to D2. * trend over time, # comparison between COVID-19 cohorts, & interaction between COVID-19 cohorts and time. * p<0.05, ** p<0.01, **** p<0.0001.*

3.5 Discussion

In this chapter the clinical data of ECMO patients in one UK tertiary ECMO centre were analysed. To the best of my knowledge, this is the largest single centre study to evaluate the incidence of MO dysfunction in patients on ECMO between those with COVID-19 and non-COVID-19 ARDS. Whilst this is a retrospective data analysis, I was able to observe differences in blood and ECMO parameters between an immunothrombotic patient cohort (COVID-19) and non-immunothrombotic cohort, both during the initial week on ECMO and in the lead up to circuit change. This observational data helps to form the basis of further studies to investigate immunothrombosis in ECMO patients, or other extracorporeal circuits.

3.5.1 Clinical differences are observed between COVID-19 and non-COVID-19 patients with severe ARDS requiring ECMO

Aetiology of ARDS is heterogenous and even in patients with respiratory failure from viral pneumonitis, there are distinct clinical differences in how they present depending on the cause. In our centre, the majority of patients who required VV ECMO before 2020 had viral pneumonitis from influenza whereas between April 2020 to September 2021 viral pneumonitis was mostly due to COVID-19. Our data shows that there are some differences at presentation to the ECMO centre, between COVID-19 and non-COVID-19 patients with severe ARDS requiring ECMO.

Demographics

The ELSO registry report from early in the pandemic did not show any difference in demographics between COVID-19 and non-COVID-19 patients [175] but the demographics of patients in our study are comparable to many later studies comparing COVID-19 with non-COVID-19 ECMO patients, many of which also report a higher proportion of patients of non-Caucasian ethnic groups, and higher BMI (>25) in COVID-19 patients [164, 167, 176, 179, 182, 183]. A meta-analysis of 59 studies showed that male patients were more likely to have higher risk for COVID-19 infection, increased severity of disease, and ICU admission [184], but was not demonstrated in this data. High BMI also increases risk of severe COVID-19 disease, ICU admission and death [185]. Furthermore, patients with high BMI may not have been optimally ventilated e.g. lower PEEP for their BMI [164], and may not have been proned due to perceived increased risks associated with prone positioning. This could mean patients with high BMI may not have received optimal ventilation strategies as per ARDS guidelines and may have received more injurious ventilation. Overall, these risk factors for severe COVID-19 disease,

and therefore potential need for ECMO may explain the demographic differences between COVID-19 and non-COVID-19 patients.

Survival to ECMO decannulation (78.5%) and hospital discharge (69.2%) in this cohort of patients was slightly higher than other studies (50-72%) [175, 179, 186-188]. There was no difference between COVID-19 and non-COVID-19 patient survival rates, similar to other studies [174, 175, 177, 189].

Laboratory tests

Regarding baseline bloods and trends in the first week of ECMO initiation, the results in this study differ slightly from those observed in other studies but were overall comparable. We observed no difference in fibrinogen, lower WCC and lower CRP in COVID-19 patients in contrast to other studies who observed higher fibrinogen and higher CRP [166, 167]. The lower creatinine, bilirubin and liver enzyme levels and higher platelet count in COVID-19 ECMO patients may contribute to the lower SOFA scores compared to non-COVID-19 patients as found in other studies [166, 167, 175]. These results do not necessarily mean lower inflammation or less organ failure but may reflect the national ECMO referral pathway and its more stringent exclusion criteria, particularly during a time with reducing ECMO capacity during the pandemic, which excludes patients who have had more than 7 days of mechanical ventilation, and established multi-organ failure [28, 174]. Some parameters such as increased platelet count, and similar D-dimer level was reported across all studies [166, 167, 175]. Despite initial reports that D-dimer could be used as a marker of COVID-19 severity [169, 170], in our study, there were no differences in fibrinogen or D-dimer levels in early ECMO between the two cohorts.

3.5.2 Thrombogenicity of COVID-19 was associated with increased MO dysfunction, and longer ECMO duration.

In patients with ARDS both the use of ECMO and having COVID-19 disease are independent thrombogenic factors [124, 129, 168]. Evidence suggests that COVID-19 is an immunothrombotic disease [93, 164, 190] therefore I hypothesised that the thrombogenic nature of COVID-19 would increase risk of thrombosis related ECMO circuit failure resulting in need for circuit change.

COVID-19 patients were twice as likely to require a circuit change than non-COVID-19 patients despite being adequately anticoagulated to higher heparin anti-Xa level (0.3-0.5U/ml). This study supports early findings by Bemtgen et al., (2020), who compared 11 COVID-19 patients to 55 non-COVID-19 patients on ECMO in their single centre study and found circuit related thrombosis leading to circuit change was more frequent in COVID-19 patients (63.6% vs 18.2%, P=0.03) with no difference in demographics or time to circuit change [179]. Similar results were found by other single centre studies [186, 191]. However, early results from the international ELSO registry showed that mechanical complications such as circuit change or MO failure occurred in only 230/983 (23%) COVID-19 patients [175] and later the ECMO-SURGES study found that only 449/1345 (33%) of COVID-19 patients required a circuit change, with increased frequency of circuit change observed in later COVID-19 variants (wild type 30%, alpha 37% and delta 46% ; P<0.0001) [192]. The ELSO studies show lower circuit change rates compared to our single centre study, but they did not compare their patients to a non-COVID-19 cohort, and participating centres were self-selected during a time of global pandemic with a higher number of small volume centres. Prior to the COVID-19 pandemic, the ELSO registry in 2016 reported oxygenator failure in 9.1% respiratory ECMO patients and 6.6% cardiac ECMO patients [125], and in 2022 reported circuit change in 25.8% respiratory ECMO patients and 17.7% cardiac ECMO patients but did not separate COVID-19 cohorts [193]. Of note, our centre has higher incidence of circuit change (38.5%) compared to the ELSO data.

COVID-19, and circuit change are both associated with longer ECMO duration (Figure 3.3). Using multivariate logistic regression, it was found that risk of circuit change was associated with increased duration of ECMO, and there was no association with COVID-19 status. The Kaplan Meier curves for incidence of circuit change (Figure 3.2), diverge after 11 days with COVID-19 patients more likely to require circuit change and have increased risk of circuit related thrombosis with longer ECMO duration. This suggests that there is another process in COVID-19 ARDS which impacts on ECMO health and ECMO duration. It can be speculated that COVID-19 is a thrombogenic condition, which increases the risk for MO dysfunction due to thrombosis and need for circuit change, which may increase the duration of the ECMO run [133]. Alternatively, COVID-19 patients had more severe respiratory failure with increased hypoxia and hypercarbia [164] which required increased ECMO flows and higher RPM to provide adequate oxygenation which can cause increased shear and activation of neutrophils and platelets and subsequent thrombus formation [194, 195]. In addition, the increased severity of COVID-19 respiratory failure takes longer to resolve due to

increased pulmonary angiopathy [93, 95] and therefore patients remained dependent on ECMO for longer which increases the risk of MO dysfunction.

Although there were differences in circuit change frequency and ECMO duration, between COVID-19 and non-COVID-19 patients, there were no differences in mortality across COVID-19 and circuit change cohorts. The non-COVID-19 circuit change frequency, ECMO duration and ECMO survival rates are comparable to another high-volume UK ECMO centre with similar practice [160]. Nevertheless, requirement for circuit change is associated with increased ECMO duration, and therefore increased ICU LOS and increased ECMO and hospital mortality [125, 133, 160]. It is therefore important to monitor MO dysfunction to decide which patients truly require circuit change for MO dysfunction.

3.5.3 Monitoring membrane oxygenator dysfunction is more difficult in COVID-19.
The initial management of patients on ECMO, and their circuit health parameters did not differ between COVID-19, and non-COVID-19 patients as previously mentioned. However, there were some differences in bloods early in the ECMO run and differences became more apparent in the days preceding circuit change in patients who did require circuit change for MO thrombosis suggesting altered pathophysiology of circuit failure in COVID-19.

COVID-19 patients had lower inflammatory markers such as CRP and total leucocyte count at ECMO initiation, lower bilirubin, creatinine and higher platelet counts which likely contribute to the lower SOFA score. COVID-19 patients were more likely to have single organ failure – lung; but had a higher degree of respiratory failure (increased hypoxia and hypercarbia) than non-COVID-19 patients and maintained higher ECMO flows and sweep gas flows compared to non-COVID-19 patients who had reducing ECMO requirements after 3-4 days of ECMO support (Section 3.4.4), however, this did not impact on TMP or TMR early in the ECMO run. Regarding ECMO circuit health parameters there were no differences in fibrinogen or PFH between the two cohorts, and the higher platelet count in COVID-19 patients was maintained early in the ECMO run which shows that despite increased ECMO blood flow settings, COVID-19 did not impact most measures of circuit health early in ECMO. The only deviation from conventional ECMO management in the COVID-19 cohort was the higher anticoagulation target which was common practice in many ECMO centres during the pandemic [167, 179, 196].

Many differences were observed in the 5-day lead up to circuit change. COVID-19 patients continued to maintain higher blood flow rates whereas the non-COVID-19 patients had reducing blood flow rates by the time of circuit change. This resulted in a rise in TMP in COVID-19 patients compared to a lower TMP in non-COVID-19 patients. The need for higher blood flow in COVID-19 patients is likely due to the higher degree of hypoxia, or higher inflammatory response in COVID-19 patients [171, 197]. It has been suggested by some groups that the change in TMR is more sensitive than TMP in predicting MO dysfunction [160]. TMR increased in the lead up to circuit change in both groups, but whilst there was also a trend for higher TMR in COVID-19 patients compared to non-COVID-19 patients, this was not statistically significant. Interestingly the RPM/blood flow is lower in COVID-19 patients at ECMO initiation and remained so in the lead up to circuit change but with no increase despite increasing blood flow requirements and TMP. This may be due to the higher anticoagulation target set for COVID-19 patients or other differences in COVID-19 pathophysiology, which are yet to be determined. Lower RPM would reduce the shear on blood and therefore lower PFH and higher haemoglobin [152]. Whilst we did not observe lower PFH, the haemoglobin was higher in COVID-19 patients compared to non-COVID-19 patients, throughout the ECMO run.

Regarding blood parameters, the expected trend for decreasing fibrinogen, platelets and increasing PFH in the lead up to circuit change is observed in all ECMO patients with no difference between COVID-19 groups, although the levels of thrombocytopenia were not as low in COVID-19 patients. The main difference between the groups was a much less exaggerated increase in D-dimer in the COVID-19 cohort despite similar baseline levels. This difference in D-dimer is also seen early in the ECMO run. D-dimer levels remained the same in both cohorts in the early ECMO run (up to day 4), however, by day 7, D-dimer was more elevated in non-COVID-19 patients compared to COVID-19 patients. When patients who required circuit change in the first 10 days of ECMO were excluded from this analysis, this difference was less apparent, highlighting the value of D-dimer in monitoring circuit health. Many centres use increasing D-dimer to monitor for need for circuit change in ECMO patients [131, 135]. However, the less exaggerated D-dimer increase, and the higher platelet counts in COVID-19 patients made monitoring for MO dysfunction difficult in this group of patients and suggests a different mechanism of MO thrombosis in COVID-19.

3.5.4 Increased thrombogenicity in COVID-19 due to lack of fibrinolysis

D-dimer is a fibrin degradation product and is often used as a marker for thromboembolic disease. Early COVID-19 risk stratification models used D-dimer as a marker for disease severity and mortality risk [198-200]. There is increased pulmonary vascular angiogenesis and thrombosis in COVID-19 [93, 95] and it has been suggested that the raised D-dimer levels in severe COVID-19 related ARDS is due local fibrinolysis within the lung [201]. In ECMO patients D-dimer is a marker of clot burden within the MO and is often used as a marker for predicting need for circuit change [130, 135]. However, the data presented here contradicts both theories that D-dimer will be elevated in COVID-19 and in the lead up to circuit change in these patients. We and Doyle et al. and found no difference in admission D-dimer levels between COVID-19 and non-COVID-19 patients who required ECMO [167]. Furthermore, the D-dimer did not increase as expected in COVID-19 patients.

The lower D-dimer levels seen in COVID-19 ECMO patients in the lead up to circuit change is likely due to fibrinolytic shutdown which has been observed in COVID-19 patients [95, 202]. There is increasing evidence that COVID-19 patients remain in a hypercoagulable state with increased clot integrity, reduced fibrinolysis and increased functional fibrinogen measured using function coagulation assays such as Thromboelastogram (TEG) [95, 202-204], with less thrombocytopenia and higher fibrinogen levels than other viral causes of ARDS requiring VV ECMO [95, 166, 167]. This suggests that there is increased thrombogenicity in COVID-19 disease and possibly altered pathogenesis of thrombogenesis.

The difference in D-dimer levels and potential increased thrombogenicity in COVID-19 disease further highlights the challenge of accurately predicting need for circuit change in a clinical setting particularly in the context of different aetiologies for ARDS and need for ECMO. Rising D-dimer is one of the most commonly used markers correlating with increased clot volume [130, 131] and is one of the first markers to change with impending circuit thrombosis [135], along with reducing fibrinogen, platelet count and increasing PFH; in combination with reduction in ECMO gas exchange and increased MO resistance. The reduced fibrinolysis associated with COVID-19 can lead to impaired thrombus dissolution and increased thrombotic phenomena seen in COVID-19, including DVT, PE, cerebrovascular accidents, myocardial infarction, and other circuit thromboses (ECMO and renal replacement therapy) [167, 168]. Over a third of COVID patients have evidence on PE on their CT scan on admission to the ECMO centres compared to only 8% in patients with

Influenza requiring ECMO [95, 167]. This contributes to the degree of respiratory failure in COVID-19 and may lead to increased risk of thrombus formation within the ECMO circuit.

Thrombocytopenia is common in ECMO patients [205]. However, we and other groups found that COVID-19 ECMO patients tend to have less thrombocytopenia than non-COVID-19 ECMO patients [166, 167, 179]. Both thrombocytopenia and thrombocytosis are seen in severe COVID-19 disease [206] and the increased inflammation seen in COVID-19 patients could lead to increased thrombocytosis [166] and platelet activation in COVID-19 patients [207].

The data presented here demonstrates that currently clinically used markers of ECMO circuit health are not enough on their own for monitoring for MO thrombosis. COVID-19 further highlighted how a disease aetiology can increase thrombosis risk, as well as alter clinically measured parameters as part of the disease process highlighting the need for better biomarkers of ECMO health or thrombosis. Whilst reduced fibrinolysis is the likely cause for reduced clot breakdown and therefore increased clot integrity, the cellular mechanisms leading up to this have not been investigated.

3.5.5 ECMO is immunothrombotic

The thrombogenicity of COVID-19 leads to a more severe respiratory failure with increased hypoxia and hypercarbia than non-COVID-19 ARDS [164], and therefore longer resolution time and longer duration on ECMO. Whilst there were differences between the two cohorts with regards to incidence of MO thrombosis and the changes in the lead up to circuit change, the multivariate logistic regression shows that ECMO duration is the greater risk factor for circuit change rather than disease aetiology. Indeed, the time to first circuit change in COVID-19 patients was longer than non-COVID-19 patients. Other centres also found ECMO related thrombosis is associated with longer ECMO duration [208, 209]. Exposure of blood to the synthetic surfaces of the ECMO circuit and large surface area of the MO leads to activation of the coagulation system and allows platelets and leucocytes to adhere to the tubing and MO surfaces, increasing thrombin generation [124]. There is evidence of immunothrombosis on the MO surface as NETs have been found on MO clots [141, 210, 211].

The impact of thrombosis on MO function has led to advances in ECMO materials including heparin bound tubing, and PMP oxygenators, and the ELSO guidelines recommend anticoagulation in patients on ECMO if there is no bleeding complication [37, 126, 212]. There is recent work using computational models investigating the impact of MO structure specifically

shape and blood inlet and outlet position on the haemodynamic features within the MO [139]. Fu and colleagues found that a round oxygenator with multiple inlets and outlets creates a more even distribution of blood flow, thereby reducing areas of low flow or dead zones and reducing thrombosis risk [139]. In their computational model the HLS Advance oxygenator with four inlets and one outlet would have a lower thrombosis risk compared to the Nautilus oxygenator which only has one inlet and one outlet. Other in vitro models of ECMO circuits suggest that the impact of the MO surface area on activating blood and platelets was insignificant but the high mechanical shear stress from the pump is a large contributing factor [194].

To date, there are no studies comparing the MO efficacy of different ECMO pump and oxygenator configurations. To fully elucidate the effect of different oxygenator/pump configurations on blood and platelet activation, larger studies comparing the Centrimag with different oxygenators such as Nautilus (Medtronic), A.L.One (Euroset), HiLITE 7000 (Medos) or the Cardiohelp pump with Quadrox (Getinge, Sweden) and HLS Advance (Maquet, Germany) oxygenators could be conducted to see what the effects the shape, inlet and outlet position and number have in vivo.

Whilst there are different aetiologies of ARDS necessitating ECMO use, and therefore varying levels of immunothrombosis, ECMO is the common facet, and the variable that can be modulated when investigating immunothrombosis in ECMO patients. However, it must also be noted that initiation of ECMO has various effects on physiology, firstly it allows the use of lung protective ventilation reducing lung injury and associated inflammation; secondly the improved oxygenated blood flow through the pulmonary vasculature reduces the effects of hypoxic pulmonary vasoconstriction, improving right ventricular afterload and therefore relief of right heart failure and associated shock [213]. Any conclusions regarding the effect of ECMO on immunothrombosis must take these factors into account.

3.5.6 Limitations

This study's main limitations are its retrospective, single centre, observational design. Whilst the single centre nature reduces inter-centre variability in practice, it may account for the variations in results when compared to larger multi-centre ELSO registry data [125, 175, 189]. Only data from patients on a Cardiohelp system was analysed. Comparisons with other UK centres where the primary ECMO configuration is with a Centrimag pump would be valuable. There is however a large range of oxygenators which can be used with the Centrimag pump and as such this study is the largest single centre study with one type of ECMO pump and

oxygenator, ensuring meaningful comparisons between the COVID-19 and non-COVID-19 groups.

Larger studies which include data from multiple centres to investigate the impact of equipment on the frequency of circuit thromboses and differences in circuit health parameters would be helpful. Whilst there are computational models of oxygenators being developed [139], these do not account for the patient factors such as disease aetiology, variations in coagulation, and cannot predict the change in laboratory parameters.

Missing data was a large issue resulting in numerous patients being excluded from the bloods trends analyses. LDH was routinely measured during the COVID-19 pandemic but was not for the non-COVID-19 patients prior. Comparing LDH trends may shed some further light into the level of haemolysis in conjunction with the PFH. In evaluating the hypercoagulability of COVID-19 and the interplay with ECMO there would have been merit in analyses of thromboelastography or platelet function assays to assess functional coagulopathy. There are small studies that have included the analysis of TEG in COVID-19 patients [214, 215]. Future work could include a prospective study, with concurrent TEG, platelet function tests and thrombin generation assays around times of circuit change to assess further biomarkers of hypercoagulability, as well as biomechanistic studies into neutrophil platelet interaction and the role in ECMO patients.
Whilst circuit change is an intervention usually due to ECMO circuit thrombosis and therefore a tangible end point to measure, it is also a weak endpoint as the decision to perform a circuit change is highly subjective between centres and clinicians, and not all parameters are measured in every centre [135, 137]. Predicting when there is a significant MO thrombosis requiring a circuit change can be difficult as there are no set guidelines nor a set single threshold or parameter for when a circuit change should be performed. The clinical variables used to monitor circuit health such as D-dimer, and platelet count can be affected by the underlying critical illness and disease process and should be considered in the context of the patient's clinical condition; for example, D-dimer is often used as a marker for MO thrombosis but early in the COVID-19 pandemic, it was thought to be a marker for disease severity [198, 199] and could have impacted the decision making for circuit change; and conditions such as HIT limit the use of platelet count as a marker for MO thrombosis [205]. Furthermore, treatments for the underlying condition could affect the thrombogenicity and immunothrombotic profile. COVID-19 induces a cytokine storm priming neutrophils to release NETs which can form aggregates with platelets leading to increased thrombosis as well as vascular endotheliopathy [94]. The RECOVERY trial found steroid treatment (dexamethasone 6mg) reduced mortality in hospitalised patients with COVID-19 [216] and

following publication of these results (July 2020), dexamethasone 6mg or equivalent dose was standard of care for hospitalised patients with COVID-19 in subsequent waves. Steroids reduce the hyperinflammation caused by the cytokine storm and therefore the potential immunothrombotic consequences such as neutrophil activation and NETosis [217], and activation of coagulation cascade [206, 218]. Unfortunately, data regarding steroids or other immunosuppressive agents was not extracted and therefore not analysed.

3.6 Concluding remarks

Development of thrombosis on the MO is common [130, 132] and we demonstrate it is more common in COVID-19 patients due to the degree of respiratory failure and need for longer duration on ECMO. There is a clinical and economic impact of this complication, particularly during the height of the pandemic where ECMO resources and intensive care beds are in demand. Predicting circuit thromboses is difficult and is even less clear in COVID-19 patients, and there are no new therapies to reduce circuit thrombosis. Simply increasing anticoagulation to prevent circuit thromboses is not a viable option as circuit thromboses developed despite higher anticoagulation targets in COVID-19 patients, and increased anticoagulation increases the risk of bleeding which is associated with poor outcomes [166, 167, 219]. The differences in blood and ECMO parameters prior to circuit change between COVID-19 and non-COVID-19 patients suggests that the mechanism underlying thrombosis in COVID-19 differs to non-COVID-19 patients.

COVID-19 has highlighted the important interplay between inflammation and coagulation in critically ill patients with increased angiogenesis and thrombosis in these patients [95, 220]. The ECMO-coagulation interaction is complex and differs in the nature and magnitude to the responses produced by other extracorporeal circuits. For example, thrombocytopaenia is particularly common in ECMO patients and the incidence of heparin-induced thrombocytopenia is far more frequent in ECMO compared with CPB [205]. These differences are a result of the more activated and dysfunctional inflammatory and coagulant conditions prevailing in ECMO patients. Neutrophils and platelets both have key roles in inflammation and coagulation. Of increasing interest is the role of NETs and their role in sepsis, ARDS and in COVID-19 leading to increased thrombosis [85, 90, 102, 220]. Other mechanisms in the pathophysiology of COVID-19 related thrombosis that necessitate further investigation include increased platelet numbers and activation, and fibrinolytic shutdown [202].

Moreover, the aetiology of severe ARDS is heterogenous and perhaps the same conventional principles of ECMO management cannot be applied to all patients. These putative drivers of ECMO failure vary considerable between patients and over time with COVID-19 being one example of a thrombogenic cohort demonstrating differences in thrombosis. We have demonstrated that ECMO thrombosis particularly in the context of COVID-19 disease is a significant problem which impacts on patient outcomes. A more comprehensive understanding of the basic processes involved is required. Being able to accurately predict future circuit change by finding novel biomarkers, and/or therapies, may help in early initiation of preventative therapies, or development of new equipment.

Chapter 4: Immune and platelet responses in ECMO patients

Abstract

An emerging area of interest in immunothrombosis is the production of NETS. Neutrophils and NETs play key roles in the pathophysiology of ARDS and are found in patients on other extracorporeal circuits such as cardiopulmonary bypass and haemodialysis, but there is little data into the role of NETs in ECMO patients.

In this chapter, I examined soluble markers of inflammation, neutrophil activation, NETosis, and platelet activation in patient plasma samples using ELISA and fluorometric assays. This was a single centre retrospective cohort study in a tertiary ECMO centre. There were high levels of neutrophil activation as measured by release of neutrophil cytoplasmic proteins neutrophil elastase (NE) and myeloperoxidase (MPO) in patients with SARF on ECMO. After ECMO initiation there were several changes: firstly, there was increased NETosis as measured by Citrullinated Histone H3 (CitH3) and nucleosomes (NuQH3.1); secondly, there was a reduction in inflammatory mediators such as vascular endothelial growth factor, angiopoietin-2, metalloproteinase-9, and tumour necrosis factor alpha, and also NE; and thirdly there was reduction in platelet activation markers platelet factor 4 and P-selectin as well as reduced platelet aggregation.

In summary, patients with SARF had high levels of neutrophil activation and NETosis. The initiation of ECMO in these patients, led to further increased NETosis despite reduction in inflammatory cytokines. It could be speculated that ultra-lung protective ventilation, which is usually initiated after transition to ECMO support, leads to the reduction of inflammatory cytokines from the alveolar epithelium and endothelium and also reduction of some neutrophil activation such as reduced NE. However, the increase in NETosis may reflect a different mode of neutrophil activation, for example as a result of shear stress from ECMO. I propose that the shear from the ECMO circuit leads to increased activation of platelets, and neutrophils. The increased NETosis may be due to increased neutrophil-platelet interactions which warrants further investigation. In addition, the increased NETosis may be a target for therapeutic intervention in patients on ECMO who have increased thrombosis or membrane lung dysfunction, for example, with histone scavengers such as Clusterin.

4.1 Introduction

4.1.1 Neutrophil activation, degranulation and NETosis

Neutrophils are among of the first cells to arrive at sites of infection and inflammation and have key roles in the host response to infection. Neutrophils are activated by ligands (antibodies, pathogens, cytokines, activated platelets etc.) binding to neutrophil receptors (TLR4, PSGL-1, HMGB1 and Fc-γ receptors) [47] leading to an influx of calcium into the cells activating NADPH oxidase and generation of ROS [48].

Generation of ROS is essential to neutrophil degranulation and release of bactericidal enzymes such as MPO and NE from the azurophilic granules. Both MPO and NE are required for NET formation. And they have been shown to regulate the formation of NETs by disrupting the charge of intracellular chromatin, and degrade specific histones [52]. ROS production also triggers activation of the calcium dependent enzyme PAD4 which leads to citrullination of histones, and subsequently NETosis (See Section 1.4.4). Histone citrullination by PAD4 is essential for NET production and CitH3 is seen as an early NET-specific biomarker [59] with many studies using this as an early biomarker for NETosis [60, 62]. The unravelling of chromatin material exposes intracellular DNA and nucleosomes hence nucleosomes are used as a surrogate marker for NETosis [64].

4.1.2 Neutrophil activation in ARDS

In ARDS, the lung injury is due to a combination of alveolar epithelial and capillary endothelial damage which leads to release of cytokines and chemokines, causing capillary leak, interstitial and alveolar oedema, and hypoxia (See section 1.1.4). The cytokines also recruit and activate neutrophils and macrophages into the alveolar space [7]. The activated neutrophils release ROS, granular enzymes and NETs to defend against the invading pathogens and interact with the epithelium causing further cytokine release [18, 19].

NETosis markers are found in bronchoalveolar lavage fluid (BALF) [85, 89] and plasma of patients with pneumonia and ARDS are found to correlate with disease severity and mortality [64, 87, 88]. NETs were increased in patients with COVID-19 related ARDS [90-92] and many hypothesised that NETs were involved in the immunothrombosis of COVID-19.

4.1.3 NETosis in extracorporeal circuits

Whilst NETs have been shown to be increased in patients with ARDS and COVID [92, 220-222], there is limited evidence regarding NETs in ECMO or other extracorporeal circuits. There are some reports of increased neutrophil activation, NET formation or presence of NET components after initiation of CPB [105-107] and haemodialysis [108, 110, 223] and is associated with increased risk of thrombosis. Some studies have found that NETs and NET components such as nucleosomes, MPO or cfDNA were associated with higher rate of haemodialysis vascular access thrombosis of both arterio-venous fistulas and grafts [109] and central venous catheters [224]. NETs and their components can interact with coagulation cascade, platelet activation and pathways that modulate thrombin formation (Section 1.5.3 and Figure 1.9). Both CPB and haemodialysis exposes blood to an extracorporeal circuit for a short period of time (only a few hours), whereas duration of ECMO is much longer: for days, often weeks and in very rare cases for months; and often in patients with established severe neutrophil activation. Therefore, the potential for NET production is higher, and the effect of NETs on inflammation and thrombosis within the patient and the ECMO circuit are much greater. Indeed, it has been found that levels of cfDNA are increased with longer CPB times (>100minutes) compared to shorter runs [106].

There are only a limited number of small studies investigating NETs in ECMO and the reports in the literature are conflicting. Haus et al. found ECMO patients have higher rates of NETs and NET precursors compared to healthy volunteers [225]. Another study examined NET markers in 12 COVID-19 ECMO patients using ELISA but did not show any difference in NET markers (cfDNA, MPO-DNA complexes) or inflammation (as measured by IL-8) before or after ECMO initiation [226].

NETS are an emerging area of interest in many fields but knowledge regarding NETs in ECMO is lacking. Given that NETs are a prominent feature of ARDS and are found in thrombi from many vascular thrombotic conditions, it stands to reason that NETs may play a role in accelerated immunothrombosis in patients supported on ECMO.

4.1.4 Platelet activation in ECMO

Platelets are primarily known for their role in haemostasis and coagulation and are also involved in the host immune response. Platelet activation causes the release of many pro- and anti-inflammatory mediators that can modulate the immune system. For example, P-

selectin is found on endothelial cells and platelets and help recruit neutrophils to sites of injury by facilitate their “rolling” across the endothelium (Figure 1.1). In addition, platelets contain several proteins/chemokines (such as PF4/CXCL4, CXCL5 and coagulation factors), stored in the alpha granules which are released on activation. PF4 may have bactericidal properties and in general many of the platelet mediated immune effects are proinflammatory [227].

The development of thrombocytopenia during ECMO is widely reported and is also demonstrated in the data presented in chapter 3. Patients on ECMO also have reduced platelet function as measured by platelet aggregometry and thromboelastography [124, 145]. Other markers of platelet function include surface expression of proteins and receptors such as fibrinogen, GPIba and GPVI receptors and P-selectin which is decreased over the course of the ECMO run due to shear-induced shedding of surface receptors [149, 228].

Upon activation, platelets degranulate and release granule proteins such as P-selectin and PF4. P-selectin is found in Weibel-Palade bodies of endothelial cells as well as in platelet α-granules and is expressed on the surface of activated platelets and endothelium. Platelets are the main sources of plasma P-selectin and therefore are representative of platelet activity and platelet count [229]. P-selectin binds to PSGL-1 on leucocytes, mediating leucocyte adhesion, leucocyte rolling and inflammation. These pathways lead to proteolytic shedding of P-selectin from platelets releasing soluble P-selectin, a monomer. Binding of P-selectin and PSGL-1 appears to occur best when both are dimers [230]. Results from murine studies suggest monomeric P-selectin does not promote inflammation or promote coagulation [231]. However, soluble P-selectin is found in platelet extracellular vesicles and is released from platelet granules and endothelial cells after activation. Furthermore, P-selectin increases the expression of tissue factor on monocytes [232], therefore, soluble P-selectin has been proposed as a potential biomarker for sepsis [233, 234] but the interconnecting role of P-selectin between inflammation and coagulation is not fully understood.

PF4 is stored in alpha granules during platelet formation and in quiescence. The concentration of PF4 within a platelet is around 20ug/10^9 platelets [235]. PF4 is released from activated platelets and can increase the plasma levels from 5-25ng/ml at rest to over 600ng/ml when activated [236]. PF4 released from platelets plays a role in leucocyte recruitment to sites of injury and thrombus formation [237]. Platelets are activated by shear

stress caused by the ECMO pump, cannulae and connectors [238]. There are reports that compared to healthy controls, PF4 levels are increased in patients on ECMO [239] and there are increased levels of PF4 antibodies in ECMO patients [240]. The PF4-heparin ratio is important in the development of heparin induced thrombocytopenia (HIT) and the HIT immune complex (PF4-heparin-antibody complex). Since most patients on ECMO are anticoagulated with heparin infusions, the incidence of HIT is higher in this patient population [205, 241]. Despite this, there is little in the literature regarding PF4 and CD62P levels in ECMO patients.

Platelet and neutrophil interactions are increased in inflammatory states and can increase activation of both cell types. Regarding platelet activation and NETosis, mouse models show P-selectin is required for platelet induced NETosis and increased P-selectin increases neutrophil activation and NETosis [242]. Furthermore, the HIT immune complex has a high affinity for cfDNA, a key component of NETs, and levels were associated with increased risk of vascular access failure in HD patients [243]. Perdomo et al also report that neutrophil activation and NETosis are the major drivers for thrombosis in HIT [244] which may suggest a role for PF4 in neutrophil activation or modulation.

Platelet dysfunction is commonly associated with ECMO use due to the constant exposure to a foreign surface and contact activation, high mechanical shear stress from the ECMO pump, endothelial damage, and exposure to continuous heparin infusions. There are only a limited number of published studies investigating platelet function and soluble platelet activation markers in patients during ECMO.

4.2 Aims and hypothesis

This chapter aimed to investigate whether there is increased neutrophil activation, NETosis and platelet activation in patients who are managed on VV ECMO for severe ARDS.

I hypothesise:

1) Exposure of blood to the extracorporeal circuit promotes inflammatory activation leading to:
    a. increased neutrophil activation and NETosis (both soluble NET markers and cell-associated NETs)
    b. increased levels of circulating inflammatory cytokines

2) ECMO promotes platelet activation and results in increased plasma levels of the platelet activation markers PF4 and CD62P
3) ECMO affects platelet function which can be measured using clinical platelet function assays

In addition, by comparing the levels of neutrophil activation markers and NETs in an immunothrombotic condition such as COVID-19, I hoped to see if there were any biological markers of increased immunothrombosis.

4.3 Methods

4.3.1 Study design and participants

Plasma samples were collected from patients enrolled into the DeVENT and HITEC studies (Section 2.2.2 and 2.2.3). Both studies enrolled adult (age ≥18years) patients who were admitted to the Royal Brompton Hospital through a specialist SARF and ECMO service. DeVENT recruitment was open during the COVID-19 pandemic from March 2020 – April 2021 and the majority of patients enrolled had COVID-19. HITEC recruitment was open from June 2022 – May 2024 and most patients did not have COVID-19.

Sample collection schedule is described in sections 2.2.2 and 2.2.3. In brief, blood samples were collected before ECMO initiation, and shortly after enrolment to the study. Samples were collected at regular time points according to the study protocols. All samples were taken from an already indwelling arterial line or central venous catheter. DeVENT sample collection was every 3-5 days in the first 2 weeks and weekly thereafter until the patient was liberated from ventilation or were transferred out of our institution. HITEC sample collection was every 5-7 days whilst on ECMO, as well as before and after circuit change (if required) and before and after ECMO decannulation. If clinical experience allowed, for some HITEC time points, samples were collected pre-oxygenator and post-oxygenator rather than from an indwelling line, to investigate if there were any differences pre- and post-membrane.

4.3.2 Data collection and definitions

Demographic, clinical, laboratory, ECMO mechanical data were extracted from electronic medical records (Intellispace Critical Care and Anaesthetics Information Systems; Phillips, Netherlands). Clinical data were reviewed and collated by investigating clinicians.

Start of ECMO is defined as cannulation; end of ECMO is defined as decannulation (DC) or death (if the patient died whilst on ECMO).

All data was organised into 24-hour periods for analysis and averaged over the 24-hour period. 24-hour periods relating to ECMO duration were calculated from ECMO cannulation.

4.3.3 Sample collection

Blood sample processing from patients in the DeVENT and HITEC studies are described in Section 2.2.5. In short, SST tubes were left to stand for 30 minutes at room temperature before centrifugation. SST, EDTA, and heparin tubes were then centrifuged at 2000 x *g* for 10minutes, 4°C to obtain serum and plasma respectively. The samples were aliquoted into Eppendorfs and stored at -80°C until assays were run.

4.3.4 ELISA

EDTA plasma from adult patients and HV were analysed by ELISA for neutrophil activation and NETosis markers: CitH3 (Clone 11D3, Cayman), MPO (Invitrogen), NE (Invitrogen), nucleosomes (NuQ-H3.1, Volition), and fluorometric assay for cfDNA (Quant-iT PicoGreen dsDNA, Invitrogen). EDTA plasma was used for analysis of the following inflammation markers: IL-1b, IL-6, IL-8, IL-10, MCP-1, MMP9, TNFα, VEGF and Ang2 (all Duoset, BioTechne). Serum from adult patients and HV were analysed by ELISA for platelet activation markers: PF4 and CD62P (both Duoset, BioTechne). There are missing values for some samples that were not within the detection range of the assay. Markers were quantified pre-ECMO, and 24-36 hours post-ECMO initiation for ECMO patients (D0 or D1), before and after decannulation (pre-DC and post-DC) and at study enrolment for HV.

4.3.5 Flow cytometry for cell-associated NETs

EDTA anticoagulated blood was stained with antibody cocktail as described in Section 2.4.4 and table 2.13. In brief, neutrophils were identified as $CD66b^{+}$, SSc^{high} events. Neutrophils that were double positive for Sytox Green and MPO were labelled MPO-DNA NETs, and neutrophils that were double positive for Sytox Green and Histone H3 were labelled HisH3-DNA NETs (Figure 2.10). Spectroflow and FlowJo were used for flow cytometry analysis.

4.3.6 Clinical platelet function and viscoelastic assays

Platelet aggregation in patient samples was investigated by whole blood impedance aggregometry using the Multiplate Analyzer (Roche, Switzerland) (Section 2.5.3). In short, hirudin whole blood was diluted 1:1 with preheated (37◦C) isotonic saline followed by 3 minutes incubation with platelet agonists at 37°C. The agonists tested were ADP 6.5µM, TRAP-6 32µM, and AA 0.5mM (ASPI test) (all Roche, Switzerland).

The viscoelastic assay used was the TEG6 Thromboelastogram (Haemonetics, USA) (Section 2.5.4). Citrated blood (1ml) was placed into a TEG 6 cartridge for analysis.

4.3.7 Statistical Analysis

Normality testing was carried out with Kolmogorov-Smirnov tests. Descriptive statistics were used to summarise the data. Results are presented as mean and standard deviations, or medians and interquartile range, as appropriate. Categorical values were summarised as counts and percentages. Differences between groups were compared with the Mann-Whitney, t-test, Kolmogorov-Smirnov, Kruskal-Wallis or Chi-squared tests as appropriate.

Trends in variables over time and between groups were analysed using two-way ANOVA or mixed effects analysis with Geisser-Greenhouse correction, and Dunn's multiple comparisons test. Paired comparisons were analysed using paired t-test or Wilcoxon matched pairs analysis as appropriate. All statistical tests were two-sided and $P<0.05$ was considered statistically significant. Analyses were performed using Prism GraphPad Version 9.5.1 (733) Software.

4.4 Results

4.4.1 Patient demographics and baseline characteristic of patients with ECMO initiation comparisons

The DeVENT study recruited a total of 55 patients from the Royal Brompton Hospital site. The HITEC study remains open for recruitment and at the time of writing has successfully recruited 69 patients to the study (Figure 4.1).

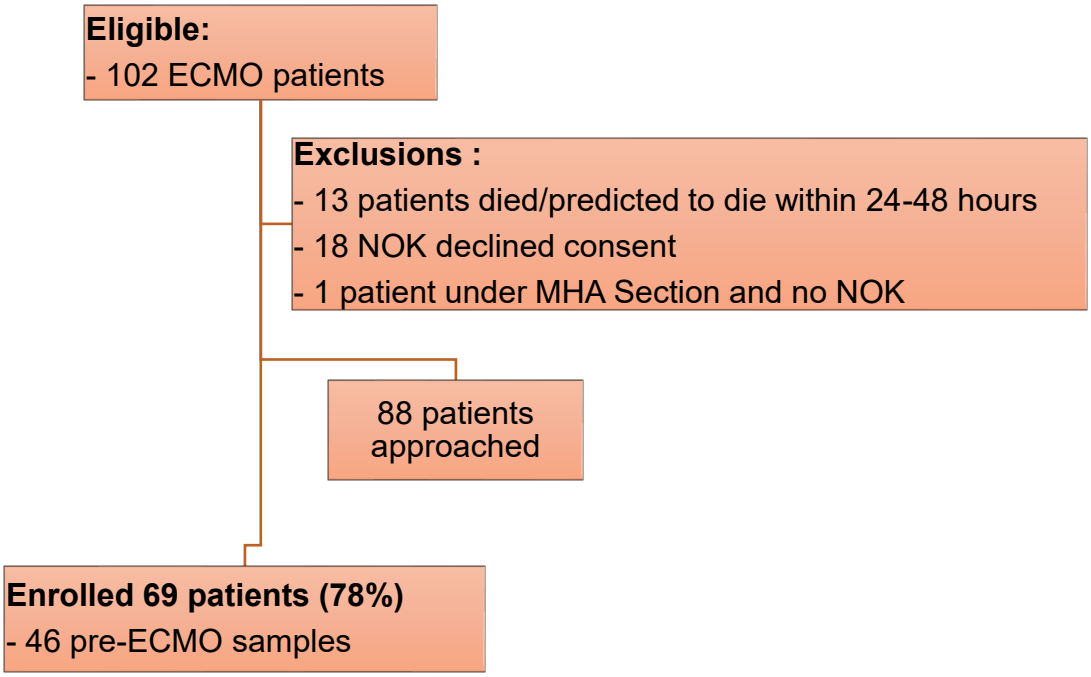


Figure 4.1 Consort diagram showing HITEC study recruitment to date.

Daily clinical data for the DeVENT and HITEC studies was electronically extracted from the electronical patient record system and pseudoanonymised for analysis.

For the purposes of this paper only HITEC patients up to and including RBH043 will be discussed. All were on ECMO (2 on VA ECMO, 39 on VV ECMO and 1 on VAV ECMO) (Table 4.1).

		DeVENT (n=55)	HITEC (n=43)
Demographics (n, %)	**Age**	50 (37-58)	46 (40-51)
	Male	39 (71%)	28 (65%)
	SOFA Score (median, IQR)	10 (8-11)	7 (6-11)
	ECMO	43 (78%)	43 (100%)
	- **VV ECMO**	55 (100%)	40 (93%)
	- **VA ECMO**	0	2 (4.6%
	- **VAV ECMO**	0	1 (2.3%)
SARF Aetiology	**COVID-19**	44 (80%)	2 (5%)
	Bacterial Pneumonia (Strep A, Staph)	3 (5.5%)	9 (21%)
	Viral Pneumonia (Influenza, Adenovirus)	0	6 (14%)
	Opportunistic infection (PJP, TB, other fungal)	0	4 (9%)
	Aspiration pneumonia	1 (1.8%)	5 (12%)
	Pulmonary embolus	1 (1.8%)	3 (7%)
	Obstructive Airways (Asthma, COPD)	0	7 (16%)
	Other Respiratory (e.g CF, Lung Cancer)	2 (3.6%)	4 (9%)
	Non-Respiratory (e.g. pancreatitis, trauma)	4 (7.3%)	3 (7%)

Table 4.1 Demographics of patients from the DeVENT and HITEC studies included in this thesis.
Novel Coronavirus disease 2019, COVID-19; chronic obstructive pulmonary disease, COPD; cystic fibrosis, CF; Extracorporeal membrane oxygenation, ECMO; pneumocystis jirovici pneumonia, PJP; severe acute respiratory failure, SARF; sequential organ failure assessment, SOFA; tuberculosis, TB; veno-arterial, VA; veno-arterial-venous, VAV; veno-venous, VV.

Samples from a total 52 ECMO patients and 8 HV were included for analysis. Due to the nature of sampling from a clinical cohort, not all patients had samples taken at both ECMO initiation and ECMO decannulation. Of the 52 ECMO patients, 44 had paired pre- and post-ECMO initiation samples, and 20 had paired pre- and post-ECMO decannulation samples.

The baseline demographics and admission bloods for HV, and ECMO patients who had pre- and post-ECMO initiation samples are presented in Table 4.2. Of the 44 patients, 15 (34.1%) had COVID-19 and 29 (65.9%) were non-COVID-19. When comparing baseline parameters between COVID-19 cohorts, there was no difference in age or gender. The non-COVID-19 patients had a higher SOFA score on admission (8.2 vs 6.1; P=0.0088). The COVID-19 patients had higher platelet count and lower CRP than non-COVID-19 patients in keeping with results presented in chapter 3.

Comparisons between bloods before and after ECMO initiation were not able to be made as the data for pre-ECMO bloods were not complete because of data missing from other hospitals, or data on the referral forms were out of date.

		HV (n=8)	All ECMO Patients (n=44)	COVID-19 (n=15)	Non-COVID-19 (n=29)	P-Value
Demographics (n, %)	**Age**	27 (24 – 40)	44.5 (32.5 – 51)	45 (34 – 52)	43 (26 – 49.5)	0.1690
	Male	3 (37.5%)	28 (63.6%)	10 (66.7%)	18 (62.1%)	0.7638
	SOFA Score	-	7.5 ± 2.8	6.1 ± 2.2	8.2 ± 2.8	**0.0088**
ARDS Aetiology	**COVID-19**		15 (34.1%)			
	Bacterial Pneumonia (Strep A, Staph, PCP)		8 (18.2%)			
	Viral Pneumonia (Influenza, Adenovirus)		5 (11.4%)			
	Aspiration pneumonia		5 (11.4%)			
	Pulmonary embolus		3 (6.8%)			
	Other Respiratory (e.g Asthma, CF, Lung Ca)		5 (11.4%)			
	Non-Respiratory		3 (6.8%)			
Baseline bloods (median, IQR)	**Hb (g/dL)**	-	97 (89 - 106)	103 (89 - 113)	94 (87.5 - 104)	0.2251
	WCC (x 10^9/L)	-	11.7 (7.7 - 20.8)	9.5 (7.2 – 12.2)	12.3 (7.9 – 23.7)	0.0987
	Neutrophils (x 10^9/L)	-	10.0 (6.7 - 18.0)	8.2 (6.5 – 10.3)	10.6 (6.8 – 21.4)	0.1272
	Platelets (x 10^9/L)	-	193 (100 - 262)	228 (195 - 300)	121 (84 - 243)	**0.0098**
	INR	-	1.1 (1.0 - 1.3)	1.0 (1.0 - 1.1)	1.2 (1.0 - 1.3)	0.1282
	APTT (s)	-	41.7 (32.4 - 59.2)	41.7 (32.4 – 59.2)	42.5 (32.5 – 60.2)	0.9849
	Fibrinogen (g/dL)	-	4.6 (3.4 - 6.5)	4.2 (2.6 – 5.6)	4.9 (3.5 - 6.8)	0.1322
	D-dimer (g/dL)	-	2386 (806 – 4145)	963 (656 – 2906)	2369 (804 – 4274)	0.1193
	CRP (mg/L)	-	168 (110 - 281)	124 (32 - 184)	180 (140 - 347)	**0.0081**
	PCT (µg/l)	-	0.8 (0.3 - 5.2)	0.4 (0.3 – 1.3)	1.7 (0.6 – 17.7)	0.1690

Table 4.2 Demographics and admission bloods of healthy volunteers and ECMO patients included for pre- and post- ECMO initiation comparisons.

Samples from 8 healthy volunteers and 44 ECMO patients were analysed. Comparisons were made between the 15 COVID-19 and 29 non-COVID-19 patients. Normality testing carried out using Kolmogorov-Smirnov test. Chi-squared test used to compare categorical data between groups. T-test and Mann-Whitney test used to compare age and bloods between groups. All statistical tests were 2-sided and P<0.05 was considered statistically significant.

Activated partial thromboplastin time, APTT; cystic fibrosis, CF; C-reactive protein, CRP; haemoglobin, Hb; extracorporeal membrane oxygenation, ECMO; international normalised ratio; INR, Pneumocystis jirovicii pneumonia, PJP; white cell count, WCC.

4.4.2 Markers of neutrophil activation and NETosis are increased in SARF and undergo a further increase after VV ECMO initiation.

Comparison of markers at baseline

Comparisons of NETs and neutrophil activation markers were made between HV, and patient admission samples (pre-ECMO). All samples were within the detection ranges of the assays used. Levels of all markers were low in HV. Levels of neutrophil activation as measured by cfDNA (389.2 [272.9 – 469.9] vs 211.1 [178.5 – 233.5]; P=0.0231), MPO (157.9 [103.0 – 343.1] vs 12.1 [9.2 – 14.8]; P<0.0001), and NE (147.9 [83.2 – 285.8] vs 16.9 [15 – 22.9]; P<0.0001) were elevated in patients at baseline compared to HV. However, CitH3 was not significantly elevated in patient samples (p=0.0705) (Table 4.3 and Figure 4.2).

Comparison of markers across ECMO initiation

Paired analysis of samples before and 24-36 hours after ECMO initiation showed CitH3, a specific marker of NETosis increased significantly after ECMO initiation (2.50 [1.16 – 5.45] vs 6.41 [2.95 – 13.64] ng/ml; P <0.0001). Levels of nucleosomes H3.1 (NuQ H3.1), a surrogate marker for NETs were measured in 18 patients, and levels also increased after ECMO initiation (1498 [257 – 4128] vs 4016 [757 – 7836] ng/ml; P = 0.0159). Interestingly, NE decreased after ECMO initiation (147.9 [83.2 – 285.8] vs 129.6 [92.3 – 213.1] ng/ml; P<0.0067) (Table 4.3 and Figure 4.2). There were no differences in the other neutrophil activation markers (MPO, and cfDNA) across ECMO initiation.

		Healthy volunteers (n=8)	ECMO Initiation (n=41-43)		ECMO Decannulation (n=20)	
			Pre-ECMO initiation	Post-ECMO initiation	Pre-decannulation	Post-decannulation
NET markers (ng/ml) (Median, IQR)	**Cit H3**	0.83 (0.41 – 2.83)	2.50 (1.16 – 5.45)	6.41 #### (2.95 – 13.64)	3.09 § (1.36 – 4.89)	1.46 ### (0.72 – 2.71)
	cfDNA	211.1 (178.5 – 233.5)	389.2 * (272.9 – 469.9)	356.5 (242.6 – 507.2)	341.6 (255.5 – 412.4)	293.1 (250.6 – 387.2)
	MPO	12.1 (9.2 – 14.8)	157.9 **** (103.0 – 343.1)	168.9 (90.2 – 283.6)	37.1 §§§§ (28.9 – 63.5)	45.8 (38.5 – 58.5)
	NE	16.9 (15.0 – 22.9)	147.9 **** † (83.2 – 285.8)	129.6 ## (92.3 – 213.1)	69.2 §§ (42.0 – 92.1)	40.1 # (33.1 – 60.1)
	NuQ H3.1 (n=18)	-	1498 (257 – 4128)	4016 # (757 – 7836)	-	-

Table 4.3 Markers of neutrophil activation and NETosis in healthy volunteers (n=8) and ECMO patients (n=44 across ECMO initiation, n=20 across ECMO decannulation).

The number of samples for matched pairs comparisons are: Cit H3 (n=42), cfDNA (n=41), MPO (n=43), and NE (n=41). Note for NuQ H 3.1 comparisons n=18; and for pre-decannulation comparisons n=20.

** denotes differences in baseline samples compared to HV*

§ denotes differences between post-ECMO initiation and pre-decannulation (Kruskal-Wallis test with Dunn's multiple comparisons).

 # denotes differences between pre-ECMO and post-ECMO initiation, and pre-decannulation and post-decannulation (Wilcoxon matched-pairs test)

** P <0.05, ** P<0.01 *** P< 0.001, **** P<0.0001.*

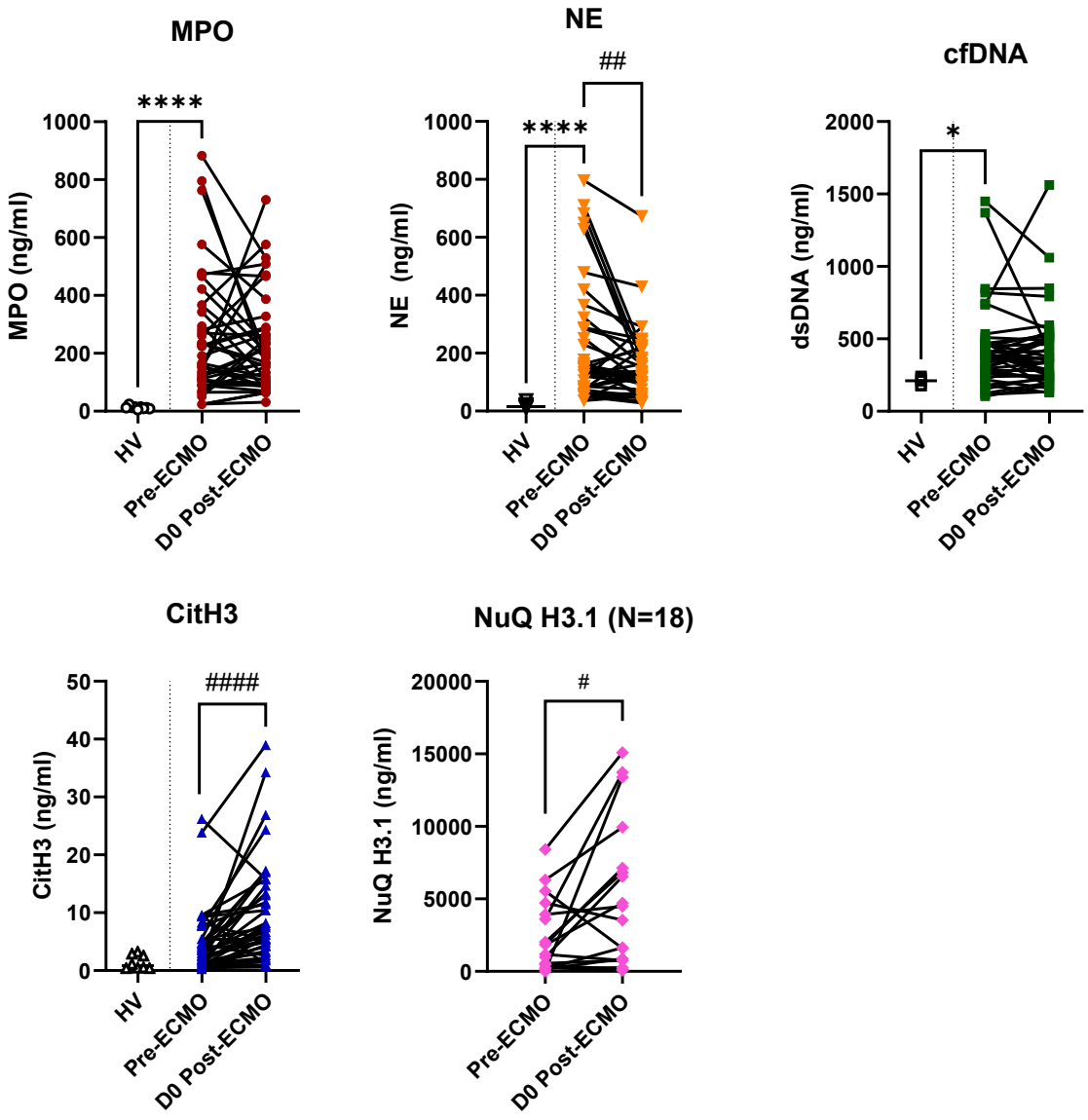


Figure 4.2 Markers of neutrophil activation and NETosis in healthy volunteers, and ECMO patients.

Plasma Citrullinated Histone H3 (CitH3), cfDNA, myeloperoxidase (MPO), neutrophil elastase (NE) and nucleosome NuQ H3.1 (NuQ H3.1) levels in healthy volunteers (HV; n=8), and ECMO patients (n=41-43) measured before ECMO initiation and 24-36 hours after ECMO initiation. Note for NuQ H 3.1 comparisons: n=18.

** denotes differences between groups (Kruskal-Wallis test with Dunn's multiple comparisons); # denotes differences between pre-ECMO and post-ECMO initiation (Wilcoxon matched-pairs test). P<0.05 was considered statistically significant. * P <0.05, ** P<0.01 *** P< 0.001, **** P<0.0001.*

4.4.3 Circulating markers of inflammation decrease after ECMO initiation

To investigate whether the increased NETosis was related to increased inflammation, plasma markers of inflammation were compared in matched pre-and post-ECMO samples. 32 patients were included in this analysis. Of these 20 (71%) were male, 17 (60%) were Caucasian, mean age 43.0±12.1 years, and 30 (94%) had non-COVID-19 aetiology. Due to some samples being out of detection range and increased dilution factors required in some samples, outliers were excluded using the ROUT method.

There was a decrease in the proinflammatory cytokines Ang-2 (1760 [816.9 – 2581] vs 2389 [1131 – 3951] pg/ml; P=0.0003), MCP-1 (66.9 [45.8 – 200.2] vs 118.3 [31.5 – 300] pg/ml; P=0.0497), MMP-9 (322.4 [169.6 – 673.9] vs 995.8 [416.1 – 1670] pg/ml; P<0.0001), sRAGE (362.6 [204.5 – 626.3] vs 711.5 [321.9 – 1673] pg/ml; P=0.0172), TNFα (34.2 [14.0 – 57.9] vs 46.3 [10.6 – 89.9] pg/ml; P=0.0272) and VEGF (32.9 [5.3 – 62] vs 77.4 [26.7 – 185.6] pg/ml; P<0.0001) after initiation of ECMO (Table 4.4 and Figure 4.3). There were no differences in other measured analytes IL-1β, IL-6, IL-10 or TGF-β.

		Pre-ECMO initiation	Post-ECMO initiation	P-Value
Inflammatory marker (pg/ml) Median, IQR)	**Ang-2 (n=31)**	2389 (1131 – 3951)	1760 (816.9 – 2581)	**0.0003**
	IL-1β (n=22)	0.97 (0.23 – 11.7)	0.69 (0.23 – 11.9)	0.0574
	IL-6 (n=26)	174.8 (69.1 – 387.2)	114.6 (34.5 – 420.2)	0.7078
	IL-8 (n=24)	30.0 (5.7 – 191.2)	21.4 (5.7 – 78.7)	**0.0448**
	IL-10 (n=20)	55.2 (27.1 – 193.1)	47.3 (15.1 – 213.1)	0.3683
	MCP-1 (n=30)	118.3 (31.5 – 300.0)	66.9 (45.8 – 200.2)	**0.0497**
	MMP-9 (n=23)	995.8 (416.1 – 1670)	322.4 (169.6 – 673.9)	**<0.0001**
	sRAGE (n=22)	711.5 (321.9 – 1673)	362.6 (204.5 – 626.3)	**0.0172**
	TGFβ (n=27)	961.1 (395.5 – 1465)	1363 (797.8 – 2422)	0.1937
	TNFα (n=26)	46.3 (10.6 – 89.9)	34.2 (14.0 – 57.9)	**0.0272**
	VEGF (n=23)	59.8 (21.2 – 110.8)	23.7 (5.0 – 49.0)	**0.0005**

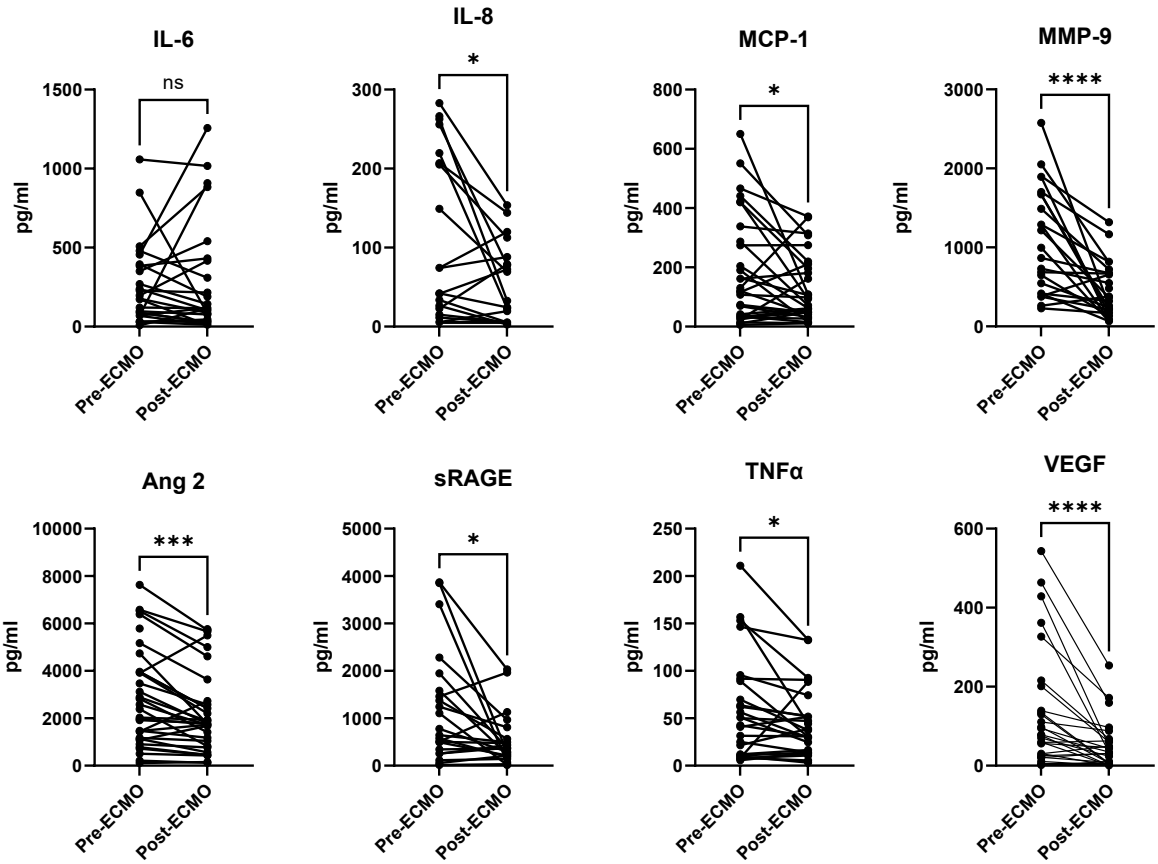


Table 4.4 and Figure 4.3 Inflammatory markers before and after ECMO initiation.

*32 paired samples had inflammatory analytes measured before and after ECMO initiation. Figure 4.2 shows significant results. Outliers were excluded using the ROUT method. Wilcoxon matched-pairs test was used to compare between pre- and post-ECMO initiation. P<0.05 was considered statistically significant. * P <0.05, ** P<0.01 *** P< 0.001, **** P<0.0001*

Angiopoietin-2, Ang-2; Interleukin 6, IL6; Interleukin 8, IL8; monocyte chemoattractant protein-1, MCP-1; metalloproteinase 9, MMP9; soluble receptor for advanced glycation end products, sRAGE; tumour necrosis factor alpha, TNFα; vascular endothelial growth factor, VEGF.

4.4.4 Markers of neutrophil activation and NETosis vary over the ECMO run

Trends across the ECMO run up to week 3 (days 20-22) were compared using mixed-effects analysis. Only patients with values for 3 or more timepoints were included in analysis. Missing values were not interpolated. After exclusions, there were 50 ECMO patients included for analysis. There was significant variance in MPO (P<0.0001), NE (P<0.0001), and CitH3 (P=0.0002) levels across the ECMO run but no change in cfDNA (P=0.2772) (see Figure 4.4).

Levels of CitH3 continue to increase after ECMO initiation with a trend to peak at days 3-5 (P=0.0600). Thereafter the CitH3 levels decrease for the remainder of the ECMO run. In contrast, levels of MPO and NE decrease after ECMO initiation and there was no change in cfDNA levels.

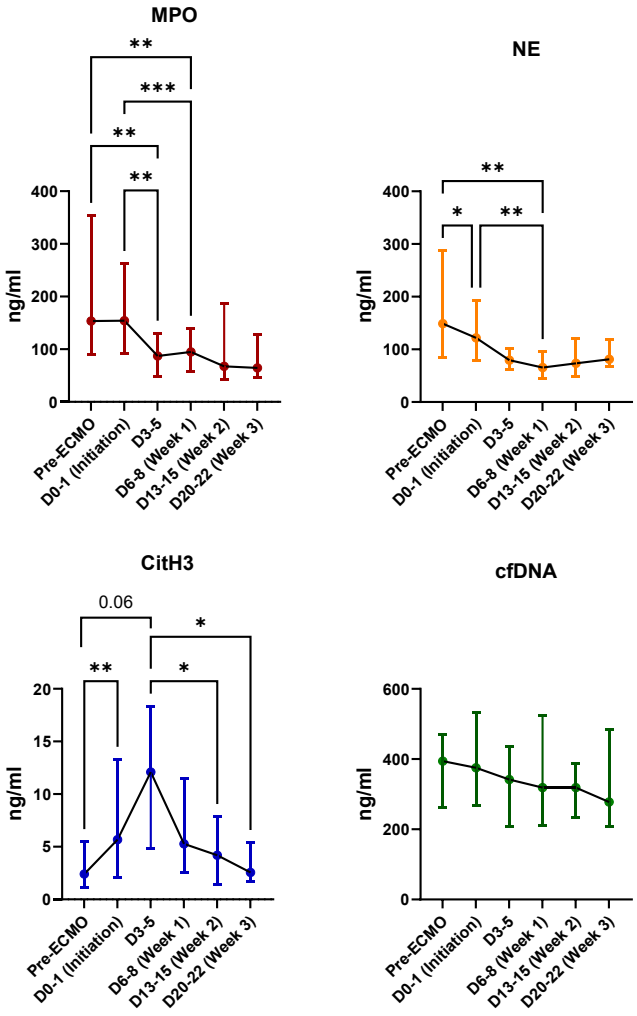


Figure 4.4 Trends in neutrophil activation and NETosis markers over the ECMO run

50 patients were included for analysis. Data is presented as median, IQR. Kruskall-Wallis test with Dunn's multiple comparisons test was used to analyse trends over time. P<0.05 was considered statistically significant. Cell-free DNA, cfDNA; citrullinated histone H3, CitH3, myeloperoxidase, MPO, neutrophil elastase, NE.

4.4.5 Markers of neutrophil activation and NETosis decreased after ECMO decannulation.

There were 20 patients who had paired samples taken on the day of decannulation (pre-DC) and the day after decannulation (post-DC). None of these patients had COVID-19. Other demographics and bloods before and after decannulation are presented in Table 4.5.

		ECMO patients with decannulation samples (n=20)
Demographics (n, %)	**Age (Median, IQR)**	47.5 (38.5 – 53)
	Male	13 (65%)
	Bacterial Pneumonia (Strep A, Staph, PCP)	3 (15)
	Viral Pneumonia (Influenza, Adenovirus)	5 (25)
	Aspiration pneumonia	2 (10)
	Asthma/Bronchospasm	6 (30)
	Other Respiratory (e.g Asthma, CF, Lung Ca)	2 (10)
	Non-Respiratory	2 (10)
	Duration of ECMO (days) (Median, IQR)	9.0 (5.2 – 14.2)

		Baseline (ECMO initiation)	Pre-decannulation	Post-decannulation	DC vs DC+1 P-value
Baseline bloods (median, IQR)	**Hb (g/dL)**	98 (91 – 105)	81.5 (79.3 – 92.3) ***	88.5 (78.3 - 101) #	**0.0323**
	WCC (x 10^9/L)	11.7 (7.9 – 15.2)	11.3 (7.8 -15.5)	11.8 (7.4 – 9.1)	0.1528
	Neutrophils (x 10^9/L)	9.9 (6.4 – 12.8)	8.0 (5.4 – 11.8)	10.0 (5.2 – 13.1)	0.2384
	Monocytes (x 10^9/L)	0.5 (0.2 – 0.8)	1.1 (0.6 – 1.2) *	1.1 (0.7 – 1.4)	0.1852
	Platelets (x 10^9/L)	177 (89 – 253)	130 (93 - 213)	139 (109 - 249)	0.0854
	INR	1.0 (0.9 – 1.2)	1.0 (0.9 - 1.1)	1.0 (0.9 - 1.1)	0.3635
	APTT (s)	36 (29.9 – 56.2)	37.8 (33.2 – 48.2)	32.7 (29.7 – 35.9)	0.0598
	Fibrinogen (g/dL)	4.5 (3.9 – 6.3)	4.5 (1.9 - 4.7)	4.2 (3.0 – 5.4)	0.3825
	D-dimer (g/dL)	2146 (731 – 3710)	3476 (1577 – 9681) *	-	N/A
	CRP (mg/L)	177 (134 – 257)	51 (28 – 106) **	53 (19 – 155)	0.7602

Table 4.5 Demographics and bloods of ECMO patients (n=20) with paired pre- and post-decannulation samples.

*Normality testing carried out using Kolmogorov-Smirnov test. Differences between groups compared using paired Wilcoxon tests. All statistical tests were 2-sided and P<0.05 was considered statistically significant. * denotes comparisons between ECMO initiation and day of decannulation. # denotes comparisons between the day of decannulation (DC) and the day after decannulation (DC+1).*

Compared to admission, by ECMO decannulation, patients had a lower haemoglobin (81.5 [79.3 – 92.3] vs 98 [91 – 105] g/dL; P=0.0001), and CRP (51 [28 – 106] vs 177 [134 – 257] mg/L; P=0.0039), higher monocyte count (1.1 [0.6 – 1.2] vs 0.5 [0.2 – 0.8] x 10^9/L; P=0.0328) and D-dimer (3476 [1577 – 9681] vs 2146 [731 – 3710] g/dL; P=0.0327). There were no differences in clinically measured ECMO health parameters before and after decannulation from ECMO. D-dimer was not routinely measured in patients after ECMO decannulation.

Levels of CitH3 (3.09 vs 6.41ng/ml; P=0.0319), MPO (37.1 vs 168.9ng/ml; P <0.0001) and NE (69.2 vs 129.6 ng/ml; P=0.0035) were significantly lower by ECMO decannulation compared to ECMO initiation (Table 4.3). Matched pairs analysis of samples before and after ECMO decannulation demonstrated further reduction in levels of Cit H3 (3.09 [1.36 – 4.89] vs 1.46 [0.72 – 2.71] ng/ml; P< 0.001) and NE (69.2 [42.0 – 92.1] vs 40.1 [33.1 – 60.1] ng/ml; P=0.0181). There were no significant changes in cfDNA or MPO (Figure 4.5). Nucleosome levels were not measured for these samples.

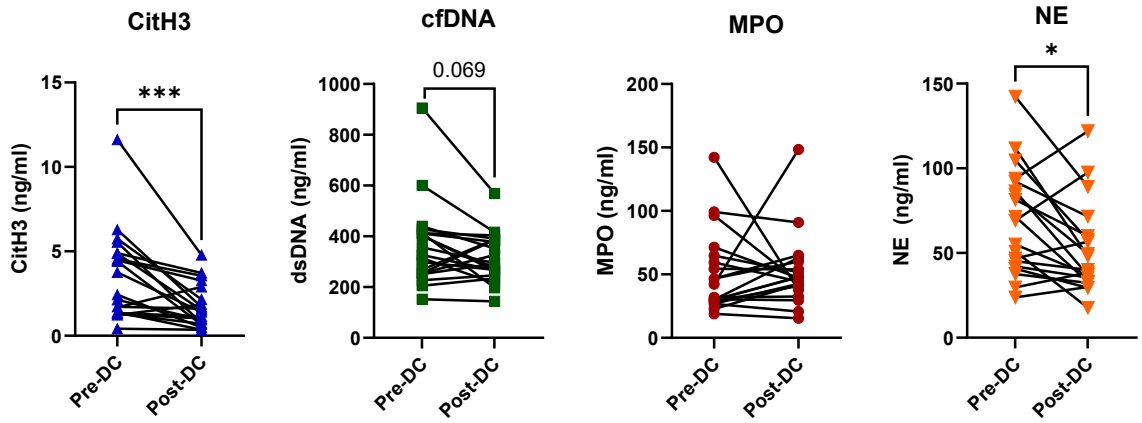


Figure 4.5 Markers of neutrophil activation and NETosis after ECMO decannulation.

*Plasma Citrullinated Histone H3 (CitH3), cfDNA, myeloperoxidase (MPO) and neutrophil elastase (NE) levels in ECMO patients (n=20) measured before ECMO decannulation (Pre-DC) and 24hours after ECMO decannulation (Post-DC). Wilcoxon matched-pairs test was used to compare between groups. P<0.05 was considered statistically significant. * P <0.05, *** P< 0.001.*

4.4.6 Sub-cohort analysis of neutrophil activation markers between COVID-19 and non-COVID-19 aetiologies of SARF

Comparisons across ECMO initiation were made between COVID-19 and non-COVID-19 patients. There were 29 non-COVID-19 patients and 12 COVID-19 patients who had matched pre- and post-ECMO initiation samples. The increase in CitH3 after ECMO initiation was seen in both COVID-19 and non-COVID-19 patients, but the decrease in NE was only seen in non-COVID-19 patients (Figure 4.6). When comparing markers between COVID-19 and non-COVID 19, the post-ECMO initiation CitH3 levels were higher in COVID-19 patients compared to non-COVID-19 patients. There were no other differences between COVID-19 and non-COVID-19 patients.

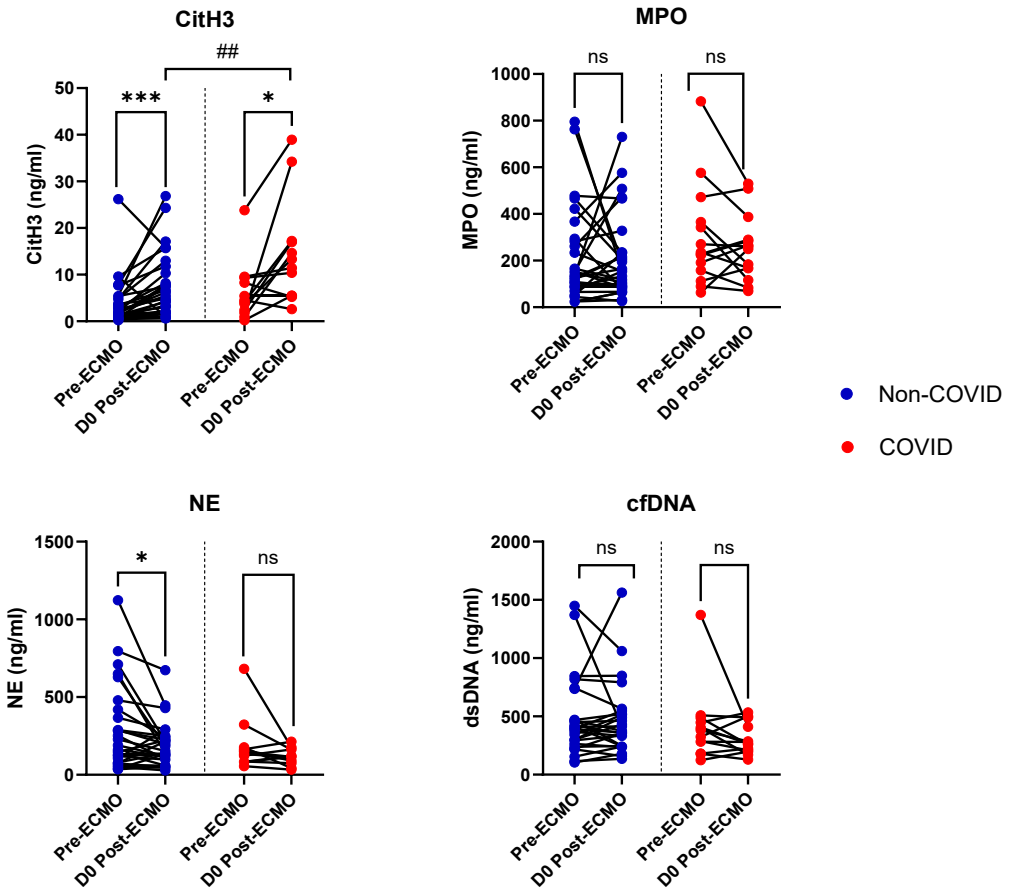


Figure 4.6 Markers of neutrophil activation on ECMO initiation separated by COVID-19 status.

*Plasma Citrullinated Histone H3 (CitH3), cfDNA, myeloperoxidase (MPO) and neutrophil elastase (NE) levels in 29 non-COVID-19 patients and 12 COVID-19 patients measured before and after ECMO initiation. Kruskal Wallis with Dunn's multiple comparisons test (denoted by #) was used to compare between COVID-19 groups, and Wilcoxon matched-pairs test (denoted by *) was used to compare between pre-and post-ECMO initiation samples. P<0.05 was considered statistically significant. * P <0.05, ** P<0.01, *** P< 0.001.*

4.4.7 Sub-cohort analysis of neutrophil activation markers pre- and post- membrane oxygenator

Part of the HITEC sampling protocol included taking blood samples from before and after the ECMO oxygenator where clinical experience allowed, to examine if there were differences in levels before and after the MO since clots form more readily on the venous (pre-oxygenator) side of the MO. A total of 34 pre-oxy and post-oxy samples from 12 ECMO patients were taken. Of these, there were 26 matched samples from 11 patients for all neutrophil activation assays. There were no differences in neutrophil activation or NETosis markers across the MO (Figure 4.6).

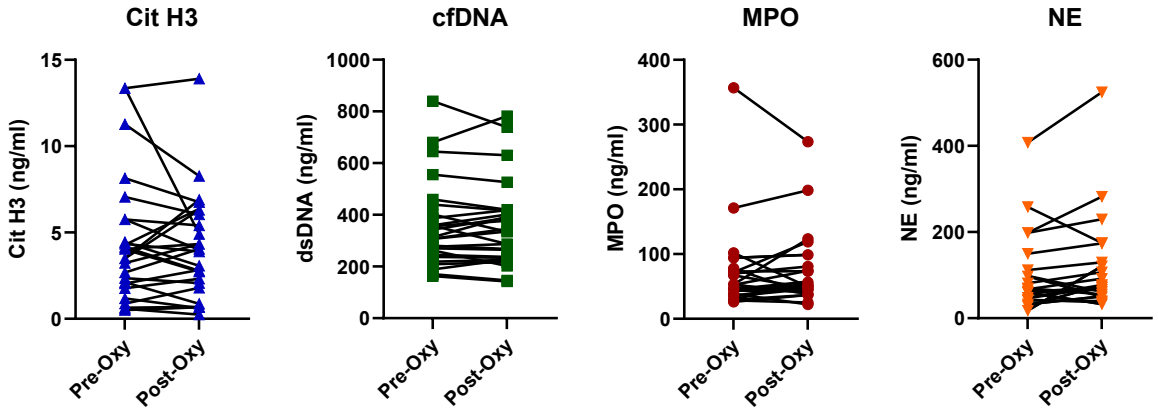


Figure 4.7 Markers of neutrophil activation before and after the membrane oxygenator

Plasma Citrullinated Histone H3 (CitH3), cfDNA, myeloperoxidase (MPO) and neutrophil elastase (NE) levels in 26 samples from 11 ECMO patients measured before (pre-oxy) and after (post-oxy) the membrane oxygenator. Wilcoxon matched-pairs test was used to compare between groups. P<0.05 was considered statistically significant.

4.4.8 Measuring cell-associated NETs

Using flow cytometry, cell-associated NETs were measured in whole blood samples from patients enrolled onto the HITEC study. The data presented in this section is preliminary data. Due to time optimising these protocols (Section 2.4.4), and with the nature of patient sampling (out of hours events, and staff availability), there were not enough data to draw significant correlations regarding changes over the ECMO run. However, some interesting trends can be observed.

After optimising the protocols, there were 5 HV and 76 samples from a total of 30 patients at various time points that had cell-associated NETs quantified in whole blood using flow cytometry. The samples were grouped into initiation, week 1 (days 6-8), week 2 (days 13-

15), decannulation or post-decannulation. There were no pre-ECMO samples due to the requirement for sample processing soon after bloods were taken.

Neutrophils were identified as CD66b positive events and the proportion of neutrophils that were double positive for MPO and dsDNA, or histone H3 and dsDNA were labelled as cell-associated NETs. Matched-pairs analysis between 15 ECMO initiation and week 1 samples, and 5 pre- and post-decannulation samples were performed. After a week on ECMO compared to at ECMO initiation, there was a reduction in cell-associated NETs as measured by MPO-DNA positive neutrophils (6.6 [2.7 – 17.4] vs 3.8 [2.3 – 6.6] %; P=0.0333) and histone H3-DNA positive neutrophils (4.8 [1.4 – 10.5] vs 2.1 [0.7 – 4.2] % P=0.0305) (Figure 4.8). There was corresponding decrease in MPO and Histone H3 expression but not in the dsDNA (Sytox Green). There was no change in neutrophil expression of CD66b from ECMO initiation to 1 week but there was a reduction in the CD66b MFI by the time ECMO was no longer required (pre-DC) compared to ECMO initiation (25,822 [20,114 – 30,542] vs 43,251 [30,826 – 62,485]; P=0.0194).

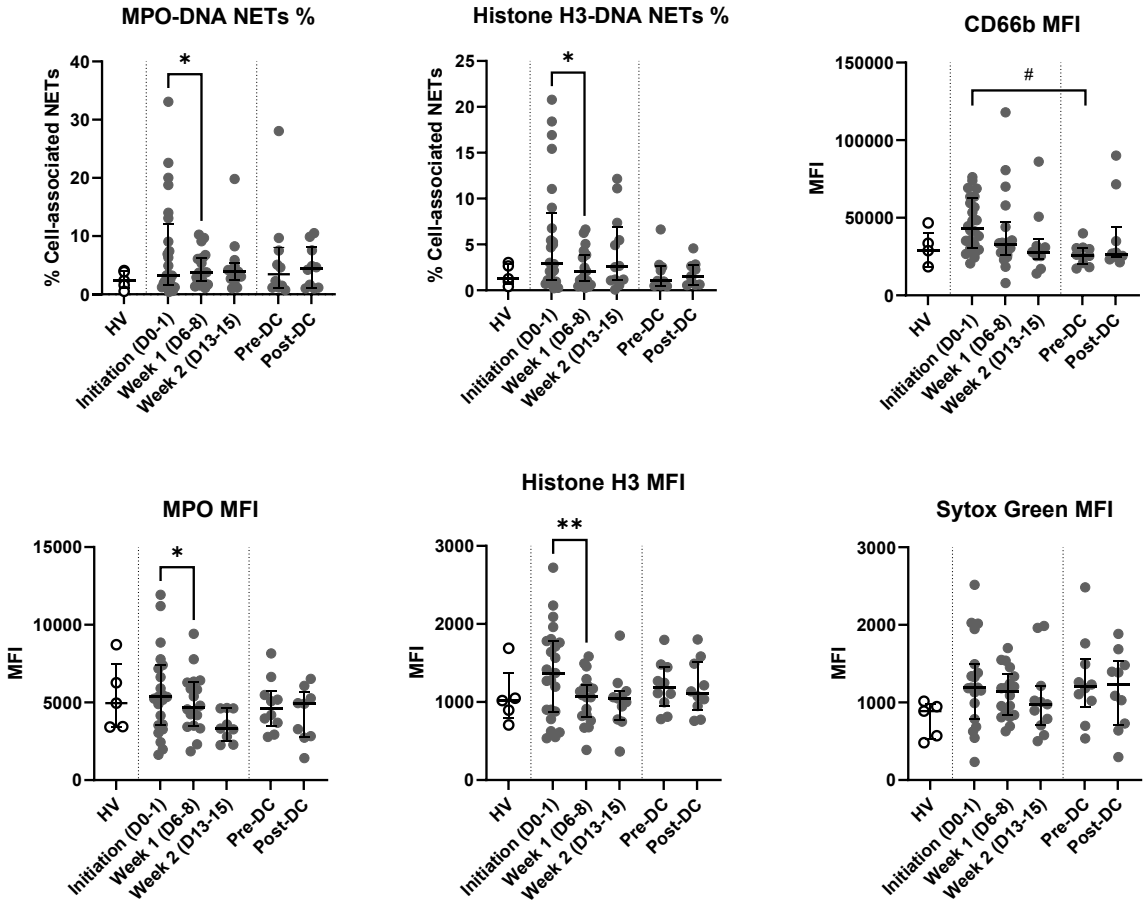


Figure 4.8 Neutrophils undergoing NETosis in patient samples.

*Whole blood from patients were stained with antibody cocktail and using flow cytometry, the proportion of cell-associated NETs were quantified, as well as neutrophil activation (CD66b) and expression of neutrophil MPO, Histone H3, and extracellular DNA (Sytox Green). Samples form healthy volunteers (HV; n=5), and ECMO patients (n=15) were analysed after ECMO initiation and weekly whilst on ECMO. Samples were also taken before (pre-DC) and after decannulation (post-DC). Comparisons between groups analysed using Kruskal-Wallis test with Dunn's multiple comparisons (denoted by #). Comparisons between Initiation and days 6-8, and pre-decannulation and post-decannulation analysed using Paired t-test and Wilcoxon matched pairs test as appropriate (denoted by *). P<0.05 was considered statistically significant. * P <0.05, ** P<0.01 ***.*

I hypothesised that the levels of cell-associated NETs would be similar to the soluble NETs measured using ELISA, therefore the levels of NETosis measured by flow cytometry was correlated with the soluble ELISA data for the same samples. There were 84 samples that had matched flow cytometry data and ELISA data. The correlation between the flow cytometry cellular data and the relevant soluble ELISA components was weak (Figure 4.9). MPO-DNA NETs had a weak correlation with soluble MPO (R=0.2776; P=0.0106), but better correlation with soluble NE (R=0.4946; P<0.0001). There was corresponding correlation of neutrophil MPO expression with soluble MPO (R=0.3744; P=0.0005) and soluble NE

(R=0.4251; P<0.0001). NETs as measured by HistoneH3-DNA did not correlate with soluble CitH3 (R=-0.1226; P=0.2666) or cfDNA (R=0.02524), and neutrophil-associated dsDNA (Sytox Green MFI) correlated weakly with soluble cfDNA (R=0.2577; P=0.0228).

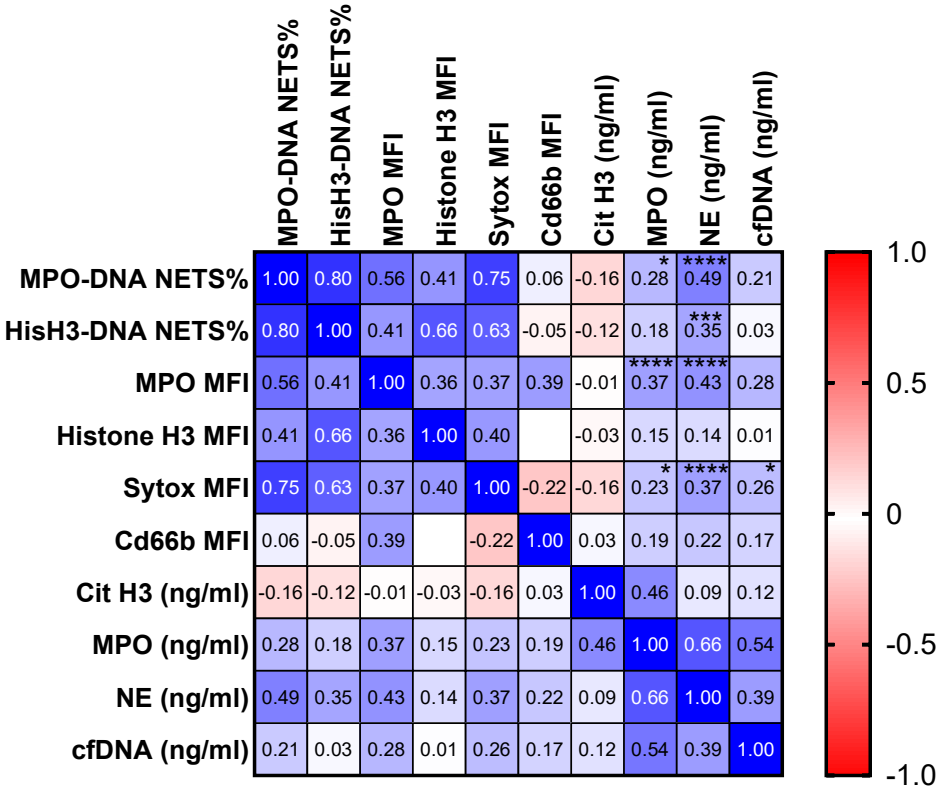


Figure 4.9 Correlation matrix between cell-associated NETs and soluble NETosis markers

The proportions of cell-associated NETs (both NPO-DNA and HistoneH3-DNA) were correlated with the soluble markers of NETosis using Spearman correlation. There were 84 patient samples with matched values. P<0.05 considered statistically significant.

4.4.9 Platelet activation markers: PF4 and CD62P decreased after ECMO initiation

To assess the effect of ECMO on platelet activation, platelet count and serum levels of the intracellular granule proteins, PF4 and CD62P, were compared. Samples from 34 ECMO patients matched across ECMO initiation and 4 HV were analysed. There were also 15 matched pre- and post-decannulation samples.

Since PF4 and CD62P are both released from platelets, it is reasonable that levels would be related to platelet count. The pre-ECMO blood results were taken when in other hospitals, and the information provided on the ECMO referral forms were often not from the day of

ECMO initiation, therefore comparisons of platelet count before and after ECMO initiation were not able to be made. To assess whether the PF4 and CD62P levels were related to platelet count, samples taken whilst in RBH (n=348) were compared with platelet count. The PF4 and CD62P levels correlated with platelet count (PF4 R= 0.5905, P<0.0001 and CD62P R=0.3770; P<0.0001) (Figure 4.9).

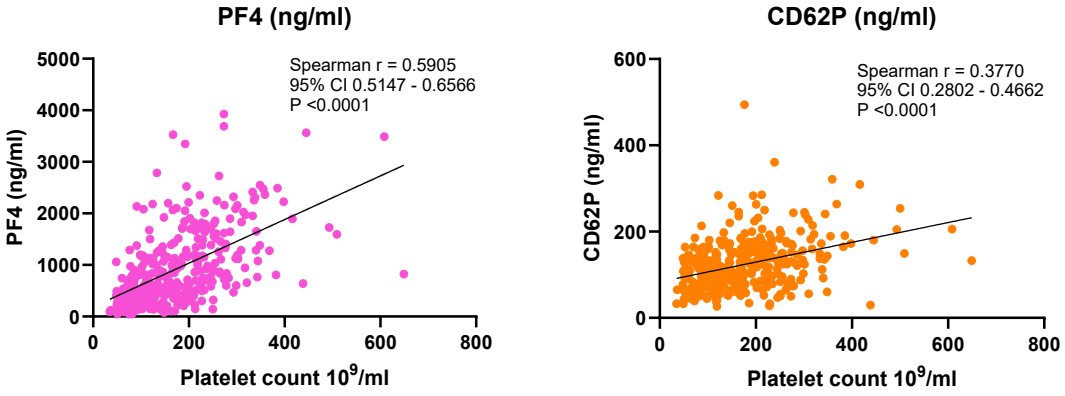


Figure 4.10 Correlation between platelet count and PF4 and CD62P levels whilst on ECMO.

Platelet count was correlated with 348 PF4 and 347 CD62P samples. Correlation computed using Spearman's correlation test. P<0.05 was considered statistically significant.

Platelet factor 4, PF4; P-selectin, CD62P.

There was no difference in PF4 levels between HV and patients' baseline levels but there were higher baseline levels of CD62P in patients compared to HV (165.9 [110.6 – 257.3] vs 61.1 [31.5 – 100.7] ng/ml; P=0.0020). There was a decrease in both PF4 (872 [384 – 1617] vs 2369 [1705 - 3259] ng/ml; P<0.0001) and CD62P (88.9 [64.9 – 129.8] vs 165.9 [110.6 - 257.3] ng/ml; P<0.0001) after ECMO initiation, but no change after ECMO decannulation (Figure 4.11). The changes across ECMO initiation in PF4 and CD62P were the same when split into COVID-19 and non-COVID-19 cohorts.

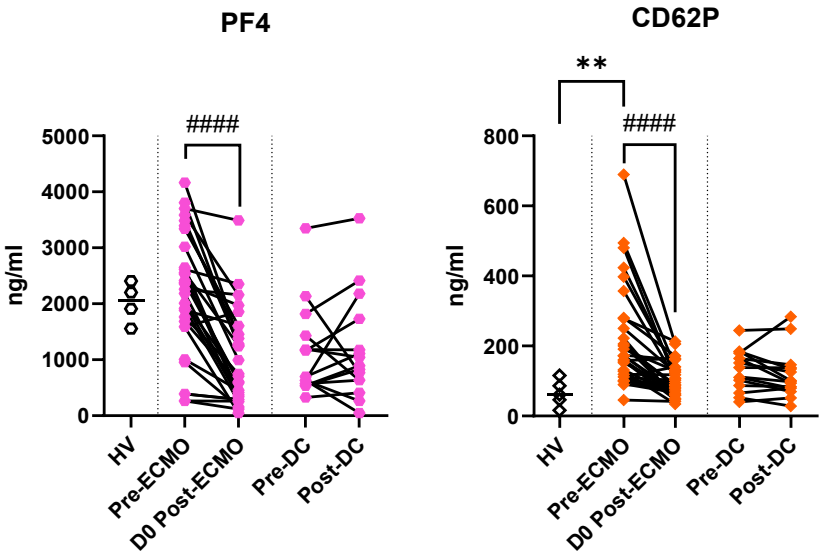


Figure 4.11 Markers of platelet activation in healthy volunteers and ECMO patients.

*Serum platelet factor 4 (PF4) and P-Selectin (CD62P) levels in healthy volunteers (HV; n=4), and ECMO patients (n=34) measured before ECMO initiation and 24-36 hours after ECMO initiation. 15 ECMO patients had levels measured before and after decannulation. Comparisons between groups analysed using Kruskal-Wallis test with Dunn's multiple comparisons (denoted by *). Comparisons between pre-ECMO and post-ECMO initiation, and pre-decannulation and post-decannulation analysed using Wilcoxon Matched pairs test (denoted by #). P<0.05 was considered statistically significant. * P <0.05, ** P<0.01 *** P< 0.001, **** P<0.0001.*

Extracorporeal membrane oxygenation, ECMO; Decannulation, DC; Healthy volunteer, HV; Platelet factor 4, PF4; P-selectin, CD62P.

Trends in platelet activation markers across the ECMO run up to week 3 were analysed. Only patients with values for 3 or more timepoints were included in analysis. After exclusions, there were 50 ECMO patients included for analysis. There was variance in platelet count (P=0.0397), PF4 (P=0.0009) and CD62P (P=0.0077) over the ECMO run. Specifically, there was a decrease in platelet count from ECMO initiation to 1 week on ECMO (199.6 [109.3 – 267.8] vs 124.3 [87.2 – 173]; P=0.0256). There was a decrease in PF4 and CD62P levels from ECMO initiation which remained low during the ECMO run (Figure 4.12).

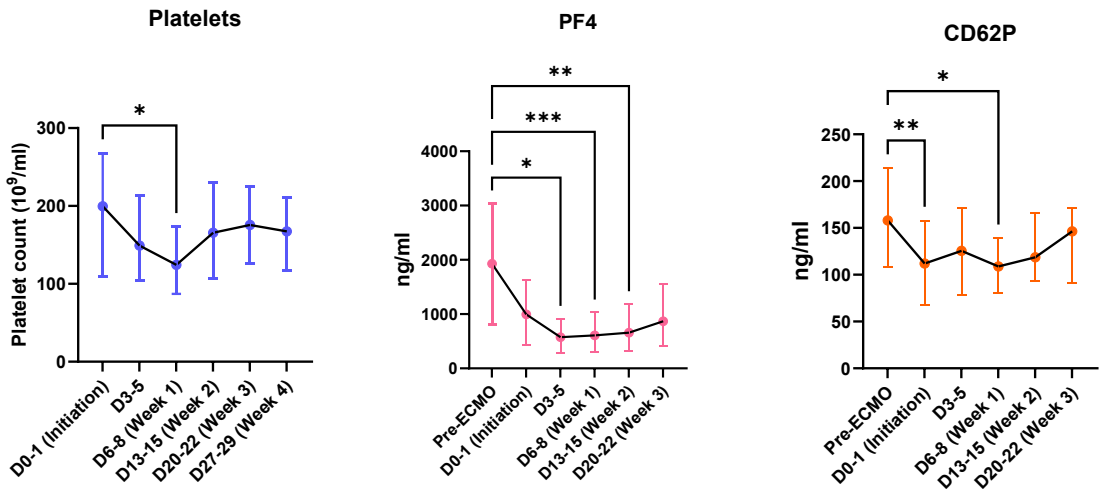


Figure 4.12 Trends in platelet count and platelet activation markers over the ECMO run

50 patients were included for analysis. Data is presented as median, IQR. Kruskall-Wallis test with Dunn's multiple comparisons test was used to analyse trends over time. P<0.05 was considered statistically significant.

Platelet factor 4, PF4; P-selectin, CD62P.

4.4.10 Clinical coagulation assays

To further assess platelet activation whilst on ECMO, platelet function tests using Multiplate aggregometry and viscoelastic assays using thromboelastogram and were run on patient samples collected from the HITEC study.

Multiplate – platelet aggregometry

In general, Multiplate tests were only run in patients who had platelet counts >100 x 10^9/L. In some cases, the platelet count was unknown at the time of sample collection (e.g. results not back from clinical lab), and the count is <100 x 10^9/L. In total 94 samples from 29 patients were analysed using the Multiplate analyser. 78 samples were taken when on ECMO and 16 samples were taken after decannulation from ECMO. There were no pre-ECMO samples as patients are initiated on ECMO outside of our hospital.

There was no difference in platelet count between samples taken on ECMO and off ECMO. Whilst on ECMO only a small proportion of samples had a response to agonists within the normal range (ADP, 28.1%; ASP, 29.5% and TRAP, 20.5%). Most samples taken whilst on ECMO had platelet dysfunction, with most samples having a reduced response to ADP (64.1%), ASP (44.9%) and TRAP (42.3%). The reduced platelet aggregation decreases after

ECMO decannulation, where most samples had a normal or increased response to agonists (Figure 4.13 and Table 4.6). These results suggest that whilst on ECMO the ability for platelet aggregation in response to simulation with ADP, AA and TRAP is impaired for most patients, but this phenomenon is reversed as soon as 24 hours after discontinuation of ECMO.

When samples taken on ECMO were compared to those off ECMO, the median response to ADP was lower whilst on ECMO compared to after ECMO decannulation (43 [25 – 70.5] vs 69 [42 – 113]; P = 0.0167). There were no differences in the ASP and TRAP tests whilst on ECMO and off ECMO (Figure 4.13).

		Proportion of results (%)		
	Test (normal AUC)	**Under**	**In Range**	**Over**
On ECMO (n=74)	ADP (51-113U)	64.1	28.1	7.7
	ASP (71-115U)	44.9	29.5	25.6
	TRAP (87-128U)	42.3	20.5	37.2
Off ECMO (n=15) (after decannulation)	ADP (51-113U)	31.2	50	18.8
	ASP (71-115U)	18.8	43.7	37.5
	TRAP (87-128U)	25	25	50

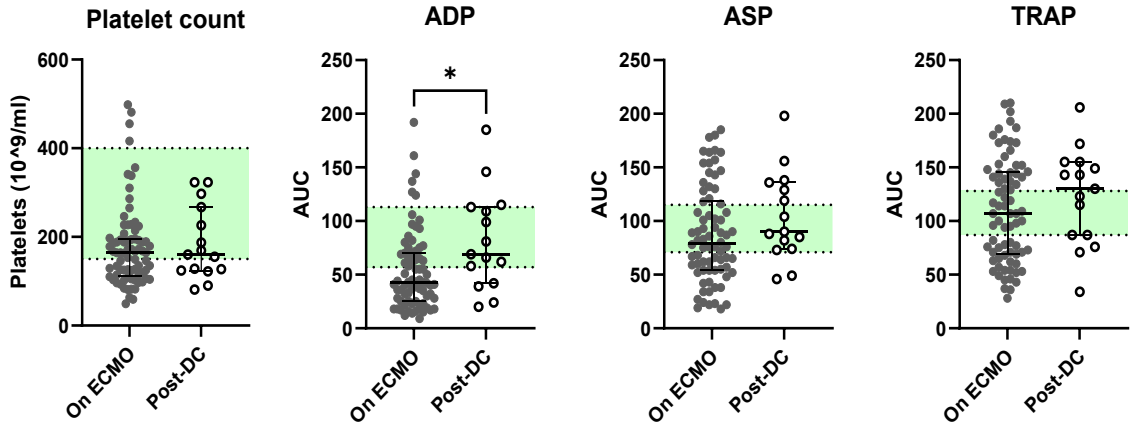


Table 4.6 and Figure 4.13 Proportion of platelet aggregation results that were within, under or over the normal range in response to three different agonists.

Platelet aggregation was measured during the ECMO run (n=74) and after decannulation (i.e. off ECMO) (Post-DC, n=15). Agonists used to stimulate platelet aggregation: Adenosine diphosphate (ADP), Thrombin receptor activating peptide (TRAP), Arachidonic acid (ASPItest). The normal limits for ADPtest are 57-113 U, ASPItest 71-115 U, and TRAPtest 87-128 U, and is represented by the green section on the graphs. Data displayed as median, IQR. Mann-Witney U test was used to compare between samples taken whilst on ECMO and off-ECMO. P<0.05 was considered statistically significant.

There was a wide variation in platelet aggregation response to agonists measured whilst on ECMO. Therefore, samples taken on ECMO were separated by duration on ECMO: D0-1 (ECMO initiation) (n=22), D6/7 (week 1) (n=17) (Figure 4.14). There were only 7 Multiplate samples for D13/14 on ECMO, therefore not included for this analysis. Due to the shorter duration of ECMO in these non-COVID-19 patients, availability of clinical expertise to run the Multiplate assay, and the sporadic nature of clinical samples, there were not enough data to complete a matched-pairs analysis or for analysis of further time points.

The effect of ECMO on reducing platelet aggregation responses seemed to be most marked in the first 1-2 days after ECMO initiation where most samples had lower than the normal response to ADP (16/22; 72.7%), AA (14/22; 63.6%) and TRAP (11/22; 50%) and median AUC for all agonists below the lower limit of normal (Figure 4.14). Whilst there was no significant change in platelet count, there was improvement in platelet function after 1 week on ECMO (D6/7) in particular the response to AA (ASPItest) (89 [71-129] vs 55 [24.5-89.5] U; P=0.0158) and TRAP-6 (122 [81-138] vs 86 [45-107] U; P=0.0286) (Figure 4.14).

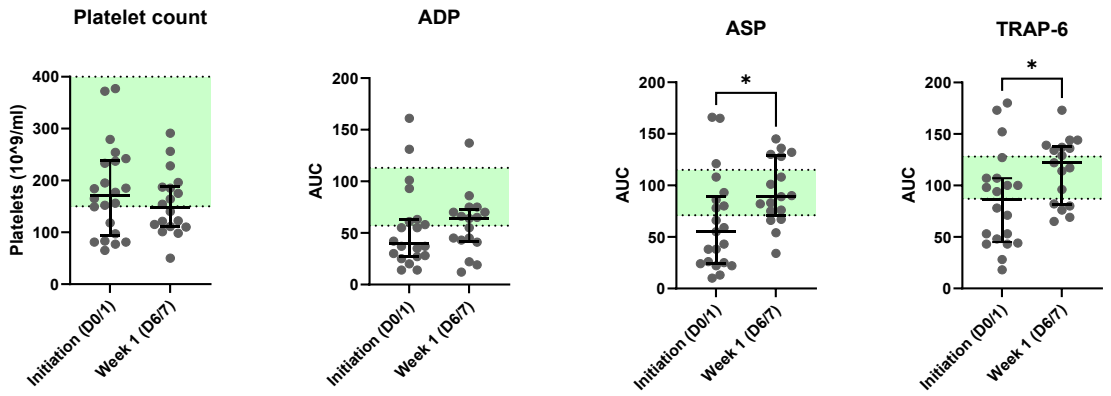


Figure 4.14 Proportion of platelet aggregation results that were within, under or over the normal range in response to three different agonists separated by duration on ECMO.

*Platelet aggregation was measured during the ECMO run on D0/1 (N=20) and D6/7 (n=17) on ECMO. Agonists used to stimulate platelet aggregation: Adenosine diphosphate (ADP), Thrombin receptor activating peptide (TRAP), Arachidonic acid (ASPI). The measured electrical impedance is expressed as area under the curve (AUC). The normal limits for ADPtest are 57-113 AUC, ASPItest 71-115 AUC, and TRAPtest 87-128 AUC, and is represented by the green section on the graphs. Data displayed as median, IQR. Comparisons between groups analysed using Mann Whitney test. All tests were two-sided and P<0.05 considered statistically significant; * P<0.05.*

Thromboelastography

Thromboelastography (TEG) was run on 198 samples from 42 patients. The majority of measured TEG parameters were within the normal ranges during ECMO and after decannulation from ECMO (Figure 4.15). There was no variation over time in any of the TEG parameters over the ECMO run and after ECMO decannulation.

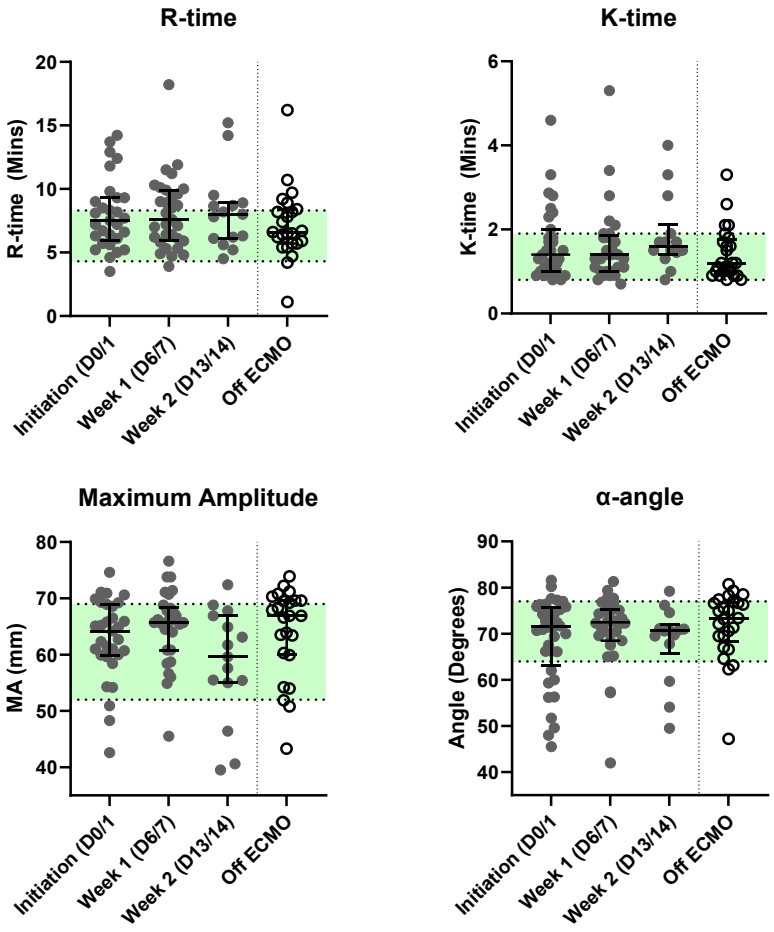
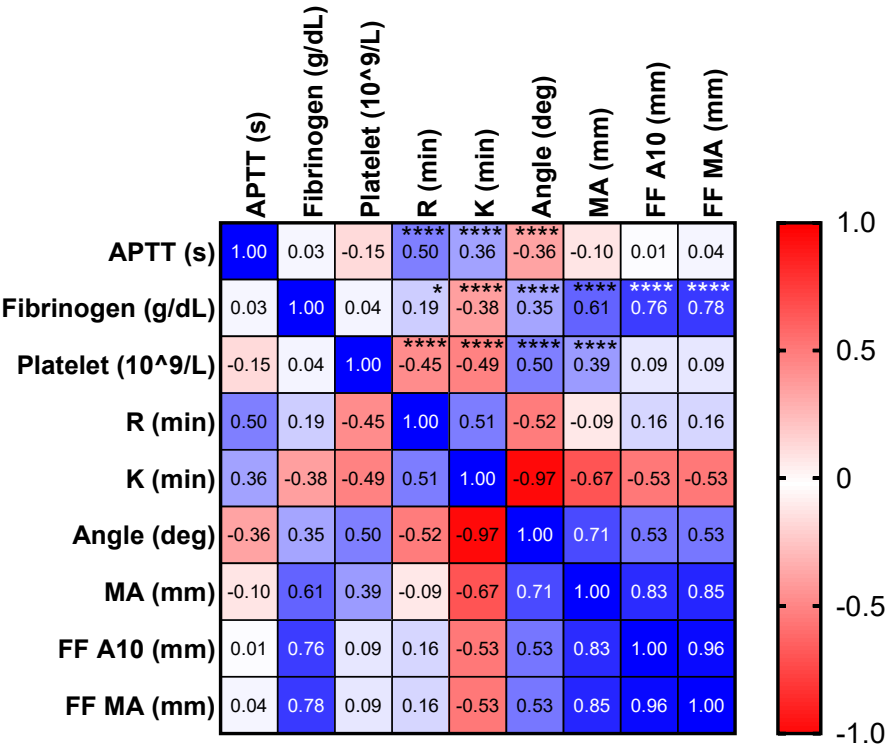


Figure 4.15 Proportion of Thromboelastogram results that were within, under or over the normal range in ECMO patients.

Thromboelastogram (TEG) was measured during the ECMO run on D0-1 (n=31), D6/7 (n=29) and D13/14 (n=14) and after decannulation (Off ECMO). The normal limits for each parameter are represented by the green section on the graphs. Data displayed as median, IQR. Comparisons between groups analysed using Kruskal-Wallis test with Dunn's multiple comparisons. All tests were two-sided and P<0.05 considered statistically significant.

To assess the reliability of TEG in patients on ECMO with traditional coagulation tests, the TEG parameters were correlated with their respective coagulation parameter. There were 137 matched clinical coagulation results with TEG samples (Figure 4.16). The APTT, a measure of plasma coagulation factors correlated with the TEG's measure of clot formation:

R-time (R=0.5, P<0.0001), and K-time (R=0.36, P=0.001) The platelet count correlated with the TEG's measure of time to form a stable clot: α-angle (R=0.5; P<0.0001) and the clot stability: MA (R=0.39; P<0.0001). The clinically measured fibrinogen had good correlation with the TEG measured functional fibrinogen, FF A10 (R0.76; P<0.0001), FF MA (R=0.78; P<0.0001) and MA (R=0.61, P<0.0001). In summary in ECMO patients the TEG correlated well with the clinical parameters each component represents.



	APTT (s)	Fibrinogen (g/dL)	Platelet (10^9/L)	R (min)	K (min)	Angle (deg)	MA (mm)	FF A10 (mm)	FF MA (mm)
APTT (s)	1.00	0.03	-0.15	**** 0.50	**** 0.36	**** -0.36	-0.10	0.01	0.04
Fibrinogen (g/dL)	0.03	1.00	0.04	* 0.19	**** -0.38	**** 0.35	**** 0.61	**** 0.76	**** 0.78
Platelet (10^9/L)	-0.15	0.04	1.00	**** -0.45	**** -0.49	**** 0.50	**** 0.39	0.09	0.09
R (min)	0.50	0.19	-0.45	1.00	0.51	-0.52	-0.09	0.16	0.16
K (min)	0.36	-0.38	-0.49	0.51	1.00	-0.97	-0.67	-0.53	-0.53
Angle (deg)	-0.36	0.35	0.50	-0.52	-0.97	1.00	0.71	0.53	0.53
MA (mm)	-0.10	0.61	0.39	-0.09	-0.67	0.71	1.00	0.83	0.85
FF A10 (mm)	0.01	0.76	0.09	0.16	-0.53	0.53	0.83	1.00	0.96
FF MA (mm)	0.04	0.78	0.09	0.16	-0.53	0.53	0.85	0.96	1.00

Figure 4.16 Correlation matrix of clinically measured coagulation parameters and the corresponding TEG.

137 samples from 39 patients had matched coagulation results and TEG samples from the same day. Normality testing using Shapiro-Wilk test showed all parameters were not normally distributed. Correlation between values were calculated using Spearman correlation coefficient. All tests were two-sided and P<0.05 deemed as significant.

Activated partial thromboplastin time, APTT; Functional fibrinogen, FF; kinetic time, K-time; maximum amplitude, MA; Reaction time, R-time.

With regards to the initial question of whether Multiplate and TEG could help predict circuit thrombosis and need for circuit change I was not able to analyse this as there were only a few patients who required circuit change and due to limitations on sampling out of hours, only 4 patients had samples taken on the day before circuit change.

4.5 Discussion

In this chapter I evaluated changes in soluble markers of inflammation, neutrophil activation, NETosis and platelet activation across ECMO initiation and decannulation. To the best of my knowledge this is the largest single cohort of ECMO patients where the markers have been quantified with up to 44 paired pre- and post ECMO initiation samples and up to 20 paired pre- and post- ECMO decannulation samples. The baseline clinical parameters match the demographic data presented in chapter 3 and other studies, where the COVID-19 patients had higher baseline platelet count, higher fibrinogen and lower CRP compared to non-COVID-19 patients [166, 167].

The data presented here has highlighted some interesting findings across ECMO initiation. Firstly, despite high levels of neutrophil activation prior to ECMO initiation, there is increased NETosis after ECMO initiation. In contrast, circulating levels of many inflammatory cytokines decrease after ECMO initiation. Secondly, levels of neutrophil activation and NETosis decrease during the ECMO run but there is further decrease in NETosis after ECMO decannulation. This suggests that ECMO may activate neutrophils via a different pathway driving NETosis and warrants further investigation into the pathways involved and could be potential therapeutic targets in this complex cohort of patients.

In addition, regarding platelet function, there are reduced numbers of platelets during the ECMO run, and evidence of platelet dysfunction as measured by clinically used platelet function assays. Levels of serum PF4 and CD62P are reduced during ECMO but it is unclear whether this represents increased platelet activation or platelet dysfunction.

4.5.1 Reductions in inflammatory cytokines after ECMO initiation are likely due to lung rest

In ARDS, the initial lung insult from the infective pathogen, lung trauma (inhalation injury, contusion, etc) or systemic inflammation leads to damage of the alveolar epithelium, release of inflammatory cytokines and recruitment of leucocytes to the alveolar space. In addition, in patients with severe ARDS, there is often secondary hit in the form of VILI which is aften due to injurious mechanical ventilation which can result in high tidal volumes (volutrauma), high airway pressures (barotrauma), increased respiratory rate (atelectotrauma), and even hyperoxia. It has been shown in many experimental animal models that VILI leads to increased inflammation and further release of inflammatory cytokines [245-247]. There are high baseline levels of inflammatory cytokines and neutrophil activation markers in severe ARDS

patients. However, against my initial hypothesis, after ECMO initiation, there is a decrease in most inflammatory cytokines, specifically TNFα, IL-6, sRAGE, VEGF, Ang-2, and monocyte chemoattractant protein 1 (MCP-1) (Figure 4.2).

At the time of ECMO initiation two interventions happen. Firstly, ECMO is initiated and secondly patients are usually put onto ultra-lung protective ventilation (UPV), a strategy to achieve lower airway pressures, tidal volumes and alveolar pressures than standard lung protective ventilation settings. The decrease in circulating inflammatory cytokines across ECMO initiation could be explained by lung rest. The aim of UPV is to reduce VILI and reduce the second hit lung injury from the endothelial and epithelial damage, thereby reducing the production of inflammatory cytokines and chemokines. There is good evidence that low volume ventilation and high PEEP strategies to reduce VILI improves survival [6, 248] and evidence that UPV whilst on ECMO can reduce biotrauma corresponding to our results. In a small single-centre study Rozenwajg and colleagues found lower levels of plasma sRAGE, IL-6, and MCP-1 after initiation of UPV [249]. Similarly, Wang and colleagues found when ventilation was guided by transpulmonary pressure monitoring whilst on ECMO, there was less injurious ventilation and also lower levels of IL-1β, IL-6 and IL-8 [250]. However, the evidence is mixed; Guervilly conducted a prospective RCT to compare UPV with conventional ventilation strategies whilst on ECMO, but found no differences in biomarkers (IL-1β, IL-6 and IL-8, surfactant protein D) and the study was stopped for futility [251]; and Guldner found that whilst UPV reduced histological damage, inflammation was not always ameliorated [252].

Being able to apply UPV to patients with severe ARDS is an attractive ventilation strategy but is not feasible in all patients on conventional mechanical ventilation due to loss of minute volume leading to hypercapnia, requirement for increased respiratory rate which may increase atelectotrauma, inability to achieve adequate oxygenation due to the lower pressures or loss of open lung ventilation. UPV can be achieved by using ECLS (including ECMO and $ECCO_2R$), and the reduced biotrauma may have added benefit of reducing the cytokine storm, systemic inflammation, and immune system activation. The current limit to this is that ECMO is associated with complications (bleeding, procedural, expert management required) which usually exceed the associated benefits [253]. If we can minimise the haematological and inflammatory complications of ECMO, then ECMO for ARDS could become standard management rather than a rescue strategy.

Although not demonstrated in this data, exposure of blood to the ECMO circuit is also associated with an inflammatory response similar to that seen in SIRS [159]. In a rat experimental model of extracorporeal circulation, Rungatscher and colleagues found increased neutrophil and monocyte activation and increased plasma levels of TNFα, NE and IL-6 after exposure to an extracorporeal circuit which was further increased when an oxygenator was incorporated in the circuit [254]. Other in vitro ECMO models found increased levels of IL-1β, IL-6, IL-8, and TNFα after short periods of 8-24 hours of perfusion [255, 256]. One study suggested that the increased cytokines may have resulted from increased mast cell degranulation [256]. In addition, exposure of blood to ECMO leads to activation of the complement cascade, activation of the endothelium which in turn secrete proinflammatory cytokines and increase expression of adhesion molecules leading to increased transmigration of leucocytes [159].

Many studies into inflammation and extracorporeal circuits looked at patients on CPB which are more inflammatory than modern ECMO circuits and the role of inflammation from ECMO in patients is poorly defined. There is a limit to plasma-based measurements on determining immune status due to compartmentalised immune responses, e.g. localised inflammation within the lung in ARDS, and in ECMO the plasma levels of some may be altered as blood proteins and cells are absorbed onto the MO. Identified plasma proteins in the literature include fibrin [130, 144], vWF [257, 258], albumin, fibrinogen and IgG [142] and some inflammatory markers [259]. Steigel et al also found presence of LPA on membrane oxygenators independent of vWF [257]. Indeed there has been much interest recently into the addition of haemoadsorption devices such as Cytosorb to the ECMO circuit to help reduce the SIRS response [260]. More work needs to be done to separate the effects of ECMO and patient interventions such as UPV in this critically ill cohort of patients.

4.5.2 ECMO initiation leads to increased NETosis and contributes to immunothrombosis in ECMO

Many of the inflammatory cytokines implicated in ARDS have roles in macrophage and neutrophil recruitment to the alveolar space. Since there is a reduction in many cytokines after ECMO initiation, it would be reasonable to expect a similar reduction in neutrophil activation markers also. However, neutrophil activation markers (MPO, NE, cfDNA) remain elevated after ECMO initiation and NETosis markers (CitH3 and nucleosomes) increase further supporting the hypothesis that exposure of blood to ECMO leads to increase in inflammation and NETosis. In addition, markers were measured after ECMO decannulation,

and whilst all markers of neutrophil activation had decreased by the time ECMO was no longer required, removing the ECMO circuit further reduced NETosis as measured by CitH3 providing further evidence that ECMO induces NETosis. The lifespan of neutrophils is short (6-20hours) [46] which could help to explain the reduction in NETosis markers within 24 hours of ECMO decannulation.

Whilst there are some studies that have found increased NETosis markers in extracorporeal circuits such as CPB [105, 107], and haemodialysis [108-110], little is known about ECMO mediated soluble NET release. An animal model using sheep on both VA and VV ECMO found neutrophils and NET markers (cfDNA and CitH3) were elevated after 6 hours on ECMO compared to baseline, and that the thrombi from the blood vessels and the MO contained NETs [211]. There are only two other studies examining NETs in ECMO patients in the literature, and neither showed increase NETosis [225, 226]. Haus et al. used immunofluorescence to stain blood smears from 10 ECMO patients and found ECMO patients have higher rates of NETs and NET precursors compared to HV. They also report that a high NET rate prior to initiation of ECMO was associated with increased inflammation as measured by TNF-α, and IL-6 levels; and more prominent thrombocytopenia and antithrombin 3 activity [225]. Another study examined NET markers in 12 COVID-19 ECMO patients using ELISA but did not show any difference in NET markers (cfDNA, MPO-DNA complexes) or inflammation (as measured by IL-8) before or after ECMO initiation [226]. Furthermore, both are small single centre studies with only 10-12 patients and used generic markers of neutrophil activation (cfDNA and MPO). The data presented in this chapter comes from over 50 ECMO patients and examined specific NETosis markers such as CitH3 and nucleosomes as well as the generic markers (MPO, NE and cfDNA) used in many other studies.

CitH3 is seen as a NET specific biomarker [60, 61], and nucleosomes appear to be a good surrogate marker for NETosis [64, 222, 261], which my data supports. Some groups have developed assays combining markers to increase specificity for NETosis such as MPO-DNA complex or NE-DNA complex ELISAs [262-264] but there are varying reports of their usefulness in detecting NETs [265]. During this research period I also tried to develop an MPO-DNA complex ELISA using these protocols, but the sensitivity was highly variable when used with ECMO patient samples and therefore this work was not pursued.

One of the initial aims of the HITEC study was to investigate whether there was increased NETosis in patients who required circuit change with sampling before and after circuit change where possible. Many of the plasma samples were previously collected during the DeVENT study which followed a different sampling protocol and did not include additional samples around circuit change or decannulation. For patients recruited to the HITEC study, there was also difficulty obtaining samples at the time of circuit change. Of the11 patients who had a circuit change only 4 patients had samples taken prior to circuit change despite all 11 having samples taken after circuit change. This is because the circuit changes occurred out of hours (evenings or weekends) or were emergent and research samples were not prioritised. The HITEC study is still recruiting and analysis of NETosis and inflammation across circuit change will be of interest in future work.

4.5.3 Comparison of cell-associated and soluble NETs

Many studies have used only one method to quantify NETosis. A novel aspect of this chapter is the measurement and comparison of cell-associated NETs as well as soluble NETs. The NET components measured using ELISA are detached from the neutrophils and do not give a true indication of the proportion of neutrophils that are undergoing NETosis. Flow cytometry allows measurement of the proportion of neutrophils that are actively undergoing NETosis and is an increasing area of interest used by many other groups but with varying levels in similar patient cohorts: Schneck found low levels of NETs in control samples (1.6 [1-2] %), patients in septic shock (2.7 [1.9-3.9] %) and after cardiac surgery (2.7 [2.1-3.7] %) [266], whereas Gavillet found low levels in control samples (7.3 ± 1.4%) and increased levels in septic patients (65.7 ± 31.4%) [267]. Lee et al quantified NETotic neutrophils as the number of MPO/CitH3 double positive neutrophils per ul/blood and found an increase in patients with sepsis (281.8 ±77.1/µl) and thrombosis (258.2 ± 52.9/µl) compared to controls (63.6 ± 12.0/µl) [63].

I was able to develop a protocol for measuring cell-associated NETs in whole blood using flow cytometry. I adapted the protocol already used in the lab for measuring NETs in isolated neutrophils, by incorporating aspects from the aforementioned studies [63, 267]. However, the levels of cell-associated NETs did not correlate with the soluble NETosis markers in this cohort of ECMO patients. This could be a limitation of a new flow cytometry protocol or a true representation of NETs in vivo, representing lytic and vital NETosis. The cell-associated NETs measured by flow cytometry likely represent neutrophils that have gone through lytic NETosis whereby the NETs are released from lysed cells and the NETs remain attached to

the cell body [48, 66]. This contrasts with vital NETosis, where the NETs and individual NET components such as the granule proteins are expelled from the cell via degranulation or in extracellular vesicles, and are not attached the parent neutrophil [66, 67], which is likely represented by the soluble NETosis markers. The triggers for the two forms of NETosis differ, for example, PMA, fungal and bacterial infections activate NADPH oxidase dependent pathways and trigger lytic NETosis, whereas calcium ionophore, LPS and platelets induce vital NETosis via NADPH oxidase independent pathways [66, 67, 268].

There is still debate regarding whether NETs are beneficial or harmful. NETs are part of the defensive strategy against invading pathogens as they entrap and bind microorganisms, preventing their spread and ensuring a high local concentration of antimicrobial proteins and enzymes, assisting in phagocytosis and clearance [58 45, 87]. However, overactivation of neutrophils and NETosis contributes to increased inflammation and multi-organ dysfunction. In ALI, increase in neutrophil recruitment to the alveolar space leads to increased ROS production, and release of neutrophil granule proteins and NETs within the alveolar space contributes to inflammation and dysregulation of the lung injury [18, 19, 87]. They also have a bidirectional role in immunothrombosis with activation of the coagulation system, and which can lead to the thrombotic complications of sepsis such as disseminated intravascular coagulation, venous thromboembolism, or microangiopathy of COVID-19 [57, 112, 269]. In inflammatory states neutrophils are more likely to be pushed into lytic cell death such as NETosis, and necroptosis rather than apoptosis (non-lytic cell death) [54]. Whilst beneficial initially, if dysregulated for example in hyperinflammatory states, NETosis may become harmful to the host and therefore understanding the roles of cell-associated NETs, their soluble components and their pathways of activation are key to mediating the harmful effects of NETs.

Limitations

Whilst we can measure soluble NETs and cell-associated NETs, there are limitations to both these methods. Many groups have used flow cytometry to measure NETs from whole blood with varying protocol deviations including red cell lysis, addition of fixative, use of different centrifugation speeds (100 – 1000 x *g*) for washing steps, and use of conjugated and primary and secondary antibodies [63, 266, 267, 270, 271]. NETs are very fragile, and fixation may help to stabilise them. It is thought that low concentrations of paraformaldehyde fixation (1-4%) fix but do not permeate the cell [272]. During the development of my protocol, I trialled paraformaldehyde 2-4% fixation with variable effects on antibody staining after fixing as well

as loss of NETs during the additional wash steps. I also trialled use of an unconjugated primary Citrullinated Histone H3 antibody (ab5103, Abcam) following methods as described by Lee et al [63] and Shneck et al [266]. However, following the additional washing and fixative steps I could not detect many neutrophils and therefore this two-stage staining was not pursued. It must be noted that there is no flow cytometry protocol that has been consistently replicated in the literature highlighting the difficulty in handling NETs from whole blood samples with potential neutrophil activation and loss of NETs during the centrifugation and washing steps [271, 273]. There may also be operator variability between the protocols described in the literature and lack of reproducibility. Fluorescent microscopy protocols also require fixation and multiple washing steps, as well as 2-day staining protocols and therefore was not used for the clinical samples in this study.

ELISA is a commonly used assay used in many laboratories and is reproducible. However, it measures only the NET components which remain in the plasma after processing and are a surrogate marker for NETosis. Measuring the individual components of cfDNA, MPO and NE is not specific to NETosis. MPO and NE can be released from activated neutrophils during degranulation [51, 52] and although most cfDNA originates from leucocytes, it can come from a number of other sources (erythrocyte progenitors, vascular endothelial cells and hepatocytes) [274]. Whilst CitH3 has been reported as a specific marker for NETosis it does not tell us the proportion of neutrophils undergoing NETosis. It would be useful to determine which neutrophil phenotypes are likely to undergo NETosis and how these pathways are activated. Use of flow cytometry allows identification of neutrophil phenotypes and immunofluorescent microscopy visualisation of neutrophils with attached NETs. Due to difficulties of quantifying NETs and the lack of an established gold standard marker, ideally two approaches should be used to validate results particularly in patient samples, and therefore the use of flow cytometry and ELISA in this study, however the results do not correlate making it difficult to interpret these results without further validation of the NETosis.

4.5.4 Platelet activation and dysfunction in ECMO patients

Soluble markers of platelet activation

In the absence of the inflammatory cytokines released from the alveolar epithelium due to lung rest, there must be an alternative pathway by which neutrophils continue to be activated and pushed into NETosis in patients on ECMO. One pathway could be the interaction between platelets and neutrophils and the link to immunothrombosis particularly whilst on ECMO. To determine whether platelets were related to NETosis in ECMO patients I first

needed to measure platelet activity across ECMO by measuring serum levels of platelet granule proteins CD62P and PF4. Against my initial hypothesis, both CD62P and PF4 levels decreased after ECMO initiation, with no change whilst remaining on ECMO, or after ECMO decannulation. These results are in contrast the other studies who found either increase in plasma CD62P [146] or no significant differences in PF4 levels [239, 275] after ECMO initiation.

Thrombocytopenia and platelet dysfunction is widely reported in ECMO patients [205, 241], through a combination of consumption due to adsorption to the ECMO artificial surfaces, formation of microthrombi, increased platelet surface receptor shedding due to shear or activation, or increased platelet extracellular vesicle formation [82, 124, 146, 276]. The decrease in PF4 and CD62P levels after ECMO initiation could be due to thrombocytopenia that develops whilst patients are on ECMO as the PF4 and CD62P levels correlate with the platelet counts. It is known that thrombocytopenia is associated with reduced platelet degranulation [277]. It could also be related to these proteins being bound to NETs themselves which leads to stabilisation of NETs and increased thrombogenicity [278]. Whilst I did not measure platelet extracellular vesicles, they are increased in patients on extracorporeal circuits due to shear which can contribute to thrombocytopenia and contain PF4 or CD62P within their cargo [279, 280].

The relevance of soluble PF4 and CD62P levels remains to be determined. Firstly, P-selectin is found on endothelial cells as well as platelets and therefore is not just a marker for platelet activation. Secondly, P-selectin is involved in many cell-cell interactions which involve binding to PSGL-1 on leucocytes. It has been suggested that there are two roles by which P-selectin contributes to thromboinflammation: 1) the membrane bound P-selectin promotes leucocyte adhesion to the endothelium, facilitating leucocyte migration to sites of tissue injury and inflammation, and leucocyte-platelet interactions and leading to increased platelet activation and thrombosis 2) the soluble form of P-selectin promotes extracellular vesicle formation and activation of the coagulation cascade [18, 281, 282]. Conversely, it has also been suggested that soluble P-selectin binding to leucocytes prevents leucocyte adhesion to the vessel wall reducing inflammation [283], and that monomeric soluble P-selectin might have use as a biomarker, but it is unlikely to directly contribute to disease; whereas dimeric P-selectin might have a role in the coagulation-inflammation pathway [231, 240, 284]. Furthermore, the levels of soluble P-selectin may be inversely proportional to cell-bound P-selectin, if it is involved in cell-cell interactions promoting inflammation [231]. If activated platelets are bound to endothelial cells and leucocytes via the P-selectin-PSGL-1 pathway, this may explain the

decrease in levels of P-selectin and increase in neutrophil activation and NETosis across ECMO initiation.

There are not many studies that investigate PF4 levels alone, and most measure the HIT immune complex. Mazzeffi and colleagues investigated whether PF4 levels would be related to development of the HIT immune complex by measuring PF4-heparin complexes but did not find a difference in their small study [239]. The development of HIT is related to PF4-heparin complexes and development of the HIT immune complex therefore correlation of PF4 with heparin levels or dose may be useful as HIT formation is dependent on the ratio of PF4 to heparin. In addition, PF4 combines to form large multimers and forms ultra-large PF4-heparin complexes which contribute to HIT [285]. However, the relevance still remains to be determined, as the presence of the HIT immune complex is common in ECMO but most are non-pathogenic [240].

Clinical platelet function tests

I also assessed platelet function using the Multiplate analyser and found reduced platelet aggregation in response to ADP, AA and TRAP-6 from samples taken whilst on ECMO with recovery of platelet function after ECMO decannulation. These results suggest there is platelet dysfunction whilst on ECMO which recovers as early as 24 hours off ECMO. This is in keeping with other studies who found thrombocytopenia and reduced platelet aggregation in response to ADP, AA, TRAP, ristocetin, collagen, and adrenaline in patients whilst on ECMO [145, 148, 286]. It has been reported that the reduced response to platelet agonists can occur as early as after 6 hours on ECMO initiation [287] and continues during ECMO but appears to recover after ECMO decannulation [148, 288]. In my data, platelet aggregation in response to ADP, AA and TRAP was improved 1 day after ECMO decannulation, similar to Tauber and colleagues [288], whereas Kalbhenn found recovery in platelet function may take up to 3 days after ECMO decannulation [148].

Many reviews regarding platelet function in ECMO report reduced platelet function (adhesion, activation and aggregation) and appears to be correlated with thrombocytopenia [82, 276], which is often found in ECMO patients [145, 286, 287]. This is supported by Winnersbach et al who found reduced platelet activation in platelet poor blood perfused within an in vitro model of ECMO, compared to platelet rich blood, and also resulted in reduced NET formation [84].

Whilst platelet counts drop after initiation of ECMO, there is not always further decrease with increased duration of ECMO, a finding seen in other studies [149, 289]. It has been suggested that the measured platelet dysfunction and reduced ability to respond to agonists is due to hyperactivation of platelets in the ECMO circuit [82]. During ECMO initiation there is contact activation via coagulation factor XII when blood comes into contact with the large surface area of the ECMO circuit and oxygenator, leading to increased platelet activation and clot deposition [290]. In addition, the increased shear stress of blood through the MO, leads to loss of platelet surface receptors GPIbα and GPVI which are important for platelet adhesion [149, 194, 291]. Others found that although there was increased platelet surface expression of P-selectin in ECMO patients, there was reduced response to ADP and TRAP-6 stimulation and lower fibrinogen binding [291, 292]. Excessive platelet activation, adhesion and aggregation of platelets may leave the circulating platelets partially degranulated, and in an exhausted state and therefore having a reduced response to exogenous agonist stimulation [82]. The increased expression of P-selectin may have a role to play in leucocyte-platelet interactions and formation of LPA. Platelet adhesion to leucocytes may have a role to play in the excess platelet activation or the thrombocytopenia that develops whilst on ECMO.

Thromboelastography

Regarding thromboelastography, in our samples the TEG R-time, K-time, MA, and α-angle corresponded to the measured APTT, fibrinogen and platelet counts in ECMO patients similar to results in other studies [293, 294]. There was no correlation of TEG results to thrombotic events or bleeding events in ECMO in the few patients where this was measured as with other groups [286]. In one paediatric study a short R-time was an independent predictor of significant thrombotic events on ECMO, but no parameters were related to bleeding events [295], and another found TEG based monitoring result in lower anti-xa levels but not related to clinical events [296]. Overall, there is limited data regarding use of viscoelastic assays in ECMO patients. There does not seem to be a benefit of using viscoelastic assays in ECMO unless there is a particular clinical bleeding concern where results are required sooner than clinical lab assays allow, but larger multi-centre trials may be helpful to validate these findings.

4.5.5 What is the impact of increased NETosis on platelet activation?

It has been reported that the presence of NETs and their components in patients on extracorporeal circuits is related to thrombosis [63, 109, 110, 211, 243], post-op complications [105, 106], thrombocytopenia [84, 225], and may be involved in the development of HIT [244]. Many groups have investigated the mechanisms of how NETS lead to thrombosis and the evidence is conflicting. Intact NETs increase thrombin generation and clot formation via platelet dependent and independent mechanisms [114], as well as through NET-bound von Willebrand factor [112]. Noubouossie and colleagues compared individual NET components (cfDNA and histones) and cell-associated NETs on coagulation in vitro. They found purified DNA triggered contact pathway and amplified contact dependent factor XI activation; and that individual histones H3 and H4 triggered thrombin generation in human plasma but intact NETs and nucleosomes did not produce any of these procoagulant effects [113]. In addition, NE has modulating effects on tissue factor pathway inhibitor leading to increased thrombin generation [117]. The difference in measured cell-associated NETs and soluble NET components may impact the immunothrombotic potential of NETs but mechanisms need to be better understood.

HIT is a common complication in ECMO patients due to the requirement of continuous heparin infusions, and the risk of HIT is increased with longer ECMO durations [205, 241]. The HIT immune complex activates platelets causing both thrombocytopenia and thrombosis [244]. NETs may contribute to the development and pathophysiology of HIT and therefore platelet activation and thrombocytopenia in ECMO patients. Some patient data has revealed an association of nucleosomes with HIT immune complexes in dialysis patients with vascular access thrombosis [63], presence of NETs in patients with HIT [244] and it has been suggested that NETs may be the trigger for thrombocytopaenia in ECMO patients [225]. Perdomo found that neutrophil activation and NETosis appeared to be the major drivers of thrombosis in HIT. They demonstrated that the HIT immune complex can induce NETosis by interacting with the FcγRIIa on neutrophils and increase neutrophil-platelet interactions [244]. Furthermore NETs, form a scaffold for platelets to adhere to increasing thrombosis, and thrombocytopenia [112, 297]. NETs also increase platelet activation and increase thrombosis by releasing prothrombotic molecules [111, 298].

The finding that NETosis is increased whilst patients are on ECMO, highlights a potential therapeutic target to reduce thrombotic complications in a population with high risk of haemostatic complications. More specifically, the increase in NET specific markers CitH3,

and nucleosomes in our data highlight a potential pathway for intervention. Augusto and colleagues found Clusterin (CLU), a scavenger protein that binds to circulating histones, can reduce the proinflammatory, cytotoxic and platelet aggregating effects of histones in a dose dependent manner in vitro. Furthermore, in septic patients, CLU-histone complexes correlated with disease severity, and low levels of CLU in patients were associated with increased mortality [299]. As CLU binds to all histone compositions including CitH3, it has potential to neutralise the deleterious effects of Cit H3 and nucleosomes released from NETosis [65]. Another pathway for potential therapeutic intervention is inhibition of PAD4. PAD4 inhibition of neutrophils in vitro reduces NETosis [244], and in animal models of disease has been shown to reduce inflammation and disease progression [300-302].

4.5.6 The role of platelets in neutrophil activation and NETosis

Conversely, activated platelets could be the driver for increased neutrophil activation and NETosis in ECMO. In a pre-clinical model of ECMO, platelet poor and platelet rich heparinised blood was perfused in test circuits. The platelet poor group showed less platelet activation and lower levels of NET formation compared to the platelet rich group [84]. There are many pathways by which activated platelets induce NETosis. Platelet CD62P binding to neutrophil PSGL-1 [242], platelets interacting with TLR4 on neutrophils [83], and presentation of HMGB1 by activated platelets to neutrophils [303] have all been shown to increase NETosis. In addition, platelets can increase stability of NETS contributing to their thrombogenicity. It has previously been found that PF4 binds to NETs, making them more compact and DNase resistant thereby increasing thrombogenicity [278]. However, others found that PF4 stabilises NETs and reduces thrombogenicity and endothelial cell injury by interfering with the contact activation pathway [304].

There are two forms of NETosis described: lytic or suicidal NETosis which is NADPH oxidase dependent often resulting in neutrophil cell death, and vital NETosis which is NADPH oxidase independent and does not result in cell death [48, 67]. Of particular interest to NETosis in ECMO is induced vital NETosis which is mediated by TLR2, TLR4, PSGL1 and HMGB1 [67, 83, 242] and the release of soluble NET components from the neutrophil cytoplasm. This platelet mediated pathway of NETosis may explain the difference in cell-associated NETs and soluble NETosis markers measured in my data. In addition, not all neutrophils in circulation enter NETosis. It is estimated that only 20-25% of neutrophils release NETs, and these may be a certain subset of neutrophils [66].

4.6 Concluding remarks

In this chapter I have discussed the observation there are distinct changes that happen after initiation of ECMO. Firstly, there is increased NETosis as measured by CitH3 and nucleosomes, secondly the initiation of lung rest after ECMO initiation leads to a reduction in inflammatory cytokines, and lastly there is likely platelet dysfunction on ECMO manifested by thrombocytopenia and reduction in soluble PF4 and CD62P, as well as reduced platelet aggregation measured by clinical coagulation assays.

Immunothrombosis is the recruitment and interaction of platelets and neutrophils at sites of tissue injury, regulated by the coagulation cascade and inflammatory mediators. There are many factors that may contribute; exposure of blood to the ECMO circuit and its components may lead to lead to platelet and neutrophil activation separately and activation of platelets from ECMO shear may further increase neutrophil activation and therefore NETosis. We know that NETs are involved in conditions where there is increased thrombosis and platelet dysfunction such as HIT.

The interplay between neutrophils and platelets is complex. To further understand the mechanisms of platelet activation and NETosis in vivo, we must investigate the direct neutrophil-platelet interactions. Neutrophils and platelets are often studied in isolation but there is increasing understanding into the interactions of platelets and leucocytes, and the importance of neutrophil-platelet aggregates (NPA) as markers of sepsis, thrombosis and their role in immunothrombosis [123, 282, 305]. Exposure of blood to the extracorporeal circuit leads to increased platelet activation, with subsequent increased platelet-neutrophil cross talk and NETosis. There may also be differences in NETosis between different subsets or phenotypes which may affect neutrophil activation and NET markers through different phases of the patient's illness and ECMO run. Exploring neutrophil phenotypes and direct neutrophil-platelet interactions during ECMO and their correlation to NETosis may provide more insight into the pathways involved in immunothrombosis, thrombocytopenia, and NETosis in this complex cohort of patients. As experience and understanding for managing patients on ECMO increases, knowledge about the cell-cell interactions, and relationship between machine and biology is paramount in delivering effective therapies and reducing complications that arise from ECMO use.

Chapter 5: Measuring leucocyte platelet aggregates – challenges of quantification

Abstract

Leucocyte-platelet aggregates (LPA) have recently been used as a marker of sepsis severity and have been associated with thrombotic conditions such as PE and DVT, and in atherosclerotic disease. There are very few studies characterising leucocyte phenotypes and LPA in critically ill patients supported on ECMO. ECMO is associated with haemostatic complications, both thrombotic and bleeding related. This is likely due to increased activation of neutrophils, monocytes and platelets, from the underlying critical illness, and through contact with the foreign surfaces of the ECMO circuit, as well as the increased shear to blood due to the ECMO pump. This chapter aims to investigate LPA formation in SARF patients who require VV ECMO.

Firstly, I describe the critical variables affecting measurement of measuring LPA in whole blood and validate a protocol to measure LPA and leucocyte phenotypes in heparinised whole blood. I demonstrate that LPA formation is calcium dependent and is reversible. Secondly using this protocol, I was able to quantify LPA and phenotype leucocytes in ECMO patient blood samples. There were increased neutrophil-platelet aggregates at ECMO initiation which decreased with duration on ECMO. There was also increased immune activation in patients on ECMO: neutrophils from ECMO patients had increased expression of activation markers CD66b, and shedding of CD62L, whereas monocytes had reduced expression of HLA-DR.

This chapter describes changes seen in ECMO patients with regards to LPA and immune dysregulation, highlighting the need for more work into leucocyte platelet interactions in this cohort of patients.

5.1 Introduction

5.1.1 Relationship between neutrophils and platelets in ECMO

Neutrophils and platelets are the first cells to arrive to sites of tissue injury or infection. Both have key roles in inflammation and the host response to infection with complex cross talk through contact-dependent interactions and soluble mediator release, leading to activation of signalling pathways in both cell types. ECMO is associated with an increased risk of complications such as increased SIRS, infection, bleeding, and thrombosis. This may be due to increased activation of neutrophils, monocytes and platelets by contact with the foreign and non-endothelialised surfaces of the ECMO circuit [159]. There are very few studies characterising leucocyte phenotypes and leucocyte-platelet interactions specifically heterotypic aggregates in ECMO patients. Furthermore, distinguishing ECMO-related changes from the underlying pathophysiology of the primary insult is challenging. ECMO may be a second hit to leucocytes and platelets that are already activated by the primary pathology.

NETs are increased in ECMO and other extracorporeal circuits as found in data presented in Chapter 4 as well as in the literature [105, 107, 108, 110, 211, 258], and thrombocytopenia is common in ECMO patients [205, 241]. The relationship between these two clinical phenomena requires more investigation as they are likely to be related. NETs may contribute to thrombocytopenia as they activate and increase aggregation of platelets [111, 112, 297, 298]. Conversely, activated platelets by the ECMO circuit could be the driver for the increased NETosis in ECMO [83, 242].

Binding of neutrophils to platelets to facilitate direct crosstalk between these two cell populations may lead to pseudothrombcytopenia particularly in ECMO patients [306]. Pseudothrombocytopenia is a phenomenon of falsely low platelet counts usually seen due to platelet agglutination to leucocytes (commonly neutrophils) usually in EDTA blood samples [307-309]. Automated analysers do not identify platelets bound to leucocytes resulting in pseudothrombocytopenia [309].

5.1.2 Leucocyte platelet aggregates

An emerging area of interest in sepsis and inflammatory states is in heterotypic leucocyte-platelet aggregates (LPA), where we stop thinking of the cell populations acting independently, but working co-operatively in line with the cell-based coagulation model (Section 1.3.2). Activated platelet interactions with leucocytes play an essential role in

leucocyte recruitment, adhesion, release of inflammatory mediators, oxidative burst and release of NETs [297]. Leucocyte-platelet interactions can be contact-independent through release of mediators, and extracellular vesicles, or direct through cell-cell interactions via surface proteins and receptors. Formation of LPAs facilitates direct intercellular crosstalk and triggers mutual activation and release of granular content by both leucocytes and platelets to initiate and propagate or modulate vascular inflammation [119].

An LPA is a complex of one leucocyte with one or more platelets formed during immune or thrombotic reactions, particularly during conditions where there is shear stress or vascular injury [119]. LPAs are formed through specific receptors such as platelet P-selectin (CD62P), CD40L and glycoprotein IIb/IIIa (GPIIb/IIIa) with PSGL-1 and Mac-1 (CD11b; integrin$\alpha_M\beta_2$) on leucocytes [119-121]. Platelets can bind various leucocyte subpopulations: neutrophils (NPA), monocytes (MPA), lymphocytes (LyPA) and eosinophils (EPA) (Figure 5.1). Different leucocyte subsets interact with platelets to different degrees; monocytes show the highest affinity for P-selectin, followed by neutrophils, and then lymphocytes [121]. The proportions of LPA subtypes may be determined by the proportion of leucocyte subtypes in circulation, with neutrophils the most abundant, followed by lymphocytes and then monocytes.

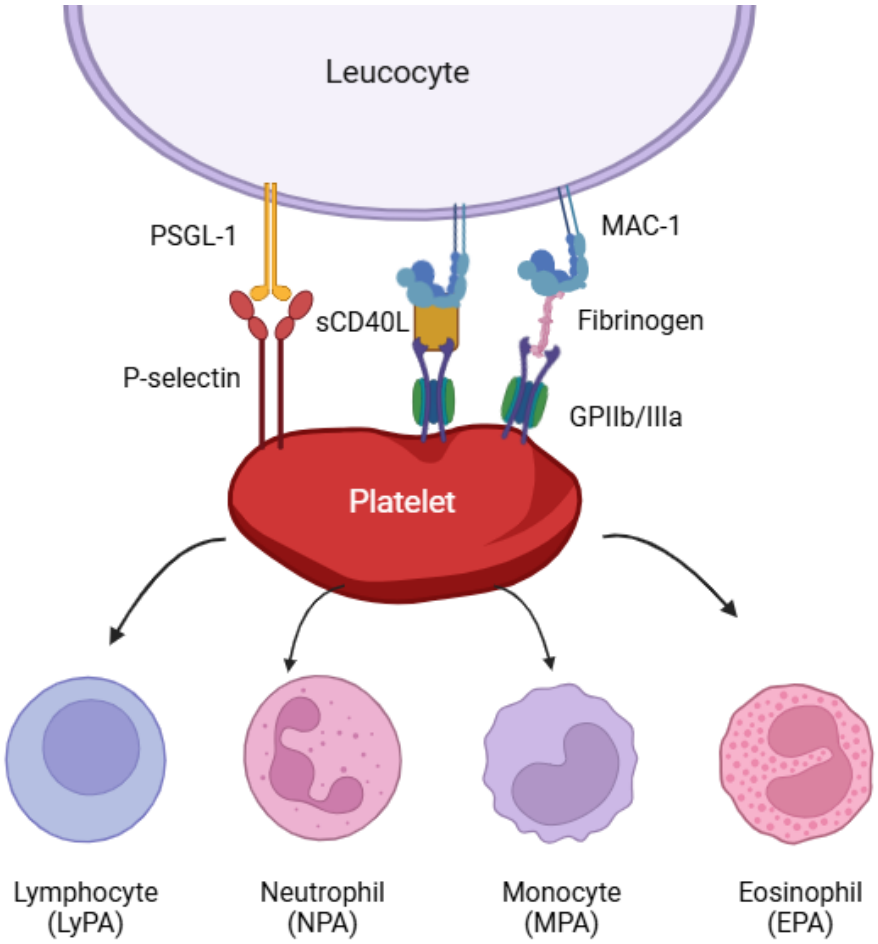


Figure 5.1 Platelets bind to leucocytes through specific receptors-ligand interactions to form leucocyte-platelet aggregates.

Activated platelets express P-selectin which binds to PSGL-1 on leucocytes, and GPIIb/IIIa which bind to Mac-1 on leucocytes via intermediary proteins such as CD40L, or fibrinogen. This leads to formation of leucocyte-platelet aggregates. Image created on Biorender.

Glycoprotein IIb/IIIa, GPIIb/IIIa; Macrophage-1 antigen, Mac-1; P-selectin glycoprotein ligand-1, PSGL-1; soluble CD40 ligand, sCD40L

Increased LPA levels are associated with a range of thrombo-inflammatory conditions including cardiovascular disease [120, 310], venous thromboembolic disease [311], acute ischaemic stroke [312], acute lung injury [313], sickle cell disease [314], and acute kidney injury [119, 315]. There are only a handful of studies to date investigating LPA in ECMO patients [276, 292], but given the increased platelet activation, leucocyte activation and inflammation that occurs after ECMO initiation it is logical that LPA and their interactions also play a role in this patient group. Leucocyte-platelet interactions could play a key role for increased neutrophil activation and NETosis, and increased immunothrombosis whilst on ECMO, and in COVID-19.

5.1.3 Leucocyte phenotypes

Changes in leucocytes numbers, phenotypes and functions have been reported in critically ill and septic patients. Activated neutrophils express increased CD66b and CD11b, and shed CD62L [71], and there are increased proportions of immature granulocytes and neutrophil CD64 expression in septic patients due to increased neutrophil turnover [72]. Neutrophil CD64 expression is upregulated in response to proinflammatory cytokines due to infection within 4-6 hours and is used as an early marker for predicting the severity and course of sepsis [316].

Monocyte subtypes are characterised based on their CD14 and CD16 expression into classic ($CD14^{++}$, $CD16^{-}$), intermediate ($CD14^{++}$, $CD16^{+}$) and non-classic ($CD14^{+}$, $CD16^{++}$). CD16 positive monocytes (non-classic) are increased in sepsis [72], and changes in monocytes counts contribute to morbidity and mortality in some fibrotic lung diseases [317, 318]. Further subdivision of intermediate and non-classic monocytes is dependent on HLA-DR expression [78]. HLA-DR is a class II major histocompatibility complex, crucial for antigen presentation by antigen-presenting cells like monocytes and macrophages. Presentation of antigens to the immune system leads to activation or suppression of T-cell responses and modification of the adaptive immune system. Usually when monocytes are activated there is increased expression of HLA-DR, but decreased monocyte HLA-DR has been widely studied in trauma, sepsis and SIRS [79-81], and is one key feature of sepsis-induced immunoparesis. In conditions where there is a massive inflammatory response, the shedding of monocyte HLA-DR leads to reduced immune activation and is associated with poor prognosis [80].

There are many ways in which neutrophils die, by apoptosis, necroptosis and NETosis and therefore exploring the phenotypes that are associated with the mode of cell death may be useful [55]. The inflammatory response associated with ARDS and with ECMO can lead to increased leucocyte activation and recruitment [159]. However, the effects of ECMO on leucocytes has not been widely reported and different phenotypes could be related to leucocyte platelet interactions and LPA formation and may contribute to morbidity and mortality.

5.2 Aims and hypothesis

The aim of this chapter was to validate a method for measuring LPA and phenotyping neutrophils and monocytes and applying this protocol to patient samples.

Using these protocols, I investigated leucocyte activation profiles and leucocyte-platelet aggregate formation in SARF patients who require VV ECMO.

I hypothesise:

1) There would be increased neutrophil and platelet interactions in patients on ECMO and throughout their ECMO run.
2) Different neutrophil or monocyte phenotypes are more likely to form leucocyte-platelet aggregates.

5.3 Methods

5.3.1 Blood sample processing

Blood was taken from HV and patients enrolled into the HITEC study as described in section 2.2.4. For patient samples, 200ul whole blood aliquots were taken from each vacutainer before processing for plasma storage. Aliquots were taken from EDTA, lithium-heparin, ACD, citrate and hirudin tubes as required and kept in a cool box with ice for transport between the hospital and the laboratory. Whole blood was stained within 90 minutes of sample collection using the whole blood staining protocol as described in section 2.4.5.

5.3.2 Whole blood stimulation/in vitro controls

In early patient LPA measurements, only EDTA blood samples were used for LPA quantification, however very low levels of LPA were measured. To validate the protocol for measuring LPA, the protocol was tested on in vitro stimulated blood samples using the whole blood stimulation protocol described in Section 2.3.4. The whole blood stimulation protocol used in our lab uses heparin blood, but many whole blood flow cytometric phenotyping protocols use EDTA blood, therefore both heparin and EDTA blood were used for evaluating LPA formation in vitro.

In summary, EDTA or heparin blood (1ml) was stimulated with PMA 100nM, LPS 100ng/ml or left untreated (UT) in 5ml Eppendorfs, in a rotator, at 37ºC for 1 hour. Whole blood (1ml) was also left static on ice for 1 hour as a control. After stimulation, aliquots of whole blood were taken to quantify LPA, and leucocyte and platelet activation markers using flow cytometry.

5.3.3 Flow cytometry for leucocyte phenotyping and leucocyte-platelet aggregates in patient samples

Neutrophil phenotyping and activation markers include CD66b, CD10, CD16, CD62L, and CD64. Monocyte markers include CD45, CD11b, CD14, CD16 and HLA-DR. Samples were also stained for CD41 to identify bound platelets and for tissue factor (CD142) as a marker of thrombogenicity. The two panels used for patient samples is shown in Table 5.1.

Fluorophore	Neutrophil-Platelet aggregates	Monocyte-Platelet aggregates
BV421	CD66b	CD45
BV605	CD10	CD11b
FITC	CD16	CD16
PE	CD142	CD142
PE-Cy7	CD41	CD41
AF647	CD62L	HLA-DR
APC-Fire 750	CD64	-
APC-Cy7	-	CD14

Table 5.1 Fluorophore conjugated antibody panels for quantification of leucocyte-platelet aggregates and phenotyping neutrophils and monocytes.

In brief, whole blood (10µl for neutrophils and 20µl for monocytes) was incubated with LPA antibody cocktail(s) at room temperature for 15 minutes, BD FACS lysis buffer (500µl for neutrophil panel and 750ul for monocyte panel) was added for 10 minutes to lyse erythrocytes and fix samples. Samples were washed with 2ml PBS and centrifuged at 300 x *g* for 7 minutes at 4°C and resuspended in 500µl of PBS. Samples were acquired on the spectral flow cytometer. For neutrophils, the stopping trigger was acquisition of 10,000 $CD66b^{+}$, SSc^{high} neutrophils, and for monocytes, the stopping trigger was acquisition of 5,000 $CD45^{+}$, $CD14^{++}$, $CD16^{-}$ monocytes.

5.4 Results

5.4.1 Anticoagulant type affects LPA formation and measurement in vitro.

Prior to examining patient samples, the effects of anticoagulants on spontaneous and stimulated LPA formation in vitro as well as their measurement needed to be determined. The antibody panel was firstly tested on EDTA and heparin HV whole blood. Whole blood left on ice was the control, and whole blood in the rotator at 37°C, without stimulation, with LPS 100ng/ml or PMA 100nM stimulation for 1 hour were the experimental conditions. There were 4 repeats for NPA panels and 3 repeats for MPA panels as there were not enough monocytes acquired for statistical analysis for one set of experiments.

There were differences in NPA levels between the two anticoagulants (ANOVA P=0.0019) and the different stimulation conditions (ANOVA P=0.0079) (Figure 5.2). When differences were compared between ETDA and heparin without stimulation in the rotator, there were higher levels of NPA in heparin blood in the rotator (78.6 [± 24.5] vs 3.0 [± 1.2]; P=0.0096) suggesting there is spontaneous NPA formation at body temperature with mixing. This is not seen when blood was kept static on ice. With stimulation, there were much higher levels of NPA in heparin blood compared to EDTA blood in the rotator with both LPS (87.6 [± 16.8] vs 16.3 [± 12.4] %; P=0.0074) and PMA (92.5 [± 8.1] vs 17.3 [± 10.1] %; P=0.0002). The levels of NPA remain unchanged in EDTA blood regardless of stimulation which suggests EDTA inhibits NPA formation.

The proportions of MPA were higher in heparin blood compared to EDTA for all conditions (ANOVA P=0.0008). There was also a difference in MPA levels between blood left on ice compared to unstimulated blood in the rotator (ANOVA P=0.0262). The proportions of MPA were maximal (>99.5%) for all conditions in the rotator in heparin blood compared to EDTA suggesting spontaneous formation of MPA in heparin blood which is not enhanced by further stimulation.

The leucocyte CD41 expression is a measure of number of platelets adhered to the leucocyte cell surface. There were differences between neutrophils and monocytes. There is a trend for increased neutrophil CD41 expression with increased stimulation, but these were not significant between anticoagulants or stimulation despite higher proportions of NPA in heparin blood compared to EDTA. In contrast, the monocyte CD41 signal was increased in heparin blood in the rotator at 37°C compared to EDTA regardless of stimulation (ANOVA P=0.0048) corresponding with the MPA proportions. The monocyte CD41 expression is low in blood kept static on ice. The increased monocyte CD41 expression may be related to the increased affinity that monocytes have for platelets compared to neutrophils and therefore more platelets are bound to each monocyte than neutrophil.

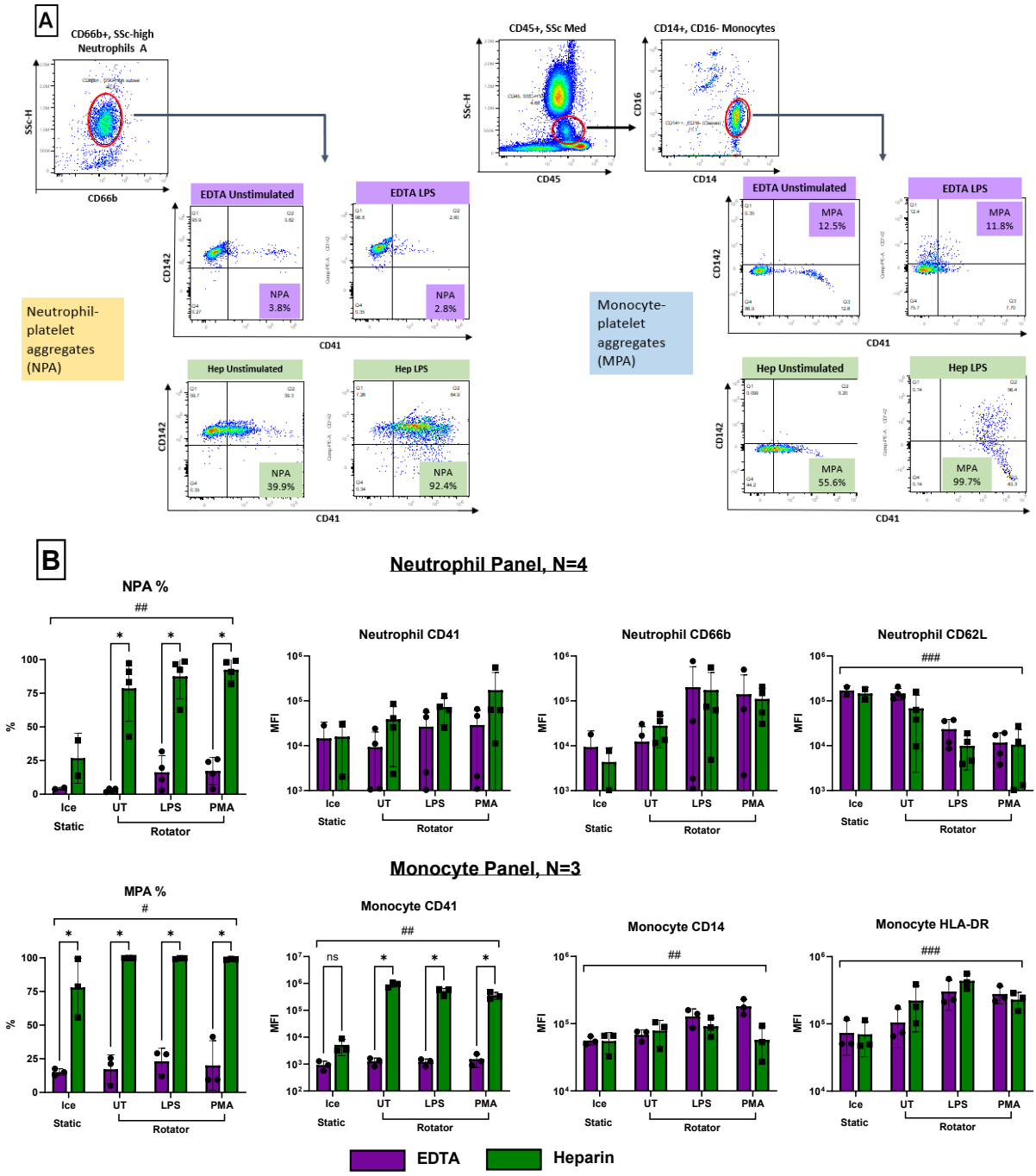


Figure 5.2 Neutrophil-platelet aggregate and monocyte-platelet aggregate formation in vitro. *Whole blood was left on ice, or in the rotator at 37°C untreated, with LPS 100ng/ml or PMA 100nM for 1 hour. N=4 for neutrophil and N=3 for monocytes. Whole blood was stained with antibodies. NPA and MPA % were quantified, as well as neutrophil (CD66b, CD62L) and monocyte (CD14, HLA-DR) activation markers and platelets (CD41) on each leucocyte determined using flow cytometry. Gating for NPA and MPA in EDTA and Heparin unstimulated and LPS stimulated blood shown in 5.2A. Summary plots for all repeats shown in 5.2B. Two-way ANOVA or mixed-effect group analyses (#) with Holm-Sidak's multiple comparisons tests (*) were performed to compare trends between anticoagulants and stimulation. Paired t-tests were used to compare between EDTA and heparin. All tests were two-sided and P<0.05 was considered statistically significant. p<0.05 *, p<0.01 **, p<0.001 ***, p<0.0001 ****.*

Lipopolysaccharide, LPS; Mean fluorescent intensity, MFI; Monocyte-platelet aggregate, MPA, Neutrophil-platelet aggregate, NPA; Phorbol myristate acetate, PMA; Unstimulated, UT.

Neutrophil activation was increased in blood in the rotator (PMA > LPS > untreated) as measured by CD62L shedding (ANOVA P=0.0004). The neutrophil CD66b expression increased with stimulation but the difference was not significant. There was some variation in monocyte activation as measured by monocyte CD14 (ANOVA P=0.0064) and HLA-DR (ANOVA P=0.0009) expression. There was no difference between the two anticoagulants in neutrophil or monocyte activation.

5.4.2 Leucocyte-platelet aggregate formation is calcium dependent and reversible.

Since platelet binding is calcium dependent, I hypothesised that cation chelation from EDTA may interfere with or reverse LPA formation. Firstly, I compared LPA quantification from patient blood in EDTA and heparin blood and to investigate the effect of EDTA on LPA measurement. In addition, 1.25mM EDTA was added to patient heparin blood samples for 10 minutes at room temperature before staining with NPA and MPA antibody cocktails.

There were 27 matched EDTA, heparin and heparin+EDTA samples from 16 patients at various time points. The proportion of measured NPA (45.8 [± 26.4] vs 1.1 [± 1.7] %; P<0.0001) and MPA (83.1 [± 21.0] vs 10.5 [± 12.8] %; P<0.0001) were higher in heparin blood samples compared to EDTA blood (Figure 5.3). Secondly, after the addition of EDTA 1.25mM to heparin blood, the proportions of NPA (6.9 [± 9.0] vs 45.8 [± 26.4] %; P<0.0001) and MPA (22.7 [± 23.1] vs 83.1 [± 21.0] %; P<0.0001) were significantly diminished compared to the heparin samples. This provides evidence that LPA formation is not fixed and that EDTA or strong calcium chelation can reverse LPA formation. These differences in NPA and MPA measured are also reflected in reduction of both neutrophil and monocyte CD41 expression after addition of EDTA to heparin blood (Figure 5.3).

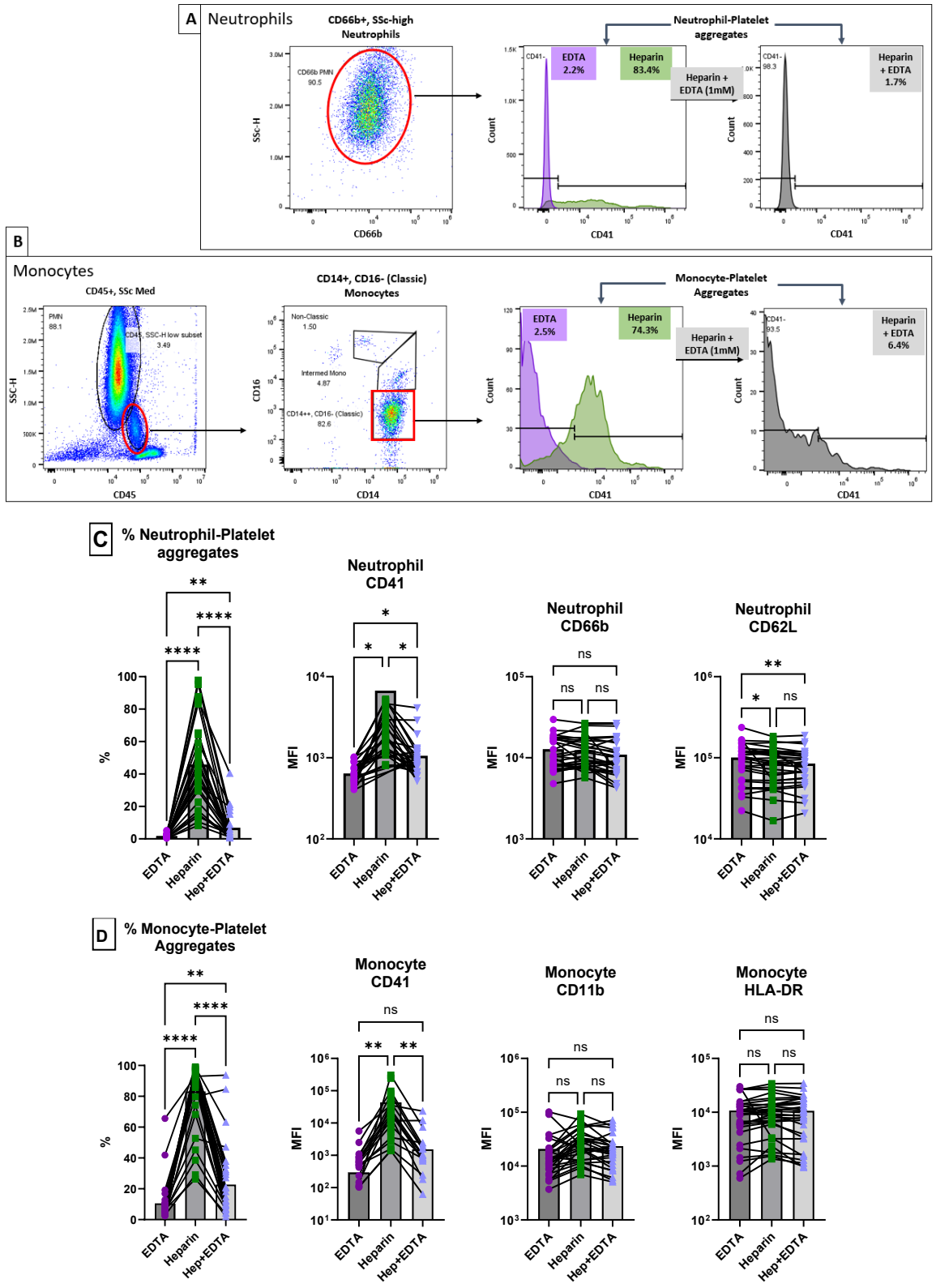


Figure 5.3 Neutrophil-platelet aggregate and monocyte-platelet aggregate measurement in patient samples in EDTA, heparin and heparin+EDTA samples. *EDTA and heparin anticoagulated whole blood from patients was stained with antibody cocktails and using flow cytometry, NPA % and MPA % were quantified, as well as neutrophil (CD66b, CD62L) and monocyte (CD14, HLA-DR) activation markers and platelet marker (CD41) on each leucocyte. EDTA (1.25mM) was added to heparin samples and stained using the same protocol. (A) and (B) shows gating for NPA and MPA respectively, (C) and (D) show summary data for NPA and MPA respectively. 27 matched samples from 16 patients were analysed. RM One-way ANOVA with Holm-Sidak's multiple comparison's test was performed to compare between groups. All tests were two-sided and P<0.05 was considered statistically significant. p<0.05 *, p<0.01 **, p<0.001 ***, p<0.0001 ****

In contrast to platelet binding, EDTA and heparin had no effect on leucocyte phenotyping, as demonstrated by the lack of difference in neutrophil (CD66b) or monocyte (CD11b, HLA-DR) activation markers (Figure 5.3). There was also no effect in heparin samples after the addition of EDTA. There was slightly lower neutrophil CD62L in heparin and heparin+EDTA compared to EDTA only samples suggesting some spontaneous neutrophil activation in heparin blood.

5.4.3 Measurement of LPA is affected by anticoagulation

To investigate the effect of different anticoagulants on LPA measurement I compared the proportions of LPA formed in critically ill patients from blood samples in different anticoagulants.

Calcium chelation

EDTA is a very potent calcium chelator and appears to completely inhibit LPA formation in vitro and reverse LPA formation in vivo in heparinised blood. To investigate if the degree of calcium chelation influenced LPA quantification and leucocyte phenotype measurement, patient samples collected in EDTA, citrate, and ACD vacutainers were compared with heparin blood. There were 11 matched samples from 5 patients who had LPA measured in all four anticoagulants. There were differences in the levels of NPA and MPA measured between the different calcium chelators and heparin. Regarding NPA, EDTA had the lowest levels (1.37 ± 0.74%), compared to ACD (9.4 ± 7.2%) and citrate (31.0 ± 15.6%) which is in line with EDTA's chelating strength compared to citrate-based anticoagulants. This was the same for MPA with levels in the order of EDTA (15.7 ± 9.3%), ACD (55.2 ± 32.6%) and citrate (84.1± 25.4%) (Figure 5.4). Similar trends were seen in neutrophil CD41 expression but in monocytes, there was no difference in CD41 expression between heparin, ACD and citrate blood suggesting MPA are less susceptible to the effects of citrate calcium chelation. The levels of NPA and MPA were comparable between heparin and citrate anticoagulation. There were no significant differences in measured neutrophil activation markers between the anticoagulants but there were some differences in monocyte activation markers with increased expression of CD11b and HLA-DR in heparin blood compared to ACD and citrate anticoagulation again suggesting some spontaneous activation in heparin blood (Figure 5.4).

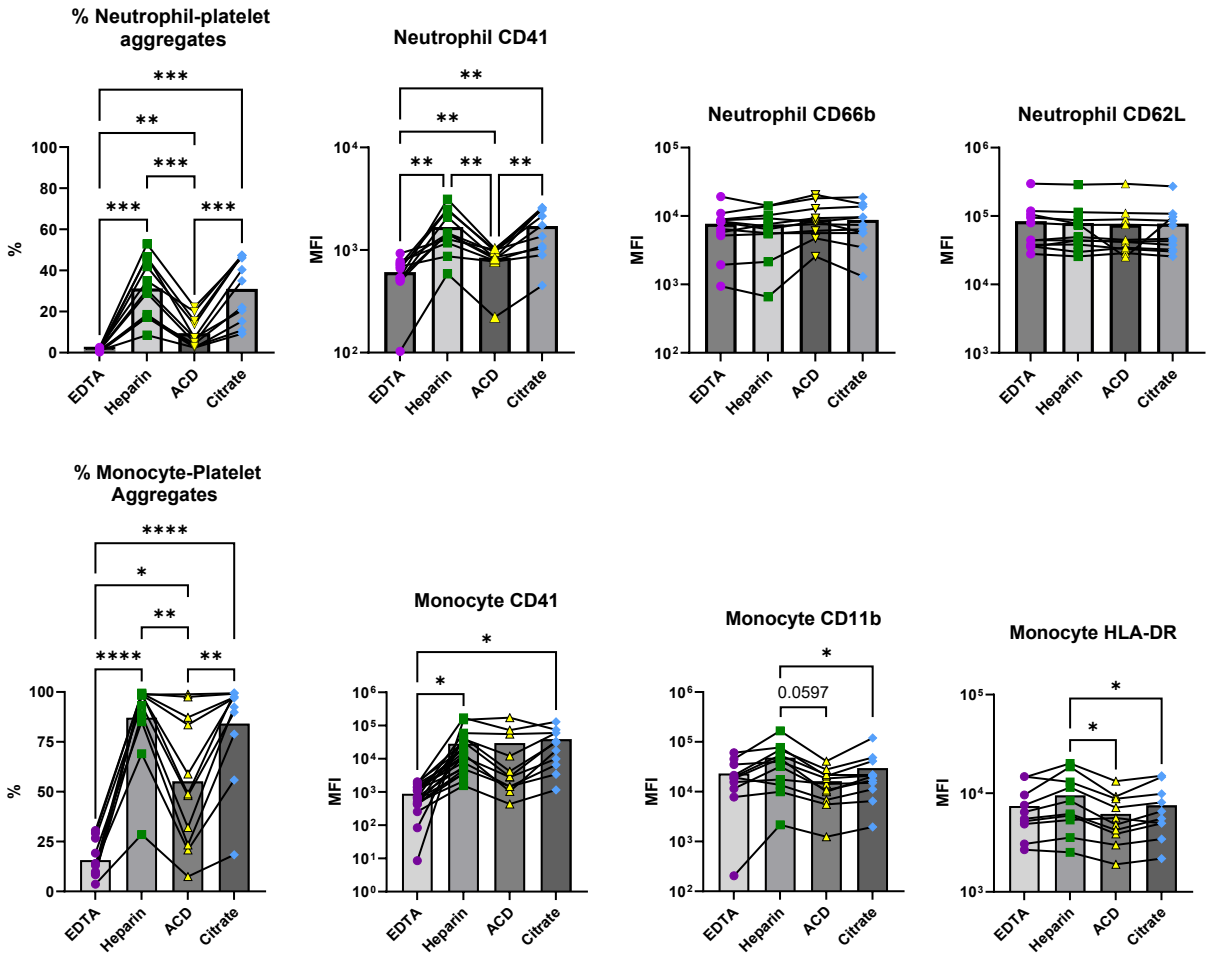


Figure 5.4 Effect of different calcium chelators on leucocyte-platelet aggregate measurement and leucocyte phenotyping.
*11 matched samples from 5 patients who had measurements from EDTA, heparin, ACD, and citrate blood were analysed. RM one-way ANOVA with Holm-Sidak's multiple comparisons test was used to compare anticoagulants. All tests were two-sided and P<0.05 was considered statistically significant. p<0.05 *, p<0.01 **, p<0.001 ***, p<0.0001 ****

Direct thrombin inhibitors

Some patients had Multiplate tests done as part of the HITEC study protocol, which requires blood to be collected in hirudin anticoagulant, a DTI. Where available the remaining hirudin blood was analysed and compared to EDTA and heparin blood (Figure 5.5). There were 15 matched samples from 8 patients who had LPA quantified in EDTA, heparin and hirudin blood. The hirudin samples had significantly higher proportions of NPA, MPA and neutrophil and monocyte CD41 expression than EDTA and heparin. There was also increased expression of neutrophil activation markers compared to both EDTA and heparin as demonstrated by increased CD66b and lower CD62L but no difference in monocyte

activation markers. This may suggest spontaneous activation in hirudin blood or could be artefact.

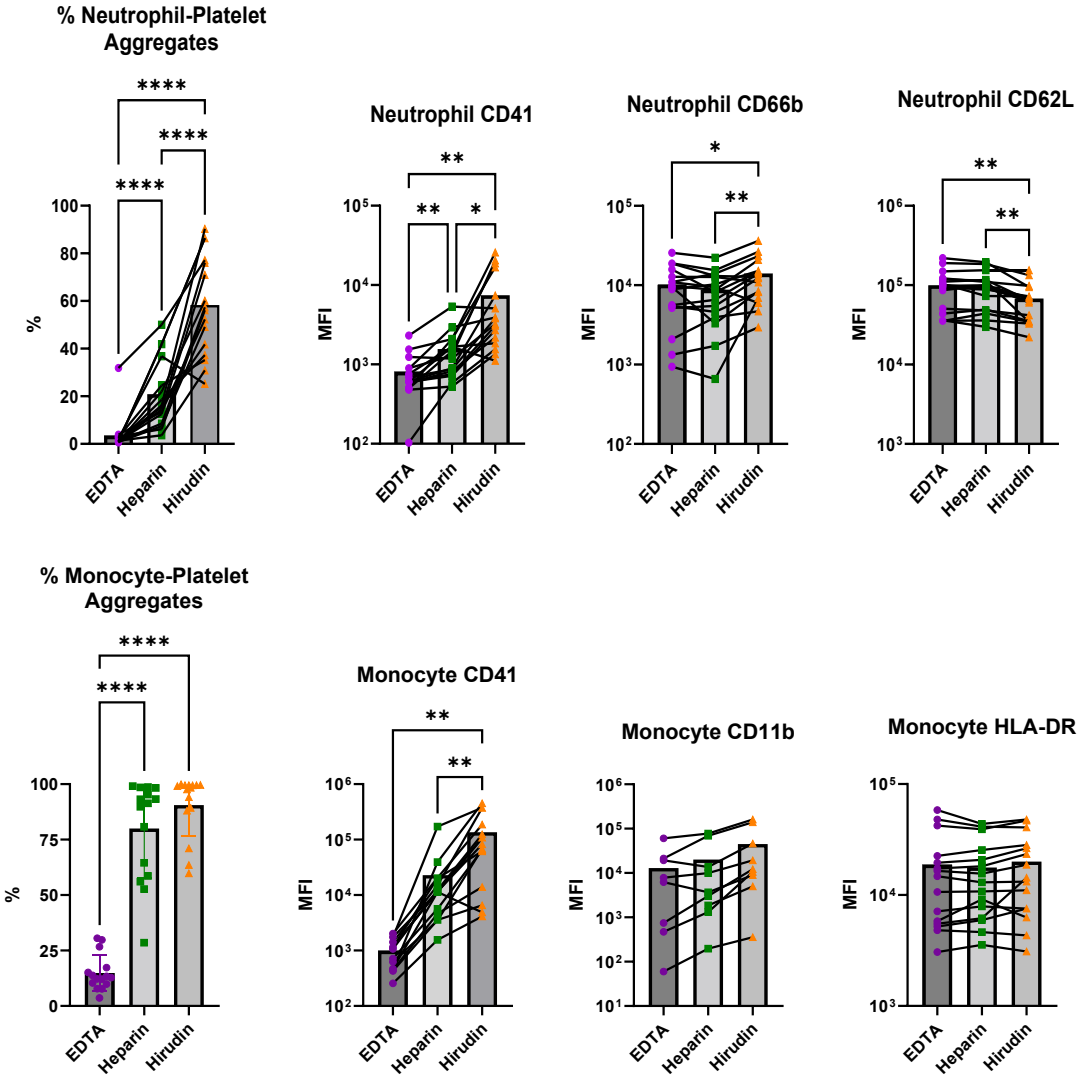


Figure 5.5 Effect of direct thrombin inhibitor on leucocyte-platelet aggregate measurement and leucocyte phenotyping.

*15 matched samples from 8 patients who had measurements from EDTA, heparin, and Hirudin blood were analysed. RM one-way ANOVA with Holm-Sidak's multiple comparisons test was used to compare anticoagulants. All tests were two-sided and P<0.05 was considered statistically significant. p<0.05 *, p<0.01 **, p<0.001 ***, p<0.0001 ****

5.4.4 NPA kinetics and neutrophil phenotypes in ECMO patients

Following the comparisons of different anticoagulants, heparin blood was used for the quantification of LPA and leucocyte phenotyping in the patient samples (See Figure 2.12 for gating strategy) as 1) this blood tube was collected at all time points for all patients enrolled on the HITEC study, 2) it eliminated the possible effect of calcium chelation on reversing LPA formation and therefore its measurement, and 3) the differences in leucocyte activation

markers were minimal when compared with calcium chelators, unlike with hirudin anticoagulation.

Samples from HV (n=4), and ECMO patients (n=20) were analysed after ECMO initiation (D0-1) and weekly whilst on ECMO. Samples were also taken before and after decannulation (Pre-DC and Post-DC). The median duration of ECMO in patients enrolled in the HITEC study was 13.1 (8.4 – 25.2) days therefore trends were examined from ECMO initiation (n=20), week 1 (n=18) and week 2 (n=13). Due to the sporadic nature of clinical sampling, matched analyses could only be performed for 14 samples between initiation and week 1 and 5 pre- and post-decannulation samples.

Compared to HV, at ECMO initiation, although there was no difference in NPA proportions, patients had higher neutrophil CD66b (10,859 [8,017 – 13,628] vs 3,930 [3,488 – 5,008]; P=0.0309), lower neutrophil CD62L (84,582 [37,262 – 118,961] vs 245,436 [187,895 – 279,995]; P =0.0256), CD10 (3,803 [1,300 – 7,491] vs 10,100 [7,784 – 13,145]; P=0.0380) and CD16 (190,881 [114,895 – 329,123] vs 624,000 [349,341 – 671,750]; P=0.0179) expression demonstrating increased activation and neutrophil turnover (Figure 5.6). There was no change in CD66b during the ECMO run, and the CD62L expression remained lower than that of HV after 1 week on ECMO. Compared to HV, the proportion of immature granulocytes ($CD66^+$; $CD16^-$, $CD10^-$) was higher in patients at ECMO initiation (4.9 [2.9 – 11.8] vs 0.09 [0.06 – 0.14] %; P=0.0054) and after a week on ECMO (5.5 [1.9 – 10.2] vs 0.09 [0.06 – 0.14] %; P=0.0127). There were no other differences in neutrophil cell surface markers whilst on ECMO (Figure 5.6).

Matched pairs analysis between ECMO initiation and 1 week on ECMO showed a decrease in the proportions of NPA (51.0 ± 29.4 vs 37.7 ± 25.4 %; P=0.0339) with corresponding decrease in neutrophil expression of CD41 (2,835 [1,153 – 9,434] vs 1,503 [1,011 – 3,742]; P=0.0353). Neutrophil CD16 expression also increased (373,188 [289,979 – 453,125] vs 177,192 [118,354 – 342,228]; P=0.0052) suggesting more mature granulocytes and there was a trend to decreasing neutrophil CD64 expression after 1 week on ECMO (P=0.0581) indicating lower levels of sepsis. There were no significant differences in NPA or neutrophil surface markers across ECMO decannulation, but there were trends towards increase in NPA and neutrophil CD41 (P=0.0625 for both) (Figure 5.6).

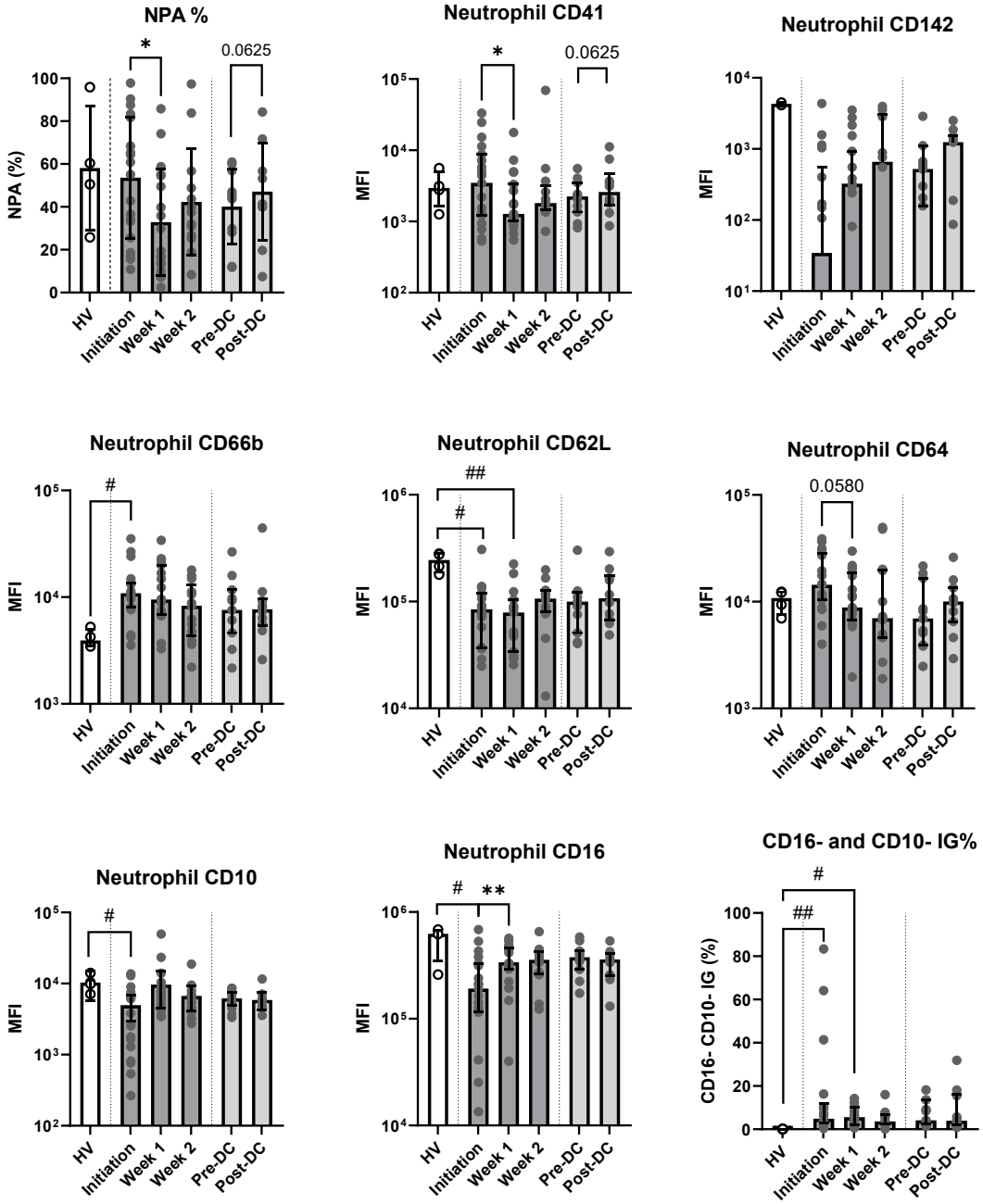


Figure 5.6 Neutrophil-platelet aggregates, and neutrophil phenotypes in ECMO patients

*Blood from patients were stained with antibody cocktail and using flow cytometry, the proportion of neutrophil platelet aggregates were quantified as well as surface expression of neutrophil activation markers, CD41 expression and immature granulocyte proportions. Samples from volunteers (HV; n=4), and ECMO patients (n=20) were analysed after ECMO initiation and weekly whilst on ECMO. Normality was determined by Kolmogorov-Smirnov test. NPA % was parametric, all other variables were non-parametric. Data presented as mean ± SD or median (IQR) as appropriate. Matched-pairs analysis between 14 ECMO initiation and week 1 samples, and 5 pre- and post-decannulation samples were performed using paired t-test or Wilcoxon matched pairs test as appropriate (denoted by *). Comparisons between groups analysed using One-way ANOVA with Holm-Sidak's multiple comparisons or Kruskal-Wallis test with Dunn's multiple comparisons as appropriate (denoted by #). P<0.05 was considered statistically significant. * P <0.05, ** P<0.01*

5.4.5 Relationship between neutrophil phenotypes, NPA and NETosis

To investigate whether different neutrophil phenotypes were more likely to form aggregates with platelets, NPA proportions were compared between immature granulocytes ($CD16^-$, $CD10^-$) and mature granulocytes ($CD16^+$, $CD10^+$); and activated ($CD62L^{low}$) and non-activated ($CD62^{high}$) neutrophils (See figure 2.12 for gating). Compared to ECMO initiation, NPA formed on immature granulocytes decreased after 1 week on ECMO (29.6 ± 22.4 vs 10.8 ± 10.1%; P=0.0010) (Figure 5.7). NPA on immature granulocytes also increased after ECMO decannulation (20 ± 20 vs 13.8 ± 18.3 %; P=0.0255). There were no differences in NPA formed on mature granulocytes. Comparisons were made between immature and mature granulocytes within the same sample. There were fewer NPA formed on immature granulocytes compared to mature granulocytes (23.3 ± 24.4 vs 46.2 ± 28%, P<0.0001).

There was a decrease in NPA in non-activated neutrophils ($CD62L^{high}$) after 1 week on ECMO compared to initiation (29.6 ± 23.8 vs 44.9 ± 31.9; P=0.0309). There were no differences in NPA over time in activated ($CD62L^{low}$) neutrophils. There were more NPA formed in non-activated neutrophils compared to activated neutrophils within the same sample (46.2 ± 28.0 vs 23.4 ± 24.4%; P< 0.0001) (Figure 5.7).

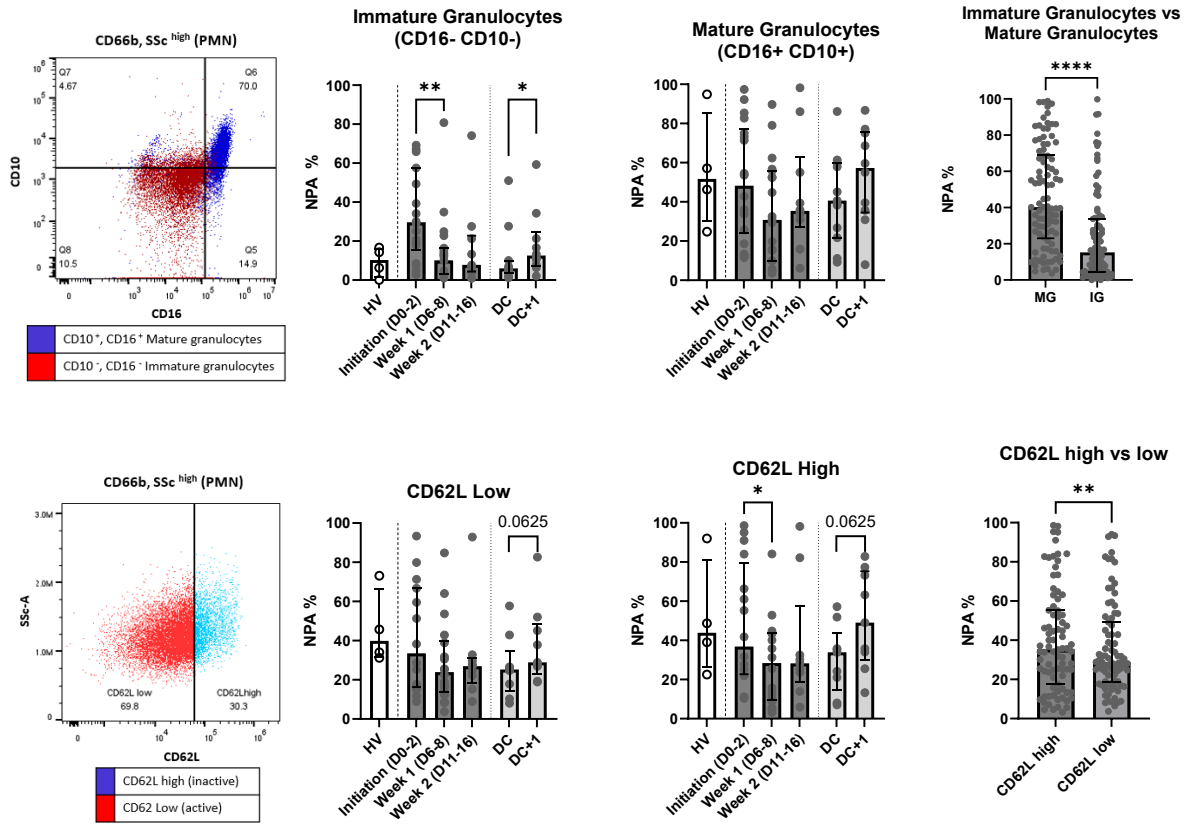


Figure 5.7 NPA proportions over time in different neutrophil sub populations.

*NPA proportions in immature granulocytes (CD10-, CD16-), mature granulocytes (CD10 +, CD16+), activated neutrophils (CD62L low) and non-activated neutrophils (CD62L high) were quantified. Samples from volunteers (HV; n=4), and ECMO patients (n=20) were analysed after ECMO initiation and weekly whilst on ECMO. Matched-pairs analysis between 13 ECMO initiation and week 1 samples, and 5 pre- and post-decannulation samples were performed using paired t-test (denoted by *). Comparisons between groups analysed using One-way ANOVA with Holm-Sidak's multiple comparisons or Kruskal-Wallis test with Dunn's multiple comparisons as appropriate. Comparisons between immature and mature granulocytes; and activated and non-activated neutrophils within the same samples were analysed using paired t-test. P<0.05 was considered statistically significant. * P <0.05, ** P<0.01*

Comparisons in neutrophil cell surface markers were made between $CD41^+$ neutrophils (NPA) and CD41- neutrophils within the same sample (see Figure 2.12 for gating strategy). There were 89 samples from 26 patients in total which had NPA quantified. $CD41^+$ neutrophils had higher expression of all neutrophil cell surface markers CD66b (8894 [6293 – 14140] vs 8607 [5991 – 13600]; P=0.0032), CD10 (6,255 [4,195 – 8,350] vs 4,715 [3,045 – 6,199]; P<0.0001) and CD16 (326,312 [210,864 – 408,500] vs 269,965 [174,157 – 349,765]; P<0.0001). There was no difference in CD64 expression or CD62L expression (Figure 5.7).

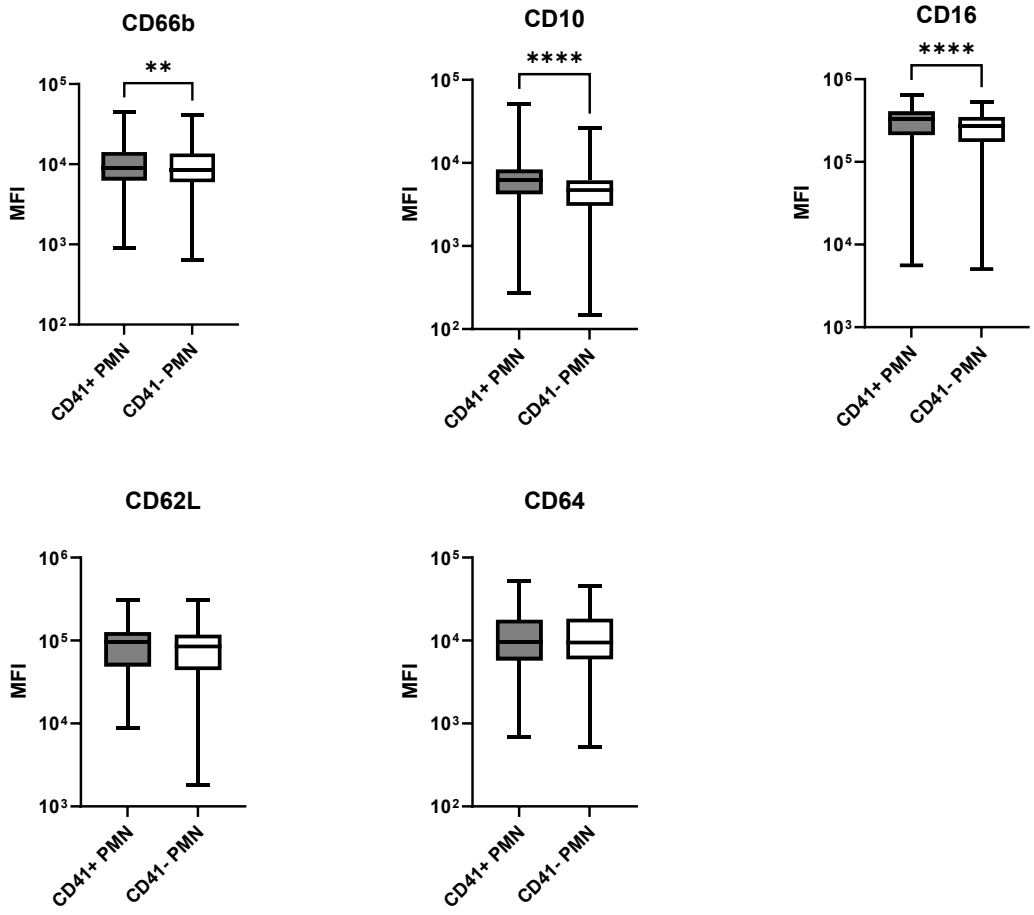


Figure 5.8 Comparison of neutrophil cell surface markers between CD41+ and CD41- neutrophils.

*A total of 89 samples from 26 patients had neutrophil-platelet aggregates quantified. All data was non-parametric. Data presented as median, IQR with full range. Wilcoxon matched pairs test was used to compare between groups. P<0.05 was considered statistically significant. * P <0.05, ** P <0.01, ***, P <0.001, **** P <0.0001.*

The proportion of NPA was compared to the proportion of cell-associated NETS, mature granulocytes and neutrophil activation markers (Figure 5.9). There was no correlation between NPA and cell-associated NETs, both MPO-DNA (R=0.04) and Histone H3-DNA (R= 0.1300). There was a negative correlation between NPA with mature granulocytes (R= -0.22, P= 0.0373) and a trend for positive correlation with immature granulocytes (R= 0.21, P=0.0518). NPA formation was associated with higher neutrophil CD62L (R=0.29, P=0.0069) and CD64 (R=0.28, P=0.0082) expression.

MPO-DNA NETs had a negative correlation with mature granulocytes (R=-0.23, P=0.0310) and CD16 (R=-0.28, P=0.0100) but not histone H3-DNA NETs (R=-0.20, P=0.0776). Both MPO-DNA NETs and Histone H3-DNA NETs had negative correlation with neutrophil CD16

expression (R=-0.28, P=0.0099 and R=-0.27, P=0.0162 respectively). There was no correlation between NETs and neutrophil CD62L or CD64 expression.

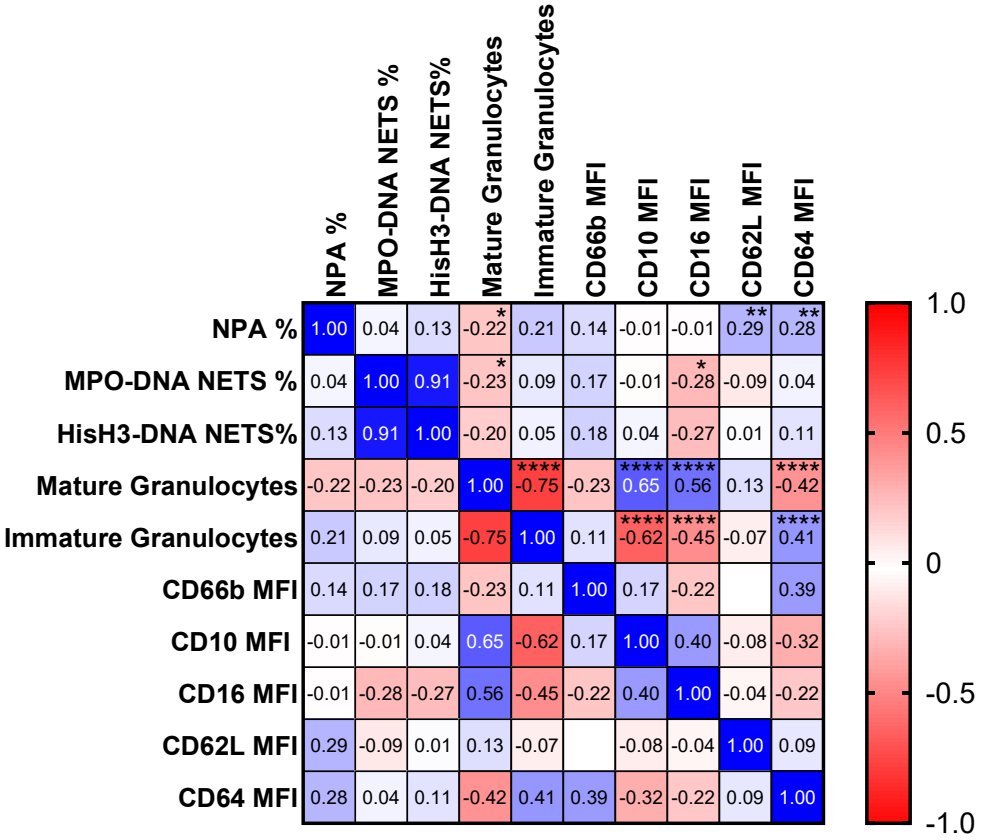


Figure 5.9 Correlation matrix of neutrophil-platelet aggregates with cell associated NETs and neutrophil activation markers.

Proportion of NPA were correlated with proportion of cell-associated NETs, mature granulocytes and neutrophil surface expression of activation markers using Spearman's correlation. There were 86 patient samples with matched values. P<0.05 considered statistically significant.

5.4.6 MPA kinetics and monocyte subsets in ECMO patients

The proportions of classic, intermediate and non-classic monocytes were compared in patient samples from ECMO initiation to week 2 of ECMO and across decannulation. There were no differences in the proportions of monocyte subtypes across the ECMO run. The majority of monocytes were classic monocytes ($CD14^{++}$ $CD16^{-}$) at ECMO initiation (80.7 ± 15.5%), week 1 (78.0 ± 13.7%) and week 2 (78.0 ± 8.4%). Proportions of intermediate and non-classic monocytes were low through the ECMO run (Figure 5.9).

The proportions of each monocyte subtype that formed MPA were also compared. The majority of classic (75-95%) and intermediate monocytes (92-97%) formed MPA, whereas only 60-70% of non-classic monocytes formed MPA. There was no variation in these proportions across the ECMO run.

Since classic monocytes were the largest subtype, the expression of CD41 and monocyte activation markers (CD11b and HLA-DR) in this subtype were compared in patient samples from ECMO initiation to week 2 and before and after decannulation, as for NPA. The monocyte cell surface markers that were used for identifying monocytes and subpopulations (CD45, CD14, and CD16) were not compared. Compared to HV, the monocyte HLA-DR expression was lower in patients at ECMO initiation (6,525 [3,340 – 13,394] vs 69,854 [61,100 – 86,451]; P=0.0017), after 1 week on ECMO (9,632 [5.989 – 24,985] vs 69,854 [61,100 – 86,451]; P=0.0242) and after 2 weeks on ECMO (22,363 [15,300 – 40,221] vs 69,854 [61,100 – 86,451]; P=0.0205). Paired analysis from ECMO initiation to week 1 confirmed the HLA-DR expression increased after 1 week on ECMO (10,300 [5,989 – 25,410] vs 6,637 [4,388 – 13,936]; P=0.0107). There was no difference in the monocyte CD41 or CD11b expression compared to HV or over the ECMO run (Figure 5.10).

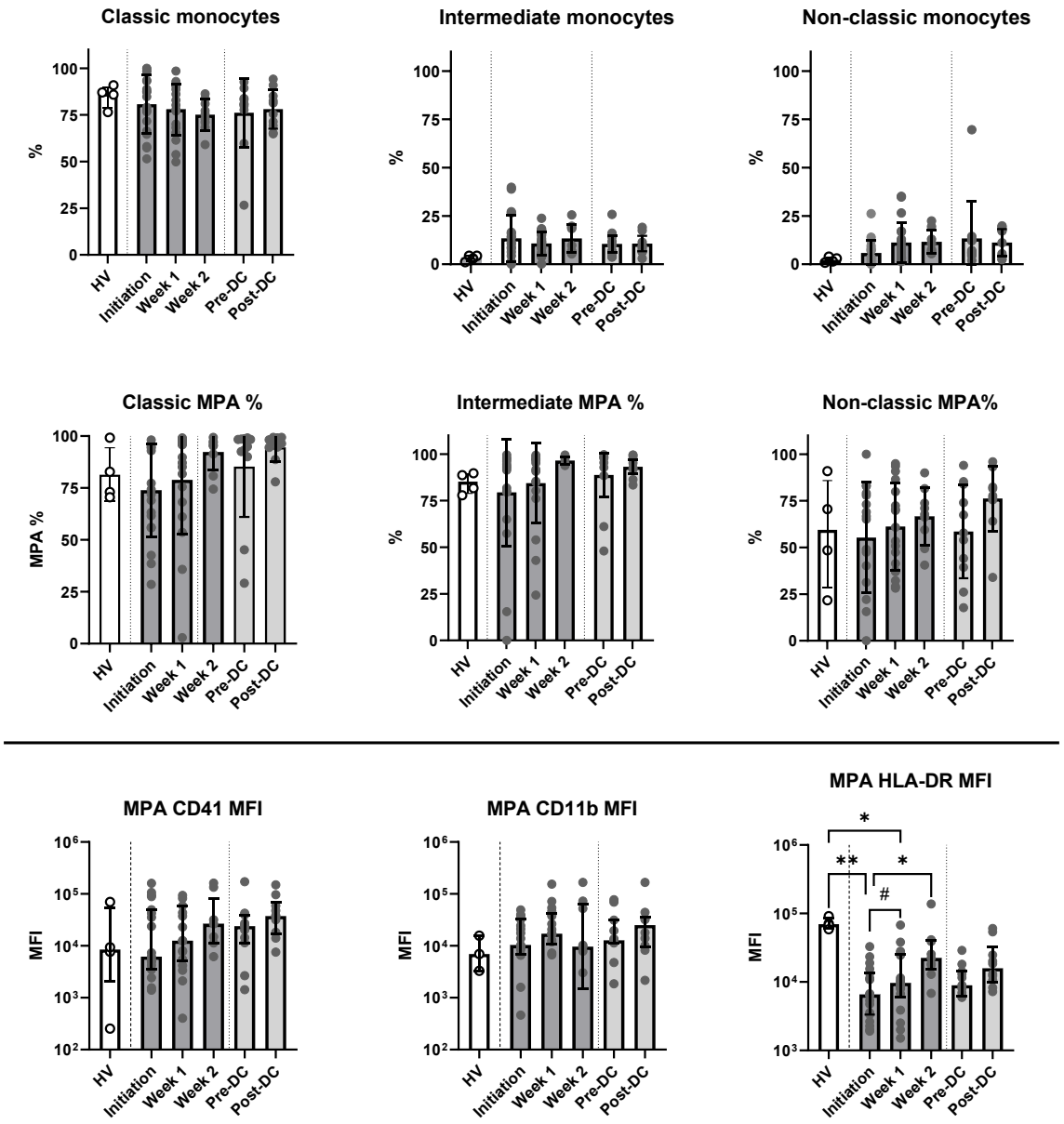


Figure 5.10 Monocyte-platelet aggregates and monocyte activation markers in ECMO patients

*Heparin blood from healthy volunteers and patients were stained with antibody cocktail and using flow cytometry the proportion monocyte subtypes, and monocyte platelet aggregates were quantified. Monocyte CD41 CD11b, and HLA-DR expression were quantified in classic monocytes. Samples from healthy volunteers (HV; n=4), and ECMO patients (n=20) were analysed after ECMO initiation and weekly whilst on ECMO. Normality was determined by Kolmogorov-Smirnov test. MPA % was parametric, all other variables were non-parametric. Data presented as mean ± SD or median (IQR) as appropriate. Matched-pairs analysis between 14 ECMO initiation and week 1 samples, and 5 pre- and post-decannulation samples were performed using paired t-test or Wilcoxon matched pairs test as appropriate (denoted by *). Comparisons between groups analysed using One-way ANOVA with Tukey's multiple comparisons or Kruskal-Wallis test with Dunn's multiple comparisons as appropriate. P<0.05 was considered statistically significant. * P <0.05, ** P<0.01 **

5.4.7 LPA formation was not related to clinically measured cell counts

The neutrophil, monocyte, and platelet count and CRP at the time of LPA measurements were also compared. There was also no variation in the clinically measured neutrophil count, platelet count, or CRP associated with these samples in the first 2 weeks of ECMO. There was a slight increase in monocyte count between ECMO initiation and 1 week on ECMO which is likely to represent recovery of the monocytopenia associated with critical illness (Figure 5.11).

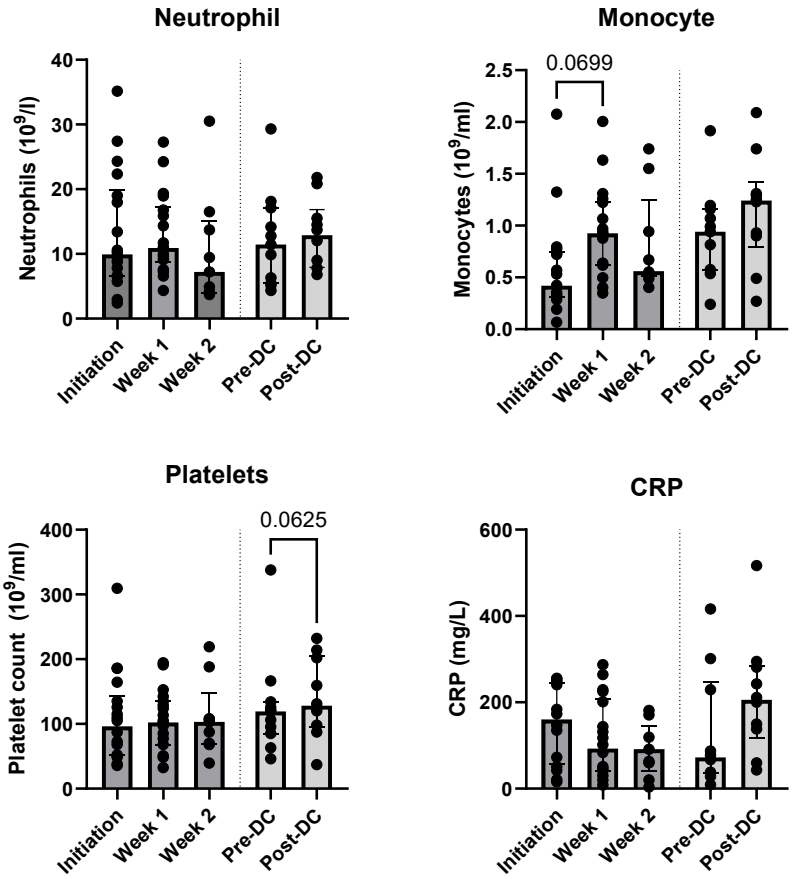


Figure 5.11 Clinically measured parameters over the ECMO run.

Neutrophil, monocyte and platelet counts and CRP from ECMO initiation to week 2 and across ECMO decannulation were compared in 20 ECMO patients. Data presented as median, IQR. Matched pairs analysis between initiation and week 1 (n=13), and before and after decannulation (DC; n=6) were performed using Wilcoxon matched pairs test. P<0.05 was considered statistically significant.

There was no correlation between NPA proportion and platelet count or CRP. There was weak negative correlation between NPA and neutrophil count (R = -0.2454; P = 0.0205) (Table 5.2). The MPA proportion correlated with platelet count (R = 0.3884; P = 0.0002) and negatively with CRP (R = -0.3422; P = 0.0011), but there was no correlation with monocyte count.

		Number of Pairs	Spearman R coefficient	95% confidence interval	P-value
NPA	NPA % vs Hb	89	0.2693	0.05842 to 0.4571	**0.0107**
	NPA % vs. Plt	89	-0.02516	-0.2381 to 0.1901	0.8150
	NPA % vs. MPV	89	0.2011	-0.01368 to 0.3982	0.0588
	NPA % vs. WBC	89	-0.2502	-0.4408 to -0.03804	**0.0180**
	NPA % vs. Neutrophil	89	-0.2454	-0.4367 to -0.03289	**0.0205**
	NPA % vs Monocyte	89	-0.1967	-0.3943 to 0.01831	0.0647
	NPA % vs CRP	88	0.0142	-0.2018 to 0.2290	0.8948
MPA	MPA % vs Hb	89	-0.0004	-0.2087 to 0.2078	0.9966
	MPA % vs. Plt	89	0.3884	0.1960 to 0.5520	**0.0002**
	MPA % vs. MPV	89	-0.1543	-0.3513 to 0.05571	0.1487
	MPA % vs. WBC	89	-0.4407	-0.5944 to -0.2559	**<0.0001**
	MPA % vs. Neutrophil	89	-0.5078	-0.6476 to -0.3350	**<0.0001**
	MPA % vs Monocyte	89	0.1532	-0.05682 to 0.3503	0.1516
	MPA % vs CRP	88	-0.3422	-0.5148 to -0.1430	**0.0011**

Table 5.2. Correlation between NPA and MPA proportions and clinical parameters.

*Correlations between LPA and clinical parameters for 89 patients were analysed using Spearman's coefficient. P<0.05 was considered statistically significant. * P <0.05, ** P<0.01 *** P< 0.001, **** P<0.0001.*

5.5 Discussion

Following the observations in Chapter 4 of increased NETosis, and thrombocytopenia during ECMO, I hypothesised that neutrophil-platelet interactions and their crosstalk could be driving enhanced activation of both cell populations and subsequent NETosis and thrombocytopenia. I therefore aimed to investigated NPA as well as MPA in this patient population.

I firstly developed a method for measuring LPA and phenotyping neutrophils and monocytes using whole blood flow cytometry. I was able to adapt protocols used by others [72, 119, 319] for measuring LPA, and take advantage of the advantages of spectral flow cytometry by creating a complex panel to also measure leucocyte subsets. Having developed a protocol, I needed to validate its use in patient samples and determine the best anticoagulant to use to measure both LPA and leucocyte phenotypes, that was both practical and replicable. Through this process I also found that LPA formation can be reversed by strong calcium chelation. With the validated and optimised protocol, I was able to measure LPA and leucocyte phenotypes in patient samples.

5.5.1 Impact of calcium chelation on LPA measurement

Being able to investigate platelet function and aggregation ex-vivo is important to understand platelet biology and their role in haemostasis and pathological conditions. But the question regarding which is the optimum anticoagulant for preserving platelet function/dynamics while avoiding spontaneous activation/inactivation remains. In the case of LPA formation, it has previously been reported that measured MPA were greatest in heparin, PPACK (a DTI), citrate then EDTA [320], which my findings support with highest levels of both NPA and MPA in heparin and citrate, followed by ACD, and EDTA anticoagulated blood (Section 5.4.3).

Blood was collected in three different calcium chelating anticoagulants (citrate, ACD and EDTA), enabling us to be able to better explore the effects of different strengths of calcium chelation on LPA measurements. In addition to the coagulation cascade, platelet activation and many cellular functions are calcium dependent. The choice of which anticoagulant to use for clinical sampling depends on the cell and type of assay that needs to be run. In many assays, limiting cell or platelet activation is desirable. EDTA has traditionally been used for phenotyping leucocytes as it does not affect the leucocyte cell surface markers [72, 321], but is a very strong calcium chelator, with very low numbers of LPA measured and therefore is not suitable for LPA measurement or platelet aggregation studies [119, 320]. Furthermore, EDTA anticoagulated blood can give falsely low platelet counts due to a platelet clumping related phenomenon called pseudothrombocytopenia [307]. Most haematology labs use EDTA blood tubes for the full blood count which includes the platelet count. In pseudothrombocytopenia, some patients have specific antiplatelet antibodies against platelet membrane glycoproteins that are activated by exposure to anticoagulants such as EDTA which leads to clumping of platelets [308]. Conversely, in some patients, EDTA can cause antibodies against GPIIb/IIIa resulting in NPA and MPA formation via FCɣRIII [322] lowering the measured platelet count. To overcome this a citrated sample is usually requested as citrate calcium chelation is not strong enough to alter GPIIb/IIIa [308].

Trisodium citrate 3.2% vacutainers are the most commonly used anticoagulant for clinical coagulation tests and platelet function testing including thromboelastography [323, 324], as well as the alternative anticoagulant when pseudothrombocytopenia occurs with EDTA, and in my data gave comparable LPA measurements as heparin blood. ACD is one of the most commonly used anticoagulants in extracorporeal therapies such as plasmapheresis and has been used for NPA measurement in some studies [314]. ACD-A tubes contain less much less trisodium citrate compared to citrate tubes (3.3mg/ml vs 32mg/ml) but also contain citric acid

and dextrose which lowers the pH considerably to 4.9 (compared to 7.8 for citrate). The difference in pH reduces platelet aggregation, and LPA formation in ACD compared to citrate anticoagulation [325] which my data confirms. Schmuckenschlager et al also investigated the effect of platelet count, temperature and pH on platelet activity and leucocyte-platelet interactions. They found that thrombocytopenia and acidosis impair platelet activation and degranulation, and reduced MPA and NPA formation in vitro. Furthermore, although there were fewer LPA formed in thrombocytopenic conditions, this did not affect CD11b activation or CD62L shedding indicating platelet-mediated leucocyte activation is independent of the platelet count [277]. My results support existing literature that if a calcium chelator is to be used for platelet aggregation work including LPA quantification, citrate would be the best option.

5.5.2 Impact of other anticoagulants on LPA measurement

Given the problems with calcium chelation and therefore accurate measurement of platelet function, many groups are investigating the efficacy of other anticoagulants. Heparin is used clinically to anticoagulate patients, such as those on ECMO, but heparinised blood tubes are not often used for platelet function studies. Heparin activates antithrombin, which inhibits thrombin and factor X limiting coagulation, however there is some literature that reports heparin increases MPA formation compared to LMWH or Lepirudin, and can also lead platelets to spontaneously aggregate, therefore making it a difficult anticoagulant to work with in vitro [326-328]. More recent evidence found the responses of platelets to agonists from heparin anticoagulated blood were preserved after 24 hours of storage, whereas the responses of platelets stored in citrate were diminished [326]. I found heparin blood gave comparable LPA measurements to citrate blood. Given most ECMO patients are exposed to heparin via heparin infusions, and the mechanisms of LPA formation appear to be calcium dependent, heparin was chosen as the most appropriate anticoagulant for measuring LPA in this ECMO patient cohort to avoid discrepancies associated with calcium chelation. All samples were processed the same way and were therefore comparable within this study.

DTI such as PPACK have been reported to be the best anticoagulant for measuring LPA and for platelet function studies as they provide reliable anticoagulation without cation chelation and should not cause platelet activation [320]. In previous work, the levels of MPA in healthy volunteers measured in DTI such as PPACK and Lepirudin were similar to those in heparin [320, 327]; and in patients who were scheduled for percutaneous coronary intervention, those who were loaded with the DTI bivalirudin, had no change in their measured MPA compared

to those who were loaded with unfractionated heparin [327]. Hirudin is a leach derived DTI and is the anticoagulant of choice for clinical platelet function assays such as Multiplate aggregometry. I was able to measure LPA in hirudin anticoagulated blood but found much higher levels of NPA and MPA in compared to heparin and EDTA blood, as well as increased neutrophil activation markers (Figure 5.5). This contradicts what is reported in the literature regarding the similar levels of LPA measured in DTIs and heparin blood. It would be useful to compare different DTI, as I have done with the calcium chelators, to truly assess which yields better LPA counts without affecting leucocyte activation. It is difficult to know whether the increased neutrophil activation measured is artefact or the true baseline function, which is inhibited by other anticoagulants. Other groups are using argatroban for neutrophil phenotyping work [329] as their preliminary work demonstrated increased priming of neutrophil phagocytosis compared to citrate, heparin and EDTA anticoagulants [330]. Further work to understand the effects of anticoagulants on leucocyte activation is required.

Argatroban is a synthetic DTI often used for anticoagulation in patients who have developed HIT, as is bivalirudin. As argatroban and bivalirudin are more clinically available compared to hirudin, these may be more appropriate anticoagulants to use for LPA measurement to avoid the unwanted effects of calcium chelation or heparin interaction with the coagulation cascade, and potential for leucocyte activation. Since hirudin tubes were not collected for all patients and it affected the neutrophil activation measurements, hirudin was not used for ongoing sample collection for LPA quantification. The most crucial aspect of measuring LPA is that the same protocol is followed for all samples to ensure comparability.

5.5.3 LPA formation is calcium dependent and is reversible.

Platelet activation is a dynamic process. EDTA is not used for in vitro platelet work as it is a strong calcium chelator and addition of EDTA to PRP for only a few minutes causes platelets to irreversibly lose their ability to aggregate to each other and respond to agonists [331]. It is known that EDTA reduces the ability of leucocytes to bind to platelets [332] but addition of a cell impermeable calcium chelator, ethylene glycol-bis(β-aminoethyl ether)-N,N,N′,N′-tetraacetic acid (EGTA), also known as egtazic acid, to cold stored platelets, can reversibly inhibit platelet activation and formation of platelet aggregates, with no effect on platelet function when transfused [333]. Many platelet isolation protocols require blood to be taken using ACD or citrate anticoagulated tubes, use of calcium free wash buffers and solutions to inhibit platelet activation and aggregation in vitro, with subsequent replacement of calcium prior to stimulation confirming platelet aggregation is reversible [334-337].

As it is well known that platelet activity and aggregation are calcium dependent and its inhibition is reversible, it therefore makes sense that platelet aggregation to leucocytes is also calcium dependent and reversible, but there is little work into the effect of calcium on leucocyte-platelet aggregation specifically. Most leucocyte phenotyping work is done with EDTA anticoagulated blood to reduce further activation *ex vivo* [72, 74, 321], but this is not the best anticoagulant for measuring LPA. In whole blood in vitro stimulation (Figure 5.2), LPA did not form in EDTA anticoagulated blood compared to heparin anticoagulated blood even with potent stimulation from PMA, suggesting LPA formation is also calcium dependent and can be inhibited by strong calcium chelation. I demonstrated that the degree of calcium chelation can affect LPA measurement ex vivo, with EDTA, the strongest calcium chelator, having the lowest levels of measured LPA compared to ACD and citrate.

To determine whether the LPA formation is reversible as with platelet aggregation, EDTA was added to heparin blood and LPA quantified. The addition of a low concentration (1.25mM) EDTA to heparin blood resulted in significantly lower levels of NPA and MPA measured as well as reduced expression of CD41 on the cell surface, comparable to levels in EDTA only samples (Figure 5.3). This suggests the LPA measured in heparin blood are a true representation of levels in the patients, but also the formation of LPA is reversible by calcium chelation and could be reversed to different degrees by the strength of calcium chelation. This finding that LPA formation is reversible suggests targeted therapies may be developed to reduce LPA formation in pathological circumstances.

Whilst EDTA did inhibit and reverse MPA formation, MPA seemed less susceptible to the effects of calcium chelation with ACD and citrate (Figure 5.4). It is known that monocytes have increased affinity to platelets than neutrophils and it has been suggested this is mediated by P-selectin [121]. However, there may be alternative receptor-ligand binding that leads to increased strength of MPA [338, 339].

The finding that EDTA can reverse LPA formation and platelet aggregation, also raises a question of whether EDTA is the most appropriate anticoagulant for measuring platelet count in clinical samples. Pseudothrombocytopenia due to EDTA has already been discussed in 5.5.1. If LPA form readily in critically unwell patients with sepsis or who are on ECMO, then the number of circulating platelets is lower than normal as they are attached to the

leucocytes commonly neutrophils [307-309] leading to one form of pseudothrombocytopenia. However, the opposing effect may be true, in patients who have LPA circulating, the platelet count measured in EDTA blood may be falsely high as the LPA dissociate irreversibly, releasing the platelets back into solution. Here I have only examined the effect of EDTA and heparin on LPA formation in vitro. It would be interesting to examine different calcium chelators and their effect on LPA formation and platelet counts.

5.5.4 LPA are present in ECMO patients

We know that monocytes have highest affinity for platelets followed by neutrophils and then lymphocytes [120, 121, 337]. In patient samples, the proportions of MPA were much higher than proportions of NPA at any given time point, as expected, with corresponding expression of CD41. There was a decrease in NPA levels from ECMO initiation to 1 week on ECMO which may be expected as the patient improves clinically and has less neutrophil and platelet activation due to reduced inflammation. However, this was not reflected in the clinically measured neutrophil count, platelet count or CRP over time. There were no differences in MPA levels or monocyte phenotypes over the ECMO run. Although there were some correlations between LPA and the associated blood results, these were not strong.

LPA are increased in conditions where there is inflammation, shear stress [340] and vascular injury [341]. Since ECMO is associated with increased leucocyte and platelet activation, it has been suggested that LPA are increased in ECMO [276] but until recently there has been little data relating to LPA in ECMO. Paschke and colleagues measured LPA in 10 VV ECMO patients and 11 HV, comparing levels before ECMO, 2 and 6 hours after ECMO initiation and then every few days whilst on ECMO. They found patients had higher proportions of NPA and MPA at baseline (before ECMO initiation) compared to HV, and levels decreased within 2 hours of ECMO initiation and remained at those levels up to 10 days on ECMO [292]. Whilst I was not able to measure LPA before ECMO initiation, the lack of change in NPA and MPA proportions during ECMO correspond with the results found by Paschke et al. Siegel et al. also measured LPA levels in 30 patients on VA and VV ECMO and also found no difference in LPA levels compared to HV and during ECMO (day 1, day 3 and after ECMO decannulation) [291]. They also stimulated whole blood with ADP and PMA, and found LPA formation in response to stimulation was reduced in ECMO patients compared to healthy controls [291].

The investigation of leucocyte-platelet interactions compliments the cell-based coagulation model which considers the interaction of immune cells with the coagulation cascade particularly in the context of ECMO where patients have an activated immune system, endothelial injury and activated coagulation system from ECMO initiation.

5.5.5 Neutrophil-platelet aggregates, associated phenotypes, NETosis and thrombocytopenia

Neutrophil phenotypes

There was increased neutrophil activation in ECMO patients compared to HV as shown by increased CD66b expression, increased CD62L shedding, and increased proportion of immature granulocytes (Figure 5.6). These trends remain unchanged during the ECMO run for up to 2 weeks. There are only a few studies that look at leucocyte phenotypes in patients on extracorporeal circuits. In patients with cardiogenic shock requiring VA ECMO, there are increased circulating immature neutrophils as well as lymphocyte dysfunction compared to patients who did not require ECMO [342] however, there are opposing results in other extracorporeal circuits. One study found in patients after cardiac surgery with CPB, there are predominantly mature neutrophils with no differences in neutrophil progenitors [343], however this may be because patients are usually well prior to elective cardiac surgery, with low neutrophil turnover and therefore should have mostly mature granulocytes. Results from in vitro models vary. In one in vitro model of ECMO using whole blood, CD62L was reduced, and CD18 was increased in neutrophils and monocytes after 2-4 hours of ECMO with ongoing CD62L shedding up to 8 hours of ECMO demonstrating increased neutrophil activation [344]. In a porcine model of neonatal ECMO, expression of neutrophil activation markers CD18, CD35 and CD11b was increased after 2 hours but the expression of CD62L was upregulated [256]. In another model of ECMO comparing two different ECMO flow rates (4L/min vs 1.5L/min) on leucocyte activation, there was no difference in the measured cell surface markers with different flows [345]. Overall, these studies support my findings that there is increased neutrophil activation on ECMO, and this is true in patients on ECMO and CPB with in vitro studies demonstrating this is an effect of ECMO rather than the immune activation associated with ARDS.

I also compared neutrophil activation markers between neutrophils that had formed NPA (i.e. neutrophils that were $CD41^{+}$) with neutrophils that had not formed NPA ($CD41^{-}$) (Figure 5.8). Neutrophils that had formed NPA had increased expression of CD66b, CD10 and CD16 compared to those that had not formed NPA ($CD41^{-}$). This suggests that NPA are more

likely to form with activated mature granulocytes, which is also confirmed when mature granulocytes were gated for NPA (Figure 5.7).. Both NPA and immature granulocytes are markers of inflammation and disease and presence of circulating immature granulocytes indicates increased neutrophil turnover and granulopoiesis [70]. Moreover, the reduced NPA formation with immature granulocytes may be due to the lack of surface expression of CD11b on immature granulocytes (Fig 1.10) [70] as CD11b (Mac-1) is one of the pathways of interaction between neutrophils and platelets (Figure 5.1). However, more work needs to be done to investigate the interactions between different neutrophil phenotypes and platelets as it is likely multifactorial.

Relationship to NETosis and thrombocytopenia

Interaction between platelets and neutrophils has been reported to induce neutrophil activation and subsequent NETosis [83, 297, 298]. The increased neutrophil expression of CD66b and proportion of NPA at initiation of ECMO suggests increased neutrophil activity and corresponds with the increase in NETosis markers CitH3, and NuQH3.1 seen at this time point (Chapter 4). This could be due to the increased neutrophil-platelet interactions of NPA formation leading to increased NETosis. The lack of correlation between NPA and cell-associated NETs contradicts this. However platelet mediated neutrophil activation is thought to be via NADPH oxidase independent pathways, and initiate vital NETosis, where the neutrophil remains intact after releasing soluble NET components [66-68], such as via TLR4 pathway [83] which could explain these findings. Furthermore, NPA only measure direct platelet-neutrophil interactions and not the effects of indirect interactions of platelet-derived soluble mediators such as PF4, P-selectin, and extracellular vesicles on neutrophil activation [242, 297, 346]. The trend for decreasing NPA levels, decreasing neutrophil CD64 and increasing neutrophil CD16 over the ECMO run corresponds with decreasing plasma MPO, NE and cfDNA and CitH3 shown in section 4.4.4 suggesting less neutrophil activation over the ECMO run.

Platelets can be captured within NETs leading to thrombocytopenia [82, 86, 347]. Indeed, Haus et al found patients with increased NET release before ECMO had a more significant drop in platelet count after ECMO initiation [225]. NPA formation can lead to neutrophil phagocytosis of platelets that have bound to the neutrophil cell surface [348] or increased splenic clearance of neutrophils with bound platelets [349]. Various groups have suggested thrombocytopenia could be the result of platelet consumption due to LPA formation [350, 351]. The readiness of monocytes to form heterotypic aggregates with platelets can contribute to this. Neutrophils

are much larger in size and therefore it is reasonable to hypothesise they have more platelets attached to their cell surface. However, this this does not seem to be the case; the neutrophil/platelet and monocyte/platelet ratios are largely 1:1 or 1:2 for both types of aggregates [337]. Although there is no work into the association of NPA and thrombocytopenia, neutrophils make up 50-70% of circulating leucocytes and numbers often increase during sepsis [352], compared to monocytes which make up only 5% of circulating leucocytes, with further monocytopenia often seen in severe sepsis [353, 354]. The difference and changes in leucocyte ratios and development of LPA could account for the thrombocytopenia in sepsis.

5.5.6 Monocyte phenotypes in ECMO

Non-classic monocytes are pro-inflammatory and are associated with increased levels of sepsis [72], but there was no change in proportions of monocyte subtypes over the ECMO run. I found classic monocytes and intermediate monocytes were more likely to form MPA than non-classic monocytes in contrast to other studies [338]. The differences in my results compared to other studies may be due to the relative monocytopenia seen in ECMO patients (Figure 5.10) which limits conclusions regarding MPA subtypes.

Whilst there were no differences in the proportion of monocyte subtypes or CD11b expression, the expression of HLA-DR on monocytes was lower in ECMO patients across the ECMO run compared to HV. This persisted throughout the whole ECMO run including after ECMO decannulation. This corresponds to many studies that also show monocyte HLA-DR is downregulated after blood exposure to extracorporeal circuits. Chenouard and Rudnesky found in patients undergoing cardiac surgery, monocyte CD11b is upregulated but HLA-DR is downregulated after CPB compared to the pre-operative state [355, 356] and in a neonatal study including patients on VA and VV ECMO, there was also reduction in monocyte HLA-DR expression after ECMO initiation compared to controls, and levels remained low during the ECMO run similar to my data [357]. However, in an adult VA ECMO cohort there was no difference in monocyte HLA-DR expression [342]. ECMO is used when patients are already in a highly inflamed state due to sepsis or shock, and ECMO can elicit a SIRS response leading to monocyte dysregulation and reduced HLA-DR expression [80, 81]. The mechanisms of this immunoparesis in ECMO is yet to be determined. Whilst it may be related to the underlying sepsis in VV ECMO patients, the observation that it is also seen after CPB suggests that there is interaction between the circuit and the immune system [159].

The effect of ECMO on leucocyte phenotypes cannot be fully extrapolated in patients on VV ECMO for ARDS due to the compounding effect of leucocyte activation from ARDS, a very heterogenous condition. A comparison of patients with a more homogenous population such as cardiogenic shock on VA ECMO to those without ECMO may be better, however to date there are limited studies in this area.

5.6 Conclusions

The relationship between neutrophils, monocytes and platelets is important when discussing immunothrombosis in patients who require ECMO for SARF. LPA are a new and exciting research focus and present a potential therapeutic target to reduce immunothrombotic complications in patients with SARF, and those who require ECMO. In this chapter I have described the challenges with measuring LPA and the effects of different anticoagulants on measurement and working with LPA in vitro, but that LPA are present in patients on ECMO, are calcium dependent, and their formation is reversible.

LPA formation in this cohort may contribute to the increased immunothrombosis via NETosis or to the thrombocytopenia seen during the course of ECMO or can contribute to ongoing lung injury despite the initiation of UPV. The increase in soluble NETosis markers seen after ECMO initiation corresponds with the high levels of NPA at ECMO initiation providing evidence that this could be the pathway for vital NETosis in this cohort of patients. I have also shown during ECMO there is increased neutrophil activation with more activated neutrophils more likely to form NPA. NPA formation also appears to be calcium dependent and therefore likely dependent on platelet activation. In ECMO this is likely due to exposure of blood to the shear forces from ECMO pump and MO and contact activation from the ECMO circuit. Minimising platelet activation in ECMO by systemic anticoagulation is already part of routine management however minimising LPA formation via GPIIb/IIIa inhibition or the P-selectin pathway inhibition could also reduce thrombosis.

The interactions of leucocytes and platelets in circulation, within the alveolar space and with exogenous materials such as an ECMO circuit are complex. Understanding the role of ECMO in immune activation, inflammation and thrombosis is vital to understand the relevance of LPA and their downstream effects and can help in developing strategies to modulate these interactions in this complex cohort of patients. More in vitro work needs to be

done to investigate leucocyte-platelet interactions in extracorporeal circuits and the effect they have on thrombosis.

Chapter 6: Evaluation of leucocyte platelet aggregates in an in vitro model of flow

Abstract

Using the ibidi microfluidics system as a model for blood flow through an ECMO circuit, I investigated LPA formation in whole blood under flow conditions. Using platelet and leucocyte agonists (TRAP-6 and LPS), a P-selectin pathway inhibitor (KF38789) and GPIIb/IIIa inhibitor (Eptifibatide) I aimed to investigate the pathways involved in LPA formation.

The kinetics of LPA formation differed between neutrophils and monocytes. Monocytes readily formed aggregates with platelets compared to neutrophils where formation was more gradual over time. Stimulation with TRAP-6, increased NPA formation more than leucocyte stimulation and the subsequent NPA formation led to platelet-mediated neutrophil activation with increased CD66b and CD62L shedding. Inhibition of the P-selectin pathway did not have an effect on LPA formation. However, inhibiting the GPIIb/IIIa pathway using eptifibatide reduced baseline and TRAP-6 stimulated NPA formation but did not alter MPA formation.

In summary, the ibidi microfluidics chamber was used successfully as a model for investigating leucocyte-platelet interactions in vitro using whole blood. Reversing or inhibiting LPA formation could be a useful therapeutic target for example with GPIIb/IIIa inhibitors. This is the first demonstration of its role in LPA formation under ex vivo flow conditions.

6.1 Introduction

There is complex cross talk between leucocytes and platelets leading to further activation of each cell type, enhancing local inflammation and thrombogenesis. LPA are formed by direct cell-cell interactions between P-selectin and GPIIb/IIIa on platelets binding to PSGL-1 and Mac-1 receptors on leucocytes.

Previous work so far has been in whole blood stimulated in a rotator which creates turbulent flow or in static conditions. I aimed to investigate leucocyte-platelet interactions under more physiological flow conditions in vitro by perfusing whole blood through a microfluidics chamber, as well as investigating the effects of leucocyte and platelet stimulation on LPA formation. The ibidi microfluidics pump system can produce unidirectional laminar flow within a microchannel slide allowing different flow rates and shear rates to be applied to adhered cells within the slide (Section 2.3.5). Blood flow through an ECMO circuit can range from 3L/min up to 7L/minute for an adult circuit. The flow rate measured is usually measured using the flow sensor on the afferent limb from the ECMO pump and MO. The large surface area of the MO disperses blood across the membrane to improve gas exchange, however the exact blood flow rate at the level of the membrane is not known. Blood flow rate depends on the pump speed and high pump speeds are known to increase shear and platelet activation [194, 358].

In ECMO patients, there is increased leucocyte and platelet activation from the underlying insult causing the lung injury, but also ECMO leads to activation of both leucocytes and platelets [124, 159]. Since the shear of the ECMO pump leads to increased platelet activation [194], and LPA formation is affected by different anticoagulants, it is logical that LPA formation is platelet dependent. To investigate what drives leucocyte-platelet interactions and LPA formation, platelet- and leucocyte-specific agonists were used to stimulate each cell type separately. In addition, a GPIIb/IIIa inhibitor and P-selectin pathway inhibitor were used to determine which of the two pathways were important in LPA formation.

6.2 Aims and hypothesis

The aim of this chapter was to investigate LPA formation and kinetics in whole blood in vitro using the ibidi microfluidics system to simulate physiological flow conditions within the membrane oxygenator.

I hypothesised that:

1) LPA formation is platelet dependent and increases with platelet stimulation compared to leucocyte stimulation.
2) Flow rate may be an important determinant for LPA formation
3) LPA formation in vitro can be inhibited by blocking the P-selectin and GPIIb/IIIa pathways.

6.3 Methods

6.3.1 Platelet rich plasma stimulation and platelet activity quantification

Whole blood from HV was centrifuged at 400 x *g* for 10 minutes at 20°C to obtain platelet rich plasma (PRP) from ACD and heparin blood. PRP (0.5 ml) was stimulated in 1.5ml Eppendorfs with agonists for 1 hour in a rotator, at 37°C. Unstimulated PRP left static at room temperature, on ice, and in the rotator served as controls. After stimulation, PRP was stained with antibody cocktail as described in section 2.4.2. Samples were analysed using flow cytometry to quantify platelets and platelet activity.

6.3.2 Whole blood stimulation in ibidi microfluidics chamber

The ibidi microfluidics set up and protocols are described in detail in section 2.3.5 and 2.3.6. In brief, heparinised whole blood was perfused through 1.6mm ID 15cm perfusion sets, and 0.4mm microchannel slides at 37°C at different flow rates which equate to different shear stress (Table 6.1):

Flow rate	Shear stress within a 0.4mm microchannel slide
2.5 ml/min	10 dyn/cm^2
5 ml/min	20 dyn/cm^2
10ml/min	40 dyn/cm^2

Table 6.1 Flow rates and estimated shear stress generated within a 0.4mm microchannel slide.

These are the flow rates and shear rates that can be generated on adhered cells within a 0.4mm microchannel slide when using whole blood at 37°C (with an assumed viscosity 0.03 dyn·s/cm^2) and 1.6mm ID, 15cm perfusion sets.

For reference, shear stress in the aorta is around 10-12 dyn/cm^2, in large veins and pulmonary artery 5 dyn/cm^2 and small veins 1-10 dyn/cm^2 [359]. It should be noted that the shear stress within the microchannel slide applies to cells (e.g. endothelial cells) that have

been seeded and adhered to the slide. In this whole blood model, there are no seeded cells and therefore flow rates rather than shear stress will be discussed.

Agonists (LPS 100ng/ml, TRAP-6 10uM) were added to whole blood at room temperature and loaded straight into the ibidi reservoirs prior to perfusion.

For inhibition experiments eptifibatide (1µg/ml) and KF38789 (20µM) were added to whole blood at room temperature and incubated for 10 minutes prior to adding stimulants and perfusing in the microfluidics unit.

Samples (50ul) were taken from the sampling port using an 18G filter needle and 1ml syringe at set time points according to the experiment protocol: 0mins (baseline prior to perfusion), 5mins, 10mins, 15mins, 30mins, 45mins, and 60mins. Samples that had inhibitor added, had samples taken before the inhibitor was added and the time point labelled as "-10mins".

6.3.3 Flow cytometry for leucocyte phenotyping and leucocyte-platelet aggregates

Due to the frequency of sampling for the ibidi perfusion experiments, a single panel for both neutrophils and monocytes was created in contrast to the two separate panels used in patient samples in Chapter 5. As the project focuses on the relationship between neutrophils and platelets, more neutrophil markers were included for the in vitro work.

Fluorophore-conjugated neutrophil phenotyping and activation antibody markers included CD45, CD66b, and CD62L. Monocyte markers included CD45, and CD14. Platelet markers included CD41 and CD62P, and FITC-conjugated bovine lactadherin (BLAC) to identify bound platelets and platelet activation (Table 6.2).

Fluorophore	Leucocyte-Platelet aggregates
BV421	CD45
BV605	CD62P
FITC	BLAC
PE	CD41
PE-Cy5	CD11b
PE-Cy7	CD66b
AF647	CD62L
APC-Cy7	CD14

Table 6.2 Fluorophore conjugated antibodies for quantification of leucocyte-platelet aggregates and phenotyping neutrophils and monocytes for in vitro experiments.

All antibodies were diluted to a final concentration of 1:100.

In brief, whole blood (20µl) was incubated with LPA antibody cocktail(s) at room temperature for 15 minutes, 750µl BD FACS lysis buffer was added for 10 minutes to lyse erythrocytes and fix samples. Samples were washed with 2ml PBS and centrifuged at 300xg for 7 minutes and resuspended in 500µl of PBS. Samples were run on the flow cytometer to acquire 5,000 $CD14^{+}$, $CD16^{-}$ monocytes depending on the protocol.

6.4 Results

6.4.1 TRAP-6 is a potent platelet agonist, whereas LPS did not induce platelet activation in platelet rich plasma

To determine the best platelet agonist and anticoagulant to use within the ibidi experiments heparin and ACD PRP was stimulated in Eppendorfs with different agonists and at different temperatures. Calcium ionophore (A23187) was used as the positive control as it is known to stimulate platelets and leucocytes, LPS 100ng/ml was tested as a leucocyte agonist, TRAP-6 and thrombin were tested as platelet agonists. TRAP-6 was chosen as it is one of the agonists used in the Multiplate aggregometry as it specifically activates the thrombin receptor, and thrombin tested as a more physiological agonist. Platelet counts and platelet activation after stimulation was quantified. Platelet activation was quantified by measuring the proportion of CD62P positive platelets.

The platelet counts as measured by flow cytometry in PRP left static on ice was lower in heparin PRP compared to ACD PRP (115.2 vs 290.3 $x10^{6}$/ml; P=0.0011), with a corresponding increase in platelet activation in heparin as measured by platelet CD62P expression (80.2 vs 37.9%; P=0.0114) (Figure 6.1). The difference between ACD and heparin suggests that there may be spontaneous platelet activation in heparin PRP, but calcium chelation inhibits this. These changes were not observed with platelets kept at room temperature suggesting cooling induced lower counts by aggregation in heparin blood and a higher total P-selectin signal from such aggregates as a plausible explanation. Unstimulated PRP in the rotator at 37°C was not different to PRP left static at room temperature in both platelets count and CD62P signal.

In contrast, the platelet counts in PRP stimulated with thrombin were lower in ACD compared to heparin PRP (31.9 vs 188.6 $x10^{6}$/ml; p=0.0149) with some increase in CD62P expression (65.1 vs 30.6%; P=0.0806). In ACD PRP stimulated with thrombin there was formation of large, coagulated material within the Eppendorfs that were visible

macroscopically, which were seen on repeated experiments. These are likely platelet clumps due to platelet activation.

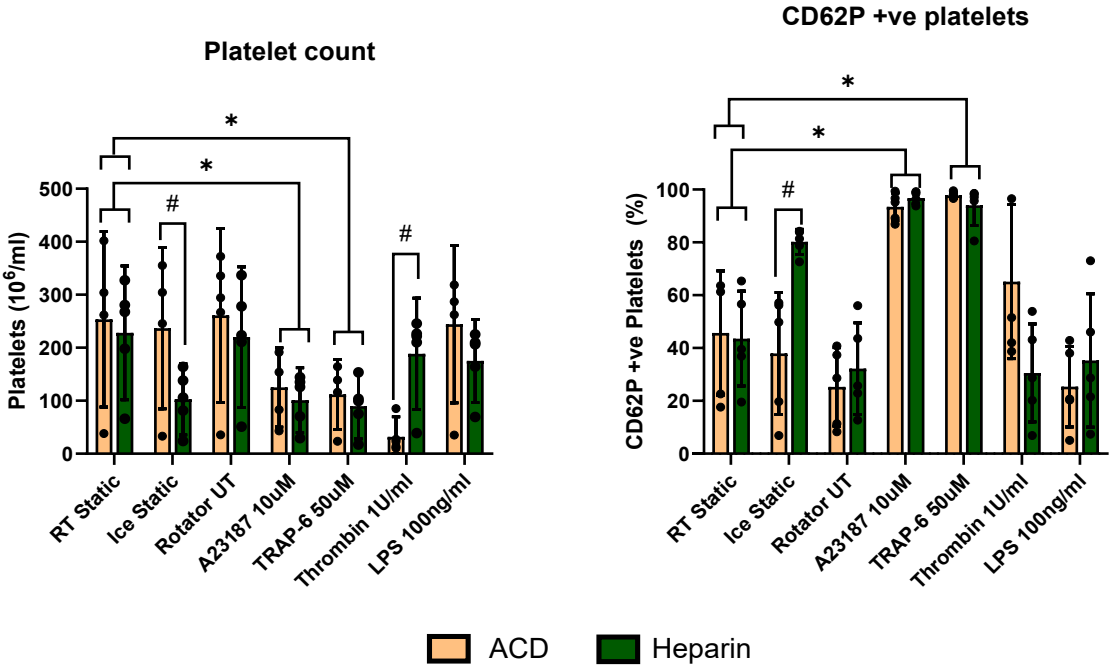


Figure 6.1 Platelet count and platelet CD62P expression in response to different agonists.

*Heparin and ACD PRP (N=5) was left static at room temperature (RT) and on ice and stimulated in the rotator without stimulation (UT), with A23187 10μM, TRAP-6 50μM, thrombin 1U/ml or LPS 100ng/ml for 1 hour. Using flow cytometry, the number of platelets, and platelet CD62P expression was quantified. N=5. Data presented as Mean ± SD. 2-way ANOVA was used to compare between stimulation and anticoagulant groups (differences between stimulation denoted by *, differences between anticoagulants denoted by #). P<0.05 considered statistically significant. p<0.05 **

Calcium ionophore, A23187; Lipopolysaccharide, LPS; P-selectin, CD62P; Room temperature, RT; Thrombin receptor activating peptide-6, TRAP-6; Untreated, UT.

With regards to stimulation, the number of platelets decreased with increased stimulation which likely indicates platelet aggregation. Calcium ionophore (A23187 10μM), and TRAP-6 (50μM) led to the highest level of platelet activation as measured by CD62P expression (96.8% and 94% respectively in heparin PRP). Stimulation with LPS 100ng/ml did not significantly affect platelet numbers or platelet CD62P expression when compared to platelets left static and in the rotator at room temperature.

Calcium ionophore was the positive control for this set of experiments and was not used as a stimulant for in vitro LPA experiments as it is known to stimulate leucocytes as well as

platelets. LPS is a well-known leucocyte agonist, and this is demonstrated in the whole blood model in section 5.4.1 with activation of both neutrophils and monocytes. LPS did not induce platelet activation in PRP, therefore was used as the leucocyte agonist in ongoing experiments. TRAP-6 has not been reported to directly activate neutrophils and was used as the platelet agonist in further experiments, but at a much lower dose of 10uM rather than the commonly used doses of 25-50uM for platelet investigations. This was chosen to avoid excessive platelet activation. Thrombin was not used due to the immediate clumping effect. Heparin blood was used for in vitro experiments to avoid the calcium chelating effects of ACD, which is demonstrated again in this set of experiments, and mimics the heparinised blood of ECMO patients.

6.4.2 Laminar blood flow appears to generate less LPA than turbulent blood flow

The ibidi microfluidics chamber can be used to generate unidirectional laminar flow within the microchannel slide chamber, similar to physiological blood flow within most small blood vessels and within the venous system. Pulsatile laminar flow can also be generated using this system to simulate blood flow in large arteries, but since I am investigating ECMO, where blood flow through the ECMO tubing and return to the inferior vena cava is non-pulsatile, unidirectional laminar flow was chosen for the ibidi microfluidics experiments.

Prior to using the ibidi microfluidics chamber, I compared NPA and MPA proportions within this model to previously used stimulation models at static and rotator conditions. To do this heparinised whole blood was stimulated in Eppendorfs left standing (static), in a rotator to generate turbulent flow/mixing, and in flow conditions (2.5ml/min through 15cm 1.6mm ID tubing, without the ibidi microchannel slide). The microchannel slide was not included as this was pilot data of flow rather than shear stress. Blood samples were taken at 0, 30 and 60 minutes. LPS 100ng/ml was used as the leucocyte agonist and TRAP-6 10μM was used as the platelet agonist.

Regarding NPA formation, in unstimulated whole blood after 30 minutes there was increased NPA formation in the rotator compared to static (93.4% vs 36.5%; P=0.0056), and flow conditions (46.7%; P=0.094). There was further increased NPA formation with LPS and TRAP stimulation in static and flow conditions, but no further increase in rotator since unstimulated NPA was already maximal at 30 minutes. The largest differences in NPA formation were between 0 to 30 minutes (Figure 6.2) with all agonists. There was further

increase in NPA formation in static and rotator conditions between 30 to 60 minutes but not significantly different, and with no differences between different agonists. In general, blood left at static conditions had the lowest proportion of NPA formation compared to rotator and flow conditions suggesting that movement or mixing of platelets and neutrophils increases NPA formation (Figure 6.2).

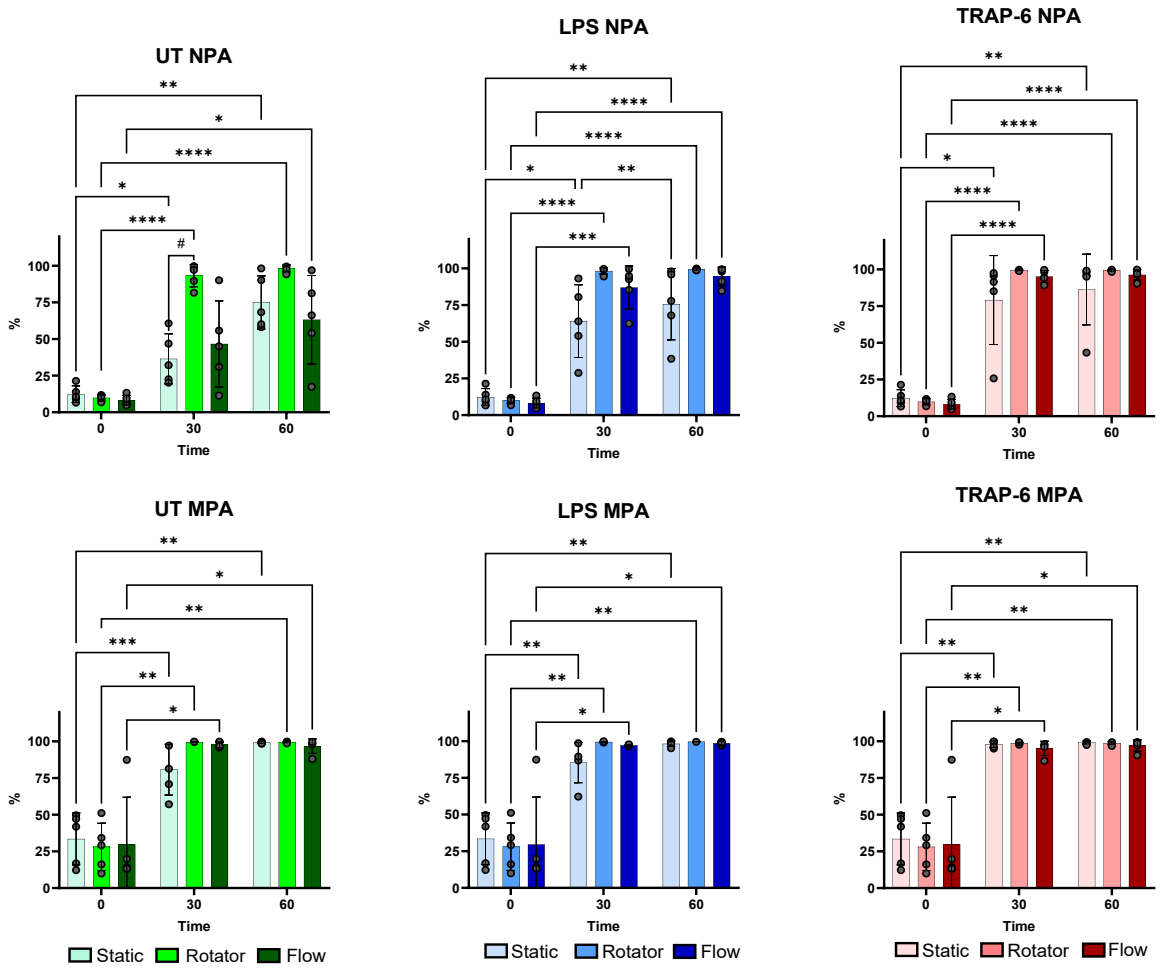


Figure 6.2 Neutrophil and monocyte platelet aggregate formation at static, rotator and flow conditions with no stimulation, LPS and TRAP-6.

*Heparinised whole blood was stimulated in static, rotator, and flow (2.5ml/min through 15cm 1.6mm ID tubing) conditions at 37°C (N=5). Blood samples were taken at 0, 30 and 60 minutes. Data presented as mean ± SD. Two-way ANOVA with Geisser Greenhouse correction and Tukey's multiple comparison test were performed. Comparisons between groups over time denoted by *, and comparisons between flow conditions at the same time points denoted by #. P<0.05 considered statistically significant. P<0.05 *, P<0.01 **, P<0.001 ***, P<0.0001 ****.*

Lipopolysaccharide, LPS, Monocyte-platelet aggregates, MPA; Neutrophil-platelet aggregates, NPA; Thrombin receptor activating peptide-6, TRAP-6, Untreated, UT.

MPA formation increased after stimulation for 30 minutes and was maximal (>99%) in all conditions with no difference between static, rotator and flow conditions, or different agonists. There was no further increase in MPA between 30 and 60 minutes of stimulation.

These results also show that the lower dose of TRAP-6 10μM was adequate stimulation for both NPA and LPA formation as demonstrated by the increase in NPA seen at 30 minutes in the static conditions.

6.4.3 Flow rates did not affect leucocyte-platelet aggregation in vitro

To compare the effect of different flow rates on LPA formation in vitro, the experiments were run at 2.5ml/min, 5ml/min and 10ml/min with unstimulated, LPS and TRAP-6 stimulated whole blood. Proportion of NPA, neutrophil CD41 and CD66b expression, and proportion of MPA, monocyte CD41 and monocyte CD14 expression were quantified.

NPA formation, and neutrophil activation (neutrophil CD66b expression) differed between different stimulants, but there were no differences between different flow rates on NPA formation or neutrophil activation. This was the same for MPA formation, and monocyte activation (as measured by monocyte CD14 expression). Despite no differences in NPA or MPA formation, there appears to be higher neutrophil and monocyte CD41 expression in LPS stimulated blood at perfusion flow rate of 10ml/minute compared to 2.5ml/minute and 5ml/minute (Figure 6.3). Therefore, to minimise any excess platelet activation at higher flow rates, the lower flow rate of 2.5ml/minute was used for ongoing experiments. This lower flow rate also minimises risk of air entrainment into the perfusion set when samples are aspirated from the injection port.

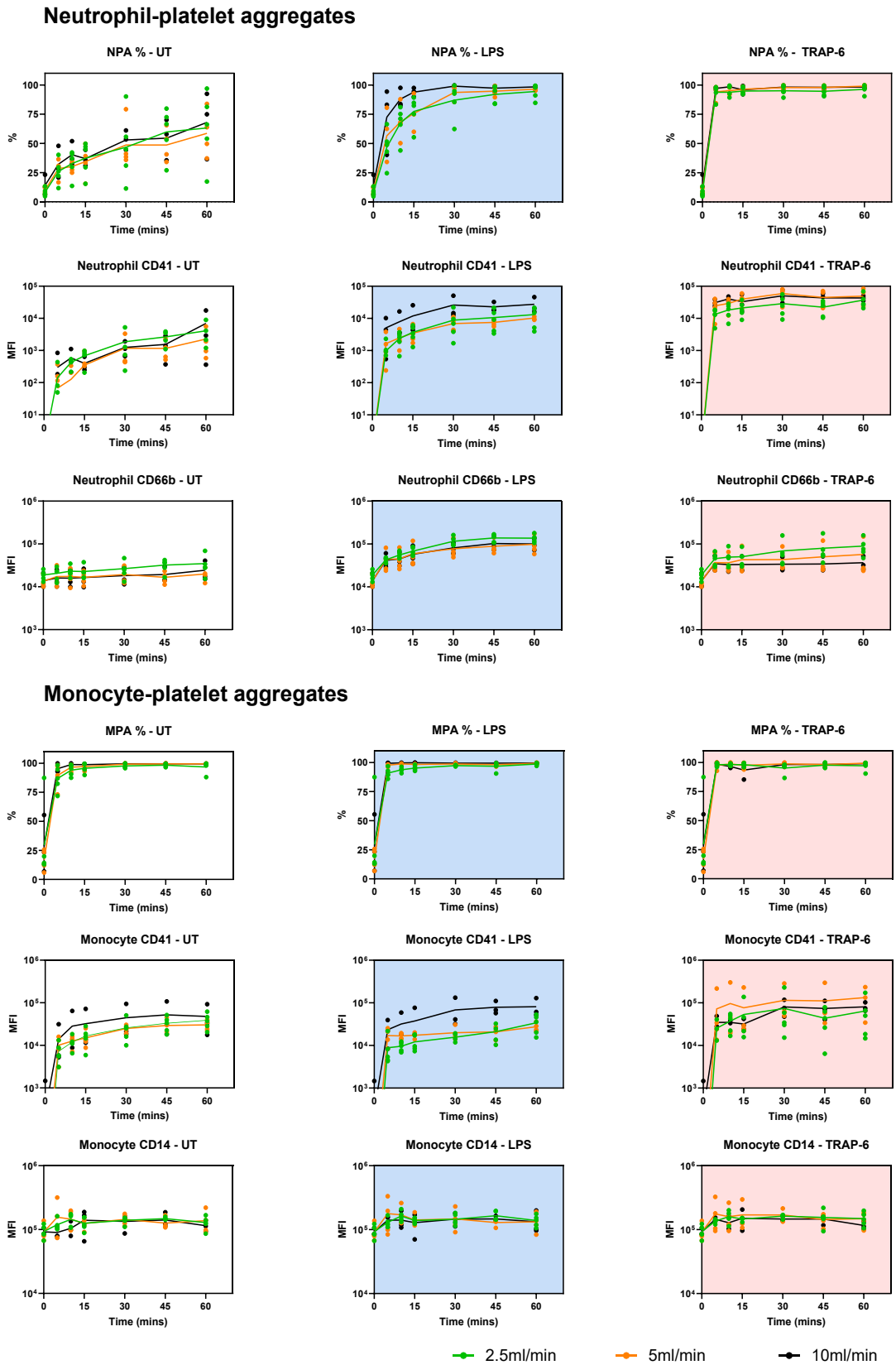


Figure 6.3 Neutrophil and monocyte platelet aggregate formation with no stimulation (UT; white), LPS (blue) and TRAP-6 (red) at different flow rates.

Blood was perfused at flow rates of 2.5ml/min (n=5), 5ml/min (n=4) and 10ml/min(n=3) through 0.4mm μ-slides and 15cm 1.6mm ID tubing at 37°C. Mean lines shown with all replicates. Mixed-effects model with Geisser Greenhouse correction performed. P<0.05 considered statistically significant.

6.4.4 Formation of neutrophil-platelet aggregates is increased with platelet stimulation, compared to leucocyte stimulation

To examine LPA formation under physiologically relevant conditions in vitro, heparinised whole blood was perfused in the ibidi microfluidics system under flow conditions of 2.5ml/min through a 0.4mm microchannel slide and 15cm 1.6mm ID tubing. Blood was perfused without stimulation, with LPS 100ng/ml or TRAP-6 10μM to investigate the effect of leucocyte and platelet activation on LPA formation.

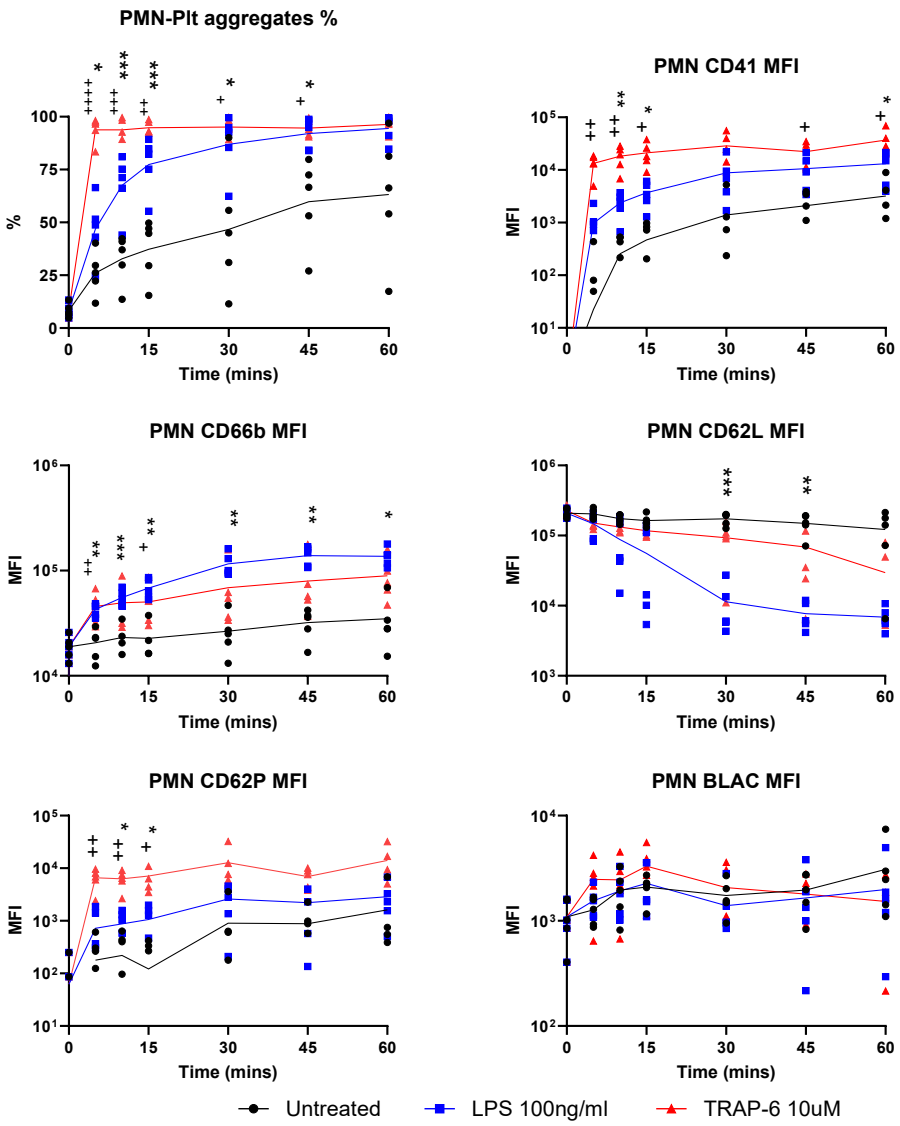
Firstly, there are differences in NPA formation and neutrophil activation with different stimuli. Under flow conditions, without stimulation there was a gradual increase in NPA formation over time (P<0.0001). Without stimulation, the proportion of NPA after 30 minutes and 60 minutes were 46.7 ± 29.4% and 63.2 ± 30.2% respectively, compared to a baseline of 8.2 ± 3.3 %. There was increased NPA formation with leucocyte stimulation using LPS 100ng/ml and further exaggerated with platelet stimulation using TRAP-6 10μM (Figure 6.4). After 30 minutes mean proportions of NPA were 46.7 ± 29.4%, 86.9 ± 14.7% and 95.1 ± 4.01% for unstimulated, LPS and TRAP respectively (two-way ANOVA P=0.0014). After 1 hour, with stimulation the proportions of NPA were near maximal for both LPS (94.5 ± 6.4 %) and TRAP (96.3 ± 3.5 %). In fact, in TRAP-6 stimulated blood the proportion of NPA is already maximal (93.8 ± 6.1%) after only 5 minutes, whereas with LPS stimulation after 5 minutes the NPA proportion was much lower (46.9 ± 15.2%). The degree of NPA formation corresponds with neutrophil CD41 expression e.g. at 30 minutes the CD41 expression was 1,398 ± 2,246, 8,787 ± 7,917 and 28,691 ± 19,113 for unstimulated, LPS and TRAP respectively (two-way ANOVA P=0.0004). There was no difference in neutrophil CD62P expression over time but there are differences in CD62P expression with each stimulant with higher neutrophil CD62P in TRAP-6 stimulated whole blood (P=0.0014) (Figure 6.4).

There was a different pattern with neutrophil activation. LPS 100ng/ml is a more potent neutrophil agonist than TRAP-6 10μM as measured by the higher CD66b expression and increased CD62L shedding over time in the LPS stimulated blood (Figure 6.4). Differences in CD66b expression were highest early in the experiment, for example, after 15 minutes of stimulation, the neutrophil CD66b expression was highest in LPS (64427 [54,441 – 83,690]; P=0.0025), then TRAP-6 (50,998 [31,839 – 68,817]; P=0.0231) when compared to untreated (21,673 [16,311 – 29,617]). Whereas differences in neutrophil CD62L expression were greater later in the experiment with lower CD62L expression after 30 minutes with LPS (6,048 [5,088 – 20,372] vs 192,923 [137,954 – 199,291]; P 0.0005) than with TRAP-6

(96,069 [50,438 – 133,824] vs 192,923 [137,954 – 199,291]; P=0.1046) when compared to unstimulated. These results indicate increased neutrophil activation with LPS stimulation compared to TRAP-6.

Platelets and their expression of activation markers, CD41, CD61 and CD62P were quantified at 0, 30 and 60 minutes in early experiments to determine platelet activation (Figure 6.5). Compared to baseline, there was increase in platelet CD41 (58,500 [49,946 – 64,277] vs 22,816 [18,538 – 33,452] and CD62P expression (21,763 [11,631 – 25,134] vs 866 [351 – 2,216]; P=0.0078) after 30 minutes with TRAP-6 stimulation. There was further increase in CD62P expression after 60 minutes (22,219 [28,896 – 25,703] vs 866 [351 – 2,216]; P=0.0015), indicating increased platelet activation. There was no platelet activation with LPS stimulation.

Taken together, these results suggest that platelet activation may be a more critical early determinant of NPA formation as NPA are increased early with platelet stimulation, compared to neutrophil activation.



Two-way ANOVA	Time	Stimulation
Neutrophil platelet aggregates (%)	**<0.0001**	**0.0014**
Neutrophil CD66b	**0.0022**	**0.0063**
Neutrophil CD62L	**<0.0001**	**0.0007**
Neutrophil CD41	**0.0177**	**0.0004**
Neutrophil CD62P	0.1057	**0.0014**
Neutrophil BLAC (Phosphatidylserine)	0.1525	0.2862

Figure 6.4 Neutrophil platelet aggregates form under flow conditions and increase with leucocyte and platelet stimulation.

*Heparinised whole blood was perfused in the ibidi microfluidics chamber at 2.5ml/min through 1.6mm tubing and 0.4mm μ-slides for 1 hour. Samples were taken at 5, 10, 15, 30, 45 and 60 minutes for flow cytometry. Whole blood was stimulated with LPS 100ng/ml, TRAP-6 10μM, or unstimulated. N=5 for all conditions. Mean lines shown with all replicates. 2-way ANOVA with Geisser-Greenhouse correction and Tukey's multiple-comparisons test was used to compare trend over time and between stimulation. Differences between LPS and unstimulated denoted by *, differences between TRAP-6 and unstimulated denoted by #. P<0.05 considered statistically significant. p<0.05 *, p<0.01 **, p<0.001 **.*

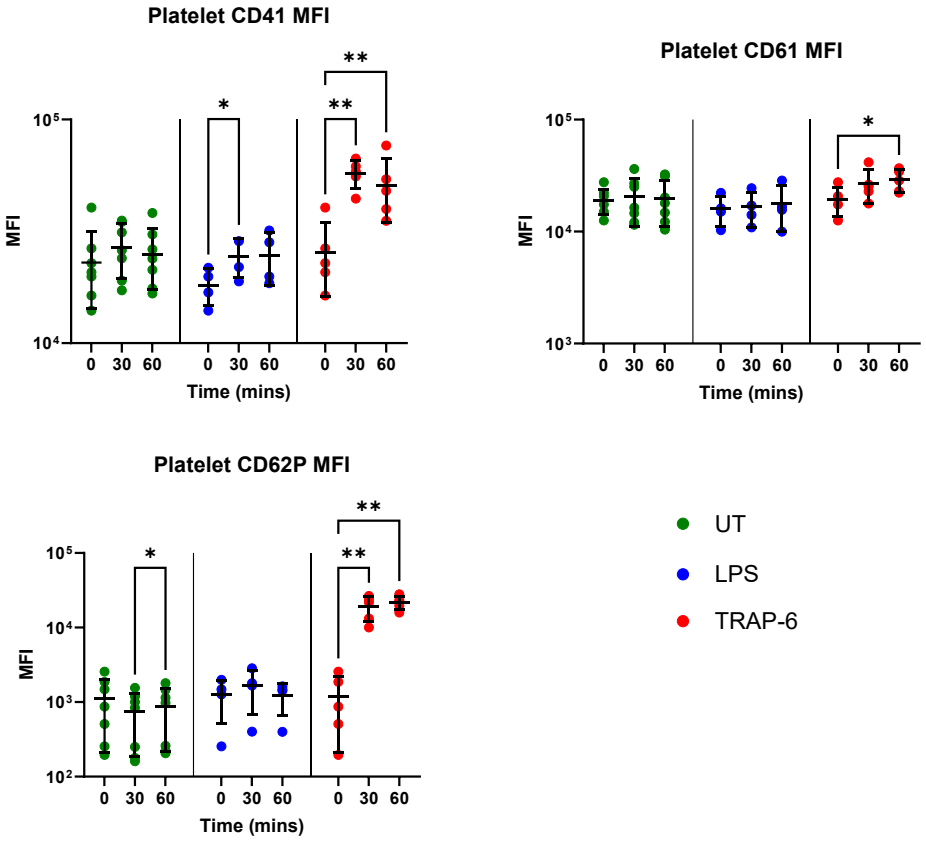


Figure 6.5 Platelet activation was increased after TRAP-6 stimulation but not LPS stimulation

*Platelets were identified as CD41 and CD61 positive events. Expression of platelet markers CD41 and CD61, and platelet activation marker CD62P were quantified at 0, 30 and 60 minutes without stimulation (UT, n=7), LPS 100mg/ml (n=4), or TRAP-6 10μM (n=5). Mixed effects analysis with Geisser-Greenhouse correction and Tukey's multiple comparison test was used to compare within groups. P<0.05 considered statistically significant. P<0.05 *, P<0.01 **.*

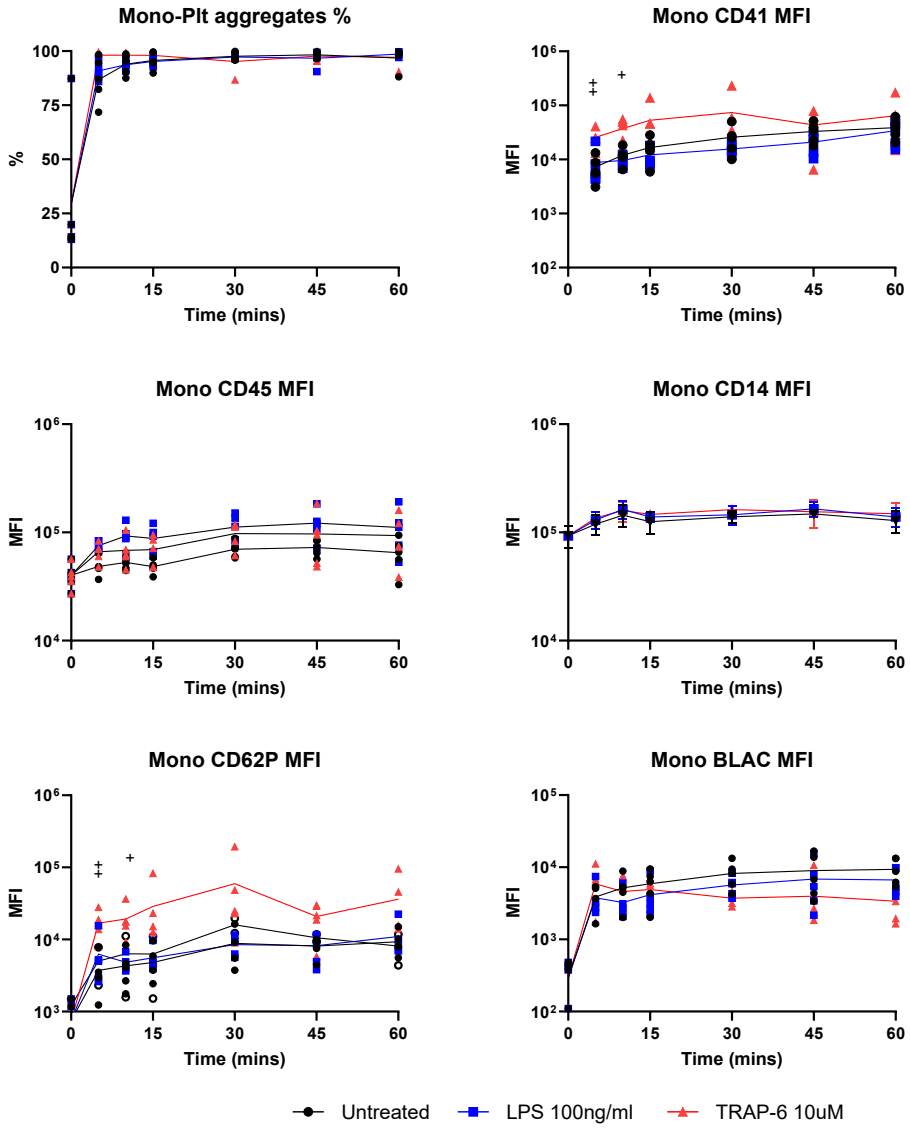
6.4.5 There is no difference in formation of monocyte-platelet aggregates with leucocyte or platelet stimulation

In contrast to the agonist-induced acceleration of NPA formation, MPA formation was maximal after 5 minutes for all conditions: unstimulated 86.8 ± 10.5%, LPS 90.9 ± 4.1% and TRAP 98.1 ± 1.5% with no significant differences between different stimulations (P=0.2689) (Figure 6.6). There were some early differences in monocyte CD41 expression after TRAP-6 stimulation when compared with unstimulated: at 5 minutes (24,657 [18,822 – 32,706] vs 5,777 [4,322 – 10,979]; P=0.0066) and at 10 minutes (42,517 [19,557 – 52,196] vs 11,641 [8,771 – 15,284]; P=0.0333). There were similar differences in monocyte CD62P expression at the same time points. This suggests that although most monocytes have formed aggregates with platelets, after TRAP-6 stimulation there is further upregulation of CD41 and

CD62P on platelets due to increased platelet activation. There were no differences in monocyte CD41 or CD62P expression when LPS was compared to unstimulated.

When examining monocyte activation, there were no differences between LPS or TRAP-6 stimulation in monocyte CD14 expression, but there was some variation in monocyte CD45 expression (P=0.0199). Unfortunately, as this was a single panel for both neutrophil and monocyte with limited monocyte activation markers, conclusions about monocyte activation cannot be drawn from this data.

These results show MPA form more readily than NPA both with and without stimulation, confirming the affinity of monocytes to platelets is higher than that of neutrophils. Whilst monocytes appear to be saturated with platelets after initial stimulation, the aggregation of platelets to neutrophils increases gradually over time.



Two-way ANOVA	Time	Stimulation
Monocyte platelet aggregates (%)	**0.0095**	0.2689
Monocyte CD14	**0.0184**	0.1567
Monocyte CD45	**0.0297**	**0.0199**
Monocyte CD41	0.0771	**0.0075**
Monocyte CD62P	0.1995	**0.0214**
Monocyte BLAC	0.0704	0.0539

Figure 6.6 Monocyte platelet aggregates form immediately and do not change under flow conditions with leucocyte and platelet stimulation.

*Heparinised whole blood was perfused in the ibidi microfluidics chamber at 2.5ml/min through 1.6mm tubing and 0.4mm μ-slides for 1 hour. Samples were taken at 5, 10, 15, 30, 45 and 60 minutes for flow cytometry. Whole blood was stimulated with LPS 100ng/ml, TRAP-6 10μM, or unstimulated. N=5 for all conditions. Mean lines shown with all replicates. 2-way ANOVA with Geisser-Greenhouse correction and Tukey's multiple-comparisons test was used to compare trend over time and between stimulation. Differences between LPS and unstimulated denoted by *, differences between TRAP-6 and unstimulated denoted by +. P<0.05 considered statistically significant. p<0.05 *, p<0.01 **, p<0.001 ***, p<0.0001 ****.*

6.4.6 Inhibitors had no effect on baseline LPA formation or leucocyte activation

To inhibit the leucocyte platelet interaction Eptifibatide, a GPIIb/IIIa pathway inhibitor, and KF38789 (Cat 2748; Biotechne), a selective inhibitor of P-selectin mediated cell adhesion was incubated with whole blood for 10 minutes prior to stimulation with LPS or TRAP-6. To ensure no priming effect of these inhibitors or LPA formation, samples were taken after incubation with inhibitors to quantify LPA formation, and leucocyte activation, prior to stimulation. There was no effect of eptifibatide or KF38789 on LPA formation (both NPA and MPA), or neutrophil or monocyte activation (as measured by neutrophil CD66b, and monocyte CD11b) (See figure 6.7).

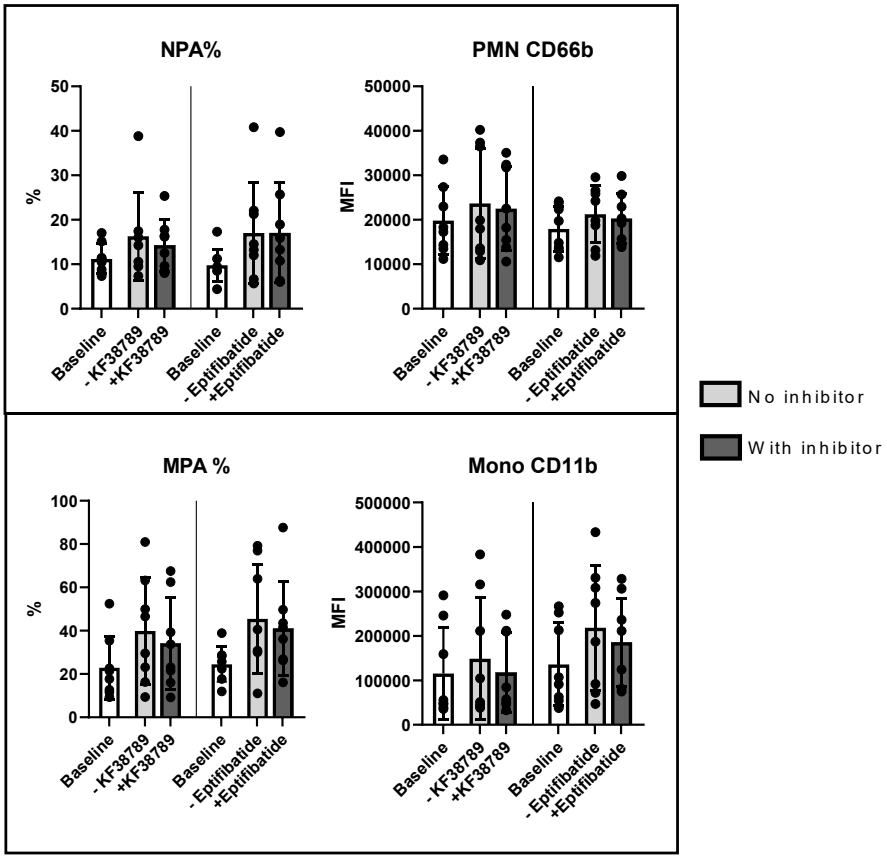


Figure 6.7 No effect of incubation with P-selectin inhibitor (KF38789) or GPIIb/IIIa inhibitor (Eptifibatide) on neutrophil and monocyte activity and leucocyte-platelet aggregates.

Heparinised whole blood was incubated with inhibitors for 10 minutes at 37°C prior to stimulation with LPS or TRAP-6 (N=8). Paired samples of whole blood with and without each inhibitor were stained with antibody cocktail. Neutrophil-platelet aggregates, neutrophil activation (CD66b), monocyte-platelet aggregates, and monocyte activation (CD11b) were measured. Bars show mean with SD. Two-way ANOVA with Geisser Greenhouse correction performed. P<0.05 considered statistically significant.

Mean fluorescence intensity, MFI; Monocyte-platelet aggregates, MPA; Neutrophil-platelet aggregates, NPA.

6.4.7 Effect of GPIIb/IIIa inhibition and P-selectin pathway inhibition on neutrophil-platelet aggregation

The ibidi 'Quad' microfluidics system in our lab has 4 fluidics units, enabling experiments to be run paired with one stimulant and one inhibitor. Experiments with both stimulants or both inhibitors were not able to be run together in parallel. Comparisons are therefore made with its unstimulated control. CD11b was also included in these antibody panels in this set of experiments to better quantify leucocyte activation particularly of monocytes. In addition, Eptifibatide, the GPIIb/IIIa inhibitor interacts with Mac-1(CD11b) on leucocytes.

Eptifibatide significantly reduced NPA formation over time in unstimulated (P=0.0201) and TRAP-6 stimulated blood (P=0.0090), but not in LPS stimulated blood (P=0.5500) (Figure 6.8). There was corresponding reduction in neutrophil CD41 expression with eptifibatide inhibition in unstimulated/TRAP-6 experiments (P=0.0167) but not the combined unstimulated/LPS experiments. There were no differences in neutrophil CD62P expression.

The P-selectin inhibitor, KF38789 had no effect on the NPA formation in unstimulated, LPS and TRAP-6 stimulated conditions but there was lower neutrophil CD41 expression in TRAP-6 experiments (P=0.0103) suggesting lower numbers of platelets attached to each neutrophil with KF38789 (Figure 6.9).

Neither eptifibatide nor KF38789 affected neutrophil activation as measured by neutrophil CD66b, CD62L or CD11b in unstimulated, LPS and TRAP-6 stimulated conditions (Figure 6.10).

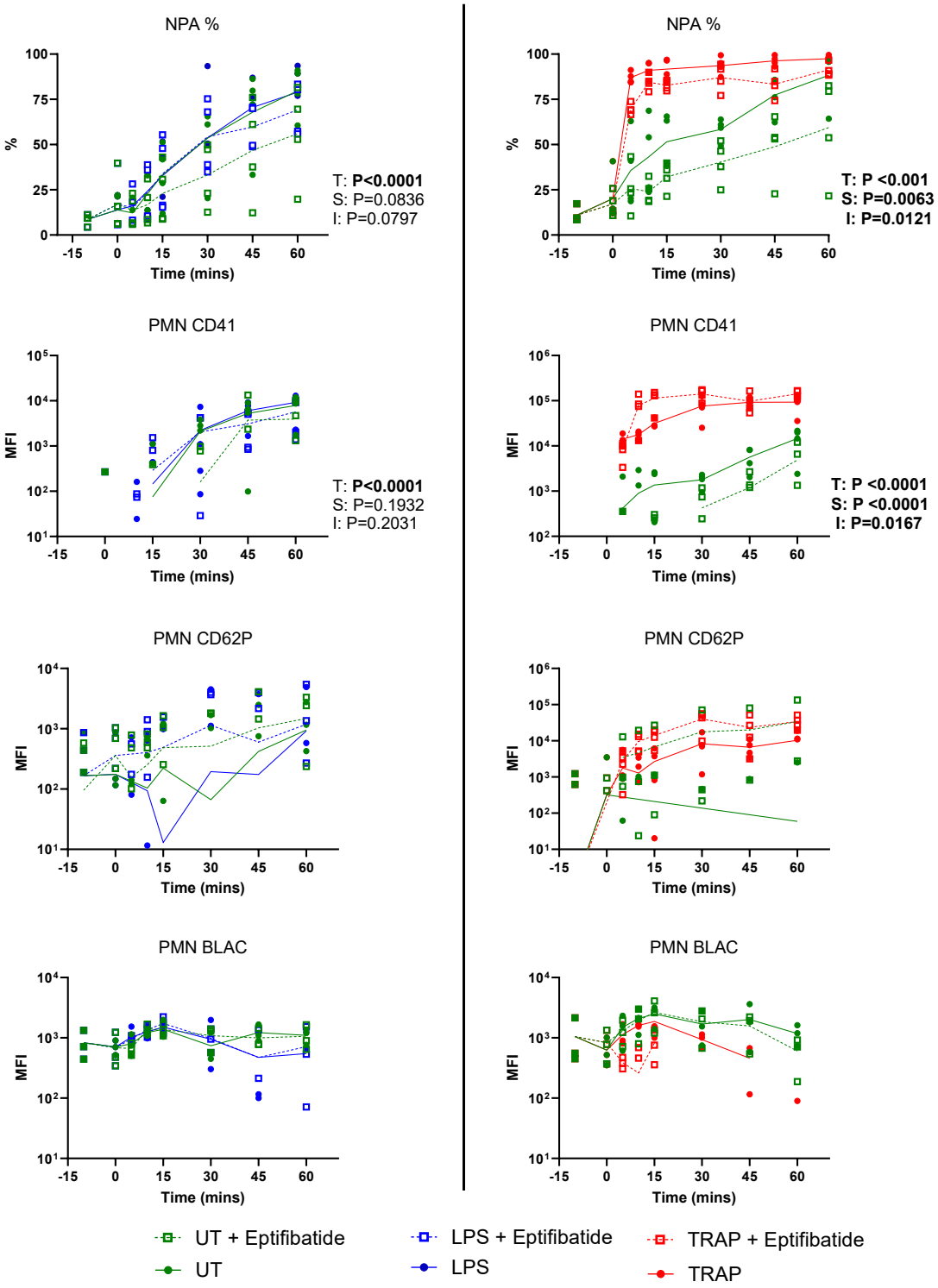


Figure 6.8 The effect of Eptifibatide, a GPIIb/IIIa pathway inhibitor on neutrophil platelet aggregation in vitro.

Paired experiments (N=4) comparing unstimulated (UT; green) with A) TRAP-6 (red) or B) LPS (blue) stimulated whole blood; with or without Eptifibatide were run in parallel. Mean lines shown with all replicates. Three-way ANOVA with Geisser Greenhouse correction used to analyse the effect of stimulation and inhibition for each paired set of experiments. P<0.05 considered statistically significant. ANOVA variation T: Time, S: Stimulation, I: Inhibition.

Lipopolysaccharide, LPS, neutrophil-platelet aggregate, NPA; neutrophil, PMN; thrombin receptor activating peptide-6, TRAP-6; untreated, UT.

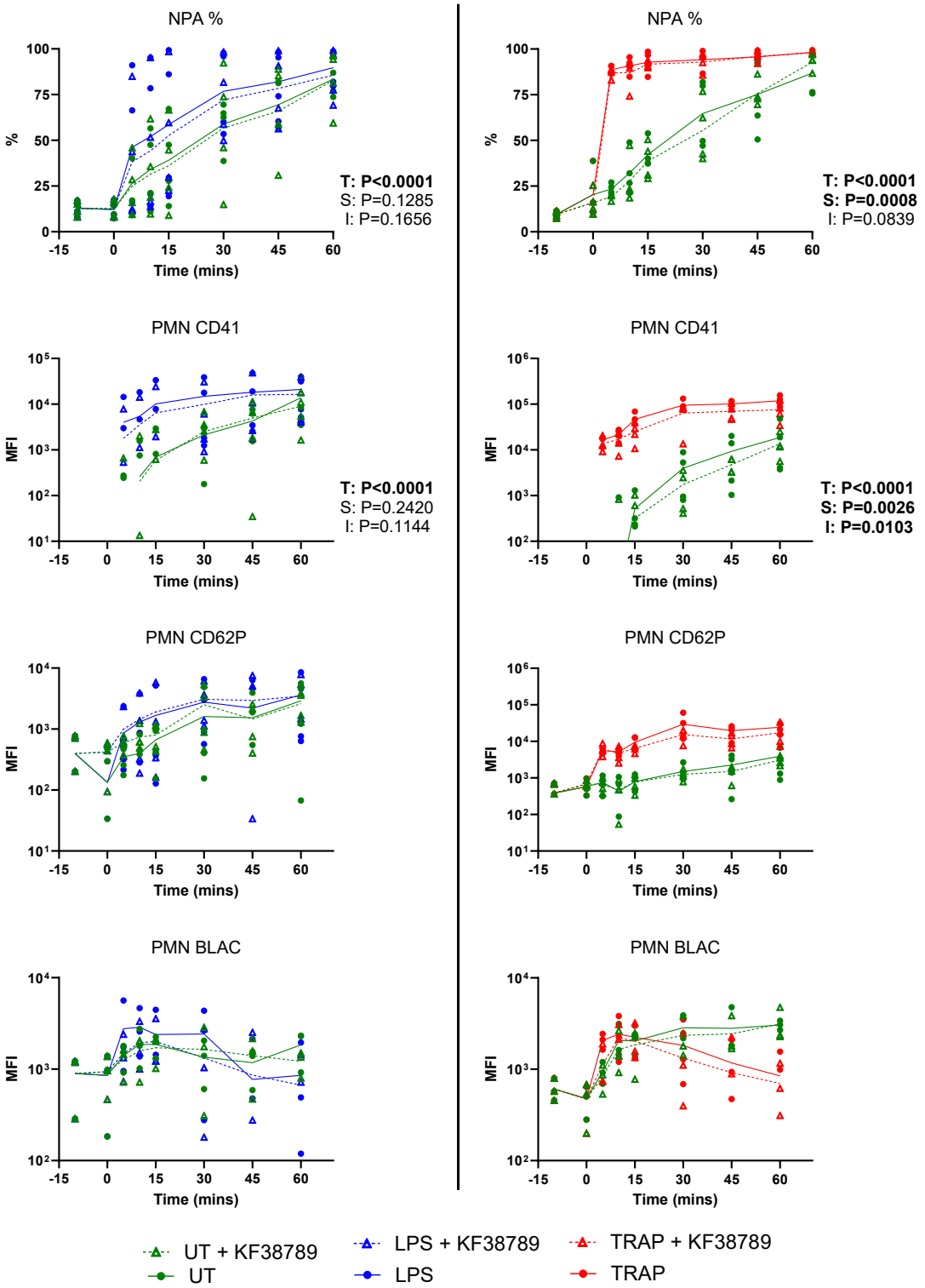


Figure 6.9 The effect of KF38789, a P-selectin pathway inhibitor on neutrophil platelet aggregation in vitro.

Paired experiments (N=4) comparing unstimulated (UT; green) with A) TRAP-6 (red) or B) LPS (blue) stimulated whole blood; with or without KF38789 were run in parallel. Mean lines shown with all replicates. Three-way ANOVA with Geisser Greenhouse correction used to analyse the effect of stimulation and inhibition for each paired set of experiments. P<0.05 considered statistically significant. ANOVA variation T: Time, S: Stimulation, I: Inhibition. Lipopolysaccharide, LPS, neutrophil-platelet aggregate, NPA; neutrophil, PMN; thrombin receptor activating peptide-6, TRAP-6; untreated, UT.

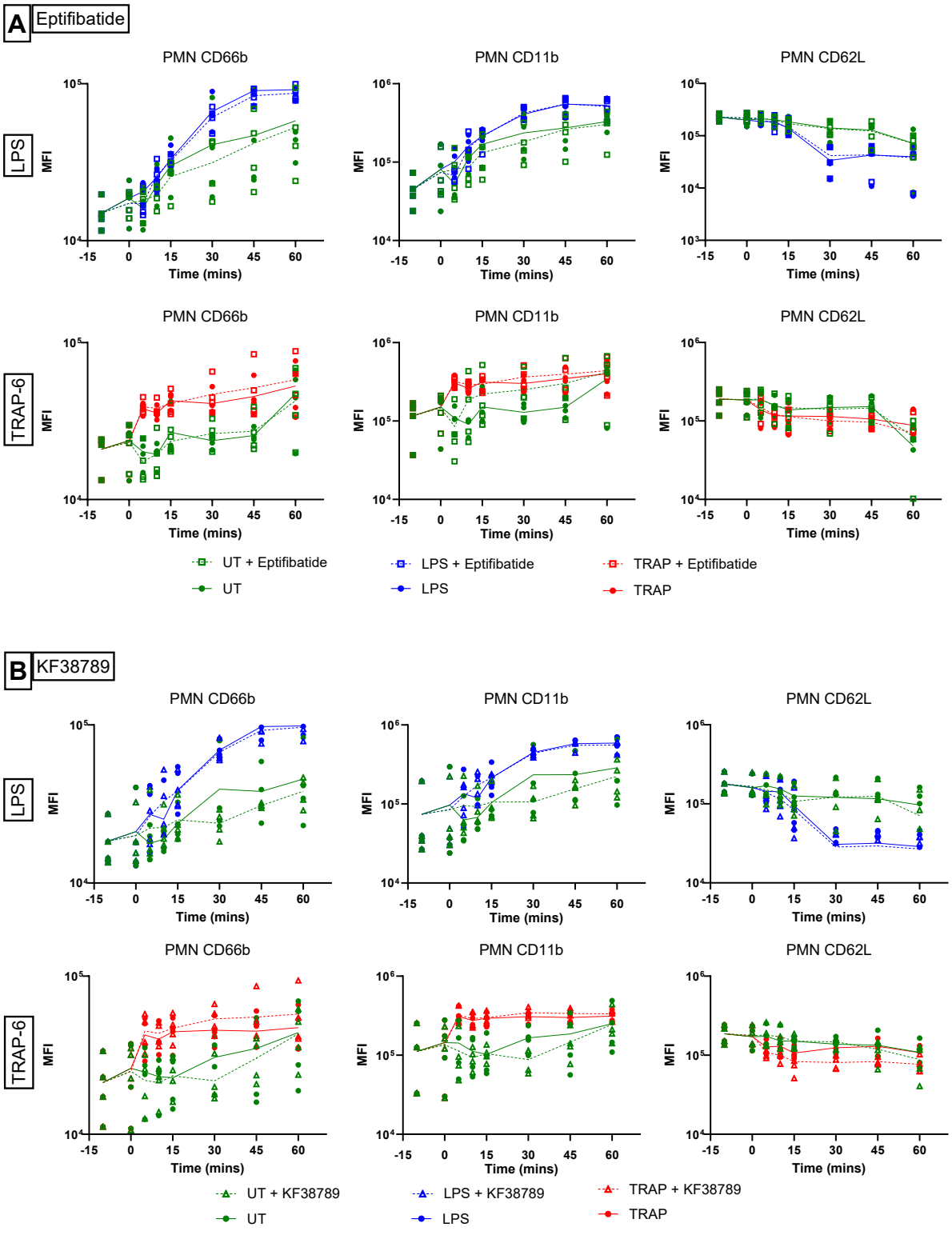


Figure 6.10 There was no effect of Eptifibatide, a GPIIb/IIIa inhibitor or KF38789 a P-selectin pathway inhibitor on neutrophil activation with LPS or TRAP-6 stimulation. *Paired experiments (N=4) with untreated (green) with LPS (blue) or TRAP-6 (red) stimulated; with or without A) Eptifibatide or B) KF38789 were run in parallel. Mean lines shown with all replicates. Three-way ANOVA with Geisser Greenhouse correction used to analyse the effect of stimulation and inhibition for each paired set of experiments. P<0.05 considered statistically significant. Lipopolysaccharide, LPS, thrombin receptor activating peptide-6, TRAP-6; untreated, UT.*

6.4.8 There is no effect of GPIIb/IIIa inhibition or P-selectin inhibition on monocyte-platelet aggregation

There was no effect of eptifibatide nor KF38789 on MPA formation or monocyte CD41 expression in unstimulated, LPS or TRAP stimulated condition (Figure 6.11 – data for MPA % and monocyte CD41 shown only as no difference between other platelet markers).

There was also no effect of eptifibatide or KF38789 on monocyte activation markers (Figure 6.12). This could be due to the high affinity of monocytes to binding platelets and corresponds with earlier results using different strength calcium chelation and little difference in MPA (Figure 5.4 in section 5.4.3).

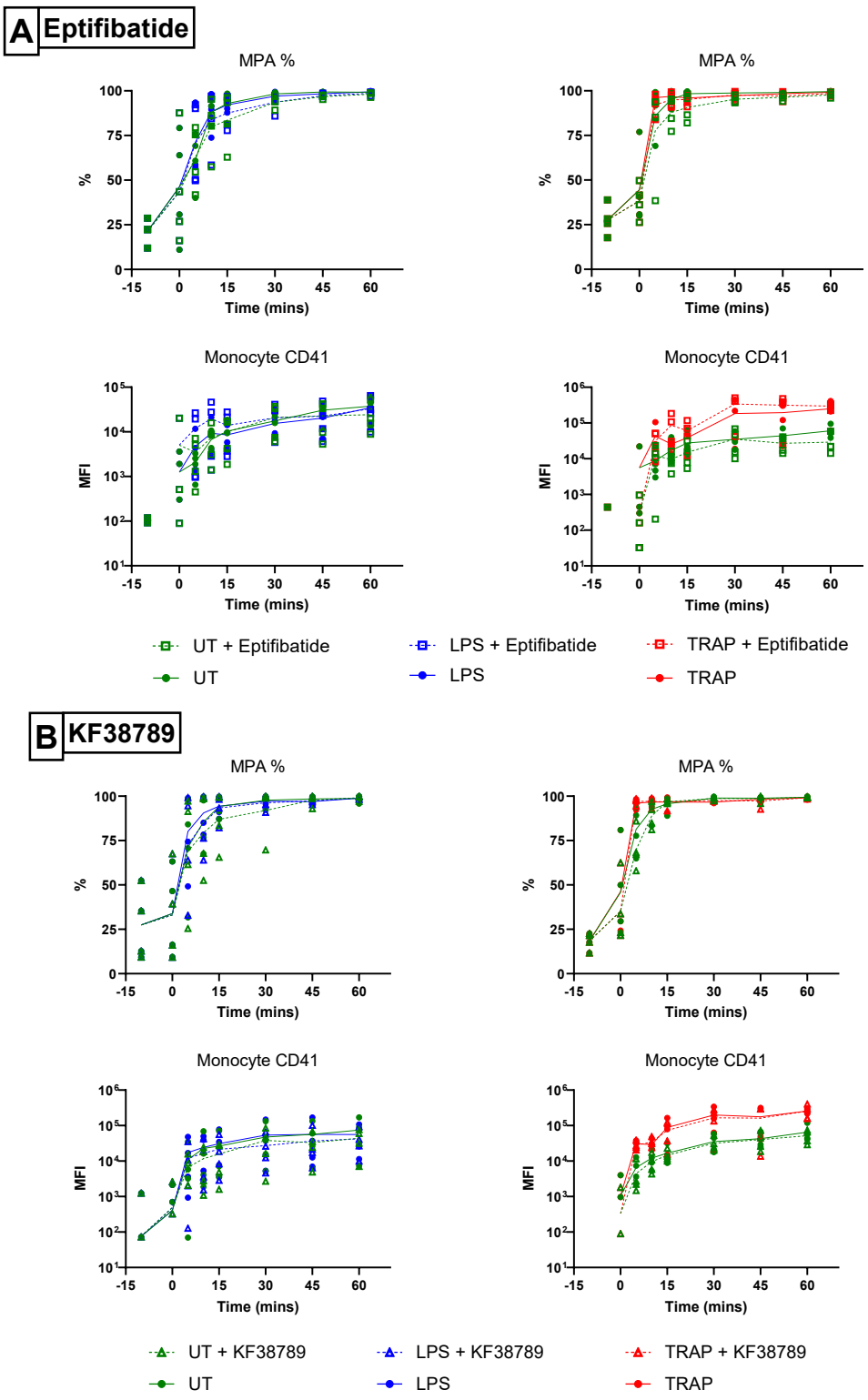


Figure 6.11 There was no effect of eptifibatide or KF38789 on monocyte platelet aggregation in vitro.

Paired experiments (N=4) comparing untreated (green) with LPS (blue) or TRAP-6 (red) stimulated whole blood; with or without A) Eptifibatide or B) KF38789 were run in parallel. Mean lines shown with all replicates. Three-way ANOVA with Geisser Greenhouse correction used to analyse the effect of stimulation and inhibition for each paired set of experiments. P<0.05 considered statistically significant. Lipopolysaccharide, LPS, monocyte-platelet aggregate, MPA, thrombin receptor activating peptide-6, TRAP-6; untreated, UT.

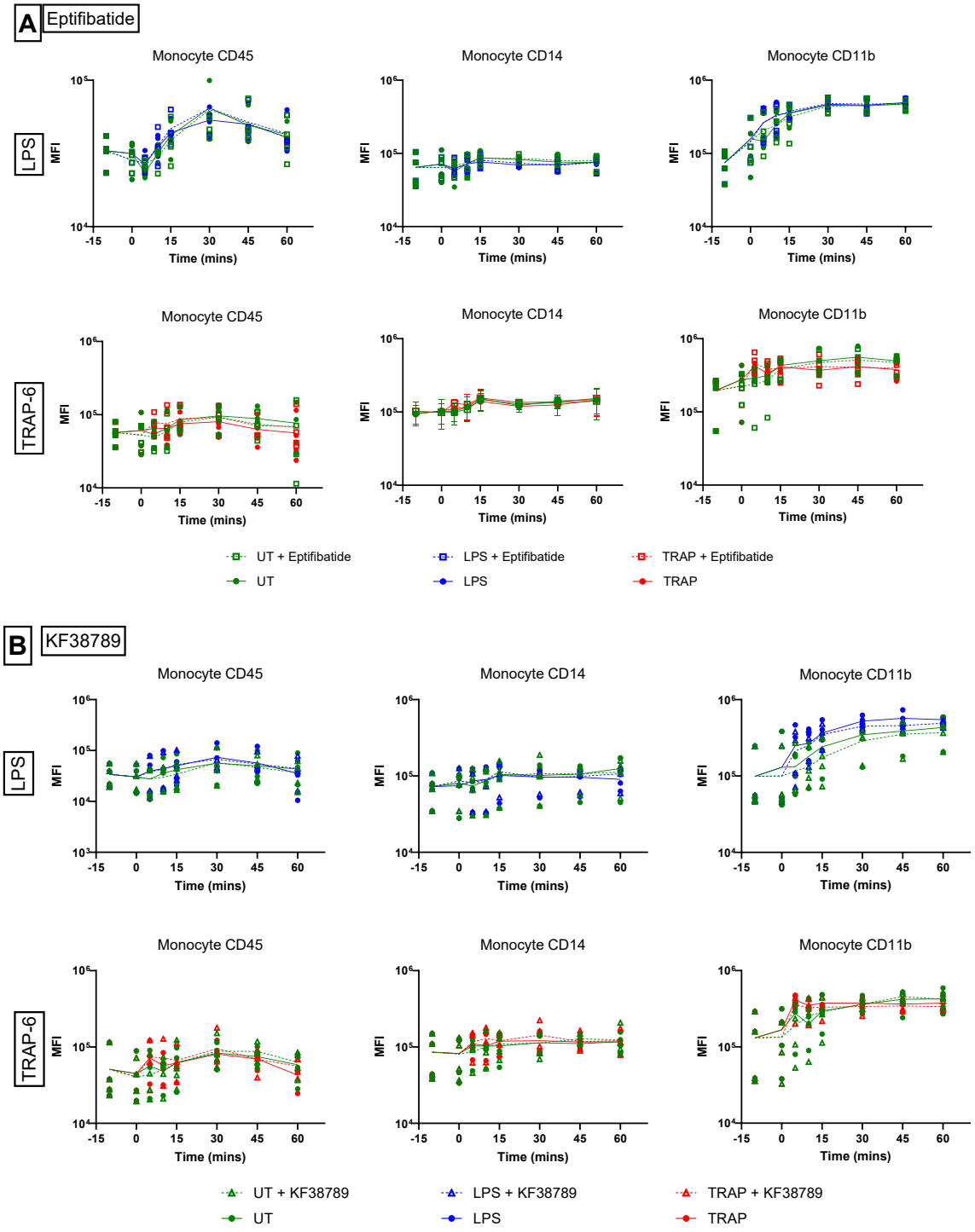


Figure 6.12 There was no difference of Eptifibatide, a GPIIb/IIIa inhibitor or KF38789 a P-selectin pathway inhibitor on monocyte activation with LPS or TRAP-6 stimulation.

Paired experiments (N=4) with untreated (green) with LPS (blue) or TRAP-6 (red) stimulated; with or without A) Eptifibatide or B) KF38789 were run in parallel. Mean lines shown with all replicates. Three-way ANOVA with Geisser Greenhouse correction used to analyse the effect of stimulation and inhibition for each paired set of experiments. ANOVA variation T: Time, S: Stimulation, I: Inhibition. P<0.05 statistical significance. Lipopolysaccharide, LPS, thrombin receptor activating peptide-6, TRAP-6; untreated, UT.

6.5 Discussion

In this chapter, I discuss the development of a protocol for using the ibidi microfluidics parallel flow chamber to assess LPA formation in whole blood in laminar flow conditions. Using this model there is spontaneous baseline NPA formation in flow conditions which increases over time. This is increased with leucocyte and platelet stimulation. Inhibition of GPIIb/IIIa reduces spontaneous and platelet stimulated NPA formation. Interestingly the kinetics observed between NPA and MPA were different with MPA being formed more readily compared to NPA and were not affected by GPIIb/IIIa or P-selectin pathway inhibition.

6.5.1 Developing an experimental flow model for investigating LPA formation

Before using the ibidi microfluidics chamber for investigation of LPA formation in flow conditions preliminary work to determine the best agonists, and flow conditions was conducted.

LPS is an established leucocyte agonist used for mimicking sepsis conditions within our lab. LPS did not appear to activate platelets within the PRP assay and was used as the leucocyte specific agonist in the whole blood model. Analysis of platelet activation within PRP and whole blood ibidi flow model showed LPS did not cause platelet activation. LPS inability to activate platelets was also found by others [337].

Platelet work was new to the lab and therefore little experience with the use of platelet agonists. Thrombin was chosen as a naturally occurring enzyme and the end point of the coagulation cascade, and TRAP-6 as it is used clinically in platelet function tests, such as the Multiplate analyser, and in many other studies of platelet function in vitro [335, 360]. In PRP, thrombin caused significant platelet clumping which were visible macroscopically and platelet activation was not able to be measured. This may be because thrombin is a very potent platelet agonist. Thrombin cleaves PAR1 on platelets triggering platelet activation and also activates multiple pathways and receptors including PAR1-4. TRAP-6 is a synthetic specific agonist of the PAR1 receptor and is therefore platelet specific since neutrophils do not constitutively express PAR-1 receptors (but may do in pregnancy) [361, 362]. Thrombin's actions on multiple pathways does not make it platelet specific and may have a role in neutrophil activation via PAR-2 [363, 364]. Therefore TRAP-6 was used as the platelet agonist in the ongoing experiments.

Whole blood stimulation models used within our lab have used blood in Eppendorfs in a rotator as described in section 2.3.4 and 5.4.1 with samples taken at the end of the experiment for quantifying biomarkers. This was not a suitable model for measuring LPA formation and kinetics over time. Preliminary work comparing blood in static, turbulent flow (Eppendorf in rotator) and laminar flow (in ibidi microfluidics chamber) conditions was carried out to determine if there were differences in LPA formation between these conditions (section 6.4.2). There was almost maximal NPA formed in turbulent flow conditions compared to static and laminar flow conditions after 30 minutes, as well as increasing NPA formation in static and laminar flow conditions up to 60 minutes demonstrating the laminar flow model influenced NPA formation with different kinetics to the turbulent flow/rotator model. The changes in MPA formation were less apparent due to maximal MPA formed after 30 minutes in both turbulent and laminar flow conditions.

In addition, the stimulation in the rotator did not allow for frequent sampling e.g. every 5 minutes without stopping the stimulation or removing from the 37°C incubator. Using the ibidi microfluidics flow system allows addition of a sampling port to the perfusion set so that samples can be taken at more frequent intervals without disrupting the experimental conditions such as flow and temperature, allowing allows better characterisation of the kinetics of LPA formation in stable conditions. Against my hypothesis, within the ibidi model, there was no difference in NPA or MPA formation at different flow rates, with and without additional stimulation, but there was slightly higher neutrophil and monocyte expression of CD41 with the highest flow rate (10ml/min) which may indicate increased leucocyte-platelet interactions. Although there were no adhered cells within the ibidi slide, and therefore shear is not discussed, it may be the influential factor at higher flow rates. The lower flow rate (2.5ml/min) was chosen for ongoing work as this would equate to similar shear (10dyn/cm^2) within small veins or in aorta where blood flow is 5L/min similar to blood flow in ECMO circuit.

6.5.2 Formation of neutrophil-platelet aggregates under flow conditions is increased with platelet activation.

There were low baseline levels of NPA measured shortly after HV venepuncture and prior to perfusion. In unstimulated blood under flow conditions, there was NPA formation which increases gradually over time but with no change in neutrophils associated platelet-derived CD41 or CD62P expression suggesting little platelet activation. There was also no change in

neutrophil CD66b expression or CD62L shedding suggesting no increase in neutrophil activation with spontaneous NPA formation (Figure 6.4). It seems quite likely that this phenomenon of low level spontaneous NPA formation would occur also during ECMO initiation where blood is exposed to altered flows within the ECMO circuit. Changes in blood flow can lead to marginalisation of neutrophils to the vessel periphery where platelets are located increasing neutrophil-platelet interactions and therefore NPA formation [365]. Without further activation by inflammatory stimuli, NPA formation via P-selectin binding PSGL-1 appears to be short-lived and transient, which plays a role in neutrophil transmigration on endothelial surfaces or possibly causing temporary NPA formation [366, 367]. The observation that NPA formation is reversible in chapter 5 also supports this theory. The findings of significantly increased numbers of aggregates therefore predicts ongoing formation of NPA such as in pathological conditions of inflammation and thrombosis [368].

To investigate whether the NPA formation was impacted more by neutrophil or platelet activation, I used TRAP-6, a platelet agonist and LPS, a leucocyte agonist to simulate more pro-immunothrombotic conditions in this in vitro model. Formation of NPA was more pronounced when using TRAP-6, compared to LPS. After TRAP-6 stimulation, the proportion of NPA formed was near maximal (>90%) after only 5 minutes, with much higher platelet-derived CD41 and CD62P signals on neutrophils compared to with LPS stimulation. In addition, despite increased neutrophil activation (increased CD66b, and decreased CD62L) with LPS compared to TRAP-6 at all time points, the speed and levels of NPA formed were greater with TRAP-6 stimulation. These findings suggest that platelets are more readily activated than neutrophils supporting the view that NPA formation in whole blood is primarily dependent on platelet activation [337, 367]. Mauler and colleagues also found stimulation of platelets with ADP for 15 minutes increased NPA formation compared to controls in mouse and human neutrophils. However, in their model, stimulation with PMA, led to higher NPA formation than with ADP [369]. Peshkova and colleagues compared NPA formation in citrated whole blood with LPS 100ng/ml, PMA 100nM, ADP 20μM, and TRAP-6 50μM and also found PMA caused the highest NPA formation (37.7%), compared to TRAP-6 (24%), ADP (17.1%) and LPS (0.5%) [337]. Further work with isolated neutrophils and PRP with LPS and PMA stimulation showed that whilst LPS caused strong activation of neutrophils, it did not activate platelets compared to PMA which activated both. From this they concluded that platelet activation is necessary for NPA formation [337]. Since TRAP-6 is not known to stimulate neutrophils, the increased neutrophil activation (CD66b expression and some CD62L shedding) after 1 hour of perfusion with TRAP-6 stimulation suggests that there is platelet-mediated neutrophil activation after formation of NPA.

The findings from these experiments that there is baseline NPA formation within flow conditions in a new perfusion circuit, which is enhanced by both leucocyte and platelet activation could explain the increased immunothrombosis seen in ECMO. Firstly, the baseline NPA formation seen in unstimulated blood could represent increased interactions from increased blood mixing due to changes in flow, and there is contact activation from blood exposure to the ECMO circuit leading to increased platelet activation and adherence, as well as thrombin generation [124, 159], leading to increased NPA formation. Secondly, patients who require ECMO are usually inflamed from the underlying condition e.g. infection, ARDS and have primed leucocytes and platelets which increases ligand-receptor expression and binding on neutrophil and platelet cell surfaces increasing NPA formation [282, 367]. And thirdly in whilst an air pump was used in this in vitro model, in ECMO a blood pump is used to generate the blood flow which can increase platelet and neutrophil activation due to high mechanical shear stress (HMSS). Sun and colleagues investigated the impact of HMSS from mechanical circulatory devices on platelet and neutrophil activation in whole blood models. They found platelet activation as measured by platelet microvesicle production and adhesion capacity to fibrinogen increased over time with no difference in circuits with and without the MO [194] suggesting HMSS from the blood pump played a dominant role in this activation. They also found increased neutrophil activation (as measured by increased CD11b, and decreased CD62L), and increased neutrophil phagocytosis after exposure to HMSS, which increased with duration of exposure up to 1 hour [370, 371].

6.5.3 Differential formation of LPA depends on cell type and stimulant

Until recently, there has been little work investigating NPA and MPA formation concurrently. Whilst there are clear differences in NPA formation in unstimulated, LPS and TRAP-6 stimulated blood, there is immediate and maximal formation of MPA at after only 5 minutes of perfusion with no difference between unstimulated, LPS or TRAP-6 stimulated blood. Therefore, the same conclusions regarding platelet activation mediating NPA formation cannot be made regarding MPA. The only difference is that monocyte expression of platelet-derived CD41 and CD62P was higher with TRAP-6 stimulation indicating increased platelet activation.

Peshkova and colleagues investigated the formation and morphology of NPA and MPA in response to various cellular activators in whole blood and in plasma [337]. After stimulating citrated whole blood for 15 minutes, they found higher levels of MPA compared to NPA in all

conditions: PMA (73.8% vs 37.7%), ADP (61.3% vs 17.1%) and TRAP-6 (77.5% vs 24%), and that both NPA and MPA formation correlated with platelet aggregation and expression of P-selectin, similar to my findings. Since PMA and TRAP-6 caused potent LPA formation whereas LPS did not, they suggest that platelets are the rate limiting step for LPA formation and LPA formation may be mediated by protein kinase C pathway since PMA and TRAP-6 activate protein kinase C [337]. In another study, Ahn et al combined isolated monocytes, neutrophils and platelets under different shear conditions in a cone-and-plate-rheometer and also found increased levels of MPA (12%) compared to NPA (8%) at baseline and that MPA formed preferentially over NPA at earlier time points and increased with increasing shear stress and shear exposure time [372] supporting my findings.

It is known that monocytes have the highest affinity for P-selectin compared to neutrophils and lymphocytes [121], which explains the increased MPA found in all in vitro models (static, rotator and flow) of whole blood stimulation as well as other studies [337, 372]. PSGL-1 is expressed constitutively on monocytes binding P-selectin and the initial binding of platelets to monocytes is strengthened further by ligand-receptor interactions such as platelet CD40L binding to monocyte CD40, and Mac-1 with CD18 [338, 339]. In contrast, whilst PSGL-1 is expressed on inactive neutrophils, there have been some studies that report neutrophil surface PSLG-1 is downregulated or cleaved after neutrophil activation [373, 374] which could explain the differences in MPA and NPA formation between LPS and TRAP-6 stimulation. In addition, monocytes express tissue factor on their cell surface whereas neutrophils do not, and therefore monocytes are more likely to activate platelets via the cell-based coagulation model (Figure 1.7) [39] further enhancing platelet mediated MPA formation. With regards to stimulation, whilst neutrophils have not been shown to constitutively express PAR-1, monocytes and other antigen presenting cells do [375], therefore TRAP-6 would activate monocytes which can further increase MPA formation compared to NPA leading to the increased monocyte CD41 and CD62P expression.

6.5.4 Inhibiting GPIIb/IIIa using eptifibatide reduced NPA formation but inhibition of P-selectin pathway by KF38789 did not

The observation that LPA formation is reversible could lead to potential treatment options for conditions where immunothrombosis due to LPA formation is high. Leucocytes and platelets interact predominantly via platelet P-selectin binding to leucocyte PSLG-1, and platelet GPIIb/IIIa binding to leucocyte Mac-1 via intermediary proteins such as fibrinogen and

CD40L [119, 120]. Therefore, I hypothesised that inhibiting these pathways would reduce LPA formation.

GPIIb/IIIa inhibition

Eptifibatide is a competitive inhibitor of the GPIIb/IIIa receptor preventing binding to intermediary proteins CD40 and fibrinogen, as well as VWF and prothrombin [376]. Incubation with eptifibatide prior to stimulation and perfusion within the microfluidics channel reduced NPA formation in unstimulated whole blood and in TRAP-6 stimulated blood, supporting the view that NPA formation is dependent on platelet activation and there is involvement of the GPIIb/IIIa pathway. Patko and colleagues were one of the first groups to report that CD40L and fibrinogen mediated formation of heterotypic platelet aggregates with Mac-1 presenting cells, and inhibition of GPIIb/IIIa with eptifibatide reduced this interaction [377] and Polanowska-Grabowska et al found anti-platelet agents such as clopidogrel suppressed NPA formation and platelet-dependent activation in sickle cell mice [314]. There was no effect of eptifibatide on LPS stimulated NPA formation, which suggests that although LPS did not activate platelets the increased leucocyte activation from LPS has some effect on NPA formation independent of platelet activation or that LPS activation leads to a different pathway of LPA formation such as through TLR4 activation on platelets [83]. In contrast to NPA, there was no effect of eptifibatide on MPA formation, which is likely due to the increased affinity of platelets to monocytes and additional increased stability by their various pathways of receptor-ligand interactions after monocyte activation [338, 339]. It could also be related to the low dose of eptifibatide used in these experiments since eptifibatide is administered clinically as a continuous infusion, and a dose titration or repeated dosing in vitro may yield different results for MPA. One study found contrasting results, with GPIIb/IIIa blockade increasing LPA formation in unstimulated and ADP stimulated blood and suggested that the P-selectin pathway is the principle pathway of interaction between leucocytes and platelets [340].

GPIIb/IIIa inhibitors such as eptifibatide, tirofiban and abciximab are used as adjunctive anti-platelet drugs in patients with unstable angina and those undergoing high risk percutaneous coronary intervention [378]. There are a few small case series reporting on the use of eptifibatide for patients with LVAD thrombosis. Al-Quthami reports on a case series of 3 patients with LVAD thrombosis and Tellor et al evaluated the use of an eptifibatide infusion for 17 patients with LVADs with suspected pump thrombosis, and found clots within the LVAD circuits were able to be dissolved in a small number of patients, however bleeding

complications occurred in the majority of patients [379, 380]. Another case describes the use of eptifibatide in a patient on VA ECMO after myocardial infarction who had in stent thrombosis, however the bleeding events were high [381]. Whilst eptifibatide may be effective at reducing clot burden in patients on ECLS, the risk of bleeding and its consequences remain high and limits its use in this high-risk cohort of patients.

Other anti-platelet drugs have been investigated in modulating LPA formation. In patients receiving the influenza vaccine, the increased MPA formation leads to a pro-inflammatory phenotype in circulating monocytes [382]. They and others found antiplatelet drugs such as aspirin and clopidogrel reduces MPA formation and the number of pro-inflammatory monocytes in patients who received the influenza vaccine, with aspirin being the most effective [382, 383]. The circulating P-selectin was also reduced and correlated with the changes in pro-inflammatory monocytes and CRP suggesting that the pro-inflammatory effect was dependent on the amplitude of P-selectin reduction [383]. However, the evidence regarding the effect of anti-platelet drugs on LPA formation is conflicting. Recent evidence shows that whilst LPA and platelet degranulation is increased in patients with coronary artery disease, there was no difference in LPA in patients on antiplatelet therapy (aspirin, clopidogrel or prasugrel) suggesting a platelet independent mechanism of LPA formation [384].

P-selectin pathway inhibition

To inhibit the P-selectin pathway, I used the compound KF38789, a selective inhibitor of P-selectin mediated cell adhesion which has no effect on E-selectin or L-selectin. KF38789 has been shown to inhibit P-selectin mediated cell adhesion and leucocyte recruitment in mouse peritonitis [385], and facilitates movement of human corneal epithelial cells [386] but has not previously been investigated in mediating leucocyte-platelet interactions. In this whole blood flow model, there was no effect of KF38789 on LPA formation. The lack of effect from KF38789 on LPA formation is not necessarily because KF38789 has no effect on the P-selectin pathway, but perhaps it modulates the interaction between endothelial cells and leucocytes, rather than between platelets and leucocytes. KF38789 was the only commercially available P-selectin pathway inhibitor I was able to procure. Future work into inhibiting the P-selectin mediated leucocyte-platelet interactions within this whole blood model could include dose titrations of KF38789 or use of an anti-P-selectin antibody which has been shown reduce NPA and MPA formation in vitro in many other studies. Peshkova used Inclacumab, an anti-P-selectin monoclonal antibody, which prevented formation of NPA induced by TRAP-6 [337], Mauler found that blocking P-selectin prevented ADP induced NPA

formation but not in PMA stimulated whole blood [369], and Ahn found both anti-P-selectin and anti-PSGL-1 antibodies were able to inhibit shear induced MPA and NPA formation, but blocking GPIIb/IIIa did not [372]. Harding found blocking P-selectin reduced MPA formation in heparinised blood [327] and Hu found P-selectin blockade abolished LPA formation under static conditions but not shear enhanced LPA formation [340]. These correspond to the many reports that LPA formation is mediated mainly by the P-selectin pathway.

P-selectin blockade has been found to have clinical benefit in some immunothrombotic conditions. Patients with sickle cell disease have both increased NPA [314] and MPA [387] compared to controls. Crizanlizumab, an anti-P-selectin monoclonal antibody, reduces rates of vaso-occlusive crises in patients with sickle cell disease and has been approved for clinical use [388, 389]. Zarbock found that anti-P-selectin antibodies reduced neutrophil-platelet interactions and led to improved gas exchange and less lung injury in an acid model of ALI in mice [313]. As COVID-19 is an immunothrombotic condition characterised by microvascular thrombi, some groups hypothesized that Crizanlizumab would reduce the interactions between platelets, leucocytes and endothelial cells in COVID-19 however there have not been any positive findings [390, 391]. The effect of anti-P-selectin monoclonal antibodies in these clinical studies is not specific to endothelial cell or platelet interactions and the effect cannot be contributed to leucocyte-platelet interactions alone. The true effect of P-selectin blockade on leucocyte-platelet interactions in clinical use remains to be determined and warrants further investigation.

Other pathways

The P-selectin and GPIIb/IIIa pathways are not the only pathways by which platelets are activated and interact with neutrophils. Li et al found FMLP and collagen activation of platelets and leucocytes of whole blood under physiological shear could be inhibited by GPIIb/IIIa and P-selectin blockade; and platelet activating factor (PAF) antagonists, superoxide anion scavengers and 5-lipoxygnase products inhibited FMLP activation of platelets, however collagen induced leucocyte activation could not be inhibited by Thromboxane A2 or PAF antagonists [123]. This study suggests multiple mechanisms and mediators involved in leucocyte-platelet interactions. Others also found LPS does not activate platelets in the same way as TRAP-6, thrombin or ADP, and LPS activation of platelets via TLR4 likely modulates their response to other agonists rather than direct activation [83, 392] which may explain why neither KF38789 or eptifibatide influenced LPA formation in LPS stimulated blood. Some studies have shown inhibiting TLR4 reduces

platelet induced neutrophil degranulation and NETosis [83, 346]. TLR4 inhibition may present another therapeutic target for reducing platelet-neutrophil interactions particularly as this pathway appears to mediate NETosis.

6.5.5 Significance of leucocyte-platelet aggregates and interactions

LPA have been suggested as an alternative, more sensitive marker for platelet activation since they remain detectable in the peripheral blood for significantly longer and are easily detected by flow cytometry [119, 393]. The investigation of leucocyte-platelet interactions compliments the cell-based coagulation model which considers the interaction of immune cells with the coagulation cascade particularly in the context of ECMO where patients have an activated immune system, endothelial injury and activated coagulation system from ECMO initiation.

LPA are thrombogenic

LPA, particularly MPA are considered a marker of increased thrombogenicity. Monocytes play an important role in atherogenesis where platelets facilitate their adhesion and extravasation through the endothelium [394]. Monocytes express tissue factor which initiates the coagulation cascade and results in the formation of thrombin and fibrin, key steps in thrombus formation, and stabilisation [395]. MPA have been proposed as a sensitive marker of platelet activation and are raised in ACS, after PCI and during CABG [310, 327, 393, 396]. They are also associated with the hypercoagulability observed in nephrotic syndrome [397], and play roles in HIV [351] and liver cirrhosis [350].

The role of NPA in atherothrombosis has not been studied as extensively as for MPA but have been found in patients with DVT [311], atherosclerosis and coronary artery disease [303], and sickle cell disease [314, 388]. NPA may have a larger role in immunothrombosis, and NETosis [101-103]. Both NPA and MPA were higher in patients with moderate and severe COVID-19 disease which could contribute to the thrombogenic phenotype of COVID-19 patients [305]. The increased NPA formation due to platelet activation with subsequent neutrophil activation provides a mechanism for increased NETosis seen in ECMO.

Platelets enhance leucocyte migration and endothelial adhesion by CD11b activation and CD62L shedding [398] and this observation that platelet-mediated activation of leucocytes is

unchanged in thrombocytopenia may explain the ongoing inflammation seen in ECMO patients, where there is often thrombocytopenia within a short period of initiating ECMO as described in Chapter 3, as well as ongoing platelet activation from the shear generated by the ECMO blood pump. The local acidosis at sites of active site of inflammation or in hypercarbic respiratory failure may also impair LPA formation and counteract immunothrombosis but increase the neutrophil inflammatory response, which is mediated by P-selectin [277, 399].

LPA contribute to acute lung injury

Neutrophil recruitment to the alveolar space is a key event in the pathophysiology of ALI. Platelet binding to neutrophils has been reported to increase neutrophil adhesion to endothelium and may be responsible for endothelial activation and ALI in murine models of acid lung injury and sickle cell disease [313, 314]. Zarbock et al. found acid aspiration induced P-selectin mediated platelet-neutrophil interactions in blood and lung capillaries as early as 30 minutes after injury, which increased vascular permeability and leucocyte recruitment. They found both reducing blood platelet count and blocking P-selectin inhibited NPA formation, resulting in increased gas exchange, and improved survival [313]. Polanowska-Grabowska et al. using similar methods also found platelet depletion and P-selectin blockade was associated with reduced pulmonary neutrophils and reduced pulmonary vascular leakage, and that platelet derived P-selectin and not endothelial P-selectin was responsible for the ALI [314]. Both these studies implicate platelet activation in the development of ALI which is P-selectin dependent. Leucocyte-platelet interactions are also found in TRALI [86] and LPS induced lung injury [347] with platelet depletion reducing the degree of lung injury in these models. The leucocyte-platelet interactions mediate neutrophil recruitment, activation and NETosis contributing to the degree of lung injury [86, 87, 97, 347]

More work needs to be done to reduce the formation of NPA and MPA in order to reduce their damaging effects in inflammation and immunothrombosis. Having robust models to investigate their interactions in physiological conditions and how to inhibit or reduce them is of importance to many clinical presentations.

6.5.6 Limitations

Whilst I was able to generate NPA in the ibidi microfluidics chamber, I was not able to identify NETs and therefore I cannot refute my initial hypothesis that LPA formation leads to

subsequent NETosis. Whilst neutrophil platelet interactions may be necessary for NETs to form, they are not sufficient and therefore it is not known whether the NPA that are identified from patient samples (in chapter 5) are related to the NETs that were identified both in whole blood and plasma samples (chapter 4). However, LPS and TRAP are not potent neutrophil agonists and were chosen for this reason to test my hypothesis, and NETosis occurs over a longer time course (4-6 hours) and therefore may not be formed in these one-hour experiments.

The ibidi microfluidics chamber can be used as a conceptual model of the ECMO circuit, but is not a perfect model of ECMO. The materials are not the same, firstly, the ibidi tubing is not heparin lined like most modern ECMO tubing, and the blood within the ibidi system is not exposed to the large surface area of the MO which adsorbs proteins, platelets and leucocytes to the oxygenator surface removing them from circulation or leading to increased activation, nor the HMSS of the ECMO pump [194, 371]. The 1 hour perfusion time within the ibidi system is short compared to perfusion through an ECMO circuit which is in use for days or weeks, with blood circulating through other organs such as the spleen, liver or lungs which can act as a reservoir, aid in the clearance of neutrophils, monocytes and platelets, and participate in uptake of inflammatory mediators [400, 401]. Furthermore the oxygen conditions are not comparable between the models; in homeostatic conditions neutrophils circulate in low oxygen concentrations (dissolved oxygen in blood 0.1-1.2%) [402], whereas in both the ibidi experimental model and in an ECMO circuit, blood and therefore neutrophils are exposed to higher FiO2 concentrations (21% for the ibidi, and 60-100% for ECMO) which has been shown to increase neutrophil activation (with reduced CD62L and increased CD11b expression) and NET formation in vitro [403].

I did not have time within the scope of this project to complete dose titrations of all reagents. Only two stimulants and two inhibitors were used with varying results. With regards to stimulants, LPS 100ng/ml is a commonly used concentration in cellular research to induce a significant inflammatory and activation response in neutrophils and monocytes and is well established within our lab in both whole blood and isolated cell stimulation [404-406]; and other groups for NPA formation [337]. However others have stimulated LPA formation using lower doses of LPS e.g. 10ng/ml [407]. Furthermore, the role of LPS in platelet activation is controversial. Galgano et al. describe the large range of LPS doses used in the literature ranging from 15pg/ml to 100 µg/ml, and the source of LPS (E.coli, salmonella, or klebsiella) is a critical factor in determining the agonist effect of LPS on platelet activation [408]. TRAP-6

was chosen as it is one of the agonists used in the Multiplate aggregometry, specifically activating the thrombin receptor, as a more physiological platelet agonist, and has not been reported to directly activate neutrophils. The dose of 10uM was used to avoid excessive platelet activation based on my own PRP stimulation data shown in 6.4.1, and from results from other platelet studies which used doses of 10-50uM ([334, 335]). The doses of the inhibitors Eptifibatide and KF38789 were selected based on the literature ([385, 386, 409]). However, Eptifibatide is commonly used as a continuous infusion rather than a singular dose and there have been no reports of KF38789 used for neutrophil-platelet interactions. KF38789 did not change LPA formation, but anti-P-selectin antibodies or PSGL-1 antibodies may increase inhibition as this shown in other studies [313, 390, 410]. Dose titration of agonists, inhibitors, and co-stimulation with both TRAP-6 and LPS as well as comparison with other stimulants and inhibitors would be useful to establish any dose-response relationship of each reagent to LPA formation, particularly if inhibitors are used clinically to determine safe and effective dosing.

6.5.7 Future work using the ibidi model for investigating LPA

This is an early model of investigating leucocyte-platelet interactions under laminar flow conditions in our lab. This model represents a reductionist system to ECMO for evaluating whole blood cellular interactions with an extracorporeal circuit, and allows evaluation of basic LPA formation, with addition of stimulants and inhibitors as well as frequency of sampling given the early platelet activation and LPA observed particularly with MPA. From these experiments I found similar findings with regards to NPA formation with different stimuli and inhibition as other groups validating the use of this model [292, 337].

Future work should include dose titrations of stimulants and inhibitors as well as co-stimulation to better represent the inflammation seen in patients who require ECMO. Other agonists could include PMA as a positive control for NETosis, calcium ionophore for both neutrophil and platelet activation, and other platelet agonists such as thrombin, or platelet activating factor. Other inhibitors which would be of interest would be P-selectin antibodies to block the P-selectin pathway, or other GPIIb/IIIa pathway inhibitors with different doses or administration e.g repeated dosing. Perfusing whole blood through the ibidi circuit represents similar conditions to ECMO initiation where the patient's circulating blood is exposed to the new ECMO circuit prior to endothelialisation. The increased NPA formation seen could help explain the increased NETosis seen after ECMO initiation in clinical samples (Chapter 4). After 24-48 hours of ECMO, there is protein and cellular deposition on the ECMO circuit.

Platelets and leucocytes interact with the protein biolayer, and the complement system propagating further activation and adhesion [124, 159]. To investigate LPA formation in a more chronic model of ECMO, the next step would be to seed endothelial cells within the ibidi microchannel slides prior to perfusion with whole blood to mimic the vasculature of an endothelialised ECMO circuit in longer term ECMO use. The change in flows would then alter the shear rates on the endothelial cells within the microchannel slides which may have further effect on LPA kinetics as found by Ahn et al, who found increased LPA formation with increased shear [372]. The model could also be reduced from whole blood to isolated cell populations using endothelial cells, isolated platelets or PRP, and neutrophils. Within this model, platelets, monocytes and neutrophils can be pre-exposed to stimulants or inhibitors to fully elucidate the cellular interactions that occur under flow or shear conditions. Using isolated cell populations can further validate whether TRAP-6 stimulation of platelet-free isolated neutrophils leads to neutrophil activation. In addition, the evaluation of aggregates containg neutrophils, monocytes and platelets together should be studied as found by Ahn who found these triple aggregates after stimulation with thrombin [372].

Despite the limitations this early work using the ibidi system shows promise and is the starting point for future work within the lab to investigating coagulation and immunothrombosis in extracorporeal circuits. The results from this work will not only apply to ECMO, but other extracorporeal circuits such as CPB and haemodialysis.

6.6 Conclusion

Understanding the mechanisms of neutrophil, monocyte and platelet activation and heterotypic aggregate formation is important in infective and inflammatory states where there is increased immune response and increased thrombosis. What is becoming clear is LPA formation leads to increased platelet-mediated leucocyte activation and therefore LPA not only increase immunothrombosis but also increase inflammation. This is exacerbated in ECMO where there are many factors contributing to the inflammation and immunothrombosis [159].

Using the ibidi microfluidics chamber, I demonstrated that NPA form in whole blood over time and is increased by platelet activation more than leucocyte activation and can be modulated by GPIIb/IIIa inhibition. This increased NPA formation due to increased platelet activation may explain the increased NETosis seen in ECMO patients, contributing to

immunothrombosis and thrombocytopenia and offers a potential therapeutic target. I also found different kinetics between NPA and MPA formation with MPA forming more readily even in unstimulated whole blood which has also been found by others. The significance of the difference between neutrophil and monocyte affinity to platelets has not been fully explored, but MPA formation also has roles in inflammation and thrombosis.

Preventing or reducing the interaction between platelets, leucocytes and endothelial cells may have multiple downstream benefits such as reduced immunothrombotic complications, reduced thrombocytopenia, and reduced lung injury. Since these interactions appear to be platelet-driven, this may already be achievable with anti-platelet drugs already in use, but we need to determine how to optimise the benefits of these drugs without increasing the bleeding risk. More work into the pathways driving platelet-mediated leucocyte activation and its inhibition is required to understand these processes and develop new therapeutic strategies.

This whole blood perfusion model is able to investigate LPA formation under flow conditions in vitro and I have validated a whole blood flow cytometry protocol for measuring NPA and MPA in vitro. The work presented in this chapter is preliminary work and the experimental models presented here can be further adapted in the future to further interrogate the effects of flow and endothelial shear on leucocyte and platelet activation.

Chapter 7 Discussion and conclusions

7.1 The mechanisms of immunothrombosis in extracorporeal circuits remain unclear

Despite decades use of ECMO, optimisation of anticoagulation regimes and advances in biomaterials, haemostatic complications of bleeding and thrombosis remain the main complications of ECMO [129, 195]. The thrombotic complications were further highlighted when patients have immunothrombotic conditions such as COVID-19 or in patients who have longer ECMO runs for other reasons [133, 179]. Over the last few decades there has been little further enhancement of ECMO biomaterials with almost all ECMO oxygenators being made with PMP since 2009 [32]. Instead, the focus has now changed to the cellular mechanisms of immunothrombosis.

Leucocyte-platelet interactions are key in immunothrombosis with both direct and indirect pathways of communication between cells. Many have examined numbers of extracellular vesicles from different cell populations, serum cytokine and chemokine levels as markers of indirect communication. Activated neutrophils release NETs and it has been shown that NETs and their individual components interact with coagulation and platelets in many ways [111]. LPA formation is an emerging area of interest in sepsis [313, 411], and other thromboinflammatory conditions [120, 282, 310, 311, 397, 412], and are a novel therapeutic target in thrombotic conditions such as sickle cell disease [388, 389]. However, there is little research into the role of LPA and their contribution to immunothrombosis in patients on ECMO. Furthermore, there are differences between monocytes and neutrophils which has not previously been explored in an ECMO population.

The primary aims of this thesis were to investigate why MO thrombosis occurs more in some patients compared to others, as well as the mechanisms leading to immunothrombosis in these patients by examining NETosis and leucocyte-platelet interactions particularly through LPA formation. I hypothesised that NETosis is a key mechanism for the development of immunothrombosis in patients on ECMO, particularly those who require circuit change and that LPA formation due to shear stress from ECMO would lead to increased NET formation. However, there is a disconnect between the clinical and in vitro work in my thesis. Whilst I was able to demonstrate the presence of NETs and LPA in patient samples, there was no relationship with circuit change, and the in vitro work has not demonstrated a relationship between LPA and NET formation. I have therefore not been able to prove my hypothesis that

neutrophil platelet interactions are a driving mechanism for increased immunothrombosis and NETosis.

Chapter 3 and 4 describe clinical observations in ECMO patients. In chapter 3, the features of MO thrombosis in ECMO patients with COVID-19 and non-COVID-19 ARDS are described, and there is increased incidence of ECMO thrombosis requiring a circuit change in patients with COVID-19, likely related to increased ECMO duration in this cohort of patients. Chapter 4 demonstrates NET formation in patients who require ECMO for ARDS with evidence of increase NETosis relating to being on ECMO which also decreases on discontinuation of ECMO. However, there were no changes in NETosis markers in patients who required circuit change and therefore the link between NETs and MO thrombosis cannot be proven from this clinical data.

I developed a method for measuring LPA for patient and in vitro work in chapter 5 and 6 and describe LPA in clinical samples however the patient LPA levels do not relate to levels of NETosis markers, and whilst there was increasing LPA formation over time in whole blood perfused through a microfluidics chamber in vitro, NET formation was not observed. Therefore, a causal relationship between LPA formation and specifically NPA, and NETosis cannot be made.

The initial hypothesised mechanisms may not be incorrect, but the data presented in this thesis do not support a clear link between neutrophil-platelet interaction, NETS and immunothrombosis in ECMO. The work described in these chapters may stand alone as individual pieces of work, but the overarching theme of ECMO related inflammation and thrombosis provides a coherent framework for discussion of mechanisms.

7.2 Summary of findings

7.2.1 ECMO is immunothrombotic and risk of MO thrombosis increases with ECMO duration

I first quantified the incidence of MO thrombosis in clinical practice, and the challenges in predicting need for circuit change as clinically there is not a biomarker or mechanical parameter that can be used alone to quantify risk of MO thrombosis. In Chapter 3, using COVID-19 as an immunothrombotic cohort, I compared circuit change frequency, and differences in clinically measured biomarkers in the lead up to circuit change in patients on VV ECMO. This was a retrospective analysis of over 270 patients from a single centre cohort of patients who were all on the same initial ECMO pump and MO (Cardiohelp with integrated HLS oxygenator). Patients with COVID-19 had twice the incidence of MO dysfunction requiring circuit change, and significantly longer ECMO runs than non-COVID-19 patients. Multiple logistic regression showed that the increased incidence of circuit change was related to the increased ECMO duration rather than directly from COVID-19 highlighting that ECMO itself is thrombogenic.

However, some clinical parameters used to predict need for circuit change differed in COVID-19 patients, in particular the lack of D-dimer rise in the lead up to circuit change. This likely represents a different mode of thrombosis in COVID-19 patients, which could be the lack of fibrinolysis seen in COVID-19, contributing to the increased thrombotic burden and pulmonary angiopathy seen in COVID-19 patients [93, 95, 202]. The immunothrombotic nature of COVID-19 could be the cause of other complications which lead to longer requirement of ECMO support. Firstly, the increased pulmonary angiopathy and microthrombi seen in COVID-19 leads to increased hypoxia and reduced native lung gas exchange resulting in increased arterial CO2 [93, 95, 413], and therefore requirement for increased ECMO blood flow, increased TMP, and MO resistance as demonstrated in the data in chapter 3. In addition, the cytokine storm associated with COVID-19 leads to increased inflammation and contributes to increased lung injury and delayed recovery time [20], and therefore increased duration of ECMO support required.

Although COVID-19 did not directly impact circuit thrombosis, it demonstrated how the lack of fibrinolysis, which likely contributes to the increased immunothrombosis of COVID-19, impacts the way ECMO circuit health is monitored. D-dimer, widely reported as the most useful predictor of need for circuit change [131, 135], was not as useful in COVID-19 patients highlighting a need for better biomarkers to monitor ECMO circuit health in general. With this

in mind, in chapter 4, I investigated biomarkers of immunothrombosis particularly neutrophil activation and NETosis in ECMO patients and found increased plasma levels of soluble NET specific markers CitH3 and nucleosome H3.1 after ECMO initiation, with a corresponding reduction in CitH3 levels after ECMO decannulation. This suggests that despite high levels of neutrophil activation (as seen by high levels of MPO, NE and cfDNA) the initiation of ECMO pushes neutrophils into a NETotic phenotype. However, at ECMO initiation, ventilation settings are also reduced to initiate lung rest with the aim of reducing ALI. The change in inflammatory mediators and cytokines could also be the mechanism of increased NETosis. Furthermore, the differences in cell-associated NETs and soluble NETs suggests that there may be 2 forms of NETosis occurring in ECMO patients with platelet-mediated activation of vital NETosis a potential pathway.

Whilst it is reported that there is increased NETosis in COVID-19 [278, 413], I did not find a difference in NETosis markers between COVID-19 and non-COVID-19 patients. These findings support the observational data from chapter 3 that ECMO is immunothrombotic, and increased duration of ECMO leads to increased risk of immunothrombosis rather than COVID-19 as an independent factor.

7.2.2 The need to distinguish between ECMO initiation or ECMO lung rest

ECMO initiation allows for lung rest ventilation settings to be initiated with the aim to reduce further lung injury, resulting in two interventions that are happening concurrently, and we need to determine which of the interventions leads to the changes in measured biomarkers. Similar to ECMO initiation, where despite high levels of neutrophil activation (high MPO, NE and cfDNA) there was an increase in NETosis markers; by decannulation, there were corresponding findings with reduction in neutrophil activation markers and further decreased in NETosis markers seen after ECMO decannulation (section 4.4.4). This supports the hypothesis that NETosis specifically is increased whilst on ECMO and this is reversed when the ECMO circuit is removed. Soluble neutrophil activation markers (CitH3, MPO and NE), and neutrophil surface markers of activation (CD66b, CD64) decrease by the time ECMO is no longer required, and this is likely related to lung recovery.

ECMO initiation is an inflammatory insult to the body often causing a SIRS reaction [159], and therefore various inflammatory mediators were also measured. There was reduction of pro-inflammatory cytokines such as IL-8, MCP-1, MMP-9, Ang-2, sRAGE TNFα and VEGF after

initiation of ECMO (section 4.4.2), many of which are released from the alveoli and contribute to endothelial injury and the pathophysiology of ARDS [7]. The decrease in these specific cytokines is therefore likely related to initiation of lung rest ventilation settings and reduction of further ventilator-induced lung injury once ECMO is initiated [245, 247, 249, 250], rather than ECMO initiation itself. To further characterise this, it would be useful to measure the levels of these inflammatory cytokines over the course of ECMO and compare levels when the patient starts to recover from their lung injury and conventional ventilation settings are initiated. To further add to this, levels can be measured in bronchoalveolar lavage fluid (BALF) before and after lung rest settings to compare the levels in the two compartments. It is not possible to apply UPV settings in a patient with severe ARDS, without the use of ECMO but if the levels of inflammatory cytokines in BALF decreases with UPV corresponding to those in plasma this would support the hypothesis that these cytokines decrease due to lung rest.

It is widely reported that ECMO induces platelet activation and dysfunction which contributes to the haemostatic complications whilst on ECMO [82, 124]. I found reduced serum levels of platelet activation markers CD62P and PF4 after ECMO initiation (section 4.4.7) which remained low during the ECMO run through to ECMO decannulation. However, these levels are related to platelet number, and this change could be due to the drop in platelet count after ECMO initiation, as platelets are adsorbed onto the ECMO circuit, or from shear of the ECMO circuit destroying the platelets [82]. There was also platelet dysfunction whilst on ECMO as measured by reduced response to agonists using Multiplate aggregometry, with recovery after decannulation of ECMO despite no change in the platelet count.

In conclusion, whilst there are two interventions at the time of ECMO initiation, my results suggest the increased NETosis and reduced platelet activation markers are likely secondary to exposure of blood to the ECMO circuit, and reductions in pro-inflammatory cytokines are due to lung rest. The decrease in NETosis markers after ECMO decannulation further supports the hypothesis that ECMO induces release of soluble free NETs components possibly through vital NETosis. Since the neutrophil lifespan is around 18 hours, we are able to see changes neutrophil related markers as soon as 24 hours after decannulation. In addition, the process of vital NETosis is reported to occur within a shorter time than lytic NETosis [68]. The changes in serum platelet activation markers after ECMO decannulation are likely less apparent as the average platelet lifespan is longer at 7-10 days, however there is change in the platelet function in response to agonists. The changes in serum platelet and

neutrophil activation markers seen in the patient samples suggests that neutrophil-platelet interactions play a part in the immunothrombosis of ECMO. To investigate this, I aimed to look at the role of LPA in this patient cohort.

7.2.3 The optimal anticoagulant for combined leucocyte and platelet work

As one of the first in our lab to investigate LPA, I needed to validate a method for quantifying LPAs in vivo as described in chapter 5. The choice of which anticoagulant the blood samples are taken can affect the levels of LPA that are measured, a finding that was common to other groups [119, 320]. Through the testing of samples from various anticoagulant tubes, I confirmed that LPA formation is calcium dependent and can be reversed by strong calcium chelation e.g. with EDTA. There was minimal LPA formation in vitro in EDTA blood compared to heparin blood and there was reversal of formed LPA after addition of EDTA to heparin patient blood samples. The order of LPA measured in different anticoagulants was Hirudin > Heparin > Citrate > ACD > EDTA in keeping with other groups [320]. The varying levels of calcium chelation did not affect the leucocyte activation markers. Due to this effect of calcium chelation on LPA formation, EDTA, citrate and ACD were not used for LPA quantification in this thesis and heparin was used instead for all leucocyte phenotyping and LPA work.

DTI have been proposed as a better anticoagulant for LPA [320]. I was able to test the LPA protocol in hirudin blood as this tube was collected in some patients who had platelet function assays at the time of sampling. The proportions of LPA were higher in hirudin anticoagulated blood compared to heparin, but there was also increased neutrophil and monocyte activation in the hirudin samples. Many studies investigating leucocyte phenotypes have used EDTA anticoagulated blood [72, 74, 321], and since there were increased neutrophil and monocyte activation markers in hirudin samples this was presumed to be artefact and hirudin was not used. However, Wood et al, used argatroban, a clinically used DTI and also found increased neutrophil activation and phagocytosis in argatroban samples compared to heparin, citrate and EDTA but suggested this was a true representation of neutrophil activity [329]. This corresponds with the findings in this thesis and perhaps DTI do give the highest yield of LPA, and neutrophil activity, as many pathways for neutrophil activation are calcium dependent [414]. In addition, there are mixed reports that heparin can both reduce and increase neutrophil activation and NETosis [415, 416]. Application of argatroban in future laboratory work will help define its utility in this setting. Like heparin, it is a commonly used anticoagulant clinically and many ECMO centres are using bivalirudin or

argatroban for anticoagulation in ECMO patients due to less immune mediated reactions such as HIT and perhaps a better side effect profile, such as less thrombocytopenia [417-419].

The best anticoagulant to use for leucocyte and platelet work with will depend on the output required and local lab processing protocols. Many studies investigating platelet work in vitro use citrate or ACD blood and replace the calcium prior to stimulation, and for clinical samples perhaps DTI are the best anticoagulant, however consistency within the lab is the main factor. Since most patients are anticoagulated with heparin in RBH, I used heparin anticoagulated blood for my work. Future work could include comparison with other anticoagulants and their effect of LPA formation.

7.2.4 LPA formation in vitro is dependent on platelet activation and can be reduced by GPIIb/IIIa inhibition

LPA formation appears to be reliant on platelet activation more than leucocyte activation. This is also shown in the in vitro stimulation work where the proportion of LPA formed was much higher with TRAP-6 stimulation of platelets compared to LPS stimulation of leucocytes (section 6.4.2). When platelet activity was inhibited by the addition of eptifibatide, a GPIIb/IIIa inhibitor, this reduced NPA formation in unstimulated and TRAP-6 stimulated samples but not in LPS stimulated samples. In addition, despite P-selectin binding to PSGL-1 being one of the major pathways for leucocyte-platelet interaction, inhibition of the P-selectin pathway using the compound KF38789 did not show any reduction in LPA formation in this set of experiments. However, this compound has not previously been applied to modulate leucocyte-platelet interactions.

Furthermore, the kinetics of LPA formation differ between monocytes and neutrophils, with increased affinity of monocytes to platelets compared to that of neutrophils which may explain the lack of difference with either inhibitor in MPA formation. The high affinity of platelets to monocytes is also seen in the high levels of MPA formation within the first few minutes of perfusion in the ibidi system being almost 100% after only 5 minutes. Whilst the differing affinity of leucocyte subtypes to platelets has previously been reported [119, 337], this is one of few studies that has compared the kinetics of NPA formation to MPA formation. But the significance of this when considering the ratio of neutrophils to monocytes in peripheral blood is yet to be determined.

Many groups have reported on the involvement of LPA in sepsis [411], coronary artery disease [120, 310, 390], sickle cell disease [387], renal disease [315, 397] and other thromboembolic diseases [311]. The contribution of LPA to disease is an area of growing interest particularly in immunothrombotic conditions e.g. COVID-19 where there were increased numbers of NPA and MPA and correlated with severity [305], and in ECMO where there is increased immunothrombosis [292]. I was able to measure LPA in ECMO patient samples of which there were varying proportions across many patients, however, not enough to make meaningful comparisons. There is only one recent study that has reported on LPA in ECMO patients and they found increased basal levels of both NPA and MPA in patients whilst on ECMO with increased platelet expression of P-selectin [292]. More work needs to be done in this area.

7.3 Clinical relevance

Many ECMO centres manage their patients in a standardised manner with the same lung rest ventilation settings, standardised protocols for anticoagulation, and monitoring of circuit health [212, 420]. Whilst this is an effective way to manage complex patients with severe respiratory failure, ARDS is a heterogenous condition, and management should also depend on the aetiology of ARDS. COVID-19 as an immunothrombotic condition highlighted the impact of immunothrombosis on the degree of respiratory failure and the requirement for increased duration of ECMO. Due to the slower resolution of respiratory failure in COVID-19 patients, and therefore longer duration of ECMO, we were able to observe more immunothrombotic complications of ECMO including the increased need for circuit change, and the difficulty in monitoring circuit health due to the mechanism of clot formation/lack of clot resolution in these patients. This highlights the need for better biomarkers to monitor for circuit health, particularly in times of pandemic when resources are more strained and decisions regarding MO thrombosis and circuit change have increased relevance.

NETosis and immunothrombosis in ECMO

The finding of increased NETosis after initiation of ECMO which decreases within 24 hours after ECMO decannulation is novel and, to my knowledge, has not previously been described. Some studies have found increased levels of NETs in patients on ECMO and other extracorporeal circuits compared to healthy volunteers [107, 108, 225, 421] but few have investigated NETs levels before, during and after ECMO and we are the first to publish positive findings on NETosis levels before and after ECMO cannulation in human samples [422]. We found increased levels of soluble NETs after ECMO initiation, which represents NET

components which are cleaved from cell-associated NETs possible due to shear, or due to vital NETosis secondary to increased leucocyte-platelet interactions leading to NADPH oxidase independent neutrophil activation. There is increased platelet activation secondary to contact activation, and shear from the ECMO pump, leading to increase direct and indirect leucocyte-platelet interactions.

This compelling evidence for NETosis due to ECMO highlights a potential pathway for ECMO related thrombosis and therefore a potential pathway for intervention for example, Clusterin supplementation has been shown to neutralise the effects of histones released from NETosis [299] . Furthermore, it has been suggested that NETosis is one of the drivers for thrombocytopenia and HIT in ECMO patients, as they can directly activate and trap platelets [84, 225, 244]. If we can limit the process that drive NETosis perhaps the degree of thrombocytopenia, immunothrombosis and incidence of thrombotic complications such as circuit thrombosis can be reduced.

LPA and thrombocytopenia

LPA are an emerging are of interest in sepsis and thromboinflammatory conditions. Leucocytes and platelets are both activated in sepsis and further activated by initiation of ECMO, therefore it is reasonable that levels of LPA would be elevated in this cohort of patients. LPA are present in ECMO patients and appears to be dependent on platelet activation. It is possible that ECMO induced activation of platelets by shear from the ECMO pump, or from contact activation from exposure to the ECMO circuit [194] leads LPA formation resulting in downstream neutrophil activation and increased NETosis [84, 346]. Furthermore, LPA formation could be another cause for thrombocytopenia during ECMO as the platelets are adhered to the leucocyte cell surface [351].

Reducing leucocyte-platelet interactions could therefore be another therapeutic target to reduce haemostatic complications of ECMO (both thrombotic and haemorrhagic). I was able to demonstrate a reduction in LPA formation in vitro by using the GPIIb/IIIa inhibitor eptifibatide. Whilst eptifibatide has been shown to cause increased bleeding in patients supported on other forms of ECLS in particular for VA ECMO where bleeding events are higher [379-381], it does not preclude its use in VV ECMO perhaps in lower doses or as a single dose, and is a practical starting point for investigating targeted therapies to reduce LPA formation in ECMO patients. P-selectin inhibition using KF38789 20uM did not reduce LPA

formation in my experiments but there are other methods of inhibiting the P-selectin PSGL-1 interaction such as P-selectin or PSGL-1 antibodies. Some P-selectin antibodies such as Crizanlizumab [388] and inclacumab [423] are used for preventing sickle cell crises, suggesting that it is possible to reduce LPA formation in thrombotic conditions. These may be useful in reducing LPA in ECMO patients. These antibodies may be better agents for reducing LPA formation compared to KF38789.

In summary, the initiation of ECMO leads to increased platelet activation, which leads to LPA formation with already primed leucocytes. The direct platelet-leucocyte interactions can modify the inflammatory properties of leucocytes, in particular increasing neutrophil activation through a separate pathway to infection driven neutrophil activation which leads to NETosis.

7.4 Limitations

It is important to recognise the limitations of both the clinical and in vitro aspects of this project.

7.4.1 Retrospective data analysis

The observational data described in chapter 3 compares 2 large cohorts of patients, but the observational, retrospective nature, and single centre population limits the analyses that can be carried out. The two main cohorts of patients were those with and without COVID-19. Whilst in general, patients with COVID-19 had longer ECMO runs and therefore increased likelihood of requiring a circuit change, practices may have differed during times of pandemic due to unfamiliarity with a new condition, and lack of resources in times of increased demand. There were missing values in many clinical indices which could be due to the pressures of the pandemic which led to exclusion of many patients from analysis. The comparison of COVID-19 to non-COVID-19 ARDS follows suit with other large cohort studies carried out by ELSO and other groups. However, the non-COVID-19 cohort includes a more heterogenous population including influenza, other types of viral pneumonitis, bacterial pneumonia and other causes of ARDS. The generalisation into two populations makes it possible for a large cohort analysis but limits the conclusions that can be drawn. A better analysis would be to compare COVID-19 to other viral pneumonitis, or include bacterial pneumonia, and indirect lung injury as individual cohorts but in our single centre data these populations were not large enough individually to make meaningful comparisons.

7.4.2 Clinical samples and analysis of biomarkers

The data presented in chapter 4 came from a total 50+ ECMO patients and includes patients with increased immunothrombosis (COVID-19). To my knowledge this is the largest study of NETosis markers in an ECMO population and shows some promising preliminary data.

Whilst the clinical samples were collected from two separate studies (DeVENT and HITEC), they were from a single centre which meant patients were managed according to the same ECMO protocols and had the same clinical data collected. However, the limitations of a single centre study still apply. The spread of samples was also impacted by the COVID-19 pandemic due to the recruitment windows for each study. The DeVENT study recruited mostly patients with COVID-19 ARDS and the HITEC study, patients with non-COVID-19 ARDS. In addition, each study followed different sampling timelines. The timing of samples in the DeVENT study were related to the day of recruitment and day of mechanical ventilation as this was the primary aim of the trial whereas the samples in the HITEC study relate to the day of ECMO. Furthermore, the sampling frequency was different for the two studies with the DeVENT study sampling every 3 days in the first 2 weeks after recruitment and HITEC study only once weekly and after significant events such as circuit change or decannulation. Although sample time points were matched where possible to the day of ECMO, this was not possible for all patients, therefore, longitudinal analyses could not be performed. The timing of sampling is crucial to characterise NETosis in the early stages of ECMO initiation and future work should involve standardised sampling timelines which may include more frequent sampling in the hours after ECMO initiation. Additionally, as a tertiary centre in a hub and spoke model the pre-ECMO data was not always available or was inaccurate due to the data entered on the referral forms, particularly during the peak of the COVID-19 pandemic. Nevertheless, this is valuable pilot data for future studies into NETosis in extracorporeal circuits.

There are no significant correlations between NETosis and inflammation in this data set, but currently there are only 20 patients with matched NETosis and inflammation data therefore it is not possible to draw meaningful conclusions. Analysis of inflammatory cytokines for all samples with neutrophil and platelet activation markers would improve this analysis. A larger study which includes data from multiple centres for example, the referral centres, would also enable recruitment of patients of different aetiologies and severities of lung injury, allowing us to fully elucidate the impact of SARF and ECMO on inflammation, neutrophil activation, NETosis and leucocyte-platelet interactions.

As well as the small number of patients with relevant samples for analysis, there is in extensive range of confounding factors beyond the ECMO circuit which can affect the results, such as aetiology of respiratory failure and its management, level of shock and potential use of steroids, patients pre-morbid state, and other organ failure and organ support e.g. haemofiltration and the addition of a second extracorporeal circuit. As such, causal relationships are not able to be inferred from this data.

7.4.3 Developing and optimising protocols

Cell-associated NETs

Measuring serum markers of NETs using ELISA is a surrogate for the level of NETosis and only represents NETs which have become detached from the neutrophil or expelled from the neutrophil within vesicles. Since neutrophils have a short life span, measuring cell-associated NETs will give a better understanding of the level of neutrophil activation at the time if correlated with neutrophil phenotypes. The advantage of using flow cytometry is the ability to measure neutrophil number, phenotype and function. It may also help to distinguish neutrophils undergoing lytic NETosis from vital NETosis and other forms of cell death [272]. The variation in the literature in protocols for measuring cell-associated NETS in whole blood demonstrates the potential lack of validity in this method. Neutrophils are also easily activated from neutrophil isolation and centrifugation protocols [273], and the ability to measure NETs in whole blood samples reduces sample manipulation compared to previous methods where the neutrophils had to be isolated from blood prior to flow cytometry measurement. The limited number of protocols which have been reproduced in the literature demonstrates how difficult it can be to measure neutrophils undergoing NETosis particularly in hyperactivated conditions such as in sepsis or thrombosis. The flow cytometry protocol used in this thesis was being developed and validated in a specific cohort of patients and whilst I was able to distinguish different populations of neutrophils with low and high proportions of cell-associated NETs in vitro, the results from patient samples is variable.

As a result, most work measuring NETs in clinical samples relies on immunofluorescence and on soluble measures of NETosis. There were some correlations between the flow cytometry measured cell-associated NETs and plasma levels of MPO and NE, but until protocols for measuring cell-associated NETs in whole blood using flow cytometry are validated, the conclusions that can be drawn are limited. Furthermore, in many studies the

terms NETs and cell-associated NETs are used interchangeably, and nomenclature should be scrutinised when reviewing the literature.

Leucocyte-platelet aggregates

The presence of LPA was analysed using flow cytometry, with further analysis of leucocyte activation markers and cell-associated NETs. There are not enough samples with LPA quantified to allow meaningful comparisons over time and limits the generalisability and applicability of the findings. This is in part due to the time taken to optimise the LPA flow cytometry protocol, and the sporadic nature of samples taken for LPA quantification due to my availability when blood samples were being taken (out of hours, or other commitments). However, the protocol developed was validated and I have demonstrated that it is possible to measure LPA in this cohort of patients. This will lead to future work in measuring LPA in other patient samples. In addition, due to the time it took to optimise these protocols and the initial focus of this project being neutrophil activation and NETosis, platelets and their activation markers were not studied in detail. Considering the findings that LPA formation is related to platelet activation, analysis of other platelet activation markers on platelets and LPA using flow cytometry would be a useful adjunct to support the current findings and correspond to work done by other groups. This would require more work and further assessment of which anticoagulant samples should be taken in which was beyond the time frame of this project.

A further weakness in the clinical analyses is that healthy controls were used to form a baseline. A useful additional comparator when looking at the effects of ECMO on NETosis, LPA, and platelet activity would be a cohort of patients with severe ARDS who did not require ECMO. In the DeVENT study there was a small number of patients who were recruited with ARDS who did not go onto have ECMO, however all these patients had COVID-19 and there were only 10 patients in this group limiting conclusions that can be drawn from this. The HITEC study did aim to recruit ARDS patients who did not require ECMO, however all these patients were managed in the referring centres and not retrieved and therefore could not be recruited. Including patients with SARG who did not go onto have ECMO, would allow further clarification of changes that happen due to lung rest or initiation of ECMO. However, these patients who do not require ECMO are more likely to have mild or moderate ARDS which may obscure the detection of truly divergent pathophysiology that occurs due to ECMO initiation.

7.4.4 In vitro work

The in vitro models used with regards to the ibidi microfluidics system and use of whole blood is the first to be carried out in this laboratory. There were many optimisation steps, and the aim was that the model would be representative of physiological blood flow in an extracorporeal circuit to examine leucocyte-platelet interactions. This relatively simple microfluidics model is not representative of the complexity of ECMO in a patient setting where blood circulates through the inflamed lungs, and other organs such as the liver or spleen which can impact the circulating cell populations; and also, the complexity and surface area of the ECMO circuit and its oxygenator. The use of LPS and TRAP-6, are relevant to sepsis and platelet activation and are established agonists in in vitro work and clinical assays. There is ongoing debate of which anticoagulant to use when carrying out in vitro experiments designed to investigate platelet activation, which has been extensively discussed in chapter 5. Heparin anticoagulated blood was used in this project to represent ECMO patient blood, but many groups have taken blood using calcium chelating anticoagulants such as ACD and replace calcium prior to stimulation within the experiment to avoid any activation between venepuncture and experiment start. There were no cells adhered to the microchannel slide and therefore shear was not able to be calculated. This could be representative of a new ECMO circuit at initiation but does not represent blood flow within an endothelialised circuit or in the native blood vessel.

The stimulation model is a one-hit model with either a platelet agonist or leucocyte agonist. In septic conditions such as in patients with severe ARDS who require ECMO, there are often multiple modes of cell activation. Comparison of simultaneous platelet and leucocyte activation with the existing single agonists may yield some interesting results. This also applies to the inhibition experiments. The inhibitors are added to the blood before any stimulation. In clinical use, eptifibatide is given as an initial bolus dose followed by a continuous infusion. Whilst a continuous infusion is not able to be simulated in the ibidi model, repeated dosing may better represent the effects of eptifibatide in vivo and produce more inhibition that that already seen. In addition, adding the inhibitors after activation has occurred (e.g. after 30minutes of perfusion) may also inform us if LPA formation is reversed by these agents as well as being inhibited. The use of KF38789 for the inhibition of LPA formation has not previously been reported, which may explain the lack of results seen, or a dose titration may be required.

With regards to the best method for measuring soluble components of NETosis, single biomarker assays are limited in the conclusions that can be drawn, which is why the use of CitH3 has been unique. Many groups have developed and used an MPO-DNA complex ELISA [263, 265, 424] using an MPO antibody (Biorad clone 4A4, 0040-0002) and the detection portion of a cell death ELISA (Roche diagnostics). I tried to develop an MPO-DNA ELISA using these previously described protocols but had poor results when analysing clinical samples. This may be due to the narrow detection range of this ELISA, and the large variability in ECMO patient samples, particularly with high levels of NETosis in ECMO patients. The narrow detection range could in part be due to poor quality antibodies. Unfortunately, I did not have time to further develop this assay, but it is generally agreed that a NET-complex ELISA for MPO, NE and DNA would be a better assay for NETosis than these components on their own as demonstrated in Chapter 4.

7.5 Future Work

There are many open questions remaining following the work in this thesis leading to several future potential work streams or projects.

7.5.1 Ongoing HITEC study recruitment

The HITEC study is still recruiting and has now recruited over 120 patients at the time of writing this chapter. Future work would be to carry out longitudinal analyses on the remaining stored plasma samples from these patients, as well as comparisons between different non-COVID-19 ARDS aetiologies. The HITEC study is an exploratory study, and the sampling time points were weekly from ECMO initiation. Since, the average ECMO run in non-COVID-19 ARDS was around 2 weeks it may be better to increase the frequency of sampling time points similar to that of the DeVENT study, which was every 3-5 days. This would give more granular data on the immunothrombotic changes that occur during the ECMO run and when there is evidence of lung recovery and ECMO support being reduced.

Furthermore, there have been two approved amendments to the study: 1) collection of BALF from recruited patients so that comparisons of inflammatory cytokines can be compared between plasma and alveolar components to determine the effects of lung rest whilst on ECMO; and 2) imaging of the membrane oxygenator after disconnection from the patient. Both these sub-studies are in the early stages.

It is known NETosis markers are found in BALF of patients with ARDS [85, 89]. To fully understand the impact of VILI and the lung rest that ECMO affords, as well as the impact of ECMO, the levels of NETosis and inflammatory cytokines could be compared across the two compartments before and after ECMO initiation, during lung recovery whilst on ECMO and after ECMO decannulation. Furthermore, a study that compares the effect of standard lung-protective ventilation with UPV whilst on ECMO could shed light on the benefits of UPV which may further support the use of ECMO for severe ARDS.

The HTIEC study was also approved for recruitment of patients on CPB and VA ECMO, but this was not possible due to time constraints. The CPB population would be a non-inflamed cohort on an extracorporeal circuit compared the inflamed ARDS ECMO cohort, and further sub-analyses could include the effects of the roller pump compared to centrifugal pump, or PP compared to PMP oxygenators. VA ECMO patients could also be a less inflammatory patient cohort depending on the aetiology of cardiac failure, whether it was post-cardiotomy and post-CPB or primary VA ECMO. Comparing differences between VA and VV ECMO patients may bring some interesting findings. Recruitment at Harefield Hospital was not possible due to the availability of research staff therefore we were not able to recruit patients on ventricular assist devices who are usually non-inflamed, but on support via an extracorporeal circuit often without MO.

The HITEC study is still open for recruitment at RBH and is now enrolling patients on VA ECMO as well as VV ECMO. The study has been approved to recruit in St Thomas' Hospital pending local research governance approval and site initiation visit. St Thomas' Hospital is a large tertiary hospital with general ICUs, cardiac ICU, and an ECMO ICU and therefore would be able to capture all the patient cohorts described. As mentioned, further studies into the effect of ECMO and initiating UPV on inflammation and immunothrombosis will be useful. The results of the upcoming ultra-ECMO trial (in VA-ECMO) [425] and Rest or Moderate Mechanical Ventilation during ECMO support (ROMEO) trial (IRAS 256932, REC 21/NW/0101, NIHR158537) [426] will be interesting.

7.5.2 Comparison of other ECMO pumps and oxygenators

In chapter 3, only patients with a Cardiohelp and integrated oxygenator as their primary circuit were included in my analysis which allowed for a better comparison between COVID-19 and non-COVID-19 cohorts. This is because the Cardiohelp is the primary mobile ECMO

circuit that is used in our centre. There were around 30 patients who were managed on a Centrimag device but with various oxygenators who were excluded from the initial analysis. A multi-centre prospective study would allow comparisons of different ECMO pumps and oxygenator combinations and their impact on circuit change frequency and blood biomarkers across the ECMO run. For example, The Royal Papworth Hospital ECMO centre uses primarily the Centrimag pump. The Centrimag pump is compatible with various oxygenators from other manufacturers e.g. A.L.One oxygenator (Euroset), Nautilus (Medtronic) and Hilite (Medos) each with vary shapes and numbers of inlets and outlets designed to improve blood flow in the oxygenator without increasing shear or activation of blood cells.

In addition, it would be worth comparing patients who are on support via percutaneous VAD or an extracorporeal circuit without an MO. It is known that the MO causes the most contact activation due to its large surface areas and it is thrombosis at the MO that requires circuit change, so the blood parameters may differ when there is no oxygenator in the circuit. Furthermore, comparison of patients on ECMO with those on CPB for cardiac surgery may be interesting. Patients on ECMO usually have a preceding infective or inflammatory insult which necessitates the need for ECMO and therefore have leucocytes and platelets that are already primed or activated, whereas patients who have elective cardiac surgery are not inflamed until initiation of surgery and CPB. This would be a realistic comparator to observe the effects of extracorporeal circuits and oxygenators on inflammation and thrombosis. Whilst we had ethical approval to investigate all forms of ECLS circuits, this was beyond the scope of this thesis and would be an interesting avenue to explore.

7.5.3 Visualising the thrombotic deposits

The clinical biomarkers and ECMO mechanical parameters used to monitor for circuit thrombosis are not specific and are often affected by the underlying condition. It is not known whether these markers correlate to the amount of thrombosis within the oxygenator. Some groups have used CT to image oxygenators of ECMO circuits after explantation from the patients after completion of ECMO and found that most of the thrombotic load is on the venous/inlet side of the Quadrox oxygenators [130, 138]. But there are no reports comparing the clot volume in oxygenators that have been explanted due to oxygenator thrombosis to those after decannulation. The hypothesis is that those oxygenators that have been explanted due to oxygenator thrombosis will have higher clot volume than those after circuit change, or that clot volume may correlate with ECMO duration. An amendment was approved by HRA REC

to CT image oxygenators from patients enrolled into the HITEC study however there was not enough time within this project to start this sub study.

To be able to visualise clots within the oxygenator to assess clot volume and location would be a useful assessment in cases where it is ambiguous whether a circuit change is required or not. However, it is not possible to perform CT scans whilst the ECMO circuit remains attached to the patient due artefact from the metalwork in the ECMO pump. This is an interesting avenue of investigation as others have assessed whether an ultrasound based assessment of blood flow through the oxygenator [427] or injecting fluorescent dyes and assessing using fluorescence imaging [428] could be used for real-time detection of thrombosis in a oxygenator, however these methods have not been validated in vivo yet.

7.5.4 Developing the in vitro model of ECMO circulation

Further iterations of the ibidi microfluidics experiment model can be run with other agonists, co-stimulation with leucocyte and platelet agonists, and dose titration of agonists and inhibitors, particularly lower doses. In a preliminary model of platelet stimulation, I stimulated PRP with various agonists such as thrombin and calcium ionophore, as well as LPS and TRAP-6. Thrombin caused large platelet clumps within the plasma and therefore was not used for stimulation experiments, with TRAP-6 used instead. The effect of other platelet agonists such as ADP, collagen or platelet activating factor could be used to characterise the pathways for platelet aggregation to leucocytes.

It would be ideal to progress the model complexity to include cultured endothelial cells into the microchannel slide to mimic the vasculature and therefore observe the effects of shear on LPA formation and leucocyte and platelet activation. The model could also be simplified to look at isolated endothelial cells, neutrophils or platelets within the microfluidics system to fully elucidate the pathways involved in LPA formation. Whilst my work using whole blood has allowed us to see the differential effects of NPA and MPA formation, to fully elucidate the monocyte-platelet and neutrophil-platelet interactions, a cell culture model may be better.

Regarding LPA inhibition within the ibidi model, further work could involve dose titration, or continuous infusion/repeated dosing as would be run in patients to maintain a higher blood concentration. The inhibitors could be added to the perfusion chamber after 15-30 minutes of

stimulation to investigate if the LPA formed were reversible, as well as being inhibited. EDTA can be used as a positive control for reversibility.

To further investigate the P-selectin and GPIIb/IIIa pathway, the effects of Mac-1 receptor or P-selectin inhibition using monoclonal antibodies would be useful. As well as eliminating the intermediary proteins fibrinogen or CD40L. This would help to discern if it is the interaction of GPIIb/IIIa with the Mac-1 receptor or reduced platelet-platelet aggregation that affects LPA formation. Other P-selectin pathway inhibitors such as monoclonal antibodies (Crizanlizumab and inclacumab) may have more effect than KF38789. Whilst KF38789 did not have an effect on LPA formation at the dose I used in my experiments, it may have an effect on leucocyte-endothelial interactions.

7.5.5 Platelet activation and NETosis

Following on from my findings I hypothesise that the high levels of plasma NETosis markers measured using ELISA, but low levels of cell-associated NETs measured using flow cytometry in whole blood samples could be representative of vital and lytic NETosis. It is possible that there is NETosis due to cell death and therefore lytic NETosis in patients with ARDS, however during ECMO the increased platelet activation from the ECMO pump, leads to increase NPA formation and initiation of vital NETosis which results in expulsion of NET components, but not cell death and therefore fewer cell-associated NETs.

This hypothesis requires further work to demonstrate that platelet activation and NPA formation leads to NETosis. NETosis by cell death occurs 2-4 hours after stimulation [429] and this 1-hour perfusion is not long enough to stimulate NETosis therefore NETosis markers and whole blood NETs were not measured. Early experiments were analysed for NETs but there were no NETs found. It is known that activation of platelets via LPS and by basic platelet agonists stimulates NET formation [83, 346]. Furthermore, the idea that there are two processes of NETosis remains contentious and confirmation that these two pathways exist requires more investigation.

Due to the difficulties in measuring NETs using flow cytometry and many groups relying on measuring soluble markers of NETosis using ELISA, distinguishing between two forms of NETosis is not possible using only these two techniques. It would be ideal to visualise the two forms of NETosis as well as presence of NPA and MPA using fluorescent microscopy. I had managed to develop a protocol for imaging platelets, neutrophils and NETs in cell

culture conditions using fluorescent microscopy (Figure 7.1). Real-time microscopy of the ibidi slides is possible but I was not able to adapt these protocols in the time I had.

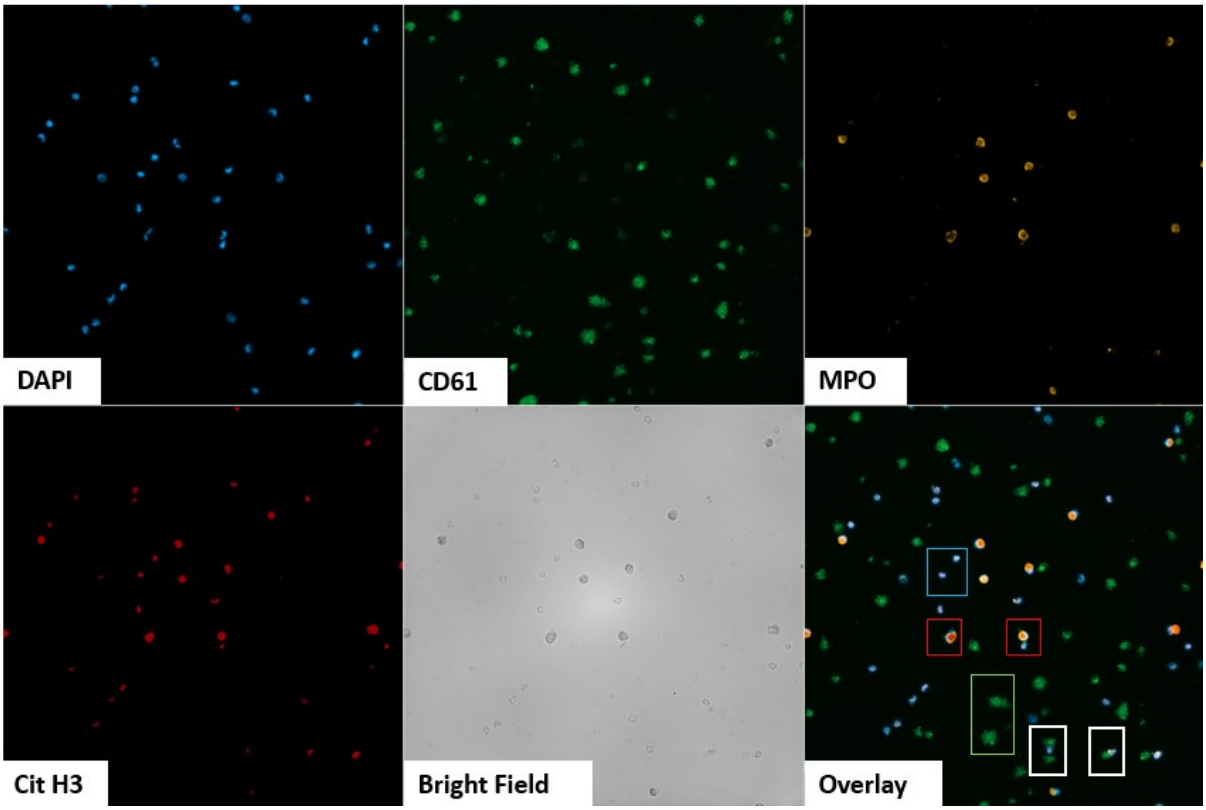


Figure 7.1 Fluorescent microscopy of neutrophils and platelets stimulated with calcium ionophore.

Neutrophils and platelets were stimulated with calcium ionophore in a tissue culture plate with calcium ionophore for 3 hours. Cells after incubation were stained for nuclei with DAPI (blue), MPO (orange), citrullinated H3 (red), and platelets with CD61 (green); and analysed by widefield microscopy (40x magnification with oil). In the overlay, neutrophils are identified as multilobed nucleated cells (blue box), NETS as nucleated cells colocalised with MPO and/or citrullinated histone H3 (red box), platelet clumps in the green box, and neutrophil-platelet aggregates as nucleated cells colocalised with platelets (white box).

REFERENCES

1. Ashbaugh DG, Bigelow DB, Petty TL, Levine BE. Acute respiratory distress in adults. Lancet. 1967;2(7511):319-23.
2. Bernard GR, Artigas A, Brigham KL, Carlet J, Falke K, Hudson L, et al. The American-European Consensus Conference on ARDS. Definitions, mechanisms, relevant outcomes, and clinical trial coordination. Am J Respir Crit Care Med. 1994;149(3 Pt 1):818-24.
3. Murray JF, Matthay MA, Luce JM, Flick MR. An expanded definition of the adult respiratory distress syndrome. Am Rev Respir Dis. 1988;138(3):720-3.
4. Griffiths MJD, McAuley DF, Perkins GD, Barrett N, Blackwood B, Boyle A, et al. Guidelines on the management of acute respiratory distress syndrome. BMJ Open Respir Res. 2019;6(1):e000420.
5. Peek GJ, Mugford M, Tiruvoipati R, Wilson A, Allen E, Thalanany MM, et al. Efficacy and economic assessment of conventional ventilatory support versus extracorporeal membrane oxygenation for severe adult respiratory failure (CESAR): a multicentre randomised controlled trial. Lancet. 2009;374(9698):1351-63.
6. Bellani G, Laffey JG, Pham T, Fan E, Brochard L, Esteban A, et al. Epidemiology, Patterns of Care, and Mortality for Patients With Acute Respiratory Distress Syndrome in Intensive Care Units in 50 Countries. JAMA. 2016;315(8):788-800.
7. Vassiliou AG, Kotanidou A, Dimopoulou I, Orfanos SE. Endothelial Damage in Acute Respiratory Distress Syndrome. Int J Mol Sci. 2020;21(22).
8. Mukhopadhyay S, Hoidal JR, Mukherjee TK. Role of TNFalpha in pulmonary pathophysiology. Respir Res. 2006;7(1):125.
9. Lucas R, Hadizamani Y, Enkhbaatar P, Csanyi G, Caldwell RW, Hundsberger H, et al. Dichotomous Role of Tumor Necrosis Factor in Pulmonary Barrier Function and Alveolar Fluid Clearance. Front Physiol. 2021;12:793251.
10. Jabaudon M, Berthelin P, Pranal T, Roszyk L, Godet T, Faure JS, et al. Receptor for advanced glycation end-products and ARDS prediction: a multicentre observational study. Sci Rep. 2018;8(1):2603.
11. Blondonnet R, Audard J, Belville C, Clairefond G, Lutz J, Bouvier D, et al. RAGE inhibition reduces acute lung injury in mice. Sci Rep. 2017;7(1):7208.
12. Audard J, Godet T, Blondonnet R, Joffredo JB, Paquette B, Belville C, et al. Inhibition of the Receptor for Advanced Glycation End-Products in Acute Respiratory Distress Syndrome: A Randomised Laboratory Trial in Piglets. Sci Rep. 2019;9(1):9227.
13. Medford AR, Millar AB. Vascular endothelial growth factor (VEGF) in acute lung injury (ALI) and acute respiratory distress syndrome (ARDS): paradox or paradigm? Thorax. 2006;61(7):621-6.
14. Bhandari V, Choo-Wing R, Lee CG, Zhu Z, Nedrelow JH, Chupp GL, et al. Hyperoxia causes angiopoietin 2-mediated acute lung injury and necrotic cell death. Nat Med. 2006;12(11):1286-93.
15. Huang X, Xiu H, Zhang S, Zhang G. The Role of Macrophages in the Pathogenesis of ALI/ARDS. Mediators Inflamm. 2018;2018:1264913.
16. Tanaka T, Narazaki M, Kishimoto T. IL-6 in inflammation, immunity, and disease. Cold Spring Harb Perspect Biol. 2014;6(10):a016295.
17. Swaroopa D, Bhaskar K, Mahathi T, Katkam S, Raju YS, Chandra N, et al. Association of serum interleukin-6, interleukin-8, and Acute Physiology and Chronic Health Evaluation II score with clinical outcome in patients with acute respiratory distress syndrome. Indian J Crit Care Med. 2016;20(9):518-25.
18. Williams AE, Jose RJ, Mercer PF, Brealey D, Parekh D, Thickett DR, et al. Evidence for chemokine synergy during neutrophil migration in ARDS. Thorax. 2017;72(1):66-73.
19. Yang SC, Tsai YF, Pan YL, Hwang TL. Understanding the role of neutrophils in acute respiratory distress syndrome. Biomed J. 2021;44(4):439-46.

20. Montazersaheb S, Hosseiniyan Khatibi SM, Hejazi MS, Tarhriz V, Farjami A, Ghasemian Sorbeni F, et al. COVID-19 infection: an overview on cytokine storm and related interventions. Virol J. 2022;19(1):92.
21. Ratano D, Fan E. Management of Severe ARDS: New Strategies and Ongoing Challenges. Respir Care. 2020;65(4):577-80.
22. Papazian L, Aubron C, Brochard L, Chiche J-D, Combes A, Dreyfuss D, et al. Formal guidelines: management of acute respiratory distress syndrome. Annals of Intensive Care. 2019;9(1):69.
23. ELSO. ELSO International Summary and Reports. 2024 [Available from: https://elso.org/registry/internationalsummaryandreports/internationalsummary.aspx.
24. Hill JD, O'Brien TG, Murray JJ, Dontigny L, Bramson ML, Osborn JJ, et al. Prolonged extracorporeal oxygenation for acute post-traumatic respiratory failure (shock-lung syndrome). Use of the Bramson membrane lung. N Engl J Med. 1972;286(12):629-34.
25. Bartlett RH, Gazzaniga AB, Toomasian J, Coran AG, Roloff D, Rucker R. Extracorporeal membrane oxygenation (ECMO) in neonatal respiratory failure. 100 cases. Ann Surg. 1986;204(3):236-45.
26. Sameed M, Meng Z, Marciniak ET. EOLIA trial: the future of extracorporeal membrane oxygenation in acute respiratory distress syndrome therapy? Breathe (Sheff). 2019;15(3):244-6.
27. Guglin M, Zucker MJ, Bazan VM, Bozkurt B, El Banayosy A, Estep JD, et al. Venoarterial ECMO for Adults: JACC Scientific Expert Panel. J Am Coll Cardiol. 2019;73(6):698-716.
28. Camporota L, Meadows C, Ledot S, Scott I, Harvey C, Garcia M, et al. Consensus on the referral and admission of patients with severe respiratory failure to the NHS ECMO service. Lancet Respir Med. 2021;9(2):e16-e7.
29. Broman LM, Taccone FS, Lorusso R, Malfertheiner MV, Pappalardo F, Di Nardo M, et al. The ELSO Maastricht Treaty for ECLS Nomenclature: abbreviations for cannulation configuration in extracorporeal life support - a position paper of the Extracorporeal Life Support Organization. Crit Care. 2019;23(1):36.
30. Thiagarajan RR. Extracorporeal Membrane Oxygenation in Infants and Children 2016 [Available from: https://thoracickey.com/extracorporeal-membrane-oxygenation-in-infants-and-children/
31. Lafc G, Budak AB, Yener AU, Cicek OF. Use of extracorporeal membrane oxygenation in adults. Heart Lung Circ. 2014;23(1):10-23.
32. Hayes MM, Fallon BP, Barbaro RP, Manusko N, Bartlett RH, Toomasian JM. Membrane Lung and Blood Pump Use During Prolonged Extracorporeal Membrane Oxygenation: Trends From 2002 to 2017. ASAIO J. 2021;67(9):1062-70.
33. Papadimas E, Leow L, Tan YK, Shen L, Ramanathan K, Choong A, et al. Centrifugal and Roller Pumps in Neonatal and Pediatric Extracorporeal Membrane Oxygenation: A Systematic Review and Meta-Analysis of Clinical Outcomes. ASAIO J. 2022;68(3):311-7.
34. Vermeer H, de Jong SF, Koers EJ, Peeters TLM, van der Lee R, de Boode WP, et al. Hemostatic Complications During Neonatal Extracorporeal Membrane Oxygenation: Roller Pump and Centrifugal Pump Driven Circuits. ASAIO J. 2023;69(6):618-24.
35. Halaweish I, Cole A, Cooley E, Lynch WR, Haft JW. Roller and Centrifugal Pumps: A Retrospective Comparison of Bleeding Complications in Extracorporeal Membrane Oxygenation. ASAIO J. 2015;61(5):496-501.
36. Bartlett RH. Physiology of Extracorporeal Gas Exchange. Compr Physiol. 2020;10(3):879-91.
37. Khoshbin E, Roberts N, Harvey C, Machin D, Killer H, Peek GJ, et al. Poly-methyl pentene oxygenators have improved gas exchange capability and reduced transfusion requirements in adult extracorporeal membrane oxygenation. ASAIO J. 2005;51(3):281-7.
38. Ho KM, Pavey W. Applying the cell-based coagulation model in the management of critical bleeding. Anaesth Intensive Care. 2017;45(2):166-76.
39. Hoffman M, Monroe DM, 3rd. A cell-based model of hemostasis. Thromb Haemost. 2001;85(6):958-65.

40. Yun SH, Sim EH, Goh RY, Park JI, Han JY. Platelet Activation: The Mechanisms and Potential Biomarkers. Biomed Res Int. 2016;2016:9060143.
41. Whiteheart SW. Platelet granules: surprise packages. Blood. 2011;118(5):1190-1.
42. Heijnen H, van der Sluijs P. Platelet secretory behaviour: as diverse as the granules ... or not? J Thromb Haemost. 2015;13(12):2141-51.
43. Peyvandi F, Garagiola I, Baronciani L. Role of von Willebrand factor in the haemostasis. Blood Transfus. 2011;9 Suppl 2(Suppl 2):s3-8.
44. McFadyen JD, Kaplan ZS. Platelets are not just for clots. Transfus Med Rev. 2015;29(2):110-9.
45. Brinkmann V, Reichard U, Goosmann C, Fauler B, Uhlemann Y, Weiss DS, et al. Neutrophil extracellular traps kill bacteria. Science. 2004;303(5663):1532-5.
46. Mayadas TN, Cullere X, Lowell CA. The multifaceted functions of neutrophils. Annu Rev Pathol. 2014;9:181-218.
47. Yang H, Biermann MH, Brauner JM, Liu Y, Zhao Y, Herrmann M. New Insights into Neutrophil Extracellular Traps: Mechanisms of Formation and Role in Inflammation. Front Immunol. 2016;7:302.
48. Fuchs TA, Abed U, Goosmann C, Hurwitz R, Schulze I, Wahn V, et al. Novel cell death program leads to neutrophil extracellular traps. J Cell Biol. 2007;176(2):231-41.
49. Metzler KD, Fuchs TA, Nauseef WM, Reumaux D, Roesler J, Schulze I, et al. Myeloperoxidase is required for neutrophil extracellular trap formation: implications for innate immunity. Blood. 2011;117(3):953-9.
50. Wang J. Neutrophils in tissue injury and repair. Cell Tissue Res. 2018;371(3):531-9.
51. Cowland JB, Borregaard N. Granulopoiesis and granules of human neutrophils. Immunol Rev. 2016;273(1):11-28.
52. Papayannopoulos V, Metzler KD, Hakkim A, Zychlinsky A. Neutrophil elastase and myeloperoxidase regulate the formation of neutrophil extracellular traps. J Cell Biol. 2010;191(3):677-91.
53. Zeng W, Song Y, Wang R, He R, Wang T. Neutrophil elastase: From mechanisms to therapeutic potential. J Pharm Anal. 2023;13(4):355-66.
54. Lawrence SM, Corriden R, Nizet V. How Neutrophils Meet Their End. Trends Immunol. 2020;41(6):531-44.
55. Perez-Figueroa E, Alvarez-Carrasco P, Ortega E, Maldonado-Bernal C. Neutrophils: Many Ways to Die. Front Immunol. 2021;12:631821.
56. Laridan E, Denorme F, Desender L, Francois O, Andersson T, Deckmyn H, et al. Neutrophil extracellular traps in ischemic stroke thrombi. Ann Neurol. 2017;82(2):223-32.
57. Savchenko AS, Martinod K, Seidman MA, Wong SL, Borissoff JI, Piazza G, et al. Neutrophil extracellular traps form predominantly during the organizing stage of human venous thromboembolism development. J Thromb Haemost. 2014;12(6):860-70.
58. Brinkmann V, Zychlinsky A. Beneficial suicide: why neutrophils die to make NETs. Nat Rev Microbiol. 2007;5(8):577-82.
59. Leshner M, Wang S, Lewis C, Zheng H, Chen XA, Santy L, et al. PAD4 mediated histone hypercitrullination induces heterochromatin decondensation and chromatin unfolding to form neutrophil extracellular trap-like structures. Front Immunol. 2012;3:307.
60. Nomura K, Miyashita T, Yamamoto Y, Munesue S, Harashima A, Takayama H, et al. Citrullinated Histone H3: Early Biomarker of Neutrophil Extracellular Traps in Septic Liver Damage. J Surg Res. 2019;234:132-8.
61. Thalin C, Daleskog M, Goransson SP, Schatzberg D, Lasselin J, Laska AC, et al. Validation of an enzyme-linked immunosorbent assay for the quantification of citrullinated histone H3 as a marker for neutrophil extracellular traps in human plasma. Immunol Res. 2017;65(3):706-12.
62. Thalin C, Aguilera K, Hall NW, Marunde MR, Burg JM, Rosell A, et al. Quantification of citrullinated histones: Development of an improved assay to reliably quantify nucleosomal H3Cit in human plasma. J Thromb Haemost. 2020;18(10):2732-43.

63. Lee KH, Cavanaugh L, Leung H, Yan F, Ahmadi Z, Chong BH, et al. Quantification of NETs-associated markers by flow cytometry and serum assays in patients with thrombosis and sepsis. Int J Lab Hematol. 2018;40(4):392-9.
64. Ebrahimi F, Giaglis S, Hahn S, Blum CA, Baumgartner C, Kutz A, et al. Markers of neutrophil extracellular traps predict adverse outcome in community-acquired pneumonia: secondary analysis of a randomised controlled trial. Eur Respir J. 2018;51(4).
65. Patel BV, Lee TML, O'Dea K. CLUSTERINg Circulating Histones in Sepsis. Am J Respir Crit Care Med. 2023;208(2):125-7.
66. Yipp BG, Kubes P. NETosis: how vital is it? Blood. 2013;122(16):2784-94.
67. Papayannopoulos V. Neutrophil extracellular traps in immunity and disease. Nat Rev Immunol. 2018;18(2):134-47.
68. Tan C, Aziz M, Wang P. The vitals of NETs. J Leukoc Biol. 2021;110(4):797-808.
69. Scapini P, Cassatella MA. Social networking of human neutrophils within the immune system. Blood. 2014;124(5):710-9.
70. McKenna E, Mhaonaigh AU, Wubben R, Dwivedi A, Hurley T, Kelly LA, et al. Neutrophils: Need for Standardized Nomenclature. Front Immunol. 2021;12:602963.
71. Ivetic A. A head-to-tail view of L-selectin and its impact on neutrophil behaviour. Cell Tissue Res. 2018;371(3):437-53.
72. Daix T, Guerin E, Tavernier E, Mercier E, Gissot V, Herault O, et al. Multicentric Standardized Flow Cytometry Routine Assessment of Patients With Sepsis to Predict Clinical Worsening. Chest. 2018;154(3):617-27.
73. Tillinger W, Jilch R, Jilma B, Brunner H, Koeller U, Lichtenberger C, et al. Expression of the high-affinity IgG receptor FcRI (CD64) in patients with inflammatory bowel disease: a new biomarker for gastroenterologic diagnostics. Am J Gastroenterol. 2009;104(1):102-9.
74. Hussein OA, El-Toukhy MA, El-Rahman HS. Neutrophil CD64 expression in inflammatory autoimmune diseases: its value in distinguishing infection from disease flare. Immunol Invest. 2010;39(7):699-712.
75. Wang X, Li ZY, Zeng L, Zhang AQ, Pan W, Gu W, et al. Neutrophil CD64 expression as a diagnostic marker for sepsis in adult patients: a meta-analysis. Crit Care. 2015;19:245.
76. Yanez A, Coetzee SG, Olsson A, Muench DE, Berman BP, Hazelett DJ, et al. Granulocyte-Monocyte Progenitors and Monocyte-Dendritic Cell Progenitors Independently Produce Functionally Distinct Monocytes. Immunity. 2017;47(5):890-902 e4.
77. Thomas GD, Hamers AAJ, Nakao C, Marcovecchio P, Taylor AM, McSkimming C, et al. Human Blood Monocyte Subsets: A New Gating Strategy Defined Using Cell Surface Markers Identified by Mass Cytometry. Arterioscler Thromb Vasc Biol. 2017;37(8):1548-58.
78. Cormican S, Griffin MD. Human Monocyte Subset Distinctions and Function: Insights From Gene Expression Analysis. Front Immunol. 2020;11:1070.
79. Hershman MJ, Cheadle WG, Wellhausen SR, Davidson PF, Polk HC, Jr. Monocyte HLA-DR antigen expression characterizes clinical outcome in the trauma patient. Br J Surg. 1990;77(2):204-7.
80. Kim OY, Monsel A, Bertrand M, Coriat P, Cavaillon JM, Adib-Conquy M. Differential down-regulation of HLA-DR on monocyte subpopulations during systemic inflammation. Crit Care. 2010;14(2):R61.
81. Monneret G, Lepape A, Voirin N, Bohe J, Venet F, Debard AL, et al. Persisting low monocyte human leukocyte antigen-DR expression predicts mortality in septic shock. Intensive Care Med. 2006;32(8):1175-83.
82. Balle CM, Jeppesen AN, Christensen S, Hvas AM. Platelet Function During Extracorporeal Membrane Oxygenation in Adult Patients: A Systematic Review. Front Cardiovasc Med. 2018;5:157.
83. Clark SR, Ma AC, Tavener SA, McDonald B, Goodarzi Z, Kelly MM, et al. Platelet TLR4 activates neutrophil extracellular traps to ensnare bacteria in septic blood. Nat Med. 2007;13(4):463-9.

84. Winnersbach P, Rossaint J, Buhl EM, Singh S, Lölsberg J, Wessling M, et al. Platelet count reduction during in vitro membrane oxygenation affects platelet activation, neutrophil extracellular trap formation and clot stability, but does not prevent clotting. Perfusion. 2021:267659121989231.
85. Bendib I, de Chaisemartin L, Mekontso Dessap A, Chollet-Martin S, de Prost N. Understanding the Role of Neutrophil Extracellular Traps in Patients With Severe Pneumonia and ARDS. Chest. 2019;156(6):1278-80.
86. Caudrillier A, Kessenbrock K, Gilliss BM, Nguyen JX, Marques MB, Monestier M, et al. Platelets induce neutrophil extracellular traps in transfusion-related acute lung injury. J Clin Invest. 2012;122(7):2661-71.
87. Lefrancais E, Mallavia B, Zhuo H, Calfee CS, Looney MR. Maladaptive role of neutrophil extracellular traps in pathogen-induced lung injury. JCI Insight. 2018;3(3).
88. Li H, Zhou X, Tan H, Hu Y, Zhang L, Liu S, et al. Neutrophil extracellular traps contribute to the pathogenesis of acid-aspiration-induced ALI/ARDS. Oncotarget. 2018;9(2):1772-84.
89. Ojima M, Yamamoto N, Hirose T, Hamaguchi S, Tasaki O, Kojima T, et al. Serial change of neutrophil extracellular traps in tracheal aspirate of patients with acute respiratory distress syndrome: report of three cases. J Intensive Care. 2020;8:25.
90. Zuo Y, Yalavarthi S, Shi H, Gockman K, Zuo M, Madison JA, et al. Neutrophil extracellular traps in COVID-19. JCI Insight. 2020;5(11).
91. Radermecker C, Detrembleur N, Guiot J, Cavalier E, Henket M, d'Emal C, et al. Neutrophil extracellular traps infiltrate the lung airway, interstitial, and vascular compartments in severe COVID-19. J Exp Med. 2020;217(12).
92. Godement M, Zhu J, Cerf C, Vieillard-Baron A, Maillon A, Zuber B, et al. Neutrophil Extracellular Traps in SARS-CoV2 Related Pneumonia in ICU Patients: The NETCOV2 Study. Front Med (Lausanne). 2021;8:615984.
93. Ackermann M, Verleden SE, Kuehnel M, Haverich A, Welte T, Laenger F, et al. Pulmonary Vascular Endothelialitis, Thrombosis, and Angiogenesis in Covid-19. N Engl J Med. 2020;383(2):120-8.
94. Iba T, Connors JM, Levy JH. The coagulopathy, endotheliopathy, and vasculitis of COVID-19. Inflamm Res. 2020;69(12):1181-9.
95. Patel BV, Arachchillage DJ, Ridge CA, Bianchi P, Doyle JF, Garfield B, et al. Pulmonary Angiopathy in Severe COVID-19: Physiologic, Imaging, and Hematologic Observations. Am J Respir Crit Care Med. 2020;202(5):690-9.
96. Gregoire M, Uhel F, Lesouhaitier M, Gacouin A, Guirriec M, Mourcin F, et al. Impaired efferocytosis and neutrophil extracellular trap clearance by macrophages in ARDS. Eur Respir J. 2018;52(2).
97. Li H, Pan P, Su X, Liu S, Zhang L, Wu D, et al. Neutrophil Extracellular Traps Are Pathogenic in Ventilator-Induced Lung Injury and Partially Dependent on TLR4. Biomed Res Int. 2017;2017:8272504.
98. Schrijver IT, Kemperman H, Roest M, Kesecioglu J, de Lange DW. Myeloperoxidase can differentiate between sepsis and non-infectious SIRS and predicts mortality in intensive care patients with SIRS. Intensive Care Med Exp. 2017;5(1):43.
99. Carr AC, Spencer E, Hoskin TS, Rosengrave P, Kettle AJ, Shaw G. Circulating myeloperoxidase is elevated in septic shock and is associated with systemic organ failure and mortality in critically ill patients. Free Radic Biol Med. 2020;152:462-8.
100. Kodama T, Yukioka H, Kato T, Kato N, Hato F, Kitagawa S. Neutrophil elastase as a predicting factor for development of acute lung injury. Intern Med. 2007;46(11):699-704.
101. de Bont CM, Boelens WC, Pruijn GJM. NETosis, complement, and coagulation: a triangular relationship. Cell Mol Immunol. 2019;16(1):19-27.
102. Iba T, Hashiguchi N, Nagaoka I, Tabe Y, Murai M. Neutrophil cell death in response to infection and its relation to coagulation. J Intensive Care. 2013;1(1):13.
103. Kapoor S, Opneja A, Nayak L. The role of neutrophils in thrombosis. Thromb Res. 2018;170:87-96.

104. Liu J, Yang D, Wang X, Zhu Z, Wang T, Ma A, et al. Neutrophil extracellular traps and dsDNA predict outcomes among patients with ST-elevation myocardial infarction. Sci Rep. 2019;9(1):11599.
105. Jung Y, Choi JW, Hwang HY, Gu JY, Kim KH, Kim HK. Elevated circulating levels of neutrophil extracellular traps after cardiopulmonary bypass surgery as risk factors of postoperative atrial fibrillation and mortality. J Thorac Dis. 2024;16(7):4319-28.
106. Paunel-Gorgulu A, Wacker M, El Aita M, Hassan S, Schlachtenberger G, Deppe A, et al. cfDNA correlates with endothelial damage after cardiac surgery with prolonged cardiopulmonary bypass and amplifies NETosis in an intracellular TLR9-independent manner. Sci Rep. 2017;7(1):17421.
107. Beaubien-Souligny W, Neagoe PE, Gagnon D, Denault AY, Sirois MG. Increased Circulating Levels of Neutrophil Extracellular Traps During Cardiopulmonary Bypass. CJC Open. 2020;2(2):39-48.
108. Bieber S, Muczynski KA, Lood C. Neutrophil Activation and Neutrophil Extracellular Trap Formation in Dialysis Patients. Kidney Med. 2020;2(6):692-8 e1.
109. Kim JH, Lee HS, Kwon MJ, Song YR, Kim SG, Kim JK. Role of neutrophil extracellular traps in vascular access thrombosis in hemodialysis patients. Thromb Res. 2023;231:121-7.
110. Korabecna M, Opatrna S, Wirth J, Rulcova K, Eiselt J, Sefrna F, et al. Cell-free plasma DNA during peritoneal dialysis and hemodialysis and in patients with chronic kidney disease. Ann N Y Acad Sci. 2008;1137:296-301.
111. Schulz C, Massberg S. Demystifying the prothrombotic role of NETs. Blood. 2017;129(8):925-6.
112. Fuchs TA, Brill A, Duerschmied D, Schatzberg D, Monestier M, Myers DD, Jr., et al. Extracellular DNA traps promote thrombosis. Proc Natl Acad Sci U S A. 2010;107(36):15880-5.
113. Noubouossie DF, Whelihan MF, Yu YB, Sparkenbaugh E, Pawlinski R, Monroe DM, et al. In vitro activation of coagulation by human neutrophil DNA and histone proteins but not neutrophil extracellular traps. Blood. 2017;129(8):1021-9.
114. Gould TJ, Vu TT, Swystun LL, Dwivedi DJ, Mai SH, Weitz JI, et al. Neutrophil extracellular traps promote thrombin generation through platelet-dependent and platelet-independent mechanisms. Arterioscler Thromb Vasc Biol. 2014;34(9):1977-84.
115. Semeraro F, Ammollo CT, Morrissey JH, Dale GL, Friese P, Esmon NL, et al. Extracellular histones promote thrombin generation through platelet-dependent mechanisms: involvement of platelet TLR2 and TLR4. Blood. 2011;118(7):1952-61.
116. Kim JE, Yoo HJ, Gu JY, Kim HK. Histones Induce the Procoagulant Phenotype of Endothelial Cells through Tissue Factor Up-Regulation and Thrombomodulin Down-Regulation. PLoS One. 2016;11(6):e0156763.
117. Petersen LC, Bjorn SE, Nordfang O. Effect of leukocyte proteinases on tissue factor pathway inhibitor. Thromb Haemost. 1992;67(5):537-41.
118. Mereweather LJ, Constantinescu-Bercu A, Crawley JTB, Salles C, II. Platelet-Neutrophil Crosstalk in Thrombosis. Int J Mol Sci. 2023;24(2).
119. Finsterbusch M, Schrottmaier WC, Kral-Pointner JB, Salzmann M, Assinger A. Measuring and interpreting platelet-leukocyte aggregates. Platelets. 2018;29(7):677-85.
120. Pluta K, Porebska K, Urbanowicz T, Gasecka A, Olasinska-Wisniewska A, Targonski R, et al. Platelet-Leucocyte Aggregates as Novel Biomarkers in Cardiovascular Diseases. Biology (Basel). 2022;11(2).
121. Rinder HM, Bonan JL, Rinder CS, Ault KA, Smith BR. Dynamics of leukocyte-platelet adhesion in whole blood. Blood. 1991;78(7):1730-7.
122. Kaiser R, Escaig R, Erber J, Nicolai L. Neutrophil-Platelet Interactions as Novel Treatment Targets in Cardiovascular Disease. Front Cardiovasc Med. 2021;8:824112.
123. Li N, Hu H, Lindqvist M, Wikstrom-Jonsson E, Goodall AH, Hjemdahl P. Platelet-leukocyte cross talk in whole blood. Arterioscler Thromb Vasc Biol. 2000;20(12):2702-8.
124. Doyle AJ, Hunt BJ. Current Understanding of How Extracorporeal Membrane Oxygenators Activate Haemostasis and Other Blood Components. Front Med (Lausanne). 2018;5:352.

125. Thiagarajan RR, Barbaro RP, Rycus PT, McMullan DM, Conrad SA, Fortenberry JD, et al. Extracorporeal Life Support Organization Registry International Report 2016. Asaio j. 2017;63(1):60-7.
126. Wahba A, Philipp A, Behr R, Birnbaum DE. Heparin-coated equipment reduces the risk of oxygenator failure. Ann Thorac Surg. 1998;65(5):1310-2.
127. Bannan S, Danby A, Cowan D, Ashraf S, Gesinde M, Martin P. Cell activation and thrombin generation in heparin bonded cardiopulmonary bypass circuits using a novel in vitro model. Eur J Cardiothorac Surg. 1997;12(2):268-75.
128. Daniel JMt, Bernard PA, Skinner SC, Bhandary P, Ruzic A, Bacon MK, et al. Hollow Fiber Oxygenator Composition Has a Significant Impact on Failure Rates in Neonates on Extracorporeal Membrane Oxygenation: A Retrospective Analysis. J Pediatr Intensive Care. 2018;7(1):7-13.
129. Murphy DA, Hockings LE, Andrews RK, Aubron C, Gardiner EE, Pellegrino VA, et al. Extracorporeal membrane oxygenation-hemostatic complications. Transfus Med Rev. 2015;29(2):90-101.
130. Dornia C, Philipp A, Bauer S, Lubnow M, Muller T, Lehle K, et al. Analysis of thrombotic deposits in extracorporeal membrane oxygenators by multidetector computed tomography. ASAIO J. 2014;60(6):652-6.
131. Dornia C, Philipp A, Bauer S, Stroszczynski C, Schreyer AG, Muller T, et al. D-dimers Are a Predictor of Clot Volume Inside Membrane Oxygenators During Extracorporeal Membrane Oxygenation. Artif Organs. 2015;39(9):782-7.
132. Hastings SM, Ku DN, Wagoner S, Maher KO, Deshpande S. Sources of Circuit Thrombosis in Pediatric Extracorporeal Membrane Oxygenation. Asaio j. 2017;63(1):86-92.
133. Distelmaier K, Wiedemann D, Binder C, Haberl T, Zimpfer D, Heinz G, et al. Duration of extracorporeal membrane oxygenation support and survival in cardiovascular surgery patients. J Thorac Cardiovasc Surg. 2018;155(6):2471-6.
134. Friedrichson B, Mutlak H, Zacharowski K, Piekarski F. Insight into ECMO, mortality and ARDS: a nationwide analysis of 45,647 ECMO runs. Crit Care. 2021;25(1):38.
135. Lubnow M, Philipp A, Dornia C, Schroll S, Bein T, Creutzenberg M, et al. D-dimers as an early marker for oxygenator exchange in extracorporeal membrane oxygenation. J Crit Care. 2014;29(3):473 e1-5.
136. Park M, Mendes PV, Hirota AS, dos Santos EV, Costa EL, Azevedo LC. Blood flow/pump rotation ratio as an artificial lung performance monitoring tool during extracorporeal respiratory support using centrifugal pumps. Rev Bras Ter Intensiva. 2015;27(2):178-84.
137. Lubnow M, Philipp A, Foltan M, Bull Enger T, Lunz D, Bein T, et al. Technical complications during veno-venous extracorporeal membrane oxygenation and their relevance predicting a system-exchange--retrospective analysis of 265 cases. PLoS One. 2014;9(12):e112316.
138. Birkenmaier C, Dornia C, Lehle K, Muller T, Gruber M, Philipp A, et al. Analysis of Thrombotic Deposits in Extracorporeal Membrane Oxygenators by High-resolution Microcomputed Tomography: A Feasibility Study. ASAIO J. 2020;66(8):922-8.
139. Fu X, Su Z, Wang Y, Sun A, Wang L, Deng X, et al. Comparison of hemodynamic features and thrombosis risk of membrane oxygenators with different structures: A numerical study. Comput Biol Med. 2023;159:106907.
140. Dornia C, Philipp A, Bauer S, Hoffstetter P, Lehle K, Schmid C, et al. Visualization of thrombotic deposits in extracorporeal membrane oxygenation devices using multidetector computed tomography: a feasibility study. ASAIO J. 2013;59(4):439-41.
141. Staessens S, Moussa MD, Pierache A, Rauch A, Rousse N, Boulleaux E, et al. Thrombus formation during ECMO: Insights from a detailed histological analysis of thrombus composition. J Thromb Haemost. 2022;20(9):2058-69.
142. Callaghan S, Cai T, McCafferty C, Van Den Helm S, Horton S, MacLaren G, et al. Adsorption of Blood Components to Extracorporeal Membrane Oxygenation (ECMO) Surfaces in Humans: A Systematic Review. J Clin Med. 2020;9(10).

143. Vandenbriele C, Vanassche T, Price S. Why we need safer anticoagulant strategies for patients on short-term percutaneous mechanical circulatory support. Intensive Care Med. 2020;46(4):771-4.
144. Lehle K, Philipp A, Gleich O, Holzamer A, Muller T, Bein T, et al. Efficiency in extracorporeal membrane oxygenation-cellular deposits on polymethylpentene membranes increase resistance to blood flow and reduce gas exchange capacity. ASAIO J. 2008;54(6):612-7.
145. Balle CM, Jeppesen AN, Christensen S, Hvas AM. Platelet Function During Extracorporeal Membrane Oxygenation in Adult Patients. Front Cardiovasc Med. 2019;6:114.
146. Cheung PY, Sawicki G, Salas E, Etches PC, Schulz R, Radomski MW. The mechanisms of platelet dysfunction during extracorporeal membrane oxygenation in critically ill neonates. Crit Care Med. 2000;28(7):2584-90.
147. Jiritano F, Serraino GF, Ten Cate H, Fina D, Matteucci M, Mastroroberto P, et al. Platelets and extra-corporeal membrane oxygenation in adult patients: a systematic review and meta-analysis. Intensive Care Med. 2020;46(6):1154-69.
148. Kalbhenn J, Schlagenhauf A, Rosenfelder S, Schmutz A, Zieger B. Acquired von Willebrand syndrome and impaired platelet function during venovenous extracorporeal membrane oxygenation: Rapid onset and fast recovery. J Heart Lung Transplant. 2018;37(8):985-91.
149. Lukito P, Wong A, Jing J, Arthur JF, Marasco SF, Murphy DA, et al. Mechanical circulatory support is associated with loss of platelet receptors glycoprotein Ibalpha and glycoprotein VI. J Thromb Haemost. 2016;14(11):2253-60.
150. Chung M, Cabezas FR, Nunez JI, Kennedy KF, Rick K, Rycus P, et al. Hemocompatibility-Related Adverse Events and Survival on Venoarterial Extracorporeal Life Support: An ELSO Registry Analysis. JACC Heart Fail. 2020;8(11):892-902.
151. Mazzeffi M, Tanaka K, Wu YF, Zhang A, Kareddy N, Tadjou Tito E, et al. Platelet surface GPIbalpha, activated GPIIb-IIIa, and P-selectin levels in adult veno-arterial extracorporeal membrane oxygenation patients. Platelets. 2022;33(1):116-22.
152. Valladolid C, Yee A, Cruz MA. von Willebrand Factor, Free Hemoglobin and Thrombosis in ECMO. Front Med (Lausanne). 2018;5:228.
153. A CLUE Study 2020 [(COVID-19 Flu ECMO)]. Available from: https://www.hra.nhs.uk/planning-and-improving-research/application-summaries/research-summaries/a-clue-study-covid-19-flu-ecmo-covid-19/.
154. Patel B, Mumby S, Johnson N, Falaschetti E, Hansen J, Adcock I, et al. Decision support system to evaluate VENTilation in the Acute Respiratory Distress Syndrome (DeVENT study) – Trial Protocol. medRxiv. 2021:2021.08.25.21262610.
155. Force ADT, Ranieri VM, Rubenfeld GD, Thompson BT, Ferguson ND, Caldwell E, et al. Acute respiratory distress syndrome: the Berlin Definition. JAMA. 2012;307(23):2526-33.
156. Authority HR. The HITEC Study 2022 [Available from: https://www.hra.nhs.uk/planning-and-improving-research/application-summaries/research-summaries/the-hitec-study/.
157. Davidson S. Monitoring of Antiplatelet Therapy. Methods Mol Biol. 2023;2663:381-402.
158. Roche. Multiplate analysed product information sheet. [Available from: https://diagnostics.roche.com/global/en/products/instruments/multiplate-5-analyzer-ins-3691.html#productInfo.
159. Millar JE, Fanning JP, McDonald CI, McAuley DF, Fraser JF. The inflammatory response to extracorporeal membrane oxygenation (ECMO): a review of the pathophysiology. Crit Care. 2016;20(1):387.
160. Vasques F, Sanderson B, Correa G, Collins P, Camarda V, Giosa L, et al. Prevalence and Indications for Oxygenator Circuit Replacement in Patients Receiving Venovenous Extracorporeal Membrane Oxygenation. ASAIO J. 2023;69(9):849-55.
161. Zakhary B, Vercaemst L, Mason P, Antonini MV, Lorusso R, Brodie D. How I approach membrane lung dysfunction in patients receiving ECMO. Crit Care. 2020;24(1):671.

162. Coronavirus disease (COVID-19) pandemic [press release]. World Health Organisation Health Emergency DAshboard: WHO2023.
163. Aslan A, Aslan C, Zolbanin NM, Jafari R. Acute respiratory distress syndrome in COVID-19: possible mechanisms and therapeutic management. Pneumonia (Nathan). 2021;13(1):14.
164. Patel BV, Haar S, Handslip R, Auepanwiriyakul C, Lee TM, Patel S, et al. Natural history, trajectory, and management of mechanically ventilated COVID-19 patients in the United Kingdom. Intensive Care Med. 2021;47(5):549-65.
165. Gattinoni L, Chiumello D, Caironi P, Busana M, Romitti F, Brazzi L, et al. COVID-19 pneumonia: different respiratory treatments for different phenotypes? Intensive Care Med. 2020;46(6):1099-102.
166. Weatherill A, Laffan M, Gasper M, Bianchi P, Passariello M, Singh S, et al. Impact of Thrombosis and Bleeding in Patients with Severe COVID-19 versus Other Viral Pneumonias in the Context of Extracorporeal Membrane Oxygenation. Semin Thromb Hemost. 2021.
167. Doyle AJ, Hunt BJ, Sanderson B, Zhang J, Mak SM, Benedetti G, et al. A Comparison of Thrombosis and Hemorrhage Rates in Patients With Severe Respiratory Failure Due to Coronavirus Disease 2019 and Influenza Requiring Extracorporeal Membrane Oxygenation. Crit Care Med. 2021;49(7):e663-e72.
168. Jenner WJ, Kanji R, Mirsadraee S, Gue YX, Price S, Prasad S, et al. Thrombotic complications in 2928 patients with COVID-19 treated in intensive care: a systematic review. J Thromb Thrombolysis. 2021;51(3):595-607.
169. Grasselli G, Tonetti T, Protti A, Langer T, Girardis M, Bellani G, et al. Pathophysiology of COVID-19-associated acute respiratory distress syndrome: a multicentre prospective observational study. Lancet Respir Med. 2020;8(12):1201-8.
170. Osuchowski MF, Winkler MS, Skirecki T, Cajander S, Shankar-Hari M, Lachmann G, et al. The COVID-19 puzzle: deciphering pathophysiology and phenotypes of a new disease entity. Lancet Respir Med. 2021;9(6):622-42.
171. Gattinoni L, Gattarello S, Steinberg I, Busana M, Palermo P, Lazzari S, et al. COVID-19 pneumonia: pathophysiology and management. Eur Respir Rev. 2021;30(162).
172. ELSO. ELSO COVID-19 Registry 2023 [Available from: https://www.elso.org/Registry/FullCOVID19RegistryDashboard.aspx.
173. Lorusso R, De Piero ME, Mariani S, Di Mauro M, Folliguet T, Taccone FS, et al. In-hospital and 6-month outcomes in patients with COVID-19 supported with extracorporeal membrane oxygenation (EuroECMO-COVID): a multicentre, prospective observational study. Lancet Respir Med. 2023;11(2):151-62.
174. Badulak J, Antonini MV, Stead CM, Shekerdemian L, Raman L, Paden ML, et al. Extracorporeal Membrane Oxygenation for COVID-19: Updated 2021 Guidelines from the Extracorporeal Life Support Organization. Asaio j. 2021;67(5):485-95.
175. Barbaro RP, MacLaren G, Boonstra PS, Iwashyna TJ, Slutsky AS, Fan E, et al. Extracorporeal membrane oxygenation support in COVID-19: an international cohort study of the Extracorporeal Life Support Organization registry. Lancet. 2020;396(10257):1071-8.
176. Schmidt M, Hajage D, Lebreton G, Monsel A, Voiriot G, Levy D, et al. Extracorporeal membrane oxygenation for severe acute respiratory distress syndrome associated with COVID-19: a retrospective cohort study. Lancet Respir Med. 2020;8(11):1121-31.
177. Garfield B, Bianchi P, Arachchillage D, Hartley P, Naruka V, Shroff D, et al. Six-month mortality in patients with COVID-19 and non-COVID-19 viral pneumonitis managed with veno-venous extracorporeal membrane oxygenation. ASAIO J. 2021.
178. Investigators R-C, Investigators AC-a, Investigators A, Goligher EC, Bradbury CA, McVerry BJ, et al. Therapeutic Anticoagulation with Heparin in Critically Ill Patients with Covid-19. N Engl J Med. 2021;385(9):777-89.

179. Bemtgen X, Zotzmann V, Benk C, Rilinger J, Steiner K, Asmussen A, et al. Thrombotic circuit complications during venovenous extracorporeal membrane oxygenation in COVID-19. J Thromb Thrombolysis. 2021;51(2):301-7.
180. Beun R, Kusadasi N, Sikma M, Westerink J, Huisman A. Thromboembolic events and apparent heparin resistance in patients infected with SARS-CoV-2. Int J Lab Hematol. 2020;42 Suppl 1(Suppl 1):19-20.
181. Medtronic. Nautilus, ECMO Oxygenator 2024 [Available from: https://www.medtronic.com/us-en/healthcare-professionals/products/cardiovascular/extracorporeal-life-support/nautilus-ecmo.html.
182. Sze S, Pan D, Nevill CR, Gray LJ, Martin CA, Nazareth J, et al. Ethnicity and clinical outcomes in COVID-19: A systematic review and meta-analysis. EClinicalMedicine. 2020;29:100630.
183. Peckham H, de Gruijter NM, Raine C, Radziszewska A, Ciurtin C, Wedderburn LR, et al. Male sex identified by global COVID-19 meta-analysis as a risk factor for death and ITU admission. Nat Commun. 2020;11(1):6317.
184. Pijls BG, Jolani S, Atherley A, Derckx RT, Dijkstra JIR, Franssen GHL, et al. Demographic risk factors for COVID-19 infection, severity, ICU admission and death: a meta-analysis of 59 studies. BMJ Open. 2021;11(1):e044640.
185. Gao M, Piernas C, Astbury NM, Hippisley-Cox J, O'Rahilly S, Aveyard P, et al. Associations between body-mass index and COVID-19 severity in 6.9 million people in England: a prospective, community-based, cohort study. Lancet Diabetes Endocrinol. 2021;9(6):350-9.
186. Bergman ZR, Wothe JK, Alwan FS, Dunn A, Lusczek ER, Lofrano AE, et al. The Use of Venovenous Extracorporeal Membrane Oxygenation in COVID-19 Infection: One Region's Comprehensive Experience. Asaio j. 2021;67(5):503-10.
187. Jäckel M, Rilinger J, Lang CN, Zotzmann V, Kaier K, Stachon P, et al. Outcome of acute respiratory distress syndrome requiring extracorporeal membrane oxygenation in Covid-19 or influenza: A single-center registry study. Artif Organs. 2021;45(6):593-601.
188. Jacobs JP, Stammers AH, Louis JS, Hayanga JWA, Firstenberg MS, Mongero LB, et al. Multi-institutional Analysis of 100 Consecutive Patients with COVID-19 and Severe Pulmonary Compromise Treated with Extracorporeal Membrane Oxygenation: Outcomes and Trends Over Time. Asaio j. 2021;67(5):496-502.
189. Barbaro RP, MacLaren G, Boonstra PS, Combes A, Agerstrand C, Annich G, et al. Extracorporeal membrane oxygenation for COVID-19: evolving outcomes from the international Extracorporeal Life Support Organization Registry. Lancet. 2021;398(10307):1230-8.
190. Eddy RL, Sin DD. Computed Tomography Vascular Tree-in-Bud: A Novel Prognostic Imaging Biomarker in COVID-19? Am J Respir Crit Care Med. 2020;202(5):642-4.
191. Ahmadi ZH, Jahangirifard A, Farzanegan B, Tabarsi P, Abtahian Z, Abedini A, et al. Extracorporeal membrane oxygenation and COVID-19: The causes of failure. J Card Surg. 2020;35(10):2838-43.
192. Schmidt M, Hajage D, Landoll M, Pequignot B, Langouet E, Amalric M, et al. Comparative outcomes of extracorporeal membrane oxygenation for COVID-19 delivered in experienced European centres during successive SARS-CoV-2 variant outbreaks (ECMO-SURGES): an international, multicentre, retrospective cohort study. Lancet Respir Med. 2023;11(2):163-75.
193. Tonna JE, Boonstra PS, MacLaren G, Paden M, Brodie D, Anders M, et al. Extracorporeal Life Support Organization Registry International Report 2022: 100,000 Survivors. ASAIO J. 2024;70(2):131-43.
194. Sun W, Wang S, Chen Z, Zhang J, Li T, Arias K, et al. Impact of high mechanical shear stress and oxygenator membrane surface on blood damage relevant to thrombosis and bleeding in a pediatric ECMO circuit. Artif Organs. 2020;44(7):717-26.
195. Wang S, Griffith BP, Wu ZJ. Device-Induced Hemostatic Disorders in Mechanically Assisted Circulation. Clin Appl Thromb Hemost. 2021;27:1076029620982374.

196. Guo Z, Sun L, Li B, Tian R, Zhang X, Zhang Z, et al. Anticoagulation Management in Severe Coronavirus Disease 2019 Patients on Extracorporeal Membrane Oxygenation. J Cardiothorac Vasc Anesth. 2021;35(2):389-97.
197. Silva MJA, Ribeiro LR, Gouveia MIM, Marcelino BDR, Santos CSD, Lima KVB, et al. Hyperinflammatory Response in COVID-19: A Systematic Review. Viruses. 2023;15(2).
198. He X, Yao F, Chen J, Wang Y, Fang X, Lin X, et al. The poor prognosis and influencing factors of high D-dimer levels for COVID-19 patients. Scientific Reports. 2021;11(1):1830.
199. Yao Y, Cao J, Wang Q, Shi Q, Liu K, Luo Z, et al. D-dimer as a biomarker for disease severity and mortality in COVID-19 patients: a case control study. Journal of Intensive Care. 2020;8(1):49.
200. Oudkerk M, Büller HR, Kuijpers D, van Es N, Oudkerk SF, McLoud T, et al. Diagnosis, Prevention, and Treatment of Thromboembolic Complications in COVID-19: Report of the National Institute for Public Health of the Netherlands. Radiology. 2020;297(1):E216-e22.
201. Nielsen ND, Rollins-Raval MA, Raval JS, Thachil J. Is it hyperfibrinolysis or fibrinolytic shutdown in severe COVID-19? Thromb Res. 2022;210:1-3.
202. Wright FL, Vogler TO, Moore EE, Moore HB, Wohlauer MV, Urban S, et al. Fibrinolysis Shutdown Correlation with Thromboembolic Events in Severe COVID-19 Infection. J Am Coll Surg. 2020;231(2):193-203.e1.
203. Hartmann J, Ergang A, Mason D, Dias JD. The Role of TEG Analysis in Patients with COVID-19-Associated Coagulopathy: A Systematic Review. Diagnostics (Basel). 2021;11(2).
204. Mortus JR, Manek SE, Brubaker LS, Loor M, Cruz MA, Trautner BW, et al. Thromboelastographic Results and Hypercoagulability Syndrome in Patients With Coronavirus Disease 2019 Who Are Critically Ill. JAMA Netw Open. 2020;3(6):e2011192.
205. Arachchillage DRJ, Laffan M, Khanna S, Vandenbriele C, Kamani F, Passariello M, et al. Frequency of Thrombocytopenia and Heparin-Induced Thrombocytopenia in Patients Receiving Extracorporeal Membrane Oxygenation Compared With Cardiopulmonary Bypass and the Limited Sensitivity of Pretest Probability Score. Crit Care Med. 2020;48(5):e371-e9.
206. Iba T, Levy JH, Levi M, Thachil J. Coagulopathy in COVID-19. J Thromb Haemost. 2020;18(9):2103-9.
207. Yatim N, Boussier J, Chocron R, Hadjadj J, Philippe A, Gendron N, et al. Platelet activation in critically ill COVID-19 patients. Annals of Intensive Care. 2021;11(1):113.
208. Rajsic S, Breitkopf R, Rugg C, Bukumiric Z, Reitbauer J, Treml B. Thrombotic Events Develop in 1 Out of 5 Patients Receiving ECMO Support: An 11-Year Referral Centre Experience. J Clin Med. 2023;12(3).
209. Trudzinski FC, Minko P, Rapp D, Fahndrich S, Haake H, Haab M, et al. Runtime and aPTT predict venous thrombosis and thromboembolism in patients on extracorporeal membrane oxygenation: a retrospective analysis. Ann Intensive Care. 2016;6(1):66.
210. Zhang M, Li S, Ying J, Qu Y. Neutrophils: a key component in ECMO-related acute organ injury. Front Immunol. 2024;15:1432018.
211. Zhang Y, Peng R, Pei S, Gao S, Sun Y, Cheng G, et al. Neutrophil extracellular traps are increased after extracorporeal membrane oxygenation support initiation and present in thrombus: A preclinical study using sheep as an animal model. Thromb Res. 2023;221:173-82.
212. McMichael ABV, Ryerson LM, Ratano D, Fan E, Faraoni D, Annich GM. 2021 ELSO Adult and Pediatric Anticoagulation Guidelines. ASAIO J. 2022;68(3):303-10.
213. Holzgraefe B, Larsson A, Eksborg S, Kalzen H. Does extracorporeal membrane oxygenation attenuate hypoxic pulmonary vasoconstriction in a porcine model of global alveolar hypoxia? Acta Anaesthesiol Scand. 2020;64(7):992-1001.
214. Kartiko S, Koizumi N, Yamane D, Sarani B, Siddique AB, Levine AR, et al. Thromboelastography Parameters do not Discriminate for Thrombotic Events in Hospitalized Patients With COVID-19. J Intensive Care Med. 2023;38(5):449-56.

215. Wang J, Hajizadeh N, Shore-Lesserson L. The Value of Thromboelastography (TEG) in COVID-19 Critical Illness as Illustrated by a Case Series. J Cardiothorac Vasc Anesth. 2022;36(8 Pt A):2536-43.
216. Horby P, Lim WS, Emberson JR, Mafham M, Bell JL, Linsell L, et al. Dexamethasone in Hospitalized Patients with Covid-19. N Engl J Med. 2021;384(8):693-704.
217. Chan L, Karimi N, Morovati S, Alizadeh K, Kakish JE, Vanderkamp S, et al. The Roles of Neutrophils in Cytokine Storms. Viruses. 2021;13(11).
218. Savla SR, Prabhavalkar KS, Bhatt LK. Cytokine storm associated coagulation complications in COVID-19 patients: Pathogenesis and Management. Expert Rev Anti Infect Ther. 2021;19(11):1397-413.
219. Arachchillage DRJ, Passariello M, Laffan M, Aw TC, Owen L, Banya W, et al. Intracranial Hemorrhage and Early Mortality in Patients Receiving Extracorporeal Membrane Oxygenation for Severe Respiratory Failure. Semin Thromb Hemost. 2018;44(3):276-86.
220. Ackermann M, Anders HJ, Bilyy R, Bowlin GL, Daniel C, De Lorenzo R, et al. Patients with COVID-19: in the dark-NETs of neutrophils. Cell Death Differ. 2021:1-15.
221. Arcanjo A, Logullo J, Menezes CCB, de Souza Carvalho Giangiarulo TC, Dos Reis MC, de Castro GMM, et al. The emerging role of neutrophil extracellular traps in severe acute respiratory syndrome coronavirus 2 (COVID-19). Sci Rep. 2020;10(1):19630.
222. Cavalier E, Guiot J, Lechner K, Dutsch A, Eccleston M, Herzog M, et al. Circulating Nucleosomes as Potential Markers to Monitor COVID-19 Disease Progression. Front Mol Biosci. 2021;8:600881.
223. Maisat W, Hou L, Sandhu S, Sin YC, Kim S, Pelt HV, et al. Neutrophil extracellular traps formation is associated with postoperative complications in neonates and infants undergoing congenital cardiac surgery. bioRxiv. 2023.
224. Chen JW, Hsu CC, Su CC, Hsu RB, Chiu YL, Jung CJ, et al. Transient Bacteremia Promotes Catheter-Related Central Venous Thrombosis through Neutrophil Extracellular Traps. Thromb Haemost. 2022;122(7):1198-208.
225. Haus M, Foltan M, Philipp A, Mueller T, Gruber M, Lingel MP, et al. Neutrophil extracellular traps - a potential trigger for the development of thrombocytopenia during extracorporeal membrane oxygenation. Front Immunol. 2024;15:1339235.
226. Odish MF, Masso-Silva JA, Pollema TL, Owens RL, Alexander LEC, Meier A. Initiation of ECMO in patients with COVID-19- related ARDS does not increase blood markers of neutrophil extracellular traps (NETs) or IL-8. J Cardiothorac Vasc Anesth. 2024;38(5):1288-9.
227. Yadav H, Kor DJ. Platelets in the pathogenesis of acute respiratory distress syndrome. Am J Physiol Lung Cell Mol Physiol. 2015;309(9):L915-23.
228. Van Den Helm S, Yaw HP, Letunica N, Barton R, Weaver A, Newall F, et al. Platelet Phenotype and Function Changes With Increasing Duration of Extracorporeal Membrane Oxygenation. Crit Care Med. 2022;50(8):1236-45.
229. Semenov AV, Romanov YA, Loktionova SA, Tikhomirov OY, Khachikian MV, Vasil'ev SA, et al. Production of soluble P-selectin by platelets and endothelial cells. Biochemistry (Mosc). 1999;64(11):1326-35.
230. Ushiyama S, Laue TM, Moore KL, Erickson HP, McEver RP. Structural and functional characterization of monomeric soluble P-selectin and comparison with membrane P-selectin. J Biol Chem. 1993;268(20):15229-37.
231. Panicker SR, Mehta-D'souza P, Zhang N, Klopocki AG, Shao B, McEver RP. Circulating soluble P-selectin must dimerize to promote inflammation and coagulation in mice. Blood. 2017;130(2):181-91.
232. Celi A, Pellegrini G, Lorenzet R, De Blasi A, Ready N, Furie BC, et al. P-selectin induces the expression of tissue factor on monocytes. Proc Natl Acad Sci U S A. 1994;91(19):8767-71.

233. Zonneveld R, Martinelli R, Shapiro NI, Kuijpers TW, Plotz FB, Carman CV. Soluble adhesion molecules as markers for sepsis and the potential pathophysiological discrepancy in neonates, children and adults. Crit Care. 2014;18(2):204.
234. Schrijver IT, Kemperman H, Roest M, Kesecioglu J, de Lange DW. Soluble P-selectin as a Biomarker for Infection and Survival in Patients With a Systemic Inflammatory Response Syndrome on the Intensive Care Unit. Biomark Insights. 2017;12:1177271916684823.
235. Yadav S, Storrie B. The cellular basis of platelet secretion: Emerging structure/function relationships. Platelets. 2017;28(2):108-18.
236. Files JM, TW, Yee E, Ritchie J, Harker L. Studies of human platelet α-granule release in vivo. Blood. 1981;58:607-18.
237. Cerletti C, de Gaetano G, Lorenzet R. Platelet - leukocyte interactions: multiple links between inflammation, blood coagulation and vascular risk. Mediterr J Hematol Infect Dis. 2010;2(3):e2010023.
238. Fuchs G, Berg N, Broman LM, Prahl Wittberg L. Flow-induced platelet activation in components of the extracorporeal membrane oxygenation circuit. Sci Rep. 2018;8(1):13985.
239. Mazzeffi M, Clark M, Grazioli A, Dugan C, Rector R, Dalton H, et al. Platelet factor-4 concentration in adult veno-arterial ECMO patients. Perfusion. 2021;36(7):688-93.
240. Vayne C, May MA, Bourguignon T, Lemoine E, Guery EA, Rollin J, et al. Frequency and Clinical Impact of Platelet Factor 4-Specific Antibodies in Patients Undergoing Extracorporeal Membrane Oxygenation. Thromb Haemost. 2019;119(7):1138-46.
241. Lubnow M, Berger J, Schneckenpointner R, Zeman F, Lunz D, Philipp A, et al. Prevalence and outcomes of patients developing heparin-induced thrombocytopenia during extracorporeal membrane oxygenation. PLoS One. 2022;17(8):e0272577.
242. Etulain J, Martinod K, Wong SL, Cifuni SM, Schattner M, Wagner DD. P-selectin promotes neutrophil extracellular trap formation in mice. Blood. 2015;126(2):242-6.
243. Lee HW, An JN, Lee HS, Song YR, Kim HJ, Kim SG, et al. Neutrophil extracellular traps and heparin-induced antibodies contribute to vascular access thrombosis in hemodialysis patients. Kidney Res Clin Pract. 2021;40(4):712-23.
244. Perdomo J, Leung HHL, Ahmadi Z, Yan F, Chong JJH, Passam FH, et al. Neutrophil activation and NETosis are the major drivers of thrombosis in heparin-induced thrombocytopenia. Nat Commun. 2019;10(1):1322.
245. Baldi RF, Koh MW, Thomas C, Sabbat T, Wang B, Tsatsari S, et al. Ventilator-induced Lung Injury Promotes Inflammation within the Pleural Cavity. Am J Respir Cell Mol Biol. 2024;71(1):43-52.
246. Koh MW, Baldi RF, Soni S, Handslip R, Tan YY, O'Dea KP, et al. Secreted Extracellular Cyclophilin A Is a Novel Mediator of Ventilator-induced Lung Injury. Am J Respir Crit Care Med. 2021;204(4):421-30.
247. Deniel G, Dhelft F, Lancelot S, Orkisz M, Roux E, Mouton W, et al. Pulmonary inflammation decreases with ultra-protective ventilation in experimental ARDS under VV-ECMO: a positron emission tomography study. Front Med (Lausanne). 2024;11:1338602.
248. Acute Respiratory Distress Syndrome N, Brower RG, Matthay MA, Morris A, Schoenfeld D, Thompson BT, et al. Ventilation with lower tidal volumes as compared with traditional tidal volumes for acute lung injury and the acute respiratory distress syndrome. N Engl J Med. 2000;342(18):1301-8.
249. Rozencwajg S, Guihot A, Franchineau G, Lescroat M, Brechot N, Hekimian G, et al. Ultra-Protective Ventilation Reduces Biotrauma in Patients on Venovenous Extracorporeal Membrane Oxygenation for Severe Acute Respiratory Distress Syndrome. Crit Care Med. 2019;47(11):1505-12.
250. Wang R, Sun B, Li X, Tang X, He H, Li Y, et al. Mechanical Ventilation Strategy Guided by Transpulmonary Pressure in Severe Acute Respiratory Distress Syndrome Treated With Venovenous Extracorporeal Membrane Oxygenation. Crit Care Med. 2020;48(9):1280-8.

251. Guervilly C, Fournier T, Chommeloux J, Arnaud L, Pinglis C, Baumstarck K, et al. Ultra-lung-protective ventilation and biotrauma in severe ARDS patients on veno-venous extracorporeal membrane oxygenation: a randomized controlled study. Crit Care. 2022;26(1):383.
252. Guldner A, Kiss T, Bluth T, Uhlig C, Braune A, Carvalho N, et al. Effects of ultraprotective ventilation, extracorporeal carbon dioxide removal, and spontaneous breathing on lung morphofunction and inflammation in experimental severe acute respiratory distress syndrome. Anesthesiology. 2015;122(3):631-46.
253. Abrams D, Agerstrand C, Beitler JR, Karagiannidis C, Madahar P, Yip NH, et al. Risks and Benefits of Ultra-Lung-Protective Invasive Mechanical Ventilation Strategies with a Focus on Extracorporeal Support. Am J Respir Crit Care Med. 2022;205(8):873-82.
254. Rungatscher A, Tessari M, Stranieri C, Solani E, Linardi D, Milani E, et al. Oxygenator Is the Main Responsible for Leukocyte Activation in Experimental Model of Extracorporeal Circulation: A Cautionary Tale. Mediators Inflamm. 2015;2015:484979.
255. Adrian K, Mellgren K, Skogby M, Friberg LG, Mellgren G, Wadenvik H. Cytokine release during long-term extracorporeal circulation in an experimental model. Artif Organs. 1998;22(10):859-63.
256. McILwain RB, Timpa JG, Kurundkar AR, Holt DW, Kelly DR, Hartman YE, et al. Plasma concentrations of inflammatory cytokines rise rapidly during ECMO-related SIRS due to the release of preformed stores in the intestine. Lab Invest. 2010;90(1):128-39.
257. Steiger T, Foltan M, Philipp A, Mueller T, Gruber M, Bredthauer A, et al. Accumulations of von Willebrand factor within ECMO oxygenators: Potential indicator of coagulation abnormalities in critically ill patients? Artif Organs. 2019;43(11):1065-76.
258. Wilm J, Philipp A, Muller T, Bredthauer A, Gleich O, Schmid C, et al. Leukocyte Adhesion as an Indicator of Oxygenator Thrombosis During Extracorporeal Membrane Oxygenation Therapy? ASAIO J. 2018;64(1):24-30.
259. Liu T, Amos SH, Ganga AL, Bullins CM, Jennings CD, Arnold WS, et al. Evaluation of cytokine response to extracorporeal membrane oxygenation. Artif Organs. 2022;46(1):146-54.
260. Napp LC, Ziegeler S, Kindgen-Milles D. Rationale of Hemoadsorption during Extracorporeal Membrane Oxygenation Support. Blood Purif. 2019;48(3):203-14.
261. Haem Rahimi M, Bidar F, Lukaszewicz AC, Garnier L, Payen-Gay L, Venet F, et al. Association of pronounced elevation of NET formation and nucleosome biomarkers with mortality in patients with septic shock. Ann Intensive Care. 2023;13(1):102.
262. Kano H, Huq M, Tsuda M, Noguchi H, Takeyama N. Sandwich ELISA for Circulating Myeloperoxidase- and Neutrophil Elastase-DNA Complexes Released from Neutrophil Extracellular Traps. Advanced Techniques in Biology & Medicine. 2016;5(196).
263. Guy A, Favre S, Labrouche-Colomer S, Deloison L, Gourdou-Latyszenok V, Renault MA, et al. High circulating levels of MPO-DNA are associated with thrombosis in patients with MPN. Leukemia. 2019;33(10):2544-8.
264. Maruchi Y, Tsuda M, Mori H, Takenaka N, Gocho T, Huq MA, et al. Plasma myeloperoxidase-conjugated DNA level predicts outcomes and organ dysfunction in patients with septic shock. Crit Care. 2018;22(1):176.
265. Hayden H, Ibrahim N, Klopf J, Zagrapan B, Mauracher LM, Hell L, et al. ELISA detection of MPO-DNA complexes in human plasma is error-prone and yields limited information on neutrophil extracellular traps formed in vivo. PLoS One. 2021;16(4):e0250265.
266. Schneck E, Mallek F, Schiederich J, Kramer E, Markmann M, Hecker M, et al. Flow Cytometry-Based Quantification of Neutrophil Extracellular Traps Shows an Association with Hypercoagulation in Septic Shock and Hypocoagulation in Postsurgical Systemic Inflammation-A Proof-of-Concept Study. J Clin Med. 2020;9(1).
267. Gavillet M, Martinod K, Renella R, Harris C, Shapiro NI, Wagner DD, et al. Flow cytometric assay for direct quantification of neutrophil extracellular traps in blood samples. Am J Hematol. 2015;90(12):1155-8.

268. Kenny EF, Herzig A, Kruger R, Muth A, Mondal S, Thompson PR, et al. Diverse stimuli engage different neutrophil extracellular trap pathways. Elife. 2017;6.
269. Laridan E, Martinod K, De Meyer SF. Neutrophil Extracellular Traps in Arterial and Venous Thrombosis. Semin Thromb Hemost. 2019;45(1):86-93.
270. Masuda S, Shimizu S, Matsuo J, Nishibata Y, Kusunoki Y, Hattanda F, et al. Measurement of NET formation in vitro and in vivo by flow cytometry. Cytometry A. 2017;91(8):822-9.
271. Zharkova O, Tay SH, Lee HY, Shubhita T, Ong WY, Lateef A, et al. A Flow Cytometry-Based Assay for High-Throughput Detection and Quantification of Neutrophil Extracellular Traps in Mixed Cell Populations. Cytometry A. 2019;95(3):268-78.
272. Masuda S, Nakazawa D, Shida H, Miyoshi A, Kusunoki Y, Tomaru U, et al. NETosis markers: Quest for specific, objective, and quantitative markers. Clin Chim Acta. 2016;459:89-93.
273. Blanter M, Cambier S, De Bondt M, Vanbrabant L, Portner N, Abouelasrar Salama S, et al. Method Matters: Effect of Purification Technology on Neutrophil Phenotype and Function. Front Immunol. 2022;13:820058.
274. Moss J, Magenheim J, Neiman D, Zemmour H, Loyfer N, Korach A, et al. Comprehensive human cell-type methylation atlas reveals origins of circulating cell-free DNA in health and disease. Nat Commun. 2018;9(1):5068.
275. Chung JH, Yeo HJ, Kim D, Lee SM, Han J, Kim M, et al. Changes in the levels of beta-thromboglobulin and inflammatory mediators during extracorporeal membrane oxygenation support. Int J Artif Organs. 2017;40(10):575-80.
276. Mansour A, Roussel M, Gaussem P, Nedelec-Gac F, Pontis A, Flecher E, et al. Platelet Functions During Extracorporeal Membrane Oxygenation. Platelet-Leukocyte Aggregates Analyzed by Flow Cytometry as a Promising Tool to Monitor Platelet Activation. J Clin Med. 2020;9(8).
277. Schmuckenschlager A, Pirabe A, Assinger A, Schrottmaier WC. Platelet count, temperature and pH value differentially affect hemostatic and immunomodulatory functions of platelets. Thromb Res. 2023;223:111-22.
278. Middleton EA, He XY, Denorme F, Campbell RA, Ng D, Salvatore SP, et al. Neutrophil extracellular traps contribute to immunothrombosis in COVID-19 acute respiratory distress syndrome. Blood. 2020;136(10):1169-79.
279. Meyer AD, Gelfond JA, Wiles AA, Freishtat RJ, Rais-Bahrami K. Platelet-derived microparticles generated by neonatal extracorporeal membrane oxygenation systems. Asaio j. 2015;61(1):37-42.
280. Diehl P, Aleker M, Helbing T, Sossong V, Beyersdorf F, Olschewski M, et al. Enhanced microparticles in ventricular assist device patients predict platelet, leukocyte and endothelial cell activation. Interact Cardiovasc Thorac Surg. 2010;11(2):133-7.
281. Carter AM, Anagnostopoulou K, Mansfield MW, Grant PJ. Soluble P-selectin levels, P-selectin polymorphisms and cardiovascular disease. J Thromb Haemost. 2003;1(8):1718-23.
282. Li J, Kim K, Barazia A, Tseng A, Cho J. Platelet-neutrophil interactions under thromboinflammatory conditions. Cell Mol Life Sci. 2015;72(14):2627-43.
283. Mehta P, Patel KD, Laue TM, Erickson HP, McEver RP. Soluble monomeric P-selectin containing only the lectin and epidermal growth factor domains binds to P-selectin glycoprotein ligand-1 on leukocytes. Blood. 1997;90(6):2381-9.
284. Gross PL. Soluble P-selectin is the smoke, not the fire. Blood. 2017;130(2):101-2.
285. Rauova L, Poncz M, McKenzie SE, Reilly MP, Arepally G, Weisel JW, et al. Ultralarge complexes of PF4 and heparin are central to the pathogenesis of heparin-induced thrombocytopenia. Blood. 2005;105(1):131-8.
286. Nair P, Hoechter DJ, Buscher H, Venkatesh K, Whittam S, Joseph J, et al. Prospective observational study of hemostatic alterations during adult extracorporeal membrane oxygenation (ECMO) using point-of-care thromboelastometry and platelet aggregometry. J Cardiothorac Vasc Anesth. 2015;29(2):288-96.

287. Wand S, Huber-Petersen JF, Schaeper J, Binder C, Moerer O. Platelet Function Disturbance During Veno-Venous ECMO in ARDS Patients Assessed by Multiple Electrode Aggregometry-A Prospective, Observational Cohort Study. J Clin Med. 2019;8(7).
288. Tauber H, Streif W, Fritz J, Ott H, Weigel G, Loacker L, et al. Predicting Transfusion Requirements During Extracorporeal Membrane Oxygenation. J Cardiothorac Vasc Anesth. 2016;30(3):692-701.
289. Abrams D, Baldwin MR, Champion M, Agerstrand C, Eisenberger A, Bacchetta M, et al. Thrombocytopenia and extracorporeal membrane oxygenation in adults with acute respiratory failure: a cohort study. Intensive Care Med. 2016;42(5):844-52.
290. Wallisch M, Lorentz CU, Lakshmanan HHS, Johnson J, Carris MR, Puy C, et al. Antibody inhibition of contact factor XII reduces platelet deposition in a model of extracorporeal membrane oxygenator perfusion in nonhuman primates. Res Pract Thromb Haemost. 2020;4(2):205-16.
291. Siegel PM, Chalupsky J, Olivier CB, Bojti I, Pooth JS, Trummer G, et al. Early platelet dysfunction in patients receiving extracorporeal membrane oxygenation is associated with mortality. J Thromb Thrombolysis. 2022;53(3):712-21.
292. Paschke L, Foltan M, Wagner MS, Lubnow M, Gruber M, Krenkel L, et al. Clinical Relevance of Platelet-Leukocyte Aggregates and Platelet P-Selectin Expression During Venovenous Extracorporeal Membrane Oxygenation. ASAIO J. 2025.
293. Wagner ML, Johnston M, Jenkins T, Palumbo JS, Rymeski BA. Use of thromboelastography in children on extracorporeal membrane oxygenation. J Pediatr Surg. 2022;57(6):1056-61.
294. Buckley MS, Benanti GE, Meckel J, Tekle LA, Gilbert B, Puebla Neira D, et al. Correlation between partial thromboplastin time and thromboelastography in adult critically ill patients requiring bivalirudin for extracorporeal membrane oxygenation. Pharmacotherapy. 2023;43(3):196-204.
295. Henderson N, Sullivan JE, Myers J, Wells T, Calhoun A, Berkenbosch J, et al. Use of Thromboelastography to Predict Thrombotic Complications in Pediatric and Neonatal Extracorporeal Membranous Oxygenation. J Extra Corpor Technol. 2018;50(3):149-54.
296. Yin EB, Bracey AW, Chatterjee S. Thromboelastography versus thromboelastometry for unfractionated heparin monitoring in adult patients on extracorporeal membrane oxygenation. Perfusion. 2025;40(1):235-42.
297. Wienkamp AK, Erpenbeck L, Rossaint J. Platelets in the NETworks interweaving inflammation and thrombosis. Front Immunol. 2022;13:953129.
298. Zucoloto AZ, Jenne CN. Platelet-Neutrophil Interplay: Insights Into Neutrophil Extracellular Trap (NET)-Driven Coagulation in Infection. Front Cardiovasc Med. 2019;6:85.
299. Augusto JF, Beauvillain C, Poli C, Paolini L, Tournier I, Pignon P, et al. Clusterin Neutralizes the Inflammatory and Cytotoxic Properties of Extracellular Histones in Sepsis. Am J Respir Crit Care Med. 2023;208(2):176-87.
300. Lewis HD, Liddle J, Coote JE, Atkinson SJ, Barker MD, Bax BD, et al. Inhibition of PAD4 activity is sufficient to disrupt mouse and human NET formation. Nat Chem Biol. 2015;11(3):189-91.
301. Shen W, Oladejo AO, Ma X, Jiang W, Zheng J, Imam BH, et al. Inhibition of Neutrophil Extracellular Traps Formation by Cl-Amidine Alleviates Lipopolysaccharide-Induced Endometritis and Uterine Tissue Damage. Animals (Basel). 2022;12(9).
302. Li M, Lin C, Deng H, Strnad J, Bernabei L, Vogl DT, et al. A Novel Peptidylarginine Deiminase 4 (PAD4) Inhibitor BMS-P5 Blocks Formation of Neutrophil Extracellular Traps and Delays Progression of Multiple Myeloma. Mol Cancer Ther. 2020;19(7):1530-8.
303. Maugeri N, Campana L, Gavina M, Covino C, De Metrio M, Panciroli C, et al. Activated platelets present high mobility group box 1 to neutrophils, inducing autophagy and promoting the extrusion of neutrophil extracellular traps. J Thromb Haemost. 2014;12(12):2074-88.
304. Ngo ATP, Sarkar A, Yarovoi I, Levine ND, Bochenek V, Zhao G, et al. Neutrophil extracellular trap stabilization by platelet factor 4 reduces thrombogenicity and endothelial cell injury. bioRxiv. 2023.

305. Le Joncour A, Biard L, Vautier M, Bugaut H, Mekinian A, Maalouf G, et al. Neutrophil-Platelet and Monocyte-Platelet Aggregates in COVID-19 Patients. Thromb Haemost. 2020;120(12):1733-5.
306. Ceran E, Schlommer C, Krockel I, Scheriau G, Angleitner P, Steinlechner B. Pseudothrombocytopenia Inducing Nonindicated Platelet Transfusion after Cardiac Surgery. Case Rep Med. 2021;2021:3695407.
307. Lardinois B, Favresse J, Chatelain B, Lippi G, Mullier F. Pseudothrombocytopenia-A Review on Causes, Occurrence and Clinical Implications. J Clin Med. 2021;10(4).
308. Tan GC, Stalling M, Dennis G, Nunez M, Kahwash SB. Pseudothrombocytopenia due to Platelet Clumping: A Case Report and Brief Review of the Literature. Case Rep Hematol. 2016;2016:3036476.
309. Wahed A, Quesada A, A D. Sources of errors in hematology and coagulation. Hematology and Coagulation. 2nd ed. Academic Press2020. p. 277-91.
310. Zeng S, Zhou X, Ge L, Ji WJ, Shi R, Lu RY, et al. Monocyte subsets and monocyte-platelet aggregates in patients with unstable angina. J Thromb Thrombolysis. 2014;38(4):439-46.
311. Zhou J, Xu E, Shao K, Shen W, Gu Y, Li M, et al. Circulating platelet-neutrophil aggregates as risk factor for deep venous thrombosis. Clin Chem Lab Med. 2019;57(5):707-15.
312. Smout J, Dyker A, Cleanthis M, Ford G, Kesteven P, Stansby G. Platelet function following acute cerebral ischemia. Angiology. 2009;60(3):362-9.
313. Zarbock A, Singbartl K, Ley K. Complete reversal of acid-induced acute lung injury by blocking of platelet-neutrophil aggregation. J Clin Invest. 2006;116(12):3211-9.
314. Polanowska-Grabowska R, Wallace K, Field JJ, Chen L, Marshall MA, Figler R, et al. P-selectin-mediated platelet-neutrophil aggregate formation activates neutrophils in mouse and human sickle cell disease. Arterioscler Thromb Vasc Biol. 2010;30(12):2392-9.
315. Yang S, Huang X, Liao J, Li Q, Chen S, Liu C, et al. Platelet-leukocyte aggregates - a predictor for acute kidney injury after cardiac surgery. Ren Fail. 2021;43(1):1155-62.
316. Patnaik R, Azim A, Agarwal V. Neutrophil CD64 a Diagnostic and Prognostic Marker of Sepsis in Adult Critically Ill Patients: A Brief Review. Indian J Crit Care Med. 2020;24(12):1242-50.
317. Kreuter M, Lee JS, Tzouvelekis A, Oldham JM, Molyneaux PL, Weycker D, et al. Monocyte Count as a Prognostic Biomarker in Patients with Idiopathic Pulmonary Fibrosis. Am J Respir Crit Care Med. 2021;204(1):74-81.
318. Scott MKD, Quinn K, Li Q, Carroll R, Warsinske H, Vallania F, et al. Increased monocyte count as a cellular biomarker for poor outcomes in fibrotic diseases: a retrospective, multicentre cohort study. Lancet Respir Med. 2019;7(6):497-508.
319. Gerrits AJ, Frelinger AL, 3rd, Michelson AD. Whole Blood Analysis of Leukocyte-Platelet Aggregates. Curr Protoc Cytom. 2016;78:6 15 1-6 0.
320. Harding SA, Din JN, Sarma J, Jessop A, Weatherall M, Fox KA, et al. Flow cytometric analysis of circulating platelet-monocyte aggregates in whole blood: methodological considerations. Thromb Haemost. 2007;98(2):451-6.
321. Conway Morris A, Datta D, Shankar-Hari M, Stephen J, Weir CJ, Rennie J, et al. Cell-surface signatures of immune dysfunction risk-stratify critically ill patients: INFECT study. Intensive Care Med. 2018;44(5):627-35.
322. Morselli M, Longo G, Bonacorsi G, Potenza L, Emilia G, Torelli G. Anticoagulant pseudothrombocytopenia with platelet satellitism. Haematologica. 1999;84(7):655.
323. Mody M, Lazarus AH, Semple JW, Freedman J. Preanalytical requirements for flow cytometric evaluation of platelet activation: choice of anticoagulant. Transfus Med. 1999;9(2):147-54.
324. Cattaneo M, Hayward CP, Moffat KA, Pugliano MT, Liu Y, Michelson AD. Results of a worldwide survey on the assessment of platelet function by light transmission aggregometry: a report from the platelet physiology subcommittee of the SSC of the ISTH. J Thromb Haemost. 2009;7(6):1029.

325. Callan MB, Shofer FS, Catalfamo JL. Effects of anticoagulant on pH, ionized calcium concentration, and agonist-induced platelet aggregation in canine platelet-rich plasma. Am J Vet Res. 2009;70(4):472-7.
326. Truss NJ, Armstrong PC, Liverani E, Vojnovic I, Warner TD. Heparin but not citrate anticoagulation of blood preserves platelet function for prolonged periods. J Thromb Haemost. 2009;7(11):1897-905.
327. Harding SA, Din JN, Sarma J, Josephs DH, Fox KA, Newby DE. Promotion of proinflammatory interactions between platelets and monocytes by unfractionated heparin. Heart. 2006;92(11):1635-8.
328. O'Brien JR, Shoobridge SM, Finch WJ. Comparison of the effect of heparin and citrate on platelet aggregation. J Clin Pathol. 1969;22(1):28-31.
329. Wood AJ, Vassallo AM, Ruchaud-Sparagano MH, Scott J, Zinnato C, Gonzalez-Tejedo C, et al. C5a impairs phagosomal maturation in the neutrophil through phosphoproteomic remodeling. JCI Insight. 2020;5(15).
330. Wood AJT. Measurement and mechanisms of complement-induced neutrophil dysfunction.: Cambridge University; 2019.
331. Zucker MB, Grant RA. Nonreversible loss of platelet aggregability induced by calcium deprivation. Blood. 1978;52(3):505-13.
332. Stephen J, Dransfield I. The Pathophysiological Relevance of Monocyte-platelet Interactions in Inflammatory Disease. Journal of Experimental & Clinical Medicine. 2010;2(6):262-8.
333. Xiang B, Zhang G, Zhang Y, Wu C, Joshi S, Morris AJ, et al. Calcium Ion Chelation Preserves Platelet Function During Cold Storage. Arterioscler Thromb Vasc Biol. 2021;41(1):234-49.
334. Aatonen M, Valkonen S, Boing A, Yuana Y, Nieuwland R, Siljander P. Isolation of Platelet-Derived Extracellular Vesicles. Methods Mol Biol. 2017;1545:177-88.
335. Ferreira PM, Bozbas E, Tannetta SD, Alroqaiba N, Zhou R, Crawley JTB, et al. Mode of induction of platelet-derived extracellular vesicles is a critical determinant of their phenotype and function. Sci Rep. 2020;10(1):18061.
336. Weiss L, MacLeod H, Comer SP, Cullivan S, Szklanna PB, Ni Ainle F, et al. An optimized protocol to isolate quiescent washed platelets from human whole blood and generate platelet releasate under clinical conditions. STAR Protoc. 2023;4(2):102150.
337. Peshkova AD, Saliakhutdinova SM, Sounbuli K, Selivanova YA, Andrianova IA, Khabirova AI, et al. The differential formation and composition of leukocyte-platelet aggregates induced by various cellular stimulants. Thromb Res. 2024;241:109092.
338. Allen N, Barrett TJ, Guo Y, Nardi M, Ramkhelawon B, Rockman CB, et al. Circulating monocyte-platelet aggregates are a robust marker of platelet activity in cardiovascular disease. Atherosclerosis. 2019;282:11-8.
339. Rolling CC, Barrett TJ, Berger JS. Platelet-monocyte aggregates: molecular mediators of thromboinflammation. Front Cardiovasc Med. 2023;10:960398.
340. Hu H, Varon D, Hjemdahl P, Savion N, Schulman S, Li N. Platelet-leukocyte aggregation under shear stress: differential involvement of selectins and integrins. Thromb Haemost. 2003;90(4):679-87.
341. Vermillion MS, Lyons CE, Najarro KM, Adams RJ, Metcalf Pate KA. Immune Activation of Platelets in Response to Serial Phlebotomy in Pigtailed Macaques (Macaca nemestrina). Comp Med. 2017;67(4):360-7.
342. Frerou A, Lesouhaitier M, Gregoire M, Uhel F, Gacouin A, Reizine F, et al. Venoarterial extracorporeal membrane oxygenation induces early immune alterations. Crit Care. 2021;25(1):9.
343. Lesouhaitier M, Gregoire M, Gacouin A, Coirier V, Frerou A, Piau C, et al. Neutrophil function and bactericidal activity against Staphylococcus aureus after cardiac surgery with cardiopulmonary bypass. J Leukoc Biol. 2022;111(4):867-76.

344. Graulich J, Walzog B, Marcinkowski M, Bauer K, Kossel H, Fuhrmann G, et al. Leukocyte and endothelial activation in a laboratory model of extracorporeal membrane oxygenation (ECMO). Pediatr Res. 2000;48(5):679-84.
345. Ki KK, Passmore MR, Chan CHH, Malfertheiner MV, Bouquet M, Cho HJ, et al. Effect of ex vivo extracorporeal membrane oxygenation flow dynamics on immune response. Perfusion. 2019;34(1_suppl):5-14.
346. Carestia A, Kaufman T, Rivadeneyra L, Landoni VI, Pozner RG, Negrotto S, et al. Mediators and molecular pathways involved in the regulation of neutrophil extracellular trap formation mediated by activated platelets. J Leukoc Biol. 2016;99(1):153-62.
347. Kornerup KN, Salmon GP, Pitchford SC, Liu WL, Page CP. Circulating platelet-neutrophil complexes are important for subsequent neutrophil activation and migration. J Appl Physiol (1985). 2010;109(3):758-67.
348. Maugeri N, Rovere-Querini P, Evangelista V, Covino C, Capobianco A, Bertilaccio MT, et al. Neutrophils phagocytose activated platelets in vivo: a phosphatidylserine, P-selectin, and beta2 integrin-dependent cell clearance program. Blood. 2009;113(21):5254-65.
349. Lee RH, Ghalloussi D, Harousseau GL, Kenny JP, Kramer PA, Proamer F, et al. Rasa3 deficiency minimally affects thrombopoiesis but promotes severe thrombocytopenia due to integrin-dependent platelet clearance. JCI Insight. 2022;7(8).
350. Panasiuk A, Zak J, Kasprzycka E, Janicka K, Prokopowicz D. Blood platelet and monocyte activations and relation to stages of liver cirrhosis. World J Gastroenterol. 2005;11(18):2754-8.
351. Metcalf Pate KA, Lyons CE, Dorsey JL, Shirk EN, Queen SE, Adams RJ, et al. Platelet activation and platelet-monocyte aggregate formation contribute to decreased platelet count during acute simian immunodeficiency virus infection in pig-tailed macaques. J Infect Dis. 2013;208(6):874-83.
352. Shen XF, Cao K, Jiang JP, Guan WX, Du JF. Neutrophil dysregulation during sepsis: an overview and update. J Cell Mol Med. 2017;21(9):1687-97.
353. Liu S, Li Y, She F, Zhao X, Yao Y. Predictive value of immune cell counts and neutrophil-to-lymphocyte ratio for 28-day mortality in patients with sepsis caused by intra-abdominal infection. Burns Trauma. 2021;9:tkaa040.
354. Chung H, Lee JH, Jo YH, Hwang JE, Kim J. Circulating Monocyte Counts and its Impact on Outcomes in Patients With Severe Sepsis Including Septic Shock. Shock. 2019;51(4):423-9.
355. Rudensky B, Yinnon AM, Shutin O, Broide E, Wiener-Well Y, Bitran D, et al. The cellular immunological responses of patients undergoing coronary artery bypass grafting compared with those of patients undergoing valve replacement. Eur J Cardiothorac Surg. 2010;37(5):1056-62.
356. Chenouard A, Rimbert M, Joram N, Braudeau C, Roquilly A, Bourgoin P, et al. Monocytic Human Leukocyte Antigen DR Expression in Young Infants Undergoing Cardiopulmonary Bypass. Ann Thorac Surg. 2021;111(5):1636-42.
357. Ziemba K, Nateri J, Hanson-Huber L, Steele L, Cismowski M, West T, et al. 625: Innate and adaptive immune function during extracorporeal membrane oxygenation. Critical Care Medicine; 2016.
358. Rauch A, Dupont A, Rosa M, Desvages M, Le Tanno C, Abdoul J, et al. Shear Forces Induced Platelet Clearance Is a New Mechanism of Thrombocytopenia. Circ Res. 2023;133(10):826-41.
359. Chatterjee S. Endothelial Mechanotransduction, Redox Signaling and the Regulation of Vascular Inflammatory Pathways. Front Physiol. 2018;9:524.
360. Baker-Groberg SM, Lattimore S, Recht M, McCarty OJ, Haley KM. Assessment of neonatal platelet adhesion, activation, and aggregation. J Thromb Haemost. 2016;14(4):815-27.
361. Walsh SW, Al Dulaimi M, Strauss JF, 3rd. Gene Expression of Pregnancy Neutrophils Differs for Protease versus Lipopolysaccharide Stimulation. Int J Mol Sci. 2022;23(9).
362. Walsh SW, Nugent WH, Al Dulaimi M, Washington SL, Dacha P, Strauss JF, 3rd. Proteases Activate Pregnancy Neutrophils by a Protease-Activated Receptor 1 Pathway: Epigenetic Implications for Preeclampsia. Reprod Sci. 2020;27(11):2115-27.

363. Bakele M, Lotz-Havla AS, Jakowetz A, Carevic M, Marcos V, Muntau AC, et al. An interactive network of elastase, secretases, and PAR-2 protein regulates CXCR1 receptor surface expression on neutrophils. J Biol Chem. 2014;289(30):20516-25.
364. Bryzek D, Ciaston I, Dobosz E, Gasiorek A, Makarska A, Sarna M, et al. Triggering NETosis via protease-activated receptor (PAR)-2 signaling as a mechanism of hijacking neutrophils function for pathogen benefits. PLoS Pathog. 2019;15(5):e1007773.
365. Goldsmith HL, Spain S. Margination of leukocytes in blood flow through small tubes. Microvasc Res. 1984;27(2):204-22.
366. Dore M, Burns AR, Hughes BJ, Entman ML, Smith CW. Chemoattractant-induced changes in surface expression and redistribution of a functional ligand for P-selectin on neutrophils. Blood. 1996;87(5):2029-37.
367. Page C, Pitchford S. Neutrophil and platelet complexes and their relevance to neutrophil recruitment and activation. Int Immunopharmacol. 2013;17(4):1176-84.
368. Entman ML, Ballantyne CM. Association of neutrophils with platelet aggregates in unstable angina. Should we alter therapy? Circulation. 1996;94(6):1206-8.
369. Mauler M, Seyfert J, Haenel D, Seeba H, Guenther J, Stallmann D, et al. Platelet-neutrophil complex formation-a detailed in vitro analysis of murine and human blood samples. J Leukoc Biol. 2016;99(5):781-9.
370. Sun W, Wang S, Zhang J, Arias K, Griffith BP, Wu ZJ. Neutrophil injury and function alterations induced by high mechanical shear stress with short exposure time. Artif Organs. 2021;45(6):577-86.
371. Sun W, Zhang J, Shah A, Arias K, Berk Z, Griffith BP, et al. Neutrophil dysfunction due to continuous mechanical shear exposure in mechanically assisted circulation in vitro. Artif Organs. 2022;46(1):83-94.
372. Ahn KC, Jun AJ, Pawar P, Jadhav S, Napier S, McCarty OJ, et al. Preferential binding of platelets to monocytes over neutrophils under flow. Biochem Biophys Res Commun. 2005;329(1):345-55.
373. Davenpeck KL, Brummet ME, Hudson SA, Mayer RJ, Bochner BS. Activation of human leukocytes reduces surface P-selectin glycoprotein ligand-1 (PSGL-1, CD162) and adhesion to P-selectin in vitro. J Immunol. 2000;165(5):2764-72.
374. Gardiner EE, De Luca M, McNally T, Michelson AD, Andrews RK, Berndt MC. Regulation of P-selectin binding to the neutrophil P-selectin counter-receptor P-selectin glycoprotein ligand-1 by neutrophil elastase and cathepsin G. Blood. 2001;98(5):1440-7.
375. Colognato R, Slupsky JR, Jendrach M, Burysek L, Syrovets T, Simmet T. Differential expression and regulation of protease-activated receptors in human peripheral monocytes and monocyte-derived antigen-presenting cells. Blood. 2003;102(7):2645-52.
376. Scharf RE. Drugs that affect platelet function. Semin Thromb Hemost. 2012;38(8):865-83.
377. Patko Z, Csaszar A, Acsady G, Peter K, Schwarz M. Roles of Mac-1 and glycoprotein IIb/IIIa integrins in leukocyte-platelet aggregate formation: stabilization by Mac-1 and inhibition by GpIIb/IIIa blockers. Platelets. 2012;23(5):368-75.
378. Hamm CW, Bassand JP, Agewall S, Bax J, Boersma E, Bueno H, et al. ESC Guidelines for the management of acute coronary syndromes in patients presenting without persistent ST-segment elevation: The Task Force for the management of acute coronary syndromes (ACS) in patients presenting without persistent ST-segment elevation of the European Society of Cardiology (ESC). Eur Heart J. 2011;32(23):2999-3054.
379. Tellor BR, Smith JR, Prasad SM, Joseph SM, Silvestry SC. The use of eptifibatide for suspected pump thrombus or thrombosis in patients with left ventricular assist devices. J Heart Lung Transplant. 2014;33(1):94-101.
380. Al-Quthami AH, Jumean M, Kociol R, Pham DT, Kiernan M, DeNofrio D, et al. Eptifibatide for the treatment of HeartMate II left ventricular assist device thrombosis. Circ Heart Fail. 2012;5(4):e68-70.

381. Gurnani PK, Bohlmann A, March RJ. Prolonged use of eptifibatide as a bridge to maintain drug-eluting stent patency in a patient receiving extracorporeal membrane oxygenation. Perfusion. 2018;33(8):699-703.
382. Passacquale G, Vamadevan P, Pereira L, Hamid C, Corrigall V, Ferro A. Monocyte-platelet interaction induces a pro-inflammatory phenotype in circulating monocytes. PLoS One. 2011;6(10):e25595.
383. Layne K, Di Giosia P, Ferro A, Passacquale G. Anti-platelet drugs attenuate the expansion of circulating CD14highCD16+ monocytes under pro-inflammatory conditions. Cardiovasc Res. 2016;111(1):26-33.
384. Schulte C, Pieper L, Frye M, Waldeyer C, Neumann JT, Brunner FJ, et al. Antiplatelet drugs do not protect from platelet-leukocyte aggregation in coronary artery disease. J Thromb Haemost. 2024;22(2):553-7.
385. Ohta S, Inujima Y, Abe M, Uosaki Y, Sato S, Miki I. Inhibition of P-selectin specific cell adhesion by a low molecular weight, non-carbohydrate compound, KF38789. Inflamm Res. 2001;50(11):544-51.
386. Gillies PJ, Richardson NA, Walshe J, Stephenson SA, Dawson RA, Harkin DG. Demonstration of P-selectin expression and potential function in human corneal epithelial cells. Exp Eye Res. 2018;176:196-206.
387. Wun T, Cordoba M, Rangaswami A, Cheung AW, Paglieroni T. Activated monocytes and platelet-monocyte aggregates in patients with sickle cell disease. Clin Lab Haematol. 2002;24(2):81-8.
388. Ataga KI, Kutlar A, Kanter J, Liles D, Cancado R, Friedrisch J, et al. Crizanlizumab for the Prevention of Pain Crises in Sickle Cell Disease. N Engl J Med. 2017;376(5):429-39.
389. Kutlar A, Kanter J, Liles DK, Alvarez OA, Cancado RD, Friedrisch JR, et al. Effect of crizanlizumab on pain crises in subgroups of patients with sickle cell disease: A SUSTAIN study analysis. Am J Hematol. 2019;94(1):55-61.
390. Solomon SD, Lowenstein CJ, Bhatt AS, Peikert A, Vardeny O, Kosiborod MN, et al. Effect of the P-Selectin Inhibitor Crizanlizumab on Survival Free of Organ Support in Patients Hospitalized for COVID-19: A Randomized Controlled Trial. Circulation. 2023;148(5):381-90.
391. Leucker TM, Osburn WO, Reventun P, Smith K, Claggett B, Kirwan BA, et al. Effect of Crizanlizumab, a P-Selectin Inhibitor, in COVID-19: A Placebo-Controlled, Randomized Trial. JACC Basic Transl Sci. 2021;6(12):935-45.
392. Ward JR, Bingle L, Judge HM, Brown SB, Storey RF, Whyte MK, et al. Agonists of toll-like receptor (TLR)2 and TLR4 are unable to modulate platelet activation by adenosine diphosphate and platelet activating factor. Thromb Haemost. 2005;94(4):831-8.
393. Michelson AD, Barnard MR, Krueger LA, Valeri CR, Furman MI. Circulating monocyte-platelet aggregates are a more sensitive marker of in vivo platelet activation than platelet surface P-selectin: studies in baboons, human coronary intervention, and human acute myocardial infarction. Circulation. 2001;104(13):1533-7.
394. Schulz C, Massberg S. Platelets in atherosclerosis and thrombosis. Handb Exp Pharmacol. 2012(210):111-33.
395. Mackman N. Role of tissue factor in hemostasis, thrombosis, and vascular development. Arterioscler Thromb Vasc Biol. 2004;24(6):1015-22.
396. Tapp LD, Shantsila E, Wrigley BJ, Pamukcu B, Lip GY. The CD14++CD16+ monocyte subset and monocyte-platelet interactions in patients with ST-elevation myocardial infarction. J Thromb Haemost. 2012;10(7):1231-41.
397. Na SP, Ning ML, Ma JF, Liang S, Wang YL, Sui MS, et al. Association of elevated circulating monocyte-platelet aggregates with hypercoagulability in patients with nephrotic syndrome. Thromb J. 2024;22(1):56.

398. da Costa Martins P, van den Berk N, Ulfman LH, Koenderman L, Hordijk PL, Zwaginga JJ. Platelet-monocyte complexes support monocyte adhesion to endothelium by enhancing secondary tethering and cluster formation. Arterioscler Thromb Vasc Biol. 2004;24(1):193-9.
399. Etulain J, Negrotto S, Carestia A, Pozner RG, Romaniuk MA, D'Atri LP, et al. Acidosis downregulates platelet haemostatic functions and promotes neutrophil proinflammatory responses mediated by platelets. Thromb Haemost. 2012;107(1):99-110.
400. Prame Kumar K, Nicholls AJ, Wong CHY. Partners in crime: neutrophils and monocytes/macrophages in inflammation and disease. Cell Tissue Res. 2018;371(3):551-65.
401. Mandel J, Casari M, Stepanyan M, Martyanov A, Deppermann C. Beyond Hemostasis: Platelet Innate Immune Interactions and Thromboinflammation. Int J Mol Sci. 2022;23(7).
402. Carreau A, El Hafny-Rahbi B, Matejuk A, Grillon C, Kieda C. Why is the partial oxygen pressure of human tissues a crucial parameter? Small molecules and hypoxia. J Cell Mol Med. 2011;15(6):1239-53.
403. Injarabian L, Skerniskyte J, Giai Gianetto Q, Witko-Sarsat V, Marteyn BS. Reducing neutrophil exposure to oxygen allows their basal state maintenance. Immunol Cell Biol. 2021;99(7):782-9.
404. Tsiridou DM, O'Dea KP, Tan YY, Takata M. Myeloid-derived microvesicles as acute mediators of sepsis-induced lung vascular inflammation European Respiratory Journal. : European Respiratory Journal; 2020.
405. Tsiridou DM, Sachouli E, Takata M, O'Dea K. Neutrophil-Derived Microvesicles Enhance Pulmonary Vascular Inflammation via a Toll-like Receptor 4 Signaling-Dependent Mechanism. The FASEB Journal. 2022;36(S1).
406. Sachouli E, Tsiridou DM, Takata M, Gordon A, O'Dea K. Stimulation of Neutrophils in Whole Blood Enhances the Pro-inflammatory Activity of Neutrophil-Derived Microvesicles. The FASEB Journal. 2022;36(S1).
407. Li Y, Becker KC, Slatkin D, Spencer F, Becker RC. The effect of temperature variation in vitro on platelet-leukocyte interactions and individual prothrombotic potential. J Thromb Thrombolysis. 2004;18(1):19-23.
408. Galgano L, Guidetti GF, Torti M, Canobbio I. The Controversial Role of LPS in Platelet Activation In Vitro. Int J Mol Sci. 2022;23(18).
409. Moser M, Bertram U, Peter K, Bode C, Ruef J. Abciximab, eptifibatide, and tirofiban exhibit dose-dependent potencies to dissolve platelet aggregates. J Cardiovasc Pharmacol. 2003;41(4):586-92.
410. Geng X, Mihaila R, Yuan Y, Strutt S, Benz J, Tang T, et al. Inclacumab, a Fully Human Anti-P-Selectin Antibody, Directly Binds to PSGL-1 Binding Region and Demonstrates Robust and Durable Inhibition of Cell Adhesion. Blood. 2020;136:10-1.
411. Wu Q, Ren J, Hu D, Wu X, Li G, Wang G, et al. Monocyte subsets and monocyte-platelet aggregates: implications in predicting septic mortality among surgical critical illness patients. Biomarkers. 2016;21(6):509-16.
412. Looney MR, Gilliss BM, Matthay MA. Pathophysiology of transfusion-related acute lung injury. Curr Opin Hematol. 2010;17(5):418-23.
413. Kvietys PR, Fakhoury HMA, Kadan S, Yaqinuddin A, Al-Mutairy E, Al-Kattan K. COVID-19: Lung-Centric Immunothrombosis. Front Cell Infect Microbiol. 2021;11:679878.
414. Hann J, Bueb JL, Tolle F, Brechard S. Calcium signaling and regulation of neutrophil functions: Still a long way to go. J Leukoc Biol. 2020;107(2):285-97.
415. Brown RA, Leung E, Kankaanranta H, Moilanen E, Page CP. Effects of heparin and related drugs on neutrophil function. Pulm Pharmacol Ther. 2012;25(2):185-92.
416. Lelliott PM, Momota M, Shibahara T, Lee MSJ, Smith NI, Ishii KJ, et al. Heparin induces neutrophil elastase-dependent vital and lytic NET formation. Int Immunol. 2020;32(5):359-68.
417. Geli J, Capoccia M, Maybauer DM, Maybauer MO. Argatroban Anticoagulation for Adult Extracorporeal Membrane Oxygenation: A Systematic Review. J Intensive Care Med. 2022;37(4):459-71.

418. Fisser C, Winkler M, Malfertheiner MV, Philipp A, Foltan M, Lunz D, et al. Argatroban versus heparin in patients without heparin-induced thrombocytopenia during venovenous extracorporeal membrane oxygenation: a propensity-score matched study. Crit Care. 2021;25(1):160.
419. Giuliano K, Bigelow BF, Etchill EW, Velez AK, Ong CS, Choi CW, et al. Extracorporeal Membrane Oxygenation Complications in Heparin- and Bivalirudin-Treated Patients. Crit Care Explor. 2021;3(7):e0485.
420. Tonna JE, Abrams D, Brodie D, Greenwood JC, Rubio Mateo-Sidron JA, Usman A, et al. Management of Adult Patients Supported with Venovenous Extracorporeal Membrane Oxygenation (VV ECMO): Guideline from the Extracorporeal Life Support Organization (ELSO). ASAIO J. 2021;67(6):601-10.
421. Lingel MP, Haus M, Paschke L, Foltan M, Lubnow M, Gruber M, et al. Clinical relevance of cell-free DNA during venovenous extracorporeal membrane oxygenation. Artif Organs. 2023;47(11):1720-31.
422. Lee TM, Retter A, O'Dea K, Patel BV. Extracorporeal membrane oxygenation for severe acute respiratory failure increases serum levels of citrullinated histone H3, a specific marker of neutrophil extracellular traps. ATS 2024; San Diego2024.
423. Mayer CL, Koeck K, Hottmann M, Redfern A, Davis M, Barth A, et al. A phase 1 study in healthy participants to characterize the safety and pharmacology of inclacumab, a fully human anti-P-selectin antibody, in development for treatment of sickle cell disease. Eur J Clin Pharmacol. 2023;79(9):1219-28.
424. Kessenbrock K, Krumbholz M, Schonermarck U, Back W, Gross WL, Werb Z, et al. Netting neutrophils in autoimmune small-vessel vasculitis. Nat Med. 2009;15(6):623-5.
425. Li W, Chen C, Hu D, Sun F, Zhang G, Zhang Z, et al. Randomized controlled trial of ultra-protective vs. protective ventilation strategy in veno-arterial extracorporeal membrane oxygenation patients with refractory cardiogenic shock: a study protocol for the ultra-ECMO trial. Front Cardiovasc Med. 2023;10:1092653.
426. NIHR. Rest Or Moderate Mechanical Ventilation During ECMO Support - ROMEO 2024 [Available from: https://fundingawards.nihr.ac.uk/award/NIHR158537.
427. Krivitski N, Galyanov G, Cooper D, Said MM, Rivera O, Mikesell GT, et al. In vitro and in vivo assessment of oxygenator blood volume for the prediction of clot formation in an ECMO circuit (theory and validation). Perfusion. 2018;33(1_suppl):51-6.
428. Sakurai H, Fujiwara T, Ohuchi K, Hijikata W, Inoue Y, Seki H, et al. Novel application of indocyanine green fluorescence imaging for real-time detection of thrombus in a membrane oxygenator. Artif Organs. 2021;45(10):1173-82.
429. Manda A, Pruchniak MP, Arazna M, Demkow UA. Neutrophil extracellular traps in physiology and pathology. Cent Eur J Immunol. 2014;39(1):116-21.